Self-Assembly of Transition Metal Dithiocarbamate Receptors for Ionic Guest Species

Neil Berry MChem (Oxon)

Exeter College, Oxford

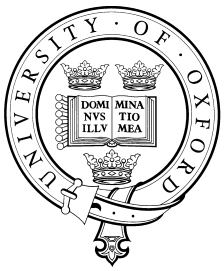

A thesis submitted for the degree of Doctor of Philosophy

Inorganic Chemistry Laboratory
University of Oxford

Trinity Term 2002

Self-Assembly of Transition Metal Dithiocarbamate Receptors for Ionic Guest Species

Neil Berry, Exeter College, University of Oxford

Abstract of thesis submitted for the degree of DPhil
Trinity Term 2002

The aim of this thesis is to develop novel receptors for the recognition of anionic, cationic and ion-pair species. The dithiocarbamate group is exploited in the metal directed self-assembly of the host molecules. Interaction between host and guest is analysed by a variety of spectroscopic methods including ^{1}H NMR, UV/visible and electrochemical techniques.

Chapter One introduces the field of supramolecular chemistry. The underlying principles of molecular recognition are discussed, followed by a review of abiotic anion, cation and ion-pair receptors reported in the literature. Various strategies for forming self-assembled architectures are presented and, in particular, the use of metal directed self-assembly highlighted.

Chapter Two investigates a new type of acyclic receptor for anions, cations or ion-pairs. The anion receptor contains amide groups, the cation receptor crown ethers and the ion-pair receptor possesses both moieties. The binding of guest ions is investigated by ^{1}H NMR, UV/visible, ESMS and electrochemical techniques. The ion-pair receptor displays positive cooperativity upon binding ion-pairs via electrostatic and conformational effects.

Chapter Three details the synthesis of macrocyclic host molecules which contain amide moieties and either one or two first row transition metal dithiocarbamate groups. Evidence for anion recognition is gained by a variety of techniques. A receptor containing a second row transition element is also investigated. Additionally, a more lipophilic receptor is synthesised and exhibits enhanced anion binding in a less competitive solvent.

Chapter Four describes the self-assembly of macrocyclic transition metal dithiocarbamate molecules which contain pyridyl or phenol groups. Bulk liquid membrane transport studies reveal a macrocyclic effect for transporting the caesium cation.

Chapter Five details the self-assembly of novel transition metal dithiocarbamate macrobicyclic anion receptors. The oxidation of a nickel(II) macrocycle to nickel(IV) affords a dicationic anionic host and the reaction of a substituted amide ligand with iron(III) creates a neutral host. Anions are sensed using a variety of techniques including electrochemistry and magnetic measurements. A new tripodal cryptand-like receptor displays a remarkable electrochemical shift upon the addition of dihydrogen phosphate.

Chapter Six reports the experimental procedures and characterisation for all products. The Appendices provide information on experimental techniques, lists the crystallographic data and summarises all the receptors studied.

Acknowledgements

Firstly, thanks must go to Professor Paul Beer for all his help, advice and ideas throughout the four years I have spent as an undergraduate and DPhil student in his research group. I am very grateful to him for the opportunity to work in his labs.

Special thanks go to Dr. Danny Fox who provided inspiration and considerable assistance during his time in the research group. I am indebted to two Part II students, Tom Shimmel and Dave Cormode, for their hard work and Tom's contribution to Chapter 2. Thanks to Dr. Andrew Cowley (Oxford University) for his expertise in determining the crystal structure and Dr. John Maher (Bristol University) for his skill in EPR spectroscopy. Thanks also to Dr. Santhosh Nair for his help with the SQUID, Dr. Nick Rees for his advice concerning NMR, Mr. Colin Sparrow for mass spectroscopy and the Inorganic Chemistry staff for elemental analyses and other assistance. I also acknowledge the Engineering and Physical Sciences Research Council for providing me with a studentship.

Thanks go to all the members of the Beer group, past and present, who have provided much help and support. I would like to thank in particular James, Andy, Rowena and Mark who have proof read this thesis and offered many valuable suggestions. Special thanks go to Michelle for being a good friend and lab partner. Outside the lab, many thanks go to Jon and Charlotte for their friendship and to members of OUHC for the time spent playing hockey.

Finally, thanks go to Tracey and my family for their continual support; this thesis is dedicated to them.

N. G. Berry

September 2002

Abbreviations

A	Ampere, area or hyperfine coupling constant
Å	Angstrom
AcOH	Acetic acid
as	Antisymmetric
AIBN	2,2'-azobis(2-methyl-propionitrile)
aq	Aqueous
Ar	Aryl
BM	Bohr magnetons
Boc	*tert*-Butoxycarbonyl
C	Concentration
°C	Degrees centigrade
$CHCl_3$	Chloroform
CH_2Cl_2	Dichloromethane
cm	Centimeters
COSY	Correlated spectroscopy
CV	Cyclic voltammetry
br	Broad
D	Diffusion coefficient
d	Doublet
DMAP	4-(Dimethylamino)pyridine
DMF	*N*,*N*-Dimethyl formamide
DMSO	Dimethyl sulphoxide
DNA	Deoxyribonucleic acid
DTC	Dithiocarbamate
E	Separation of zero point energies

E_p	Peak potential
E_{pa}	Anodic peak potential
E_{pc}	Cathodic peak potential
en	Ethylenediamine
ESMS	Electrospray mass spectrometry
Et	Ethyl
EtOH	Ethanol
Et_2O	Diethyl ether
F	Faraday constant
FC	Field cooled
g	Grams, gaseous or spectroscopic splitting factor
HSQC	Heteronuclear single-quantum correlated spectroscopy
Hz	Hertz
i	Current
IR	Infrared
J	Coupling constant
K	Kelvin
k	Boltzmann constant
K_n	n^{th} stability constant
L	Litre
LC	Ligand centred
LMCT	Ligand to metal charge transfer
M	Moles $litre^{-1}$, mega, molecular ion or metal
m	Multiplet, milli or metre
MeCN	Acetonitrile
MeOH	Methanol
min	Minute

mmol	Millimole
m/z	Mass to charge ratio
MLCT	Metal to ligand charge transfer
Nα	Temperature independent paramagnetism
n	Nano or number of electrons
NBS	*N*-Bromosuccinimide
NMR	Nuclear magnetic resonance
ppm	Parts per million
Pyr	Pyridine
Q	Charge or vibrational partition function
q	Quartet
revs	Revolutions
RNA	Ribonucleic acid
s	Singlet, second or symmetric
sh	Shoulder
SQUID	Super conducting quantum interference device
SWV	Square wave voltammogram
T	Temperature
t	Triplet
TBA	Tetrabutyl ammonium
$TBABF_4$	Tetrabutyl ammonium tetrafluoro borate
TFA	Trifluoroacetic acid
THF	Tetrahydrofuran
UV	Ultraviolet
V	Volt or volume
v/v	Volume for volume
ZFC	Zero field cooled

β	Stability constant
δ	Chemical shift
ε	Molar extinction coefficient
ξ	One electron spin-orbital coupling constant
θ	Weiss constant
λ	Wavelength
μ	Micro
μ_{eff}	Effective magnetic moment
ν	Frequency or kinematic viscosity
χ_m^{calc}	Calculated molar magnetic susceptibility
χ_m^{obs}	Observed molar magnetic susceptibility
Ω	Ohm
ω	Rate of rotation

Contents

Chapter 1

Chapter 2

Chapter 3

Chapter 4

Chapter 5

Chapter 6

Chapter One

Introduction

1 Supramolecular Chemistry

The field of supramolecular chemistry has been defined as 'chemistry beyond the molecule'[1] and involves the synthesis and study of novel molecular systems in which the components are held together reversibly by intermolecular forces. This is in contrast to traditional synthesis that uses covalent bonds to build molecules.

Examples from nature often provide inspiration for supramolecular chemistry. With this in mind, systems can be synthesised using organic and inorganic methods and the properties of the resulting supramolecular assemblies can be investigated using a variety of physical methods. Thus, supramolecular chemistry is a multidisciplinary field.

The concept of complementarity is one of the most important ideas in supramolecular chemistry. The most elegant and sophisticated examples of molecular complementarity come from nature. For example, an enzyme may catalyse a single reaction with total specificity due to the active site being complementary to the substrate. This complementarity arises from the size, shape and position of the binding sites for the substrate. Fischer introduced this idea as the 'lock and key' principle.[2]

Perhaps the most important example of this concept is the base pairing found in the DNA double helix.[3] A single strand of DNA is composed of a backbone of phosphorylated sugars on which there are a series of purine and pyrimidine bases. The double helix combines two anti-parallel strands that are held together by complementary hydrogen bonding between pairs of these bases (**Figure 1.1**).

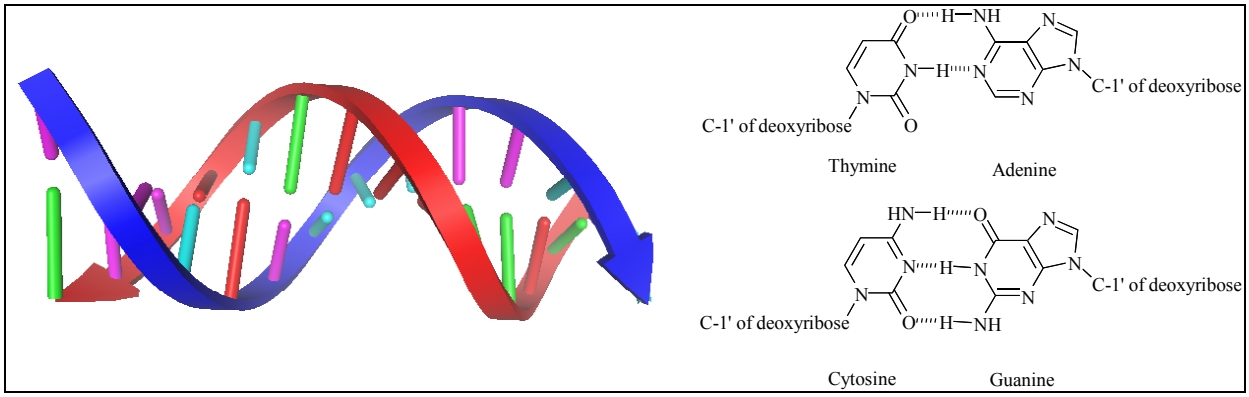

Figure 1.1 *Schematic representation of the DNA double helix and the pairing of the bases*

Hydrogen bond donors and acceptors are arranged in such a way that adenine forms two complementary hydrogen bonds with thymine and guanine forms three with cytosine. This bonding pattern extends along the double helical DNA structure so one strand is complementary to the other.

The work presented in this thesis outlines the synthesis of receptor molecules that utilise a variety of non-covalent forces to bind charged guest species. A brief outline of the non-covalent forces that can be used by the supramolecular chemist is discussed below.

1.1 Non-Covalent Forces

Inspired by the complementarity of DNA and many other examples from nature the supramolecular chemist uses various non-covalent forces to hold molecules together. These interactions include:

i) electrostatics (ion-ion, ion-dipole and dipole-dipole),

ii) hydrogen bonding,

iii) π-π stacking,

iv) dispersion and induction forces (van der Waals forces),

v) hydrophobic or solvatophobic effects.

The bond energy of a typical single covalent bond is around 350kJmol^{-1}.[4] The individual strengths of non-covalent interactions are generally much weaker ranging from 2kJmol^{-1} for dispersion forces[5] to 250kJmol^{-1} for ion-ion interactions.[6] Thus supramolecular chemistry relies upon the use of multiple weak interactions which, when correctly manipulated, may allow strong and selective recognition of specific guests to be achieved.

Electrostatic interactions are based upon the Coulombic attraction between opposite charges. Ion-ion interactions are non-directional whereas ion-dipole interactions must be suitably aligned for the strongest interaction to occur.[7] Electrostatic interactions have been used extensively in receptor molecules, e.g. cation receptors (crown ethers, cryptands, and spherands) and anion receptors (quaternary ammonium bicycles).

Hydrogen bond donor arrays have been employed in receptors designed to coordinate to neutral (e.g. barbiturate,[8] urea[9]) and anionic guest species. The fact that hydrogen bonds are highly directional and the relative ease with which they can be built into molecular architecture has made them especially attractive to the supramolecular chemist.

π-π stacking forces occur in systems that contain aromatic rings.[10] Attractive forces can occur in either a 'face to face' or 'edge to face' fashion. This attractive force is electrostatic in nature and some elegant receptors have been synthesised using such interactions including one for benzoquinone.[11]

Dispersion forces are attractive forces that occur between molecules when instantaneous dipoles in the electron clouds interact favourably.[12] These forces are believed to provide additional enthalpic stabilisation to the inclusion of a hydrophobic guest into a hydrophobic cavity.[13]

The hydrophobic effect is the driving force for the association of apolar binding partners in polar solution. Water molecules can arrange themselves around the surface of the hydrophobic cavity in a structured array. Upon guest coordination, molecules of water are released resulting in a favourable increase in entropy. In addition, there is believed to be a small favourable enthalpic effect due to the hydrogen bonds between water molecules being stronger than the bonds between water molecules and apolar species. Receptors that take advantage of this non-covalent force include cyclophanes.[14]

Although not a non-covalent force, classical coordination chemistry is widely used in supramolecular chemistry. The geometric requirements of metal ions, together with appropriate design of ligands have allowed the construction of complex architectures such as catenanes, helices and molecular grids.

1.2 Chelate and Macrocyclic Effects

The chelate and macrocyclic effects are often employed in supramolecular chemistry to form thermodynamically stable compounds.

The chelate effect is the enhanced stability of a complex containing chelate rings as compared to a similar system containing fewer or no rings.[15] This is clearly demonstrated by comparing the interaction of ammonia and ethylenediamine with a transition metal ion (**Figure 1.2**).[16]

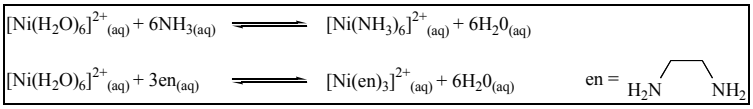

Figure 1.2 *Equilibria of ammonia and ethylenediamine binding to nickel(II)*

The bidentate ethylenediamine ligand forms a metal complex that is ten times more stable than that of ammonia. The reason is due largely due to entropic effects due to release of solvent molecules upon coordination, however enthalpic factors also play a role.[17] Another factor is that the basicity of the amino groups in ethylenediamine is greater than that of ammonia due to the positive inductive effect of the alkyl groups. Thus stronger metal-ligand co-ordinate bonds are formed.

The macrocyclic effect is related to the chelate effect and refers to the increased thermodynamic stability of macrocyclic systems as compared to their acyclic analogues.[18] For example the coordination of copper(II) by the ligands shown in **Figure 1.3** is four orders of magnitude greater for the macrocycle compared to the acyclic structure.

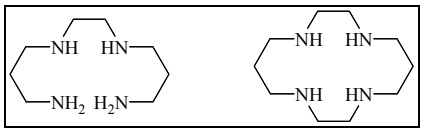

Figure 1.3 *Acylic and macrocyclic polyaza ligands*

The increased stability is caused by a combination of enthalpic and entropic factors. Macrocyclic hosts are frequently less solvated than their acyclic analogues and therefore less energy is required for desolvation. Macrocyclic ligands are also less flexible and consequently have fewer degrees of freedom to lose upon complexation of the guest species. Additionally, macrocyclic complexes are more kinetically inert than their acyclic analogues.

The enhanced binding of guest species by chelating or macrocyclic hosts has been employed in the design of many receptor molecules operating through a variety of non-covalent forces. The examples in this chapter are chosen to highlight the principles which supramolecular chemistry frequently uses.

This thesis presents a variety of novel self-assembled receptor molecules for charged guest species. The following sections briefly review the areas of cation, anion and ion-pair coordination and the topic of self-assembly.

2 Cation Binding

The following sections contain a brief overview of cation coordination chemistry that has been carried out in this field, however extensive reviews have been published.[19]

2.1 Why Bind Cations?

Cations play important roles in many biological processes. For example, concentration differences across cell membranes maintain potentials that are used to transport organic substrates into the cell. Metal cations are present in the active site of many enzymes often playing catalytic roles.[3] Medically important metal complexes include complexes of paramagnetic lanthanide cations that are used in magnetic resonance imaging as contrast agents.[20] These and many other examples have inspired a great deal of effort in producing selective receptors for cationic guest species.

2.2 Crown Ethers

In 1960 Pedersen made the chance discovery of the first polyether macrocyclic molecule.[21] He observed that a potassium ion fitted snugly inside the cavity of dibenzo[18]crown-6 and formed six attractive ion-dipole interactions with the oxygen donors in the macrocycle.[22]

Extensive cation coordination studies showed that the strongest complexes were formed between a particular Group 1 metal ion and a crown ether possessing a complementary cavity size. This is often referred to as 'the optimal spatial fit'.[23] For example [18]crown-6 forms the most stable complex with potassium cations whereas the larger cavity of [21]crown-7 forms a stronger complex with caesium (**Table 1.1**).

Cation	Diameter (Å)	Crown Ether	Cavity Diameter
Li^+	1.36	[12]crown-4	1.2-1.5
Na^+	1.94	[15]crown-5	1.7-2.2
K^+	2.66	[18]crown-6	2.6-3.2
Rb^+	2.94	-	-
Cs^+	3.34	[21]crown-7	3.4-4.3

Table 1.1 *Diameter of group 1 metal cations and various crown ethers*

Crown ethers may also form complexes of different stoichiometry with alkali metal cations. The crystal structure of K^+-(benzo[15]crown-5)$_2$ revealed that the potassium cation is sandwiched between two crown ether molecules as it is too large to fit inside the molecular cavity of benzo[15]crown-5 itself.[24] Conversely, dibenzo[24]crown-8 encapsulates two potassium cations simultaneously (**Figure 1.4**).[25]

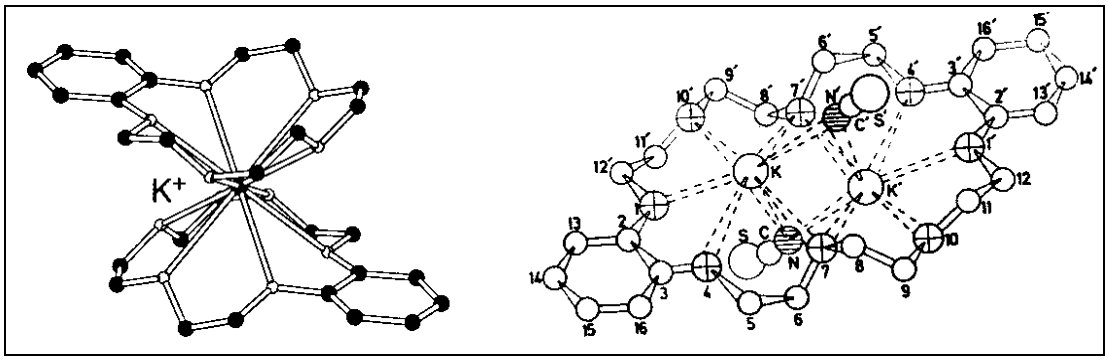

Figure 1.4 *Crystal structure of benzo[15]crown-5:potassium sandwich complex and bis(potassium thiocyanate)dibenzo[24]crown-8*

Crown ethers also form complexes with transition and lanthanide metal cations. The affinity of crown ethers for transition metals can be enhanced by replacing 'hard' oxygen donor atoms with 'softer' sulphur or nitrogen atoms (**Figure 1.5**).[26]

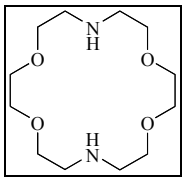

Figure 1.5 *An azacrown ether*

For example, the macrocycle shown in **Figure 1.5** exhibited a stability constant with silver over five orders of magnitude greater than potassium.[27]

Crown ethers can also form complexes with primary ammonium cations (**Figure 1.6**).[28]

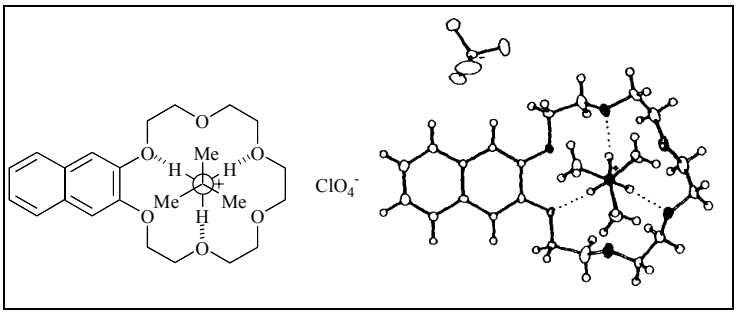

Figure 1.6 *An 18[crown]-6 cation receptor and the crystal structure of the primary ammonium:receptor complex*

This [18]crown-6 molecule binds to primary alkyl ammonium molecular cations as it possesses three oxygen atoms which are correctly orientated to form three hydrogen bonds with the guest. [15]crown-5 does not possess this symmetry and as a consequence a much weaker complex is formed.[29]

2.3 Lariat Crown Ethers

Crown ethers can be functionalised with pendant arms containing additional coordinating groups which add a 'three-dimensionality' to cation complexation. These molecules are known as lariat crown ethers and exhibit higher binding constants than analogous crown ether molecules. For example, the molecule shown in **Figure 1.7** bound sodium cations an order of magnitude more strongly than [15]crown-5.[30]

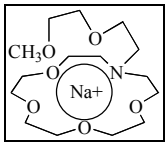

Figure 1.7 *A lariat crown ether*

2.4 Cryptands

Lehn and co-workers first reported the synthesis of cryptands in 1969.[31] Cryptands are cage-like bicyclic molecules which complex Group 1 and Group 2 metal cations with very large stability constants (**Figure 1.8**).

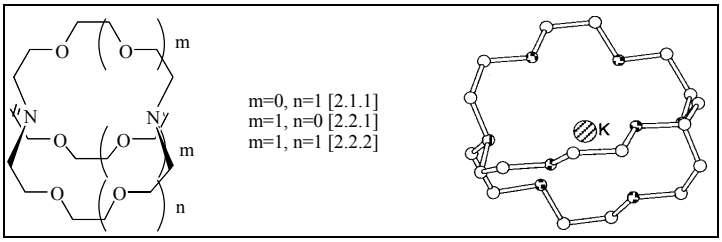

Figure 1.8 *Lehn's cryptand cation receptors and crystal structure of the potassium:[2.2.2] complex*

For example [2.2.2]cryptand binds potassium in methanol four orders of magnitude more strongly than 18[crown]-6.[32] In a series of cryptands, the highest stability constants were observed for Li^+[2.1.1], Na^+[2.2.1] and K^+[2.2.2], corresponding to a complementarity of cavity size and size of the cation.[33] The large magnitude of the stability constants are due to a combination of factors.[34] Metal complexation leads to a positive entropy effect as solvent is released upon coordination. In addition, there is less reorganisation of the receptor required, with respect to 18[crown]-6, to bind the cations.

2.5 Spherands

Cram illustrated the concept of preorganisation with the spherand ionophore shown in **Figure 1.9**.[35]

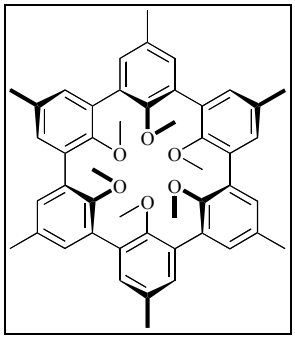

Figure 1.9 *Cram's spherand cation receptor*

This spherand bound both lithium and sodium cations very strongly, but did not complex cations larger than sodium.[36] This is an example of preorganisation which states that 'the more

highly hosts and guests are organised for binding and the lower their solvation prior to their complexation, the more stable their complexes will be'.[37] Like crown ethers, the cavity size can be altered to change the selectivity for different cations. These systems exhibited extremely slow complexation-decomplexation kinetics.

3 Anion Binding

In comparison to cation coordination, the field of anion coordination is a relatively recent development.[38] Many new molecules reported this thesis have been designed to bind anions and so the following sections present a brief overview of the main types of anionic receptors reported to date, however comprehensive reviews have been published.[39]

3.1 Why Bind Anions?

Anions play numerous important roles in both biology and chemistry. Many biologically important species are anionic, such as nucleic acids and the majority of enzyme substrates.[40] Anions also can play a role in diseases. For example, cystic fibrosis is caused by the misregulation of chloride channels[41] and the need for a selective sensor of this anion has been reported.[42] Environmentally, some anions can pose a pollution problem. For example, nitrate anions from the extensive use of fertilisers used on agricultural land can be washed into lakes which leads to excessive plant growth, thus disrupting aquatic life cycles.[43] Pertechnetate anions are toxic radioactive by-products of the nuclear industry and so selective binding and extraction of such a pollutant is an important goal.[44]

3.2 Anion Properties and Receptor Design

Anions possess a variety of characteristic features that must be considered when designing a receptor for a particular anionic guest.

Anions are larger than their isoelectronic cations and so the potential host's cavity must be of sufficient size to allow guest encapsulation (**Table 1.2**).[45]

Cation	Radius (Å)	Anion	Radius (Å)
Na^+	0.95	F^-	1.36
K^+	1.33	Cl^-	1.81
Rb^+	1.48	Br^-	1.95
Cs^+	1.69	I^-	2.16

Table 1.2 *Radii of isoelectronic cations and anions*

Unlike simple metal cations many anions only exist over a limited pH range, e.g. carboxylates, phosphates and sulphates. [46] At low pH anions become protonated and thus lose their negative charge.

The charge, size and pH alter the way in which an anion is solvated. The degree of aqueous solvation of the anion is reflected in the Hofmeister series, which indicates increasing hydrophobicity.[47] In a hydrophobic binding site, the less hydrated anions are bound more strongly.[48]

Anions exist in a range of geometries that enable a receptor to be designed with a complementarity for that particular shape (**Table 1.3**).[49]

Spherical	Linear	Trigonal Planar	Tetrahedral	Octahedral
F^-	N_3^-		PO_4^{3-}	
Cl^-	CN^-	CO_3^{2-}	VO_4^{3-}	$Fe(CN)_6^{4-}$
Br^-	SCN^-	NO_3^-	SO_4^{2-}	$Co(CN)_6^{3-}$
I^-	OH^-		SeO_4^{2-}	

Table 1.3 G*eometries of various anions*

3.3 Positively Charged Receptors

Inspired by examples from nature, anionic guest species can be bound by incorporating positive charges into a host. Carboxypeptidase A is a zinc enzyme that performs the selective cleavage of the terminal peptide at the carboxylate end of a polypeptide. X-ray structures have revealed that the positively charged zinc ion plays a vital part in coordinating the substrate in the active site of the enzyme.[50] In another example from nature, the two proteins that provide transport of phosphate and sulphate anions both rely solely on hydrogen bonds to complex their respective anions.[50] The first crystal structure of a chloride channel revealed its outer portion was lined with positive charges to attract chloride anions, however the chloride selectivity filter relied upon multiple hydrogen bonding interactions to achieve specificity.[51] The following sections present examples of anion receptors that use electrostatic interactions, commonly in combination with hydrogen bonding, to form complexes with negatively charged guest species, often in water.

3.3.1 Polyaza Macrocycles

In 1968, Simmons and Park reported a macrotricyclic receptor that used electrostatics and hydrogen bonding attractive forces to encapsulate anionic guest species (**Figure 1.10)**.[52]

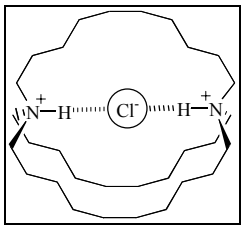

Figure 1.10 *Simmons's and Park's macrobicyclic polyammonium receptor*

It was found that the receptor bound halide anions inside the cavity with the protons on the nitrogens pointing inwards, forming hydrogen bonds with the guest. These hydrogen bonds complemented the electrostatic attractive forces thus forming a strong host:guest complex.

Lehn developed a range of polyammonium aza macrocycles one of which is shown in **Figure 1.11**.[53]

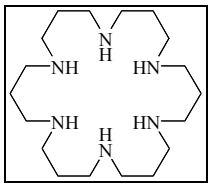

Figure 1.11 *Lehn's polyamine macrocyclic receptor*

Fully protonated, this receptor forms strong complexes with both inorganic and organic polyanions in water. However, no interaction was observed with mono anions, indicating the importance electrostatic interactions can play.

The binding of anionic species can be sterically tuned. The receptor shown below has two individual binding sites separated by an alkyl spacer group (**Figure 1.12**).[54]

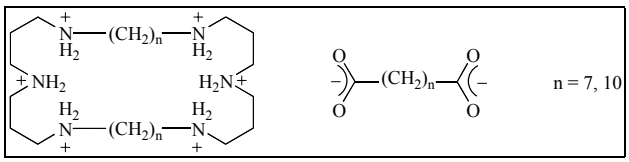

Figure 1.12 *Lehn's sterically tuned polyammonium macrocyclic receptors*

The strongest complexes are found for the dicarboxylate dianion that has a complementary fit for the receptor's cavity. These ammonium receptors have the disadvantage of only operating at low to medium pH when they are highly protonated. Many anions are only maximally negatively charged at high pH, so there is a limited pH range in which effective anionic binding can occur.

3.3.2 Expanded Porphyrins

Sessler and co-workers prepared a receptor based upon an expanded protonated porphyrin structure. This receptor complexed fluoride three orders of magnitude more strongly than chloride.[55] This sapphyrin has been further functionalised to create a receptor for biologically important anions such as anti-viral nucleic acid phosphates. Selectivity was observed for guanine monophosphate, which was attributed to a complementary hydrogen bonding triad (**Figure 1.13**).[56]

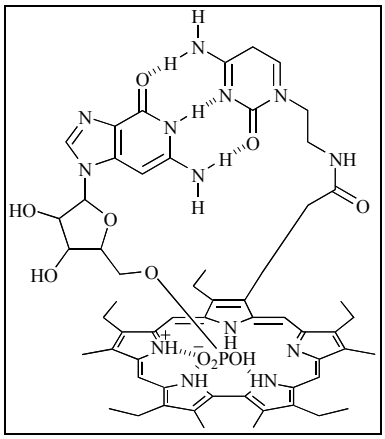

Figure 1.13 *Sessler's sapphyrin guanine receptor with bound guanine monophospate*

3.3.3 Guanidinium Receptors

One solution to the problem of the limited pH range of polyammonium hosts was the use of guanidinium-based receptors. Guanidinium is readily protonated and remains protonated up to high pH values.[57] This means that guanidinium based receptors have a much wider pH range in which they can effectively operate. Unfortunately, anion binding is much weaker than with the polyammonium analogues due to charge delocalisation.

Schmidtchen incorporated a guanidinium group into a bicyclic system in order to rigidify the hydrogen bond donor groups.[58] For example, the receptor shown in **Figure 1.14**, extracts *p*-nitrobenzoate from water into chloroform by a combination of electrostatic, hydrogen bond interactions and π-π stacking effects.[59]

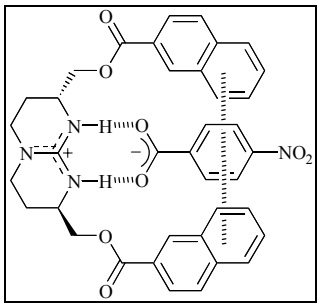

Figure 1.14 *Guanidinium receptor with bound p-nitro benzoate*

3.3.4 Quaternary Ammonium Receptors

Another solution to the problem of the limited pH range of polyamine receptors was to use pH independent quaternary ammonium receptors. Schmidtchen reported that quaternary

ammonium macrotricyclic receptors formed 1:1 complexes in water with various anions (**Figure 1.15**).[60]

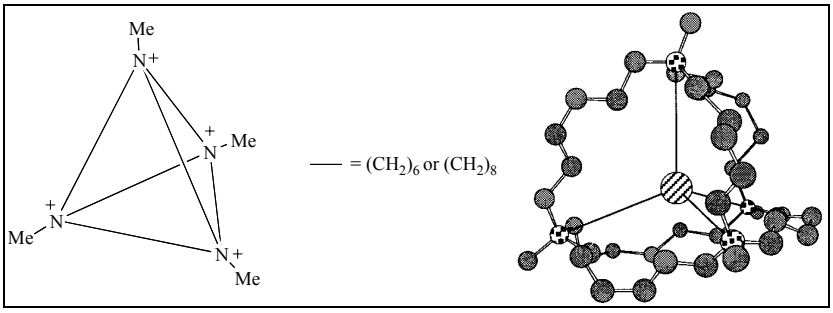

Figure 1.15 *Schmidtchen's macrotricyclic anion receptors and the crystal structure of the iodide:hexyl receptor complex*

The receptor with the hexyl spacer group bound halide anions more strongly than the receptor with the octyl spacer due to the difference in cavity size.[61] However, the larger receptor formed a stronger complex with the larger anion iodide over bromide.

A similar receptor was synthesised which contained a zwitterionic group.[62] This removed the counter anion that was present in the previous receptor and competed with the anionic guest for the binding site. It was shown that this net neutral receptor bound anions more strongly than the receptor in **Figure 1.15**.

Electrostatic forces have been used together with hydrophobic forces to create a receptor for a different type of anionic guest species. Large hydrophobic cavities containing quaternised nitrogen atoms were reported by Schneider (**Figure 1.16**).[63]

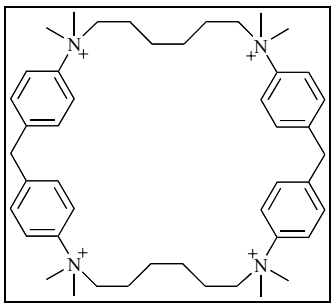

Figure 1.16 *Schneider's cyclophane receptor*

This host showed selectivity for hydrophobic anions such as nucleic acid base anions. The receptor utilised the hydrophobic cavity and the positive charge on the nitrogens to interact with the anion.

3.3.5 Metallated Cavities

Atwood took a different approach to making charged hydrophobic receptors by functionalising the hydrophobic calix[4]arene framework with positively charged metal groups.[64] This yielded an electron deficient host that has been shown to encapsulate the tetrafluoroborate anion (**Figure 1.17**). More remarkably, this molecule displayed strong binding of chloride in water.[65]

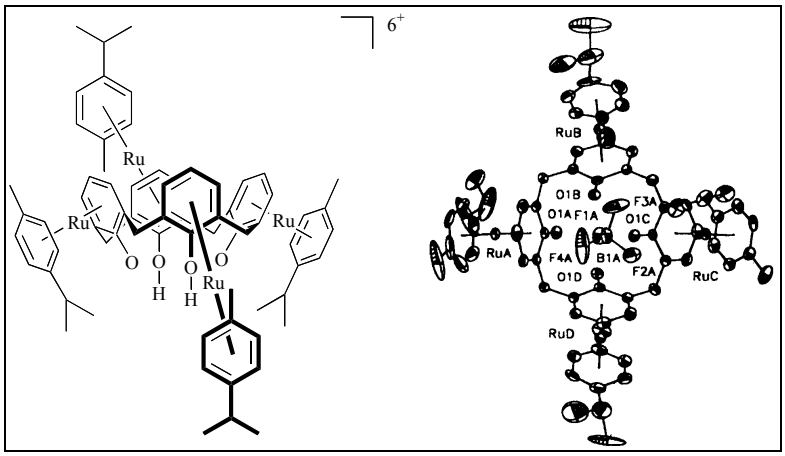

Figure 1.17 *Atwood's metallated calixarene and the crystal structure of the tetrafluoborate:receptor complex*

3.4 Neutral Receptors

Anions can be considered as electron pair donors and will therefore interact with an electron pair acceptor and are also capable of forming hydrogen bonds with hydrogen bond donor groups such as amides and thioureas. Hydrogen bonds are directional in nature and so a receptor can be designed to possess an array of such interactions which are convergent. In contrast to positively charged receptors, neutral hosts containing amide groups for example, are often studied in organic solvents due to low solubility in water.

The molecule shown in **Figure 1.18** was the one of the first anion receptor reported using amide groups.[66]

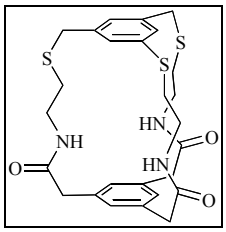

Figure 1.18 *Pascal's trisamide anion receptor*

The three convergent amide bonds point into the cavity and fluoride was shown to bind strongly in DMSO solution.

Recently steroidal podands have been modified to include convergent hydrogen bond donor groups which bind chloride anions extremely strongly in chloroform via three hydrogen bond donor groups (**Figure 1.19**).[67]

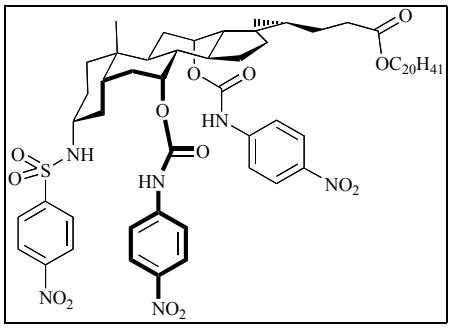

Figure 1.19 *A steroidal anion receptor*

The directionality of hydrogen bonds allows the possibility of designing receptors with specific shapes that maybe capable of differentiating between guests of different geometry. For example, the receptor in **Figure 1.20** displays strong binding of phosphate in preference to chloride even in DMSO.[68]

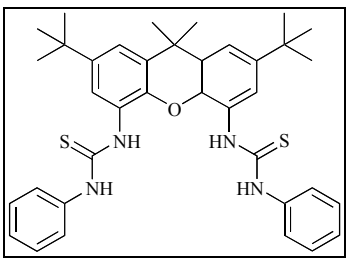

Figure 1.20 *A bisthiourea anion receptor*

3.5 Lewis Acidic Receptors

Lewis acids are capable of accepting an electron pair and so can complex anions. This fact has led to a development of receptors that utilise Lewis acidic heteroatoms.

The first ligand to utilise this interaction was an organoboron compound designed by Shriver and Biallis (**Figure 1.21 a**).[69]

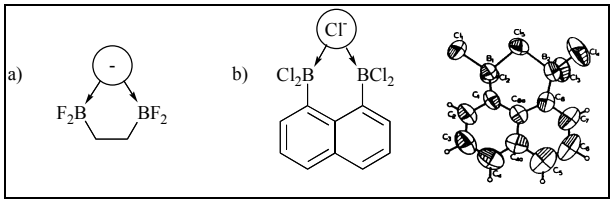

Figure 1.21 *a) Shriver and Biallis's and b) Katz's organoboron anion receptors and the crystal structure of Katz's chloride:receptor complex*

The binding of the methoxide anion by this chelating ligand was found to be greater than that of boron trifluoride. Katz synthesised a similar organoboron receptor that was more preorganised, and it bound strong σ donors such as hydride, fluoride and chloride (**Figure 1.21 b**).[70]

Lewis acidic Group 14 metals have been incorporated into macrocyclic structures. For example, a twelve membered macrocycle containing three silicon atoms was shown to transport chloride preferentially over the other halides (**Figure 1.22**).[71] Several organogermanium macrocycles were also studied in similar experiments. The Lewis acidity of the bis-methyl or bis-phenyl substituted germanium was too low for anion transport but the enhanced acidity of the methyl(chloro) substituted metal resulted in selectivity for chloride being shown over bromide (**Figure 1.22**).[72]

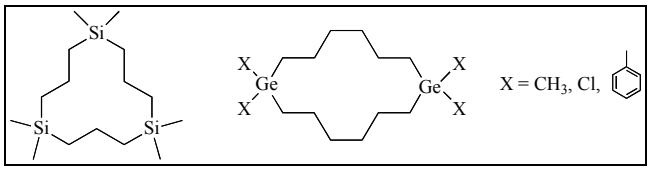

Figure 1.22 *Organosilicon and organogermanium anion receptors*

Newcomb has made extensive use of organotin macrocycles and cryptands for anionic recognition (**Figure 1.23**).[73]

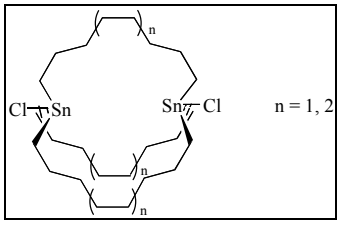

Figure 1.23 *Newcomb's organotin anion receptor*

The cryptand with an eight-carbon linkage was shown to bind to chloride anions in a 1:1 stoichiometry in $CFCl_3$, while the ten-carbon linkage bound bromide.[74] Crystallography revealed that the halide ions formed strong interactions with both metal atoms.

Organomercury receptors have also been extensively studied as the mercury atom can accept electron density. As organomercury posseses linear geometry, large macrocyclic receptors have been synthesised. For example, Hawthorne has synthesised numerous receptors using carboranes (**Figure 1.24**).[75]

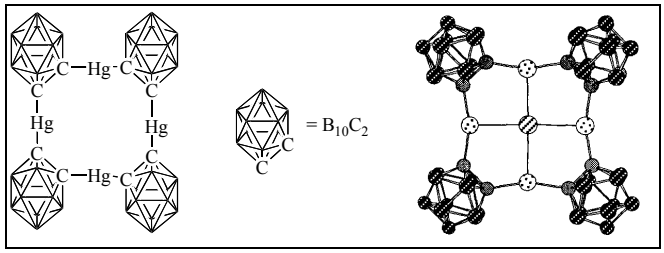

Figure 1.24 *Hawthorne's organomercury anion receptor and the crystal structure of the chloride:receptor complex*

The macrocycle was formed from carborane clusters that are linked by linear mercury atoms. The macrocycle formation was templated by the presence of a chloride anion. The crystal structure revealed that the chloride was bound in the plane of the mercury atoms and equidistant from each of them. When iodide was investigated, it was found that two anions were bound to the macrocycle, one above the plane and one below.

Lewis acid centres have also been used in conjunction with secondary amides to create anion receptors. Reinhoudt used a uranyl salene group as the metal centre and found that the receptor shown in **Figure 1.25** bound dihydrogen phosphate in DMSO with an extremely high stability constant.[76]

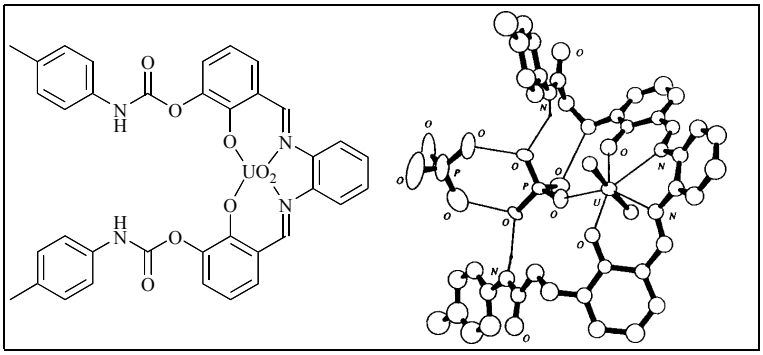

Figure 1.25 *Reinhoudt's uranyl receptor and the crystal structure of dihydrogen phosphate:receptor complex*

Anion receptors similar to this have been included in chemically modified field effect transistors.[77] They display responses that deviate from the Hofmeister series and exhibit selectivity for phosphate anions over other more lipophilic anions.

3.6 Anion Sensors

With the aim of advancing chemical sensor technology, considerable recent attention has focussed on the design of receptors that have the ability to sense the anion recognition event through a macroscopic electrochemical or optical response. Chemical sensors are molecules that can bind to a guest species and report the binding process via the change of a measurable physical property. The receptors in this thesis contain groups that have the potential to report the presence of anions by optical or electrochemical techniques. Several types of chemical sensor for anions have been reported and the examples given below highlight some of the techniques that have been employed.

3.6.1 UV/visible and Colorimetric Sensing

Ansyln has used a 1,3,5-substituted triethylbenzene scaffold to create a receptor with C_3 symmetry (**Figure 1.26**).[78]

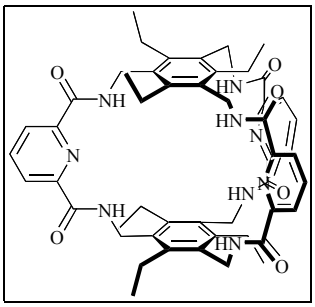

Figure 1.26 *Ansyln's anion receptor*

The receptor forms 1:1 complexes with anionic dyes such as methyl red, and upon addition of anions, the equilibrium between the receptor and the dye is perturbed resulting in large changes in absorbance in the UV/visible spectroscopy. This receptor forms strong complexes with the C_3 symmetrical nitrate anion.

The development of selective colorimetric sensors for anions is particularly challenging. Recently a porphyrin derivative with urea hydrogen bond donors and chromophoric unit (**Figure 1.27**) was reported to show dramatic colour changes upon the addition of fluoride, acetate and dihydrogen phosphate anions, while addition of the other halide anions afforded very little colour change.[79]

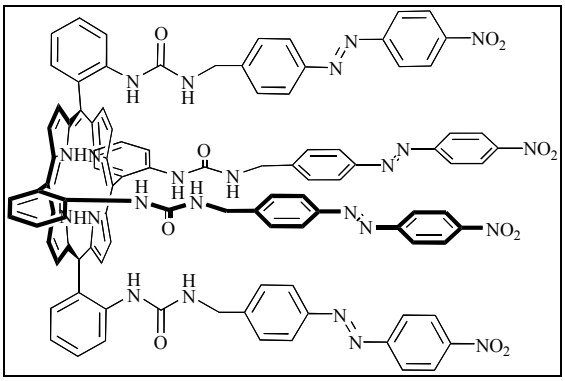

Figure 1.27 *A colorimetric anion sensor*

3.6.2 Electrochemical Sensing

Beer used a range of metallocenes derivatives to electrochemically sense anions in solution. For example, cobaltocenium appended with secondary amide units form hydrogen bonds with anionic guest species.[80] This charged moiety has been built into a range of receptors, which can electrochemically sense anions in organic solvents via a cathodic shift of the cobaltocenium/cobaltacene reduction wave (**Figure 1.28**).

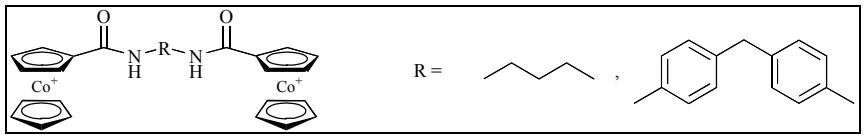

Figure 1.28 *Beer's cobaltocenium receptors*

The examples shown in **Figure 1.28** illustrate how the stoichiometry can be tuned by altering the spacer group in between the two metal centres. The short flexible chain forms a 1:1 complex with chloride whereas the longer more rigid spacer binds chloride in a 2:1 ratio.

3.6.3 Luminescence Sensing

Beer also used functionalised ruthenium(II) bipyridine molecules with hydrogen bond donating groups to report optically anion binding (**Figure 1.29**).[81]

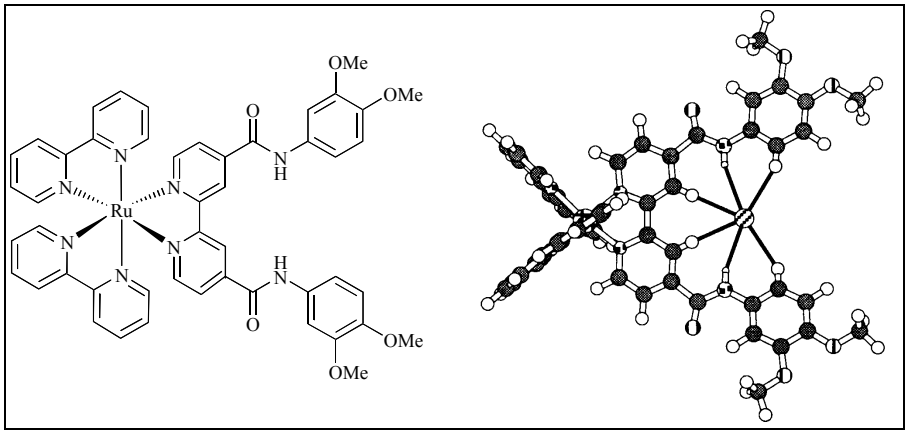

Figure 1.29 *Beer's ruthenium(II) bipyridine receptor and the crystal structure of the chloride:receptor complex*

The crystal structure shows a chloride anion bound by hydrogen bonds with the amide protons and also protons on the aromatic rings. Upon the addition of anions, the luminescence intensity of the receptor molecule increased due to guest binding perturbing the ruthenium(II) bipyridine centre.

An anion receptor based on a lanthanide metal cation has been reported.[82] The receptor consists of a europium ion coordinated by a polyamine ligand which has three amide groups attached (**Figure 1.30**). It was shown, by an increase in luminescence, that the complex strongly bound citrate and malonate anions in water at pH=7.4.

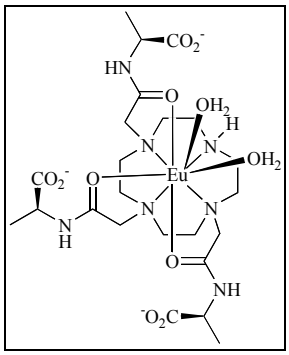

Figure 1.30 *A luminescent sensor*

4 Anion and Cation Binding

The previous two sections have highlighted the approaches that have been taken to bind cations and anions in separate receptor molecules. However, it is possible to design receptors that can bind both anions and cations simultaneously. The approaches that can be taken to achieve this goal are now discussed briefly.

4.1 Cascade Complexes

These complexes are designed to be able to bind more than one metal cation and the cations can then bind strongly to an anionic guest species. The overall complex is called a cascade complex.

Lehn synthesised a range of receptors capable of forming cascade complexes.[83] The receptor shown in **Figure 1.31** can bind two copper(II) metal ions and forms an ellipsoid shaped potential anion receptor.

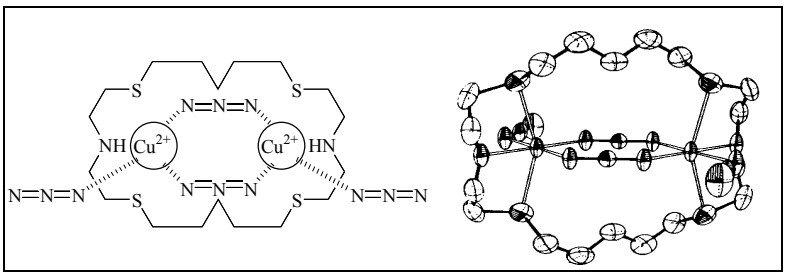

Figure 1.31 *Lehn's coordinate cascade receptor and the crystal structure of copper (II):azide cascade complex.*

It was found by magnetic susceptibility measurements that the triazide bridged the two copper atoms whereas the smaller chloride ion bound one anion to each metal. This cascade complex illustrates how a host molecule can control the relative position of metal ions and manipulate the selectivity of subsequent anion binding.

A cascade complex using non-coordinate interactions has been also been reported (**Figure 1.32**).[84]

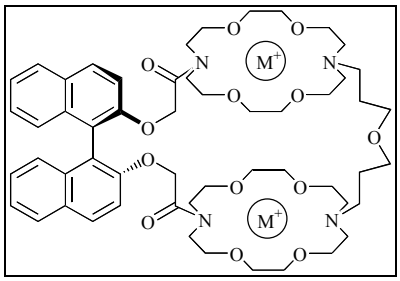

Figure 1.32 *Lehn's non-coordinate cascade receptor*

The receptor shown above binds one alkali metal cation in each crown ether ring and these are then capable of binding to an anionic guest species via electrostatic interactions. In addition, the binapthyl unit is chiral and this receptor demonstrated enhanced binding of one optical isomer of mandelate over the other.

4.2 Ion-Pair Receptors

It is possible to design ditopic receptors that contain two separate binding sites, one for a cation and one for an anion. Reetz synthesised one of the first such ion pair receptors which contains both a crown ether group for cation binding and a Lewis acidic boron for anion binding (**Figure 1.33**). [85]

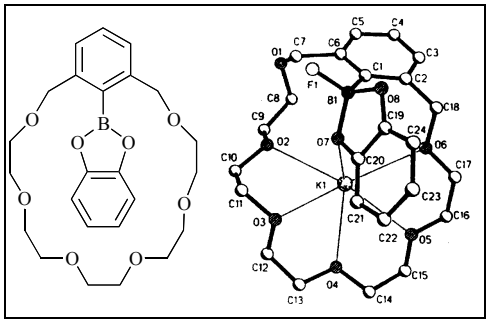

Figure 1.33 *Reetz's ion-pair receptor and the crystal structure of the potassium fluoride:receptor complex*

Remarkably, this receptor could solubilise KF in dichloromethane. NMR and crystallographic data showed that the anion was binding to the boron atom and the cation to the crown ether ring. This receptor displayed cooperative binding effects as it proved a more efficient receptor molecule than a simple 1:1 mixture of crown ether and boronic acid.

Many biologically important molecules exist as zwitterions. An effective receptor for zwitterions must possess the correct spatial arrangement of anion and cation binding motifs so both parts of the guest can be bound simultaneously.

The receptor shown in **Figure 1.34** extracts amino acids from aqueous solution into dichloromethane.[86]

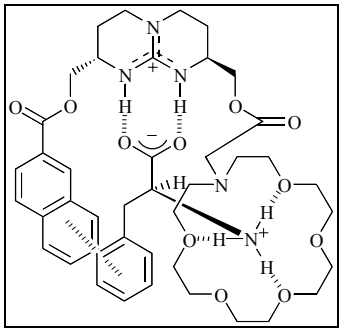

Figure 1.34 *de Mendoza's zwitterionic receptor*

Extraction experiments showed selectivity for amino acids that had an aromatic side chain such as phenylalanine and tryptophan. The binding occurs due to the carboxylate binding to the guanidinium group, the protonated amine to the azacrown and favourable π-π stacking between the amino acid side chain and the receptor's naphthalene unit. Furthermore, the receptor showed complete selectivity for L-amino acids over D-amino acids due to the particular spatial arrangements of the binding sites.

5 Self-Assembly

Self-assembly relies upon appropriately designed ligands, and the intermolecular forces that exist between the components, to control their relative orientation thus synthesising a specific supermolecule. This process allows the synthesis of novel molecular architectures that are only accessible in very small yields via traditional covalent bond formation.

Nature uses a simple, limited range of interactions to produce complex molecular assemblies. For example, the tobacco mosaic virus consists of and a RNA strand and 2130 protein sub units.[87] The proteins assemble themselves around the RNA strand and form the virus superstructure using non-covalent forces.

However, various non-covalent interactions have been used to drive the formation of self-assembled products and comprehensive reviews have been published,[88] but a brief summary is found in the following sections.

5.1 Hydrogen Bonded Assemblies

In recent years much interest has been shown in using hydrogen bonding to create a variety of assemblies.[89]

Lehn and Mascal have reported the formation of a superstructure using hydrogen bonds to self-assemble the hexameric compound shown in **Figure 1.35**. [90]

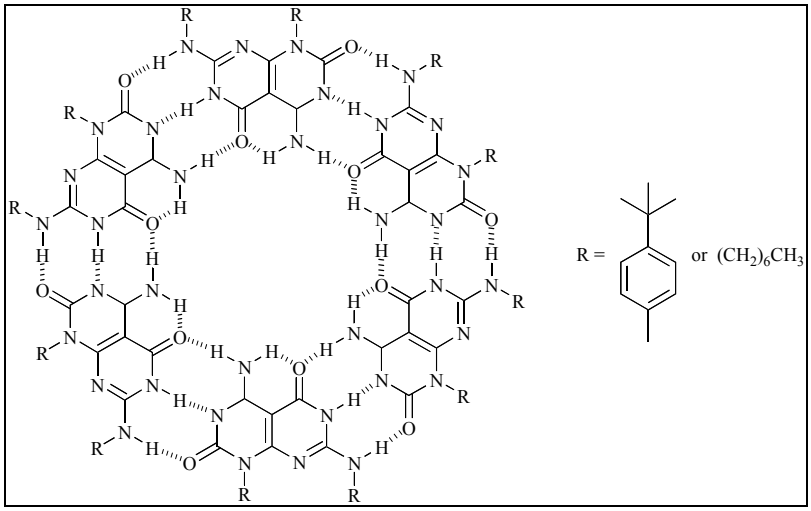

Figure 1.35 *Lehn's and Mascal's hexameric hydrogen bonded assembly*

This molecule possesses a pair of complementary acceptor-donor-acceptor and donor-donor-acceptor hydrogen bonding arrays at an angle of 120° to each other. The existence of the structure was confirmed by NMR and crystallographic studies.

Rebek and co-workers have condensed two molecules of glycoluril with durene tetrabromide to create a self-complementary unit.[91] This molecule possesses a curved surface due to steric hindrance between the ester groups. Two molecules self-assemble via eight complementary hydrogen bonds creating a 'tennis ball' molecular capsule that can bind methane molecules inside the complex (**Figure 1.36**).[92]

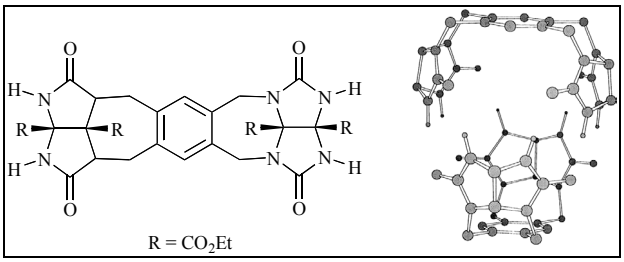

Figure 1.36 *Rebek's monomer and the crystal structure of the 'tennis ball'*
(Hydrogens attached to carbon and glycouril substituents have been omitted for clarity)

Self-replicating molecular systems have been designed to utilise hydrogen bond interactions (**Figure 1.37**).[93]

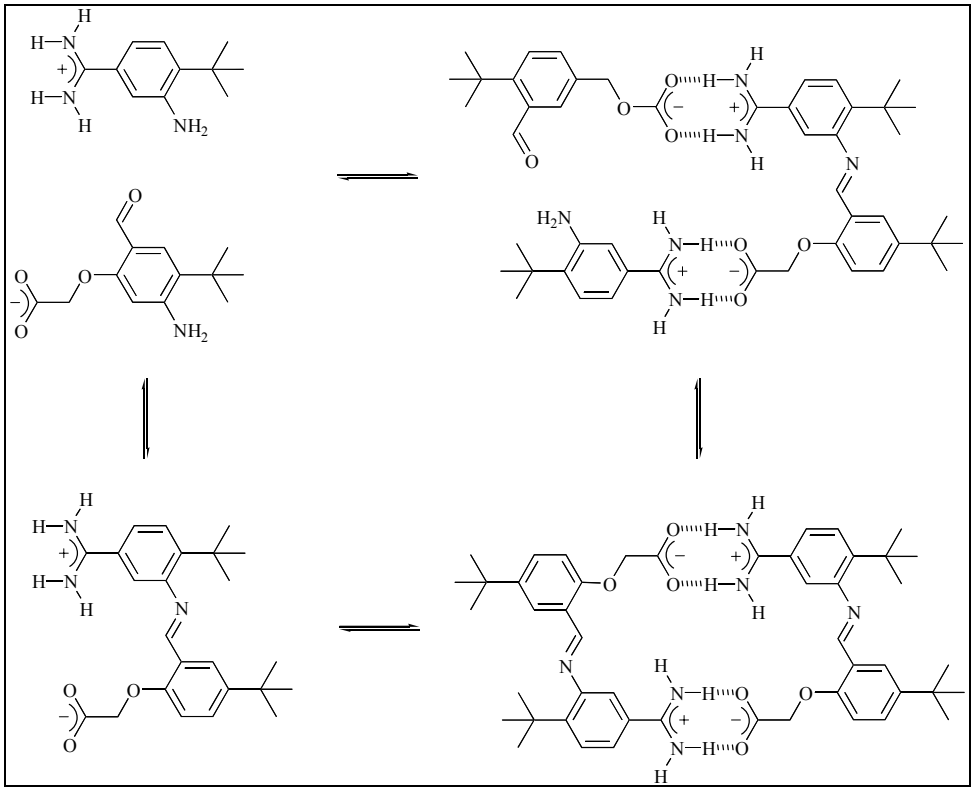

Figure 1.37 A *self-replicating molecular system*

The reaction of 2-formylphenoxyacetate with 3-aminobenzamidinium gives the product imine. This imine possesses a carboxylate and an amidinium group that can complex to the two starting materials. This complex holds the amine and aldehyde groups in close proximity increasing the rate of reaction to form the imine. This system is self-replicating as the product is a catalyst for its own formation (autocatalysis).

5.2 Catenanes and Rotaxanes

The synthesis of a supermolecule that possesses two components that are interlinked but not physically joined is a considerable challenge. [n]Catenanes consist of n interlocked macrocyclic species. Once a catenane has been formed the only way that one ring can be removed is by bond cleavage.

Hunter has prepared a [2]catenane by the reaction of isophthaloyl dichloride with a bis-amine derivative as shown in **Figure 1.38**.[94]

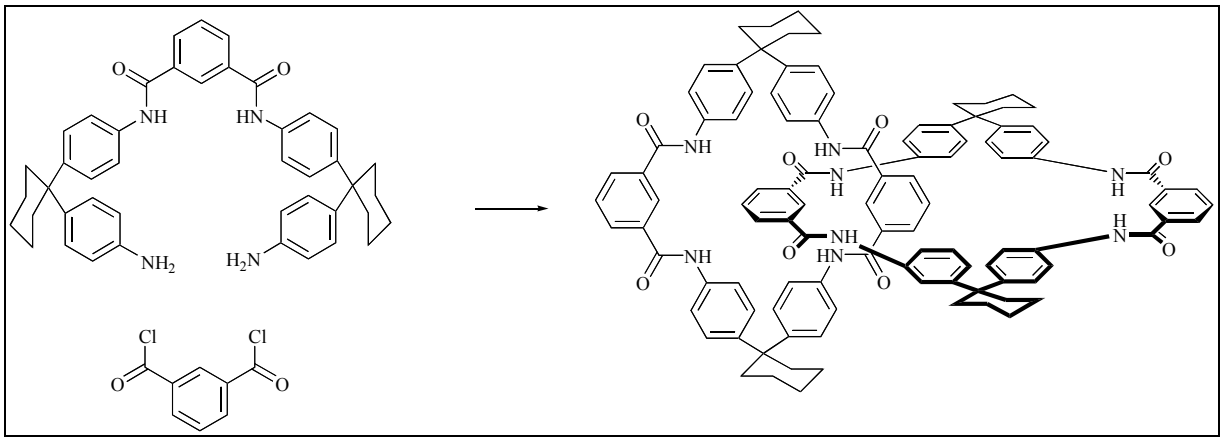

Figure 1.38 *Hunter's [2]catenane*

Hydrogen bonding interactions hold two bis-amide molecules together, perpendicularly to one another, and the reaction of the free amines with the acid chloride forms the macrocyclic structure. The [2]catenane is stabilised by a combination of π-π stacking and hydrogen bonding effects.

Stoddart synthesised a catenane using hydrogen bonding forces and π-π stacking interactions by using bisparaphenylene-[34]crown-10 and a pyridine compound with 1,4-bis(bromomethyl) benzene as shown in **Figure 1.39**.[95]

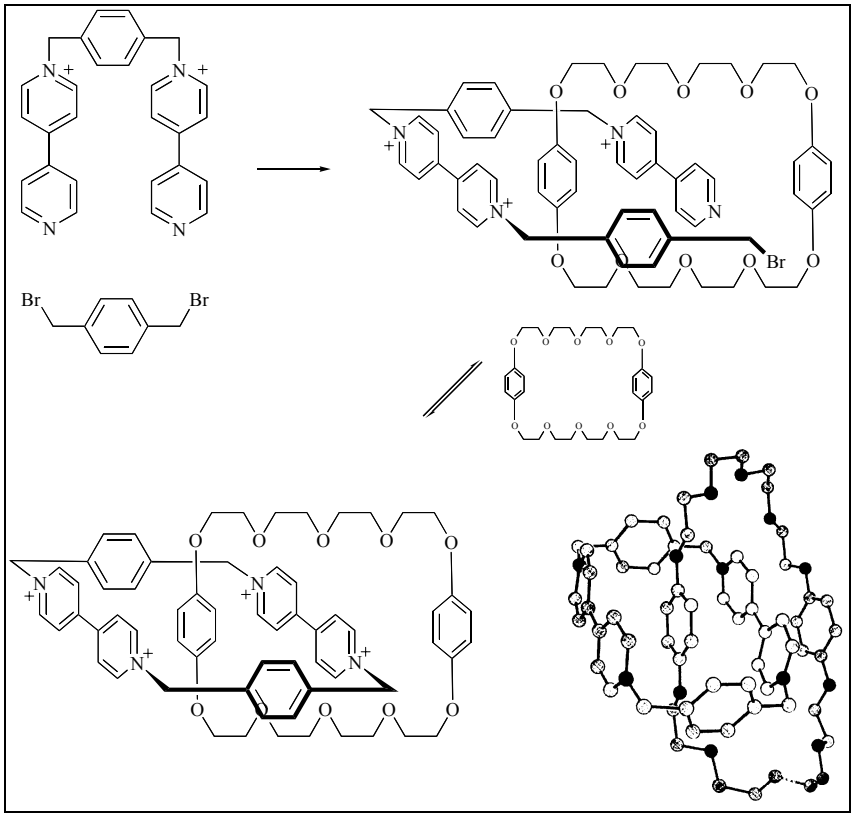

Figure 1.39 *Stoddart's [2]catenane and the crystal structure*

The pyridine nitrogen acts as a nucleophile to create a tricationic strand. This strand threads through the macrocycle forming a complex. This complex is stabilised by π-π stacking interactions between electron rich crown ether macrocycle and the electron poor paraquat cation together with hydrogen bonding interactions between the aromatic hydrogens of the paraquat and the oxygens of the crown ether. This complex is trapped by a ring closing intramolecular nucleophilic attack forming the [2]catenane.

Rotaxanes are composed of a macrocyclic component through which an axle or rod is threaded. The ends of the axle are stoppered with bulky groups that prevent the axle slipping off. Thus the components are permanently joined together but are not linked by a covalent bond.

Three approaches can be taken to form rotaxanes: threading and stoppering, clipping and the use of elevated temperature.

Threading involves mixing the components together and the self-assembly process forms a pseudorotaxane that can then be stoppered to prevent the macrocycle 'falling off'. Clipping uses a pre-stoppered component which self-assembles with the other component and undergoes macrocyclic ring closure.[96] If the stoppers are not too large then at high temperature the macrocycle maybe able to slip over them and form the rotaxane that would persist when the temperature is lowered again.[97]

Stoddart reported the assembly of rotaxanes by a 'threading followed by stoppering' approach (**Figure 1.40**).[98]

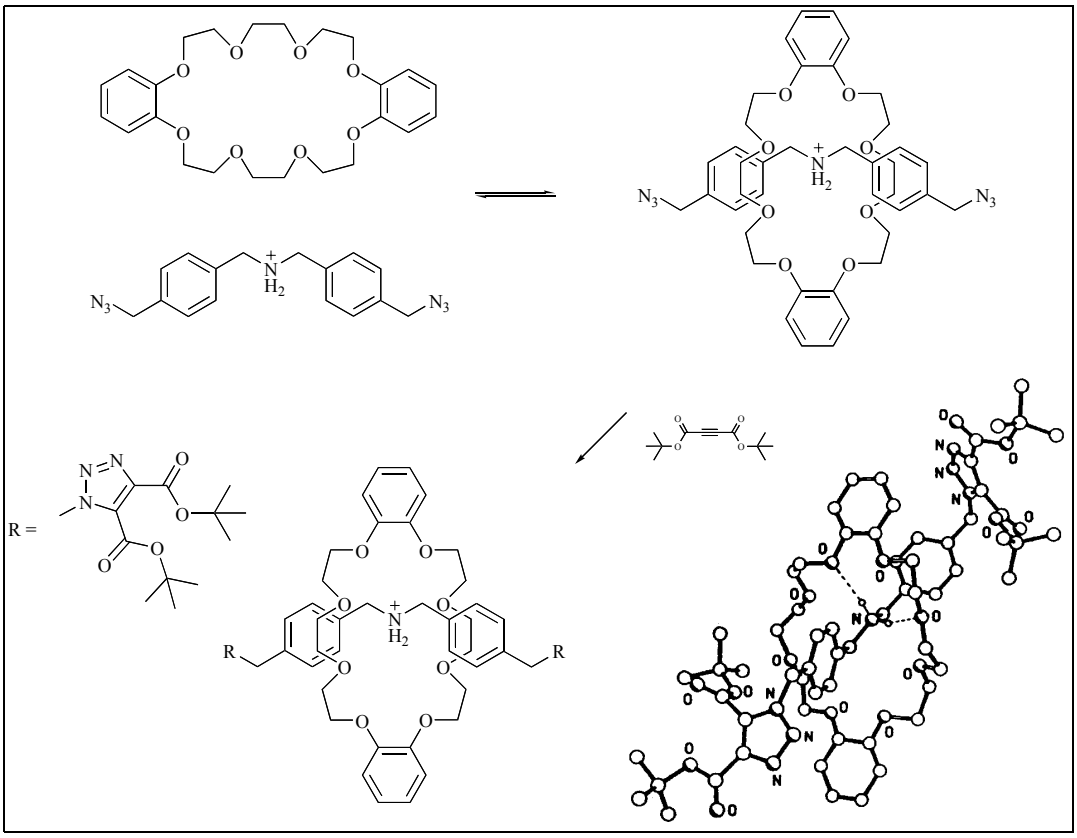

Figure 1.40 *Stoddart's [2]rotaxane and the crystal structure*

The threading of the dialkyl ammonium ion is favoured by a combination of electrostatic and hydrogen bond forces. Once threaded, the azide groups can react with the stoppers to complete the rotaxane formation. The crystal structure revealed favourable π-π stacking interactions and hydrogen bonds between the protonated amine and oxygen atoms.

5.3 Metal Directed Self-Assembly

Metal directed self-assembly is particularly relevant to this thesis as all the new transition metal receptors that have been made relied upon this process for their formation. In addition, metal ions provide a range of coordination geometries, binding strengths/labilities and photochemical/redox properties that can be exploited. Self-assembly proceeds under thermodynamic conditions, is highly convergent and generally requires fewer steps than covalent synthesis.[99] The resulting species often exhibit remarkable structures and properties as illustrated in the following sections.

5.3.1 Double and Triple Helices

Classical synthetic approaches to forming helicates in a step-by-step fashion are very difficult to accomplish due to the difficulty in attaining the required molecular geometry. By means of carefully designed components, geometric constraints maybe overcome by use of metal directed self-assembly giving rise to helicates in high yields.[88a]

Lehn has synthesised a range of polymetallic double helices based on poly-bipyridine strands with ether linkages between each bipyridine subunit. The copper(I) ions enforce a tetrahedral coordination geometry that causes the assembly of the helical structure. Helicates with up to five copper atoms have been synthesised (**Figure 1.41**).[100]

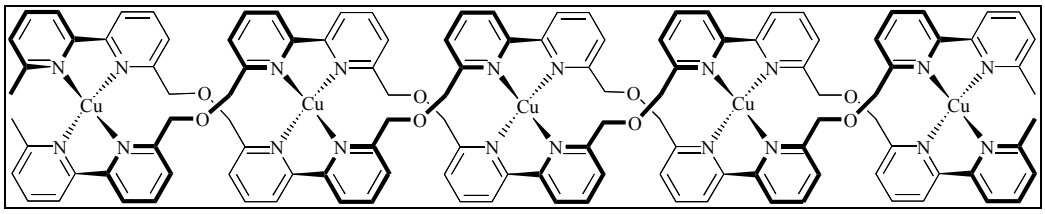

Figure 1.41 *Lehn's pentametallic double helicate*

It was found that if poly-bipyridine strands containing two, three, four and five bipyridine units were mixed together in the presence of copper(I) ions, only helices containing strands of the same length formed. This is known as 'self-recognition'.[101]

The benzimidazole-pyridine ligand shown in **Figure 1.42** forms different kinds of helicates depending upon the metal ion used.[102] The rigid strand enforces the formation of dimetallic complexes and the nitrogen atoms provide metal ion binding sites. The addition of copper(I) ions produces a double helical structure whereas addition of cobalt(II) causes the self-assembly of a triple helicate. Thus, the metal ion controls the structure of the self-assembled product.

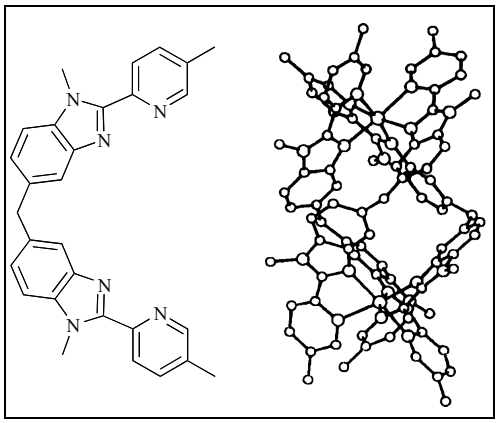

Figure 1.42 *Benzimidazole-pyridine ligand and the crystal structure of the cobalt triple helix*

In certain supramolecular systems, the addition of a guest species prompts the conversion of one structure to another. For example, Raymond reported the slow conversion of a di-nuclear triple helicate to a tetranuclear tetrahedron upon the addition of tetramethyl ammonium cation (**Figure 1.43**).[103]

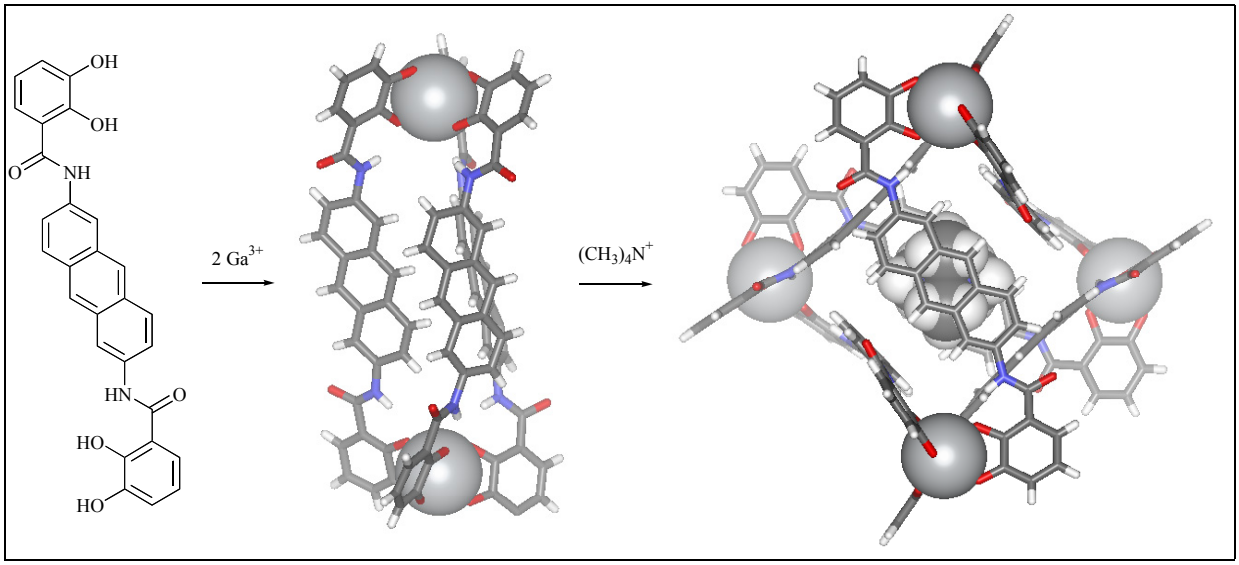

Figure 1.43 *Raymond's triple helicate/tetrahedral interconversion controlled by the addition of a tetramethyl ammonium cation*

5.3.2 Knots

A trefoil knot contains one single strand that intertwines itself with three crossing points in such a way that it cannot be unwound.

Sauvage successfully synthesised such a knot by creating a double helical structure using two phenanthroline units and copper(I) ions and then performing a macrocyclisation. When the metal is removed, a single ring that crosses itself in three places is produced (**Figure 1.44**).[104]

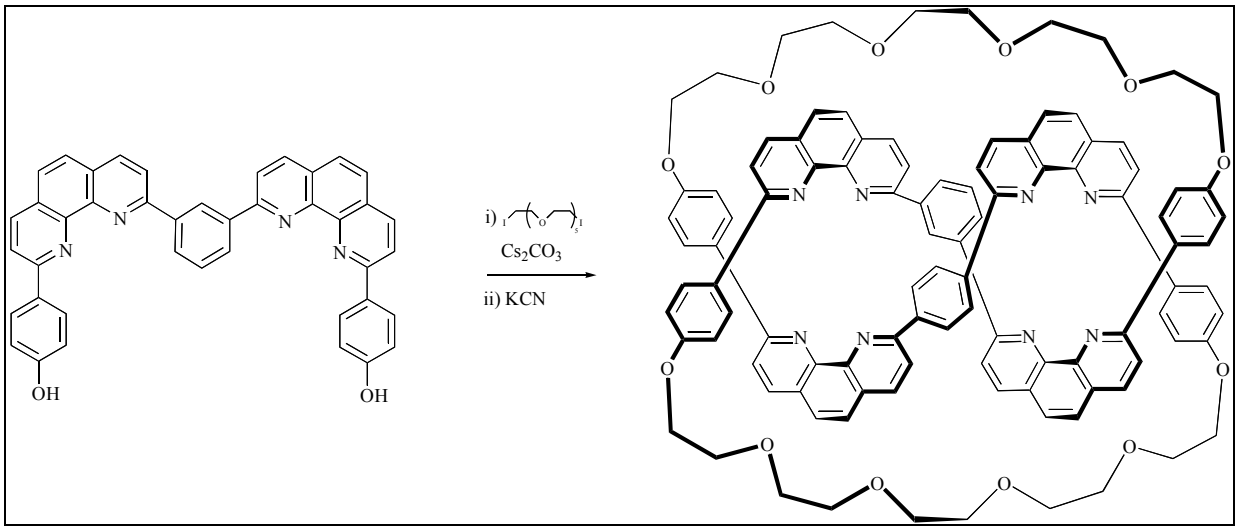

Figure 1.44 *Sauvage's trefoil knot synthesis*

5.3.3 Macrocycles

Research into the self-assembly of macrocycles has produced some novel architectures which have the potential to bind other species within their cavities.

Sanders has used self-assembly to create boxes which contain porphyrin binding sites. Addition of 1,3,5-tris(4-pyridyl)triazene to the dialkyne metalloporphyrin and subsequent copper catalysed coupling of the alkyne groups formed the trimeric macrocycle shown in **Figure 1.45**.[105]

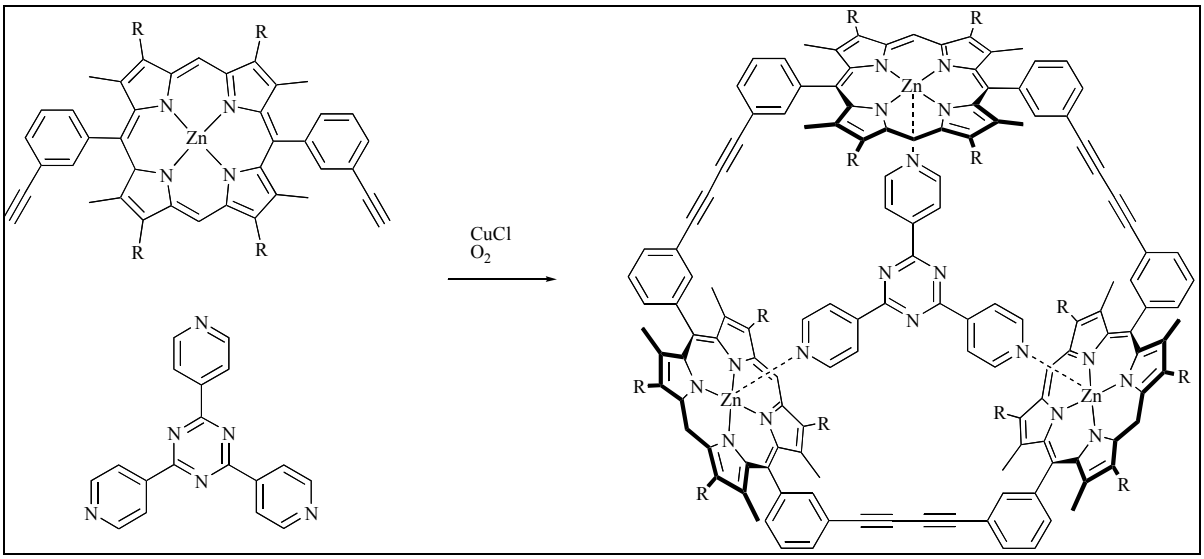

Figure 1.45 *Sander's metal assisted synthesis of a triporphyrin box*

When the triazene compound was replaced with di-coordinating 4,4'-bipyridine the dimeric capsule was predominantly formed. This indicated that the pyridine molecule was coordinating to the metal ions and templating the formation of a macrocycle. The trimeric

molecule has been used as a molecular reaction vessel with Diels-Alder reactions being catalysed within the central cavity.[106]

Hupp synthesised a tetranuclear metallomacrocycle which contains both rhenium and cationic palladium centres (**Figure 1.46**).[107]

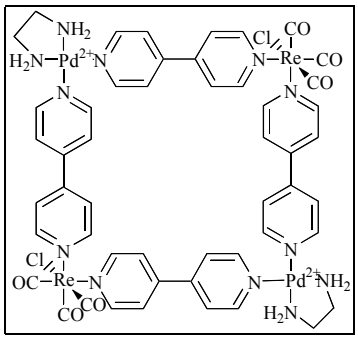

Figure 1.46 *Hupp's metallomacrocycle*

Addition of perchlorate anion increased the luminescence intensity, presumably by inclusion of the anion in the molecular cavity. This demonstrates the possible exploitation of metallocyclophanes in developing molecular sensing devices.

5.3.4 Locked and Unlocked Boxes

The lability of a metal ion can determine whether a molecular box is 'locked' or 'unlocked'. For example the palladium(II) cation has been used in the assembly of a number of boxes using the metal's square planar geometry to create 90° angles at the corners of the macrocycle. Upon mixing the a pyridyl ligand with the palladium(II) salt shown in **Figure 1.47** a mixture of [2]catenane and macrocycle was produced.[108]

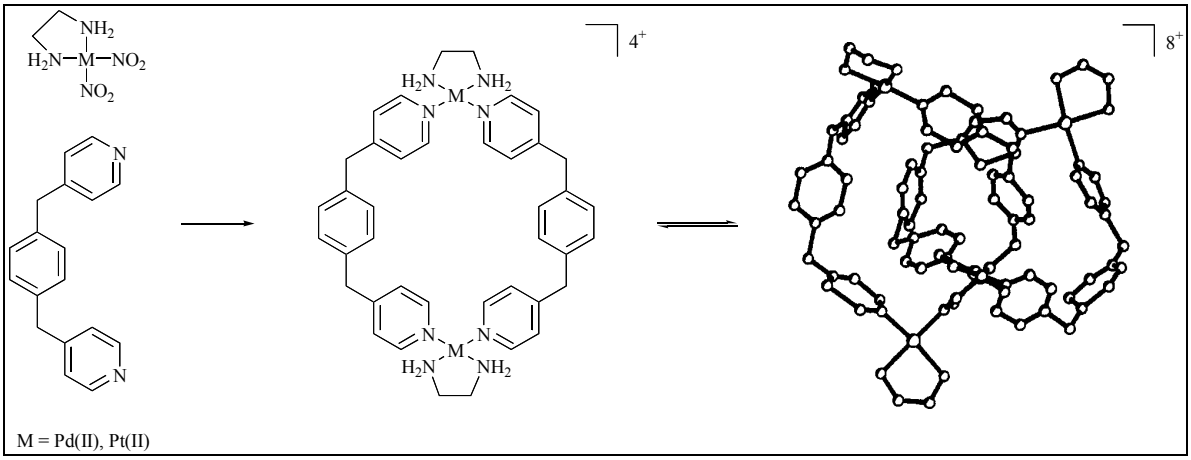

Figure 1.47 *Fujita's macrocycle:[2]catenane equilibrium and the crystal structure of the platinum(II) [2]catenane*

The nitrogen-palladium bonds are relatively labile and so equilibrium exists between the two products. At low concentration the macrocycle predominates whereas at high concentration the [2]catenane is the dominant product. In contrast, analogous systems containing platinum(II) are not labile under usual conditions and maybe isolated as discrete entities.[109] When very polar solvents are used together with high temperatures the [2]catenane assembles and upon cooling it can be isolated.

With the careful design of pyridine-based ligands and use of palladium(II) salts, a whole range of structures such as octahedrons, cones, tetrahedrons and hexadrons have been reported and their molecular recognition properties studied.[110]

5.3.5 Racks, Ladders and Grids

Metal-directed assembly allows the formation of complex molecular architectures such as racks, ladders and grids.

A rack is formed when the tris-bipyridine strand is mixed with the 1,10-phenanthroline crown ether in the presence of copper(I) ions. This rack is actually a psuedo-rotaxane with three macrocycles bound to a central axle via three metal ions (**Figure 1.48**).[111]

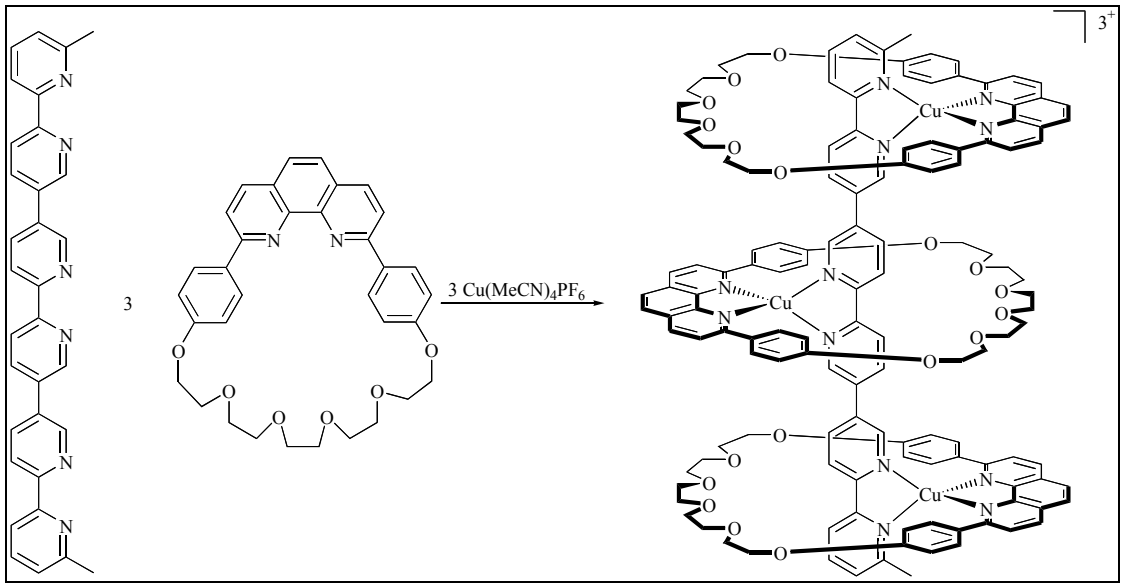

Figure 1.48 *Lehn's trimetallic molecular rack*

When the same bipyridine axle is added to six copper(I) ions and three bispyrimidine units a molecular ladder is formed (**Figure 1.49**).[112] NMR and UV/visible spectroscopy experiments confirmed the structure.

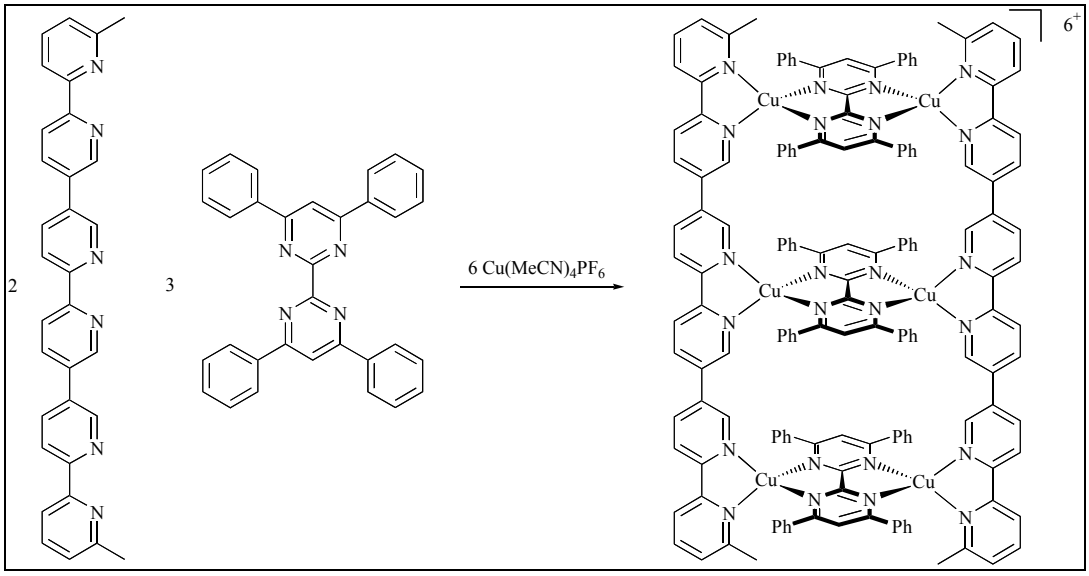

Figure 1.49 *Lehn's molecular rack*

A molecular grid was produced by Lehn by mixing four tridentate terpyridine strands with four lead(II) ions (**Figure 1.50**).[113]

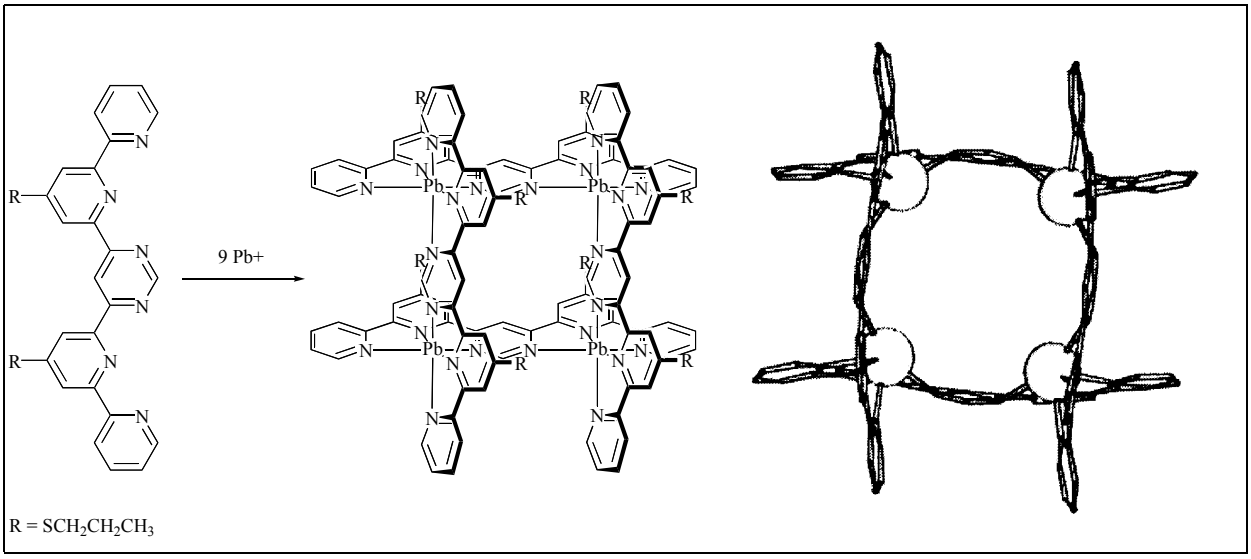

Figure 1.50 *Lehn's tetrametallic molecular grid and the crystal structure*

The structure was confirmed NMR spectrospcopy and a crystal structure. This kind of structure maybe of potential interest in molecular electronics.

5.3.6 Self-Assembly Templated by Anions

The role of anions in promoting self-assembly via templation has only recently begun to be recognised. Many of the examples reported to date were discovered by serendipity.

Lehn reported the most striking example of anion templation.[114] When a tris bipyridine ligand is added to an equimolar amount of iron(II) chloride initially a trimetallic triple helicate is formed, the kinetic product. However, upon thermodynamic equilibration a transformation occurs giving a pentametallic circular helicate (**Figure 1.51**).

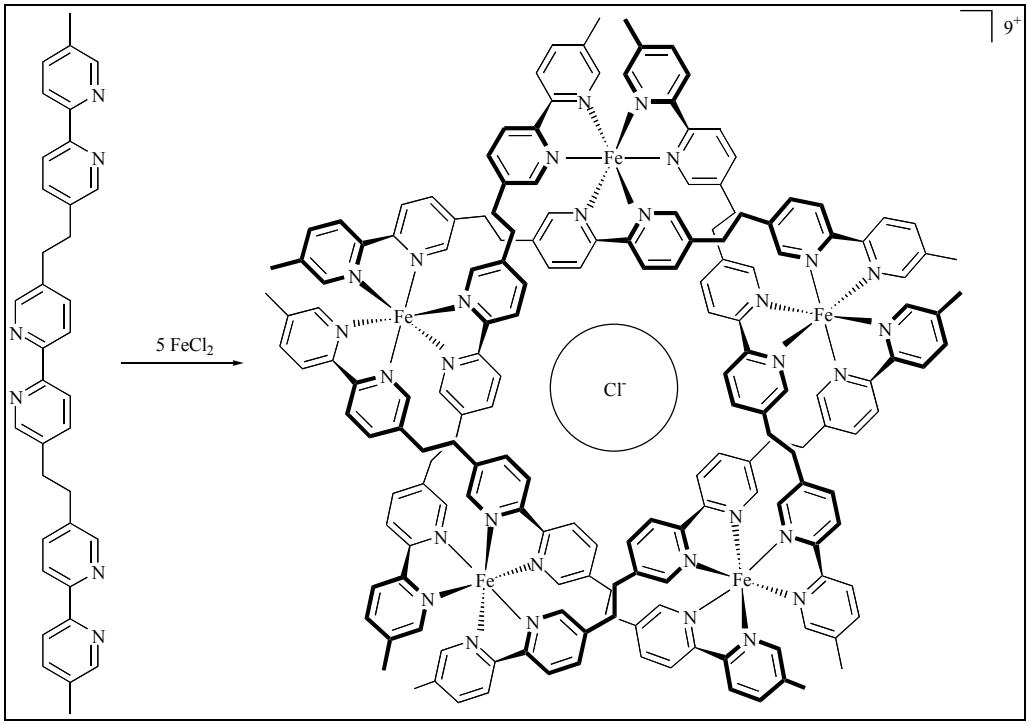

Figure 1.51 *Lehn's circular double helicate formed around a chloride ion*

The bound chloride cannot be exchanged for another anion such as hexafluorophosphate or triflate demonstrating the selectivity the helicate possesses for chloride anion.[115] When the reaction was carried out using iron(II) tetrafluoroborate the pentametallic structure does not form, but rather a hexameric complex is produced.

Mingos used a Lewis acidic metal centre in conjunction with hydrogen bonding interactions to form a cage complex templated around an anion. Addition of nickel(II) chloride to amidinothiourea in methanol yielded a cage-like molecule (**Figure 1.52**).[116] The crystal structure revealed that a chloride anion was bound inside the complex.

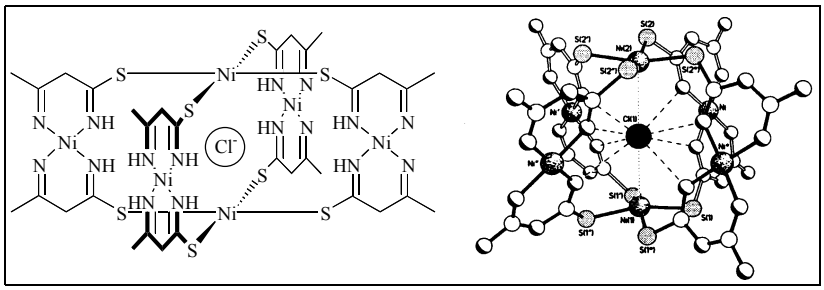

Figure 1.52 *Mingos's amidinothiourea-nickel(II) cage complex and the crystal structure of the chloride complex*

6 Aims of the Project

The aim of this thesis is to investigate the metal directed self-assembly of transition metal based dithiocarbamate receptors which are designed to bind anions, cations or ion pairs.

The host structures are based upon transition metal dithiocarbamate receptors that have been functionalised by a variety of ion binding groups. Anion receptors contain amide or thiourea groups adjacent to the dithiocarbamate linkage, cation receptors have crown ether or aromatic groups and ion pair receptors incorporate both crown ether and amide groups near the transition metal dithiocarbamate. Depending on the transition metal employed, a variety of spectroscopic properties are imparted upon the receptor molecules that can be exploited to monitor guest binding.

Chapter 2 centres on novel types of acyclic anion, cation and ion pair receptors. Guest binding is monitored using NMR and UV/visible spectroscopies, electrochemical techniques and electrospray mass spectrometry.

Chapter 3 described the synthesis of new macrocyclic structures for anion binding. Anion binding is investigated by a variety of techniques including NMR, UV/visible, electrochemistry, magnetism, electron paramagnetic resonance and electrospray mass spectrometry.

Chapter 4 outlines the formation of a range of macrocyclic molecules which contain pyridyl or phenol moieties. The receptor's cation binding ability is assessed using electrospray mass spectrometry and bulk liquid membrane experiments.

Chapter 5 explores two types of macrobicyclic cryptand-like anion receptors. The first type of receptor are synthesised by either changing oxidation state of the transition metal or by using an octahedral metal centre. A second type of cryptand-like anion receptor is synthesised by using a tripodal based ligand. Electrochemical, magnetic and UV/visible techniques are used to assess anion binding.

7 References

[1] J. M. Lehn, *Angew. Chem., Int. Ed. Engl*, 1989, **27**, 89.
[2] E. Fischer, *Ber. Dtsch. Chem. Ger.*, 1894, **27**, 79.
[3] L. Stryer, *Biochemistry*, 4th Edition, W.H. Freeman and Co., 1979.
[4] P. W. Atkins, *Physical Chemistry*, 4th Edition, Oxford University Press, 1990, 938.
[5] P. W. Atkins, *Physical Chemistry*, 4th Edition, Oxford University Press, 1990, 656.
[6] H. J. Schneider, *Angew. Chem., Int. Ed. Engl.*, 1991, **30**, 1417.
[7] H. J. Schneider, D. Guttes, W. Schneider, *J. Am. Chem. Soc.*, 1998, **110**, 6449.
[8] S. K. Chang, D. Van Engen, E. Fan, A. D. Hamilton, *J. Am. Chem. Soc.*, 1991, **113**, 7640.
[9] T. W. Bell, Z. Hou, *Angew. Chem., Int. Ed. Engl.*; 1997; **36**, 1536.
[10] C. Hunter, J. K. M. Sanders, *J. Am. Chem. Soc.*, 1994, **112**, 5525.
[11] P. A. Brooksby, C. A. Hunter, A. J. McQuillan, D. H. Purvis, A. E. Rowan, R. J. Shannon, *Angew. Chem., Int. Ed. Engl.*, 1994, **33**, 2489.
[12] P. W. Atkins, *Physical Chemistry*, 4th Edition, Oxford University Press, 659.
[13] J. Canceill, M. Cesario, A. Collet, J. Guilhem, L. Lucombe, C. Pascard, *Angew. Chem., Int. Ed. Engl.*, 1991, **30**, 1417.
[14] F. Dietrich, *Cyclophanes*, RSC, UK, 1991.
[15] A. E. Martell, *Advances in Chemistry No. 62*, 1967, 272.
[16] G. Scwarzenbach, *Helv. Chim. Acta*, 1952, **35**, 2344.
[17] J. J. R. F de Silva, *J. Chem. Edu.*, 1983, **60**, 390.
[18] D. K. Cabbiness, D. W. Margerum, *J. Am. Chem. Soc.*,1969, **91**, 6540.
[19] a) T. D. James, C. J. Ward, *J. Chem. Soc. Perkin Trans. 1*, 2000, 3155; b) B. Dietrich, *Inclusion Compounds*, Academic Press, 1984, 337; c) D. J. Cram, K. N. Trueblood, D. J. Cram, K. N. Trueblood, *Top. Curr. Chem.*, 1981, **98**, 43.
[20] J. F. Desreux, P. P. Barthelemy, *Nucl. Med. Biol.*, 1988, **15**, 9.
[21] C. J. Pedersen, *Angew. Chem., Int. Ed. Engl.*, 1988, **27**, 1021.
[22] W. R. Davidson, P. Kebarle, *J. Am. Chem. Soc.*, 1976, **98**, 6133.
[23] H. K. Frenksdorff, *J. Am. Chem. Soc.*, 1971, **93**, 600.
[24] P. R. Mallinson, M. R. Truter, *J. Chem. Soc. Perkin Trans. 2*, 1972, **12**, 1818.
[25] D. E. Fenton, M. Merce, N. S. Poonia, M. R. Truter, *Chem. Commun.*, 1972, 66.
[26] S. Ahrland, J Chatt, N.R Davis, *Quart. Rev.*, 1958, **12**, 265.
[27] J. W. Steed, J. Atwood, *Supramolecular Chemistry*, Wiley, 2000.
[28] D. J. Cram, K. N. Trueblood, D. J. Cram, K. N. Trueblood, *Top. Curr. Chem.*, 1981, **98**, 43
[29] J. M. Tinker, S. S. Moore, D. M. Walba, D. C. Hiberty, D. J. Cram, *J. Am. Chem. Soc.*, 1977, **99**, 4207.
[30] R. A. Schultz, D. M. Dishong, G. W. Gokel, *J. Am. Chem. Soc.*, 1982, **104**, 625.
[31] B. Dietrich, J. M. Lehn, J. P. Sauvage, *Tetrahedron Lett.*, 1969, 2885.
[32] J. M. Lehn, *Pure & Appl. Chem.*, 1978, **50**, 871.
[33] J. M. Lehn, *Pure & Appl. Chem.*, 1977, **49**, 857.
[34] E. Kauffmann, J. M. Lehn, J. P. Sauvage, *Helv. Chim. Acta*, 1976, **59**, 1099.
[35] K. N. Trueblood, C. B. Knobler, E. Maverick, R. C. Helgeson, S. B. Brown, D. J. Cram, *J. Am. Chem. Soc.*, 1981, **103**, 5594.
[36] D. J. Cram, G. M. Lehn, *J. Am. Chem. Soc.*, 1985, **107**, 3657.
[37] D. J. Cram, *Angew. Chem., Int. Ed. Engl.*, 1988, **27**, 1009.
[38] B. Dietrich, *Inclusion Compounds*, 1984, **2**, 387.
[39] a) D. M. Roundhill, H. F. Koch, *Chem. Soc. Rev.*, 2002, **31**, 60; b) R. J. Fitzmaurice, G. M. Kyne, D. Douheret, J. K Kilburn, *J. Chem. Soc. Perkin Trans. 1*, 2002, 841; c) P. D. Beer, P. A. Gale, *Angew. Chem., Int. Ed. Engl.*, 2001, **40**, 486; d) J. H. Hartley, T. D. James, C. J. Ward, *J. Chem. Soc. Perkin Trans. 1*, 2000, 3155; e) M. M. G. Antonisse, P. D. Beer, J. Cadman, *Coord. Chem. Rev.*, 2000, **205**, 131; f) L. Fabbrizzi, M. Licchelli, G. Rabaioli, A. Taglietti, *Coord. Chem. Rev.*, 2000, **205**, 85; g) T. S. Snowden, E. V. Ansyln, *Curr. Opin. Chem. Bio.*, 1999, 740;

h) P. A. Gale, *Coord. Chem. Rev.*, 2000, **199**, 181; i) D. N. Reinhoudt, *Chem. Commun.*, 1998, 443, 3155, 841; j) P. D. Beer, *Acc. Chem. Res.*, 1998, **31**, 2, 71; k) B. Dietrich, *Pure & Appl. Chem.*, 1993, **76**, 1457.
[40] L. G. Lange, J. F. Riordan, B. L. Vallee, *Biochemistry*, 1974, **13**, 4361.
[41] P. M. Quinton, *FASEB*, 1990, **4**, 2710.
[42] P. D. Beer, D. K. Smith, *Prog. Inorg. Chem.*, 1997, **46**, 1.
[43] C. F. Mason, Biology of Freshwater Pollution, 2nd Ed, Longman, 1991.
[44] K. Schwochau, *Technetium: Chemistry and Radiopharmaceutical Applications*, Wiley, 2000, Chapter 3.
[45] C. S. G. Phillips, R. J. P. Williams, Inorganic Chemistry, Volume 2, OUP, 1965.
[46] P. D. Beer, *Chemical Sensors*, Blackie, 1987, 50.
[47] F. Hofmeister, *Arch. Ex. Pathol. Pharmakol.*, 1988, **24**, 247.
[48] S. Goldman, R. G. Bates, *J. Am. Chem. Soc.*, 1972, **94**, 1476.
[49] L. Radom, *J. Chem.*, 1976, **29**, 1635.
[50] S. Mangani, M. Ferraroni, *Supramoelcular Chemistry of Anions*, A. Bianchi, K. Bowman-James, E. Garcia-Espana, Wiley-VCH, 1997, 63.
[51] R. Dutzler, E. B. Campbell, M. Cadene, B. T. Chait, R. MacKinnon, *Nature*, 2002, **415**, 287.
[52] C. H. Park, H. E. Simmons, *J. Am. Chem. Soc.*, 1968, **90**, 2429.
[53] B. Dietrich, M. W. Hoisseini, J. M. Lehn, R. B. Sessions, *J. Am. Chem. Soc.*, 1981, **103**, 1282.
[54] M. W. Hosseini, J. M. Lehn, *Helv. Chim. Acta*, 1986, **69**, 587.
[55] J. L. Sessler, M. Cyr, H. Futura, V. Kral, T. Mody, T. Morishima, M. Shionoya, S. J. Weyhan, *Pure Appl. Chem.*, 1993, **65**, 393.
[56] V. Kral, J. L. Sessler, H. Furuta, *J. Am. Chem. Soc.,* 1992, **114**, 8704.
[57] B. Dietrich, D. L. Fyles, T. M. Fyles, J. M. Lehn, *Helv. Chim. Acta*, 1979, **62**, 2763.
[58] F. P. Schmidtchen, *Tetrahedron Lett.*, 1989, **30**, 4493.
[59] A. Echavarren, A. Galan, J. M . Lehn, J. D. Mendoza, *J. Am. Chem. Soc.*, 1989, **111**, 4994.
[60] K. Worm, F. P. Schmidtchen, A. Schieter, A. Schafer, M. Hesse. *Angew. Chem., Int. Ed. Engl.*, 1994, **33**, 327.
[61] F. P. Schmidtchen, *Angew. Chem., Int. Ed. Engl.*, 1977, **16**, 721.
[62] K. Worm, F. D. Schmidtchen, *Angew. Chem., Int. Ed. Engl.*, 1995, **34**, 65.
[63] M. Fernandez-Saiz, H. J. Schneider, J. Sartorius, W. D. Wilson, *J. Am. Chem. Soc.*, 1996, **118**, 4739.
[64] J. W. Steed, R. K. Juneja, J. L. Atwood, 1994, *Angew. Chem., Int. Ed. Engl.*, **33**, 2456.
[65] M. Staffilani, K. S. B. Hancock, J. W. Steed, K. T. Holman, J. L. Atwood, R. K. Junela, R. S. Burkhalter, *J. Am. Chem. Soc.*, 1997, **119**, 6324.
[66] R. A. Pascal, J. Spergel, D. V. Engen, *Tetrahedron Lett.*, 1986, **27**, 4099.
[67] A. J. Ayling, S. Broderick, J. P. Clare, A. P. Davis, M. N. Perez-Payan, M. Lahtinen, M. J. Nissinen, K. Rissanen, *Chem. Eur. J.*, 2002, **8**, 2197.
[68] P. Buhlmann, S. Nishizawa, K. P. Xiao, Y. Umezawa, *Tetrahedron*, 1997, **53**, 1647.
[69] D. F. Shriver, M. J. Ballis, *J. Am. Chem. Soc.*, 1967, **89**, 1078.
[70] H. E. Katz, *Organometallics*, 1987, **6**, 1134.
[71] M. E. Jung, H. Xia, *Tetrahedron Lett.*, 1988, **29**, 297.
[72] S. Aoyagi, K. Tanaka, Y. Takeachi, *J. Chem. Soc. Perkin Trans. 2*, 1994, 1549.
[73] J. H. Hunter, M. T. Blanda, P. J. Squattrito, *J. Am. Chem. Soc.*, 1989, **111**, 6295.
[74] M. T. Blanda, J. H. Horner, M. Newcomb, *J. Org. Chem.*, 1989, **54**, 4626.
[75] X. Yang, C. B. Knobler, M. F. Hawthorne, *Angew. Chem., Int. Ed. Engl.*, 1991, **30**, 1507.
[76] D. M. Rudkevich, W. Verboom, Z. Brzozka, M. J. Palys, W. P. R.V. Stauthamer, G. J. v. Hummel, S. M. Franken, S. Harkema, J. F. J. Engbersen, D. N. Reinhoudt, *J. Am. Chem. Soc.*, 1994, **116**, 4341.
[77] M. M. G. Antonisse, B. H. M. Snellink-Ruel, I. Yigit, J. F. J. Engersen, D. N. Reinhoudt, *J. Org. Chem.*, 1997, **62**, 9034.
[78] K. Niikura, A. P. Bisson, A. V. Ansyln, *J. Chem. Soc. Perkin Trans. 2*, 1999, 1111.
[79] C. Lee, D. H. Lee, J. I. Hong, *Tetrahedron Lett.*, 2001, **42**, 8665.

[80] P. D. Beer, D. Hesek, J. E. Kingston, D. K. Smith, S. E. Stokes, M. G. B. Drew, *Organometallics*, 1995, **14**, 3288.
[81] P. D. Beer, *Acc. Chem. Res.*, 1998, **31**, 2, 71.
[82] J. I. Bruce, R. S. Dickins, L. J. Govenlock, T. Gunnlaugson, S. Lopinski, M. P. Lowe, D. Parker, R. D. Peacock, J. J. B. Perry, S. Aime, M. Botta, *J. Am. Chem. Soc.*, 2000, **122**, 9674.
[83] J. M. Lehn, S. H. Pine, E. I. Watanabe, A. K. Willant, *J. Am. Chem. Soc.*, 1977, **99**, 6766.
[84] J. M. Lehn, J. Simon, A. Moradpour, *Helv. Chim. Acta*, 1978, **61**, 2407.
[85] M. T. Reetz, C. M. Niemeyer, K. Harms, *Angew. Chem., Int. Ed. Engl.*, 1991, **30**, 1472.
[86] A. Galan, D. Andreu, A. M. Echavarran, P. Prados, J. de Mendoza, *J. Am. Chem. Soc.*, 1992, **114**, 1511.
[87] H. Fraenkel-Conrat, R. C. Williams, *Proc. Natl. Acad. Sci. USA*, 1955, **41**, 690.
[88] a) V. G. Machado, P. N. W. Baxter, J. M. Lehn, *J. Braz. Chem. Soc.*, 2001, **12**, 431; b) M. Fujita, K. Umemoto, M. Yoshizawa, N. Fujita, T. Kusukawa, K. Biradha, *Chem. Commun.*, 2001, 509; c) B. J. Holliday, C. A. Mirkin, *Angew. Chem., Int. Ed. Engl.*, 2001, **40**, 2022, C. J. Jones, *Chem. Soc. Rev.*, 1998, **27**, 289; d) L. J. Prins, D. H. Rienhoudt, P. Timmerman,. *Angew. Chem., Int. Ed. Engl.*, 2001, **40**, 2382; e) D. C. Sherrington, K. A. Taskinen, *Chem. Soc. Rev.*, 2001, **30**, 83.
[89] a) L. J. Prins, D. H. Rienhoudt, P. Timmerman, *Angew. Chem., Int. Ed. Engl.*, 2001, **40**, 2382; b) 2382, D. C. Sherrington, K. A. Taskinen, *Chem. Soc. Rev.*, 2001, **30**, 83.
[90] a) A. Marsh, M. Silvestri, J. M. Lehn, *Chem. Commun.*, 1996, 1527; b) M. Mascal, N. M. Hext, R. Warmuth, W. H. Moore, J. P. Turkenburg, *Angew. Chem., Int. Ed. Engl.*, 1996, **35**, 2204.
[91] C. Valdes, U. P. Spitz, L. Toledo, S. Kubik, J. Rebek Jr., *J. Am. Chem. Soc.*, 1995, **117**, 12733.
[92] N. Branda, R. Wyler, J. Rebek Jr., *Science*, 1994, **263**, 1267.
[93] A. Terfort, G. von Kiedrowski, *Angew. Chem., Int. Ed. Engl.*, 1992, **104**, 654.
[94] F. J. Carver, C. A. Hunter, R. J. Shannon, *Chem. Commun.*, 1992, 1277.
[95] P. R. Ashton, T. T. Goodnow, A. E. Kaifer, M. V. Reddington, A. M. Z. Slawin, N. Spencer, J. F. Stoddart, C. Vincent, D. J. Williams, *Angew. Chem., Int. Ed. Engl.*, 1989, **28**, 1396.
[96] P. T. Glink, A. I. Oliva, J. F. Stoddart, A. J. P. White, D. J. Williams, *Angew. Chem., Int. Ed. Engl.*, 2001, **40**, 1870.
[97] F. M. Raymo, K. N. Houk, J. F. Stoddart, *J. Am. Chem. Soc.*, 1998, **120**, 9318.
[98] P. R. Ashton, E. J. T. Chrystal, P.T. Glink, S. Menzer, C. Schiavo, N. Spencer, J. F. Stoddart, P. A. Tasker, A. J. P. White, D. J. Williams, *Chem. Eur. J.*, 1996, **2**, 729.
[99] S. Leininger, B. Olenyuk, P. J. Stang, *Chem. Rev.*, 2000, 853.
[100] J. M. Lehn, A. Rigault, *Angew. Chem., Int. Ed. Engl.*, 1988, **27**, 1095.
[101] R. Kramer, J. M. Lehn, A. Marquis-Rigault, *Proc. Nat. Acad. Sci. USA*, 1993, **90**, 5394.
[102] C. Piguet, G. Bernardelli, B. Bocquet, A. Quattropani, A. F. Williams, *J. Am. Chem. Soc.*, 1992, **114**, 7440.
[103] M. Scherer, D. L. Caulder, D. W. Johnson, K. N. Raymond, *Angew. Chem., Int. Ed. Engl.*, 1999, **38**, 1588.
[104] J. F. Dietrichbuchecker, J. F. Nierengerten, J. P. Sauvage, N. Armaroli, V. Balzani, L. Decola, *J. Am. Chem. Soc.*, 1993, **115**, 11237.
[105] A. Vidal-Ferran, N. Bampos, J. K. M. Sanders, *Inorg. Chem.*, 1997, **36**, 6117.
[106] M. Marty, Z. Clyde-Watson, L. J. Twyman, M. Nakash, J. K. M. Sanders, *Chem. Commun.*, 1998, **20**, 2265.
[107] R. V. Sloane, D. I. Yoon, R. M. Calhoun, J. T Hupp, *J. Am. Chem. Soc.*, 1995, **117**, 11813.
[108] M. Fujita, F. Ibukuro, H. Seki, O. Kamo, M. Imanari, K. Ogura, *J. Am. Chem. Soc.*, 1996, **118**, 899.
[109] M. Fujita, F. Ibukuro, K. Yamaguchi, K. Ogura, *J. Am. Chem. Soc.*, 1995, **117**, 4175.
[110] M. Fujita, K. Umemoto, M. Yoshizawa, N. Fujita, T. Kusukawa, K. Biradha, *Chem. Commun.*, 2001, 509.
[111] P. N. Baxter, H. Sleiman, J. M. Lehn, K. Rissanen, *Angew. Chem., Int. Ed. Engl.*, 1997, **36**, 1294.
[112] P. N. Baxter, G. S. Hanan, J. M.Lehn, *Chem. Commun.*, 1996, **17**, 2019.

[113] A. M. Garcia, F. J. Romero-Salguero, D. M. Bassani, J. M. Lehn, G. Baum, D. Fenske, *Chem. Eur. J.*, 1999, **5**, 1803.
[114] B. Hasenkopf, J. M. Lehn, N. Boumediene, E. Leize, A. Van Dorsselaer, *Angew. Chem., Int. Ed. Engl.*, **37**, 3265.
[115] B. Hasenkopf, J. M. Lehn, B. O. Kneisel, D. Fenske, *J. Am. Chem. Soc.*, 1997, **45**, 10956.
[116] R. Vilar, D. M. P. Mingos, A. J. P. White, D. J. Williams, *Angew. Chem., Int. Ed. Engl.*, 1998, **37**, 1258.

Chapter Two

Acyclic Anion, Cation and Ion Pair Dithiocarbamate Receptors

1 Introduction

Self-assembly offers several advantages over traditional covalent synthesis.[1] It is an efficient process generally resulting in high yields of the desired product, which is frequently a large structure made up from a small number of subunits. As self-assembly regularly occurs under equilibrium control reorganisation of the components can occur allowing the final product to be the thermodynamic minimum for that system. Furthermore, error checking is possible as the interactions are non-covalent and reversible, allowing defective subunits to be rejected. There are several types of non-covalent interactions that are used in self-assembly and examples of these have been discussed in **Chapter 1 Section 5**.

There are many reports of metal directed self-assembly of structures which use either polypyridine based ligands with transition metals such as palladium(II) or platinum(II),[2] or catechol ligands with gallium(III) or iron(III) ions.[3] However, the use of other ligands has been less common. The dithiocarbamate ligand's coordination chemistry has been extensively investigated[4] but not fully exploited in the field of self-assembly. *N*-substituted dithiocarbamates can be prepared simply by reacting a primary or secondary amine with carbon disulphide in the presence of a base. Subsequent reaction of the dithiocarbamate salt with a transition metal yields the dithiocarbamate complex. The dithiocarbamate group is an attractive unit for self-assembly as it forms complexes with a vast array of metal ions and can stabilise metals in high oxidation states, e.g. copper(III) and nickel(IV). Therefore, by the careful design of a multidentate ligand and the stereochemical requirements of a particular metal ion, a self-assembled structure may result that possesses unique electronic/magnetic properties and may have the potential to bind guest substrates. Despite these appealing features, it is only recently that the dithiocarbamate moiety has been used in self-assembly.

Beer and co-workers have reported the remarkable formation of a nano-dimensional molecular loop and tetrahedron by the reaction of a tetrakis-functionalised dithiocarbamate

resorcarene ligand with zinc(II)[5] (**Figure 2.1**) and copper(II) ions respectively.[6] Thus, the polymetallic structure was controlled by the nature of the transition metal ion employed.

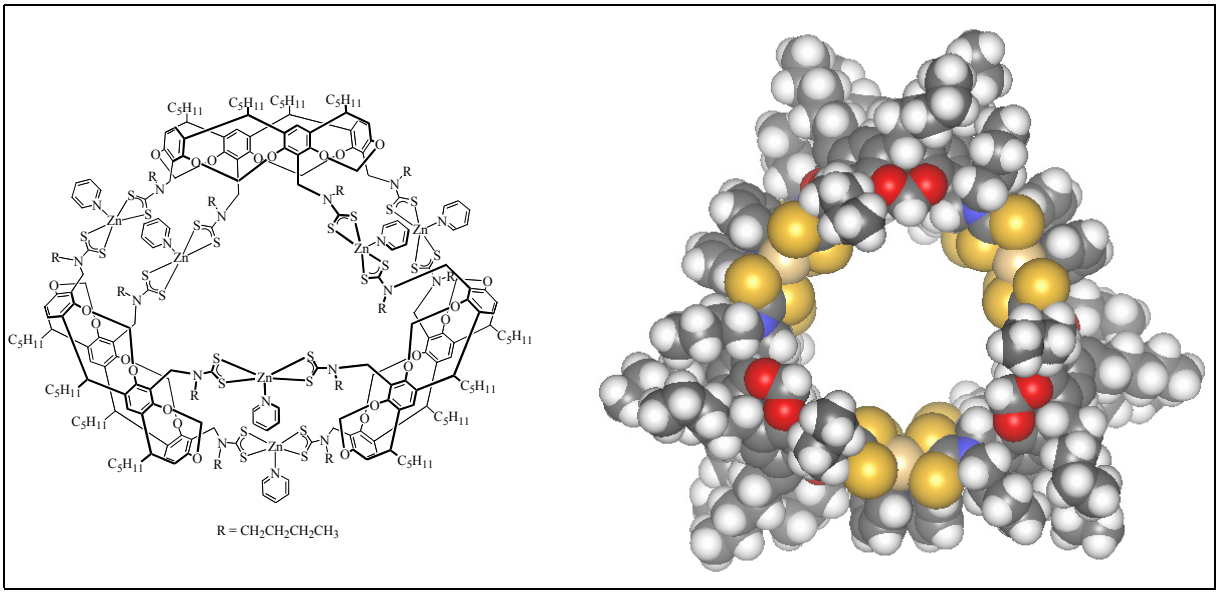

Figure 2.1 *Beer's dithiocarbamate-resorcarene molecular loop and the crystal structure*

UV/visible studies revealed that the molecular loop bound C_{60} very strongly in benzene or toluene solution. Molecular modelling of C_{60} inside the cavity revealed a possible mode of binding involved charge donation from the sulphur atoms of the dithiocarbamate linkages to the electron deficient C_{60}.

Dithiocarbamates ligands have also been utilised by Beer to construct a metal directed self-assembled redox active macrocycle (**Figure 2.2**).[7]

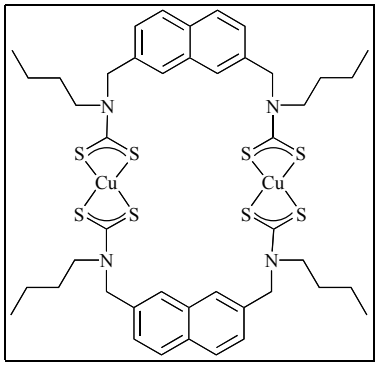

Figure 2.2 *Beer's redox active receptor for dihydrogen phosphate and perrhenate anions*

The dinuclear copper(II) dithiocarbamate based macrocycle shown in **Figure 2.2** displayed selective electrochemical recognition of perrhennate and dihydrogen phosphate anions over chloride, bromide and nitrate anions. This was presumably due to the larger tetrahedral anions possessing a better size complementarity for the molecular cavity.

In an effort to construct new types of redox active receptors for the recognition of charged species, this chapter describes the metal directed self-assembly and characterisation of novel acyclic transition metal dithiocarbamate based receptors. A schematic of the receptors' design is shown in **Figure 2.3.**

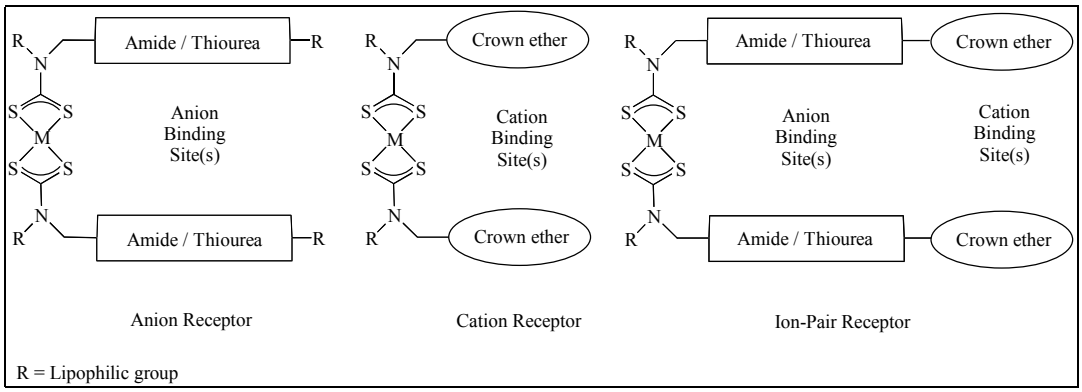

Figure 2.3 *Schematic of target receptors*

The target receptors contain recognition sites for binding anions, cations or both charged species simultaneously, whilst the transition metal dithiocarbamate centre can be used as a spectroscopic/electrochemical probe to monitor guest binding.

The target anion receptors contain either amide or thiourea groups, capable of forming hydrogen bonds with the negatively charged guest species (see **Chapter 1 Sections 3.4** and **3.6**). The cation receptors contain crown ether groups, which can bind strongly to alkali metal cations (see **Chapter 1 Section 2.2**). Ion-pair receptors contain both anion and cation binding groups (see **Chapter 1 Section 4**).

2 Amide Dithiocarbamate Anion Receptors

The following sections detail the synthesis and characterisation of a new type of anion receptor. The synthesis has incorporated two amide functionalities into the structure of self-assembled acyclic transition metal dithiocarbamate receptors.

2.1 Synthesis and Characterisation

In order to prepare the target receptors, a secondary amine moiety covalently linked to a secondary amide group had to be synthesised The amide intermediate **2** (2-benzylamino-*N*-hexylacetamide hydrochloride) was prepared in two steps as shown in **Scheme 2.1**.

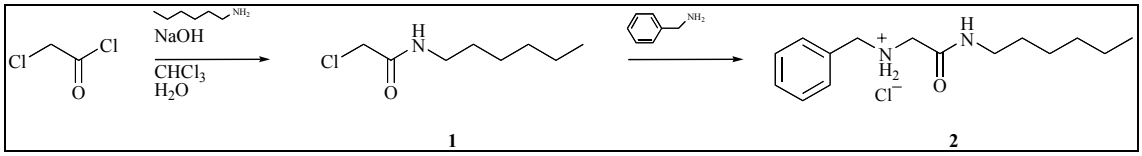

Scheme 2.1 *Synthesis of 2-benzylamino-N-hexylacetamide*

2-Chloro-*N*-hexyl-acetamide **1** was synthesised in 87% yield according to a literature route[8] using chloroacetyl chloride, hexylamine and aqueous sodium hydroxide in chloroform at 0°C. Compound **1** was successfully converted to **2** by the addition of an equimolar amount of neat benzylamine at 70°C. The structure was confirmed by electrospray mass spectrometry (ESMS) and ^{1}H NMR spectroscopy. The observed isotopic model in the mass spectrum showed agreement with the calculated pattern, and the amide proton was observed in the ^{1}H NMR spectrum in $CDCl_3$ as a characteristic triplet at 8.1ppm.[9]

New transition metal dithiocarbamate receptors **4** and **5** were synthesised in a one-pot reaction as shown in **Scheme 2.2**.

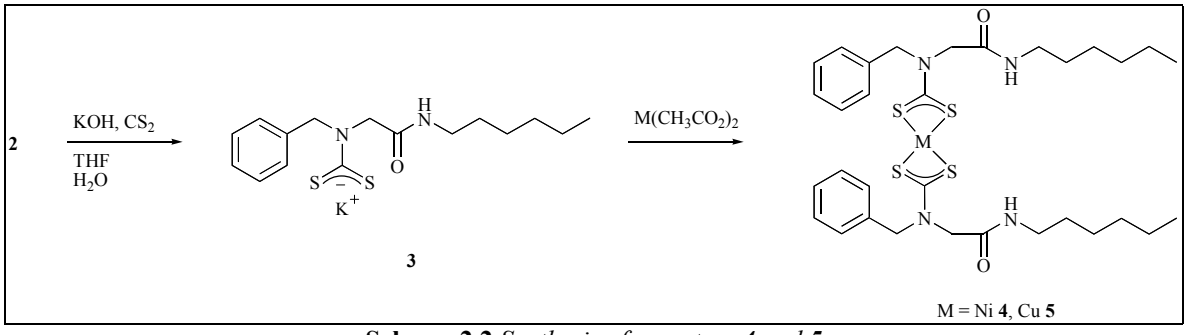

Scheme 2.2 *Synthesis of receptors **4** and **5***

An equimolar amount of carbon disulphide and potassium hydroxide was added to **2** in a tetrahydrofuran:water (2:1) mixture to form the potassium dithiocarbamate salt, **3**. This was not isolated but converted to the final product by the addition of half an equivalent of nickel(II) or copper(II) acetate.[4] Recrystallisation of **4** and **5** from dichloromethane/diethyl ether produced green and brown powders respectively in approximately 20% yield. Both receptors were

characterised by elemental analysis and ESMS showed excellent agreement with isotopic models. A summary of the receptors is shown in **Appendix 10**.

The ^{1}H NMR spectrum of receptor **4** and the peak assignments are shown **Figure 2.4**.

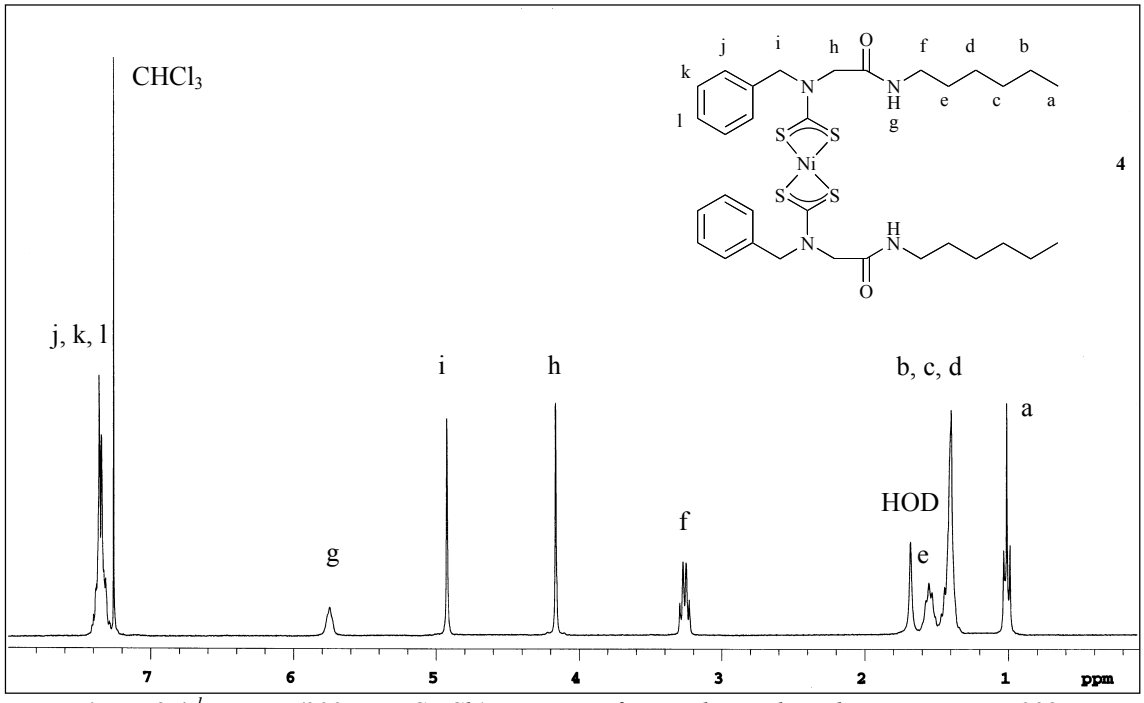

Figure 2.4 *^{1}H NMR (300MHz, $CDCl_3$) spectrum of **4** together with peak assignments at 298K*

The peaks between 7.55-7.38ppm are characteristic of aromatic protons. Receptor **4** was also characterised by ^{13}C NMR with a resonance observed at 165.4ppm due to the deshielded carbon of the carbonyl group.[10] Due to the paramagnetic properties of copper(II) dithiocarbamates[4] NMR spectroscopy could not be used to characterise receptor **5**.

Figure 2.5 displays the infrared spectrum of receptor **5** in Nujol® mull[11] together with band assignments.

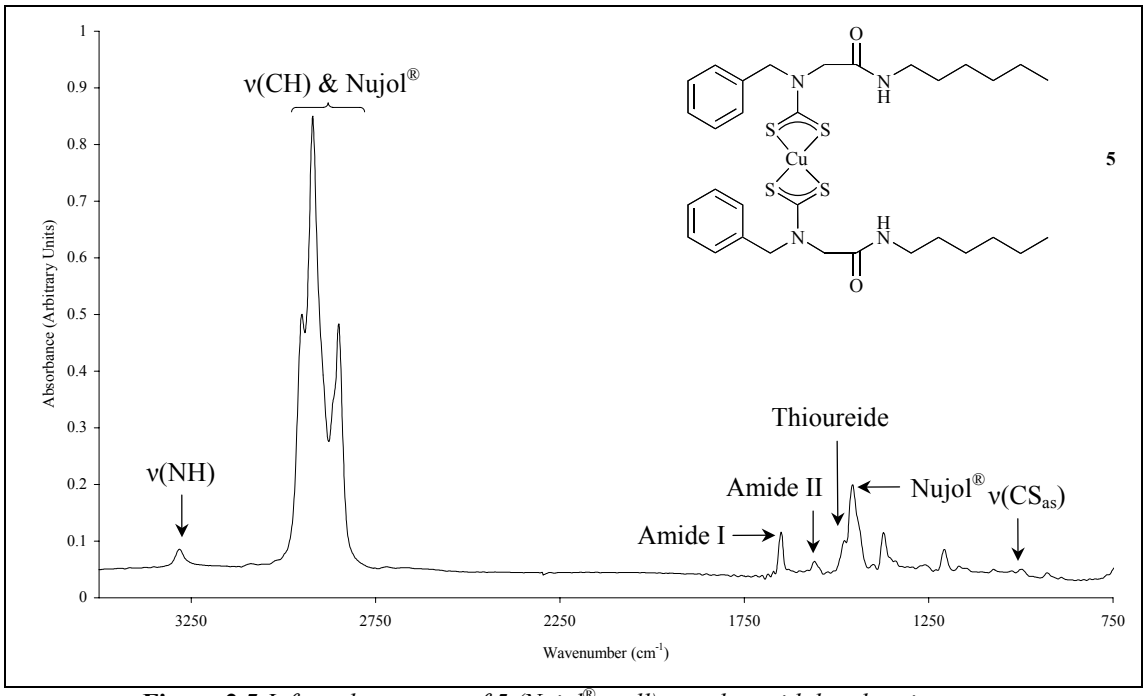

Figure 2.5 *Infrared spectrum of **5** (Nujol® mull) together with band assignments*

The band at 3286 cm^{-1} is due to the NH stretch of the amide[12] and between 2800-3000 cm^{-1} are the peaks corresponding to CH stretches of **5**[13] and Nujol®.[14] The amide I absorption, due to the carbonyl group, occurred at 1652cm^{-1}.[15] The amide II band was observed at 1572cm^{-1} and is a combination of NH bend and CN stretch of the amide group.

The peak at 1482cm^{-1} is characteristic of a dithiocarbamate CN stretch.[16] This 'thioureide' band confirms the partial double bond character between these two atoms as the resonance lies between that of a single carbon nitrogen bond and a double carbon nitrogen bond. The single band at 1006cm^{-1} is due to an anti-symmetric CS stretch and is evidence for the bidentate coordination of the metal by the sulphurs of the dithiocarbamate group.[17] A band at 676cm^{-1} has been assigned to a symmetric CS stretch.[18]

Synthesis of the analogous zinc(II) receptor, using **3** and zinc(II) acetate, gave a characteristically white powder. However, despite several attempts, it was not possible isolate and purify the molecule in order to perform binding studies.

2.2 Anion Binding Studies

The anion binding properties of **4** were studied using a variety of spectroscopic and electrochemical techniques. The anions chosen for complexation investigation were acetate, benzoate, dihydrogen phosphate and chloride as they possess contrasting shapes,[19] sizes and basicities.[20] TBA was used as the counter cation as it is large and non-coordinating.

2.2.1 ^{1}H NMR Spectroscopy

^{1}H NMR spectroscopy has often been used to provide information about the structure of the receptor:guest complex in solution and calculate receptor:guest stability constants.[21] Formation of a receptor:guest complex can alter the magnetic environments of the protons which are in close proximity to the binding site, leading to a change of the observed chemical shift in the spectrum. In all cases in this thesis, the receptor and receptor:guest complexes inter-convert rapidly on the NMR timescale and weighted mean of their chemical shifts was observed.[22]

Receptor **4** was titrated with aliquots of the TBA salts of the four different anions in DMSO-d_6:CD_2Cl_2 (4:1) solution (**Appendix 1**). The solvent mixture was employed due to the low solubility of **4**. In all cases, the amide resonance significantly shifted to lower field after the addition of 10 equivalents of anion. These downfield shifts imply favourable anion-receptor hydrogen bonding to the amide.[21] **Figure 2.6** shows the ^{1}H NMR spectra of **4** when titrated with acetate.

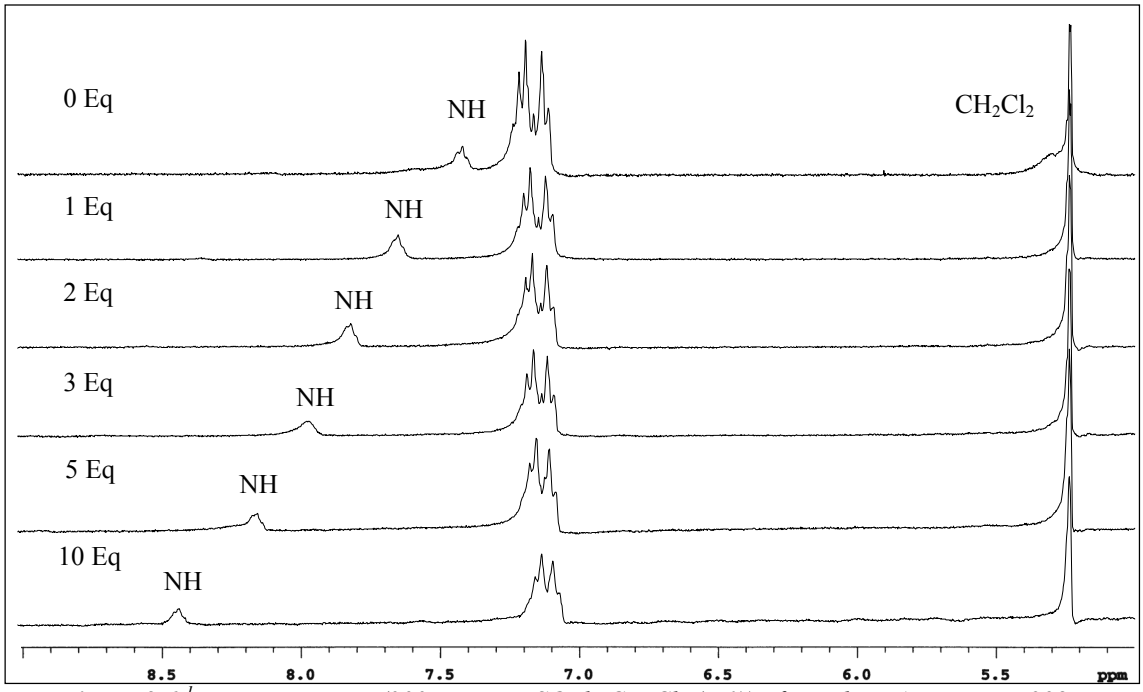

Figure 2.6 *^{1}H NMR titration (300MHz, DMSO-d_6:CD_2Cl_2 (4:1)) of **4** with TBA acetate at 298K*

Table 2.1 displays the change in chemical shift of the amide proton **4** upon the addition of equivalents of the four anions.

Anion	Change in amide proton shift (Δδ)				
	1 Eq	**2 Eq**	**3 Eq**	**5 Eq**	**10 Eq**
Acetate	0.23	0.40	0.55	0.73	1.01
Benzoate	0.11	0.25	0.34	0.51	0.79
Dihydrogen Phosphate	0.11	0.17	0.19	0.26	0.44
Chloride	0.09	0.15	0.24	0.35	0.56

Table 2.1 *Change in chemical shift of the amide protons upon addition of anions as their TBA salts to **4** at 298K*

After the addition of 10 equivalents of anion the magnitude of the downfield shift observed of the amide proton was in the order of acetate > benzoate > chloride ~ dihydrogen phosphate. This follows the trend in basicity for acetate and benzoate as shown in **Table 2.2**.[20] Interestingly, dihydrogen phosphate is much more basic then chloride but this is not reflected in the NMR titration profiles.

Anion	Acetate	Benzoate	Dihydrogen Phosphate	Chloride
pK_a	4.76	4.2	2.2	-6.1

Table 2.2 *pK_a values of the four anions in water*

Unfortunately, it was not possible to determine stability constants from this data. This was because the titration curve was very shallow which is indicative of weak binding and the stability constant could not be accurately calculated.

2.2.2 UV/visible Spectroscopy

Nickel(II) dithiocarbamate complexes display absorptions in the UV region at 230nm and 320nm due to a ligand centred (LC) π-π^* transitions.[23] A metal to ligand (MLCT) charge transfer band occurs at ~390nm together with another weaker MLCT band in the visible region at ~430nm. At ~490nm and ~650nm d-d Laporte forbidden, spin allowed transitions occur.

All the nickel(II) receptors displayed three characteristic peaks between 250-500nm. The lower wavelength LC peak was hidden by absorption of the DMSO solvent, however the tail of this absorption was often observed. In this case the d-d transitions were not observed due to their very low intensity.[24]

Table 2.3 displays the wavelengths and molar extinction coefficients of receptor **4** and the control compound, nickel(II) bis(*N*,*N*-diethyl dithiocarbamate) ($Ni(DTCEt_2)_2$),[25] in MeCN:DMSO (4:1) solution.

Assignment	$Ni(DTCEt_2)_2$	4
LC	327 (36.9)	331 (30.7)
MLCT	399 (5.8)	399 (5.0)
MLCT	427 sh (1.6)	434 (1.3)

Table 2.3 *Wavelength λ/nm (molar extinction coefficient $\varepsilon/10^3$ $M^{-1}cm^{-1}$) of $Ni(DTCEt_2)_2$ and **4***

UV/visible spectroscopy was used to prove the number of nickel(II) dithiocarbamate centres per molecule of **4** by monitoring the oxidation of nickel(II) to nickel(IV) (see **Chapter 4 Section 2.1.1**).

Figure 2.7 shows the change in UV/visible absorption spectrum upon the addition of aliquots of *N*-bromosuccinimde (NBS) solution to a chloroform solution of receptor **4**.

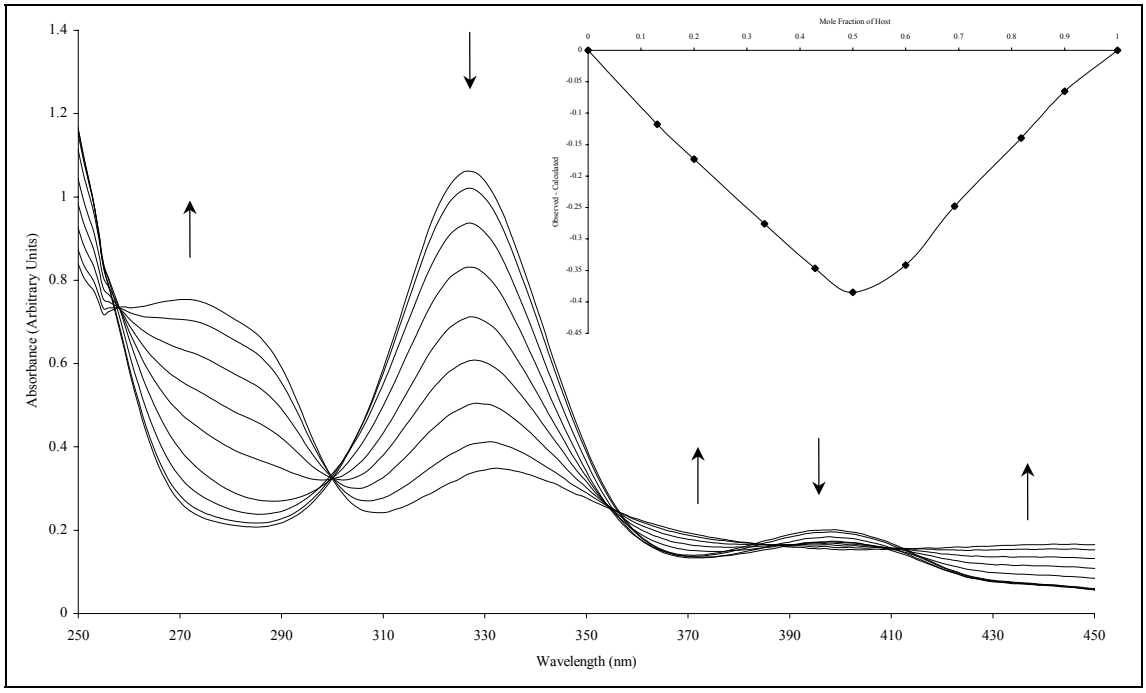

Figure 2.7 *UV/visible oxidation of **4** with NBS in $CHCl_3$*
*(Inset) Job Plot of **4** with NBS in $CHCl_3$*

The initial spectrum is typical of a nickel(II) dithiocarbamate and the final spectrum shows peaks characteristic of a nickel(IV) dithiocarbamate species (see **Chapter 5 Section 2**). The Job plot for the oxidation displays a minimum ~0.5, clearly indicating that one equivalent of NBS was required to perform the oxidation,[26] confirming that **4** contained one nickel(II) dithiocarbamate centre.

Anion titrations were carried out with **4** in a MeCN:DMSO (4:1) solvent mixture (**Appendix 2**) and the data was analysed with the computer program Specfit™.[27] This is a curve-fitting program that uses the whole spectrum to calculate stability constants. This solvent mixture was used as anion titrations carried out with **4** in MeCN resulted in calculated stability constants which were very large and outside the range of accuracy of the computer program used.[6b] Thus a more competitive solvent mixture has been used throughout.

Upon addition of TBA acetate to a solution of receptor **4** very large changes in the charge transfer bands were seen together with an isosbestic point at 304nm as shown in **Figure 2.8**. Specfit™ was able to calculate stability constant values as shown in **Table 2.4**.

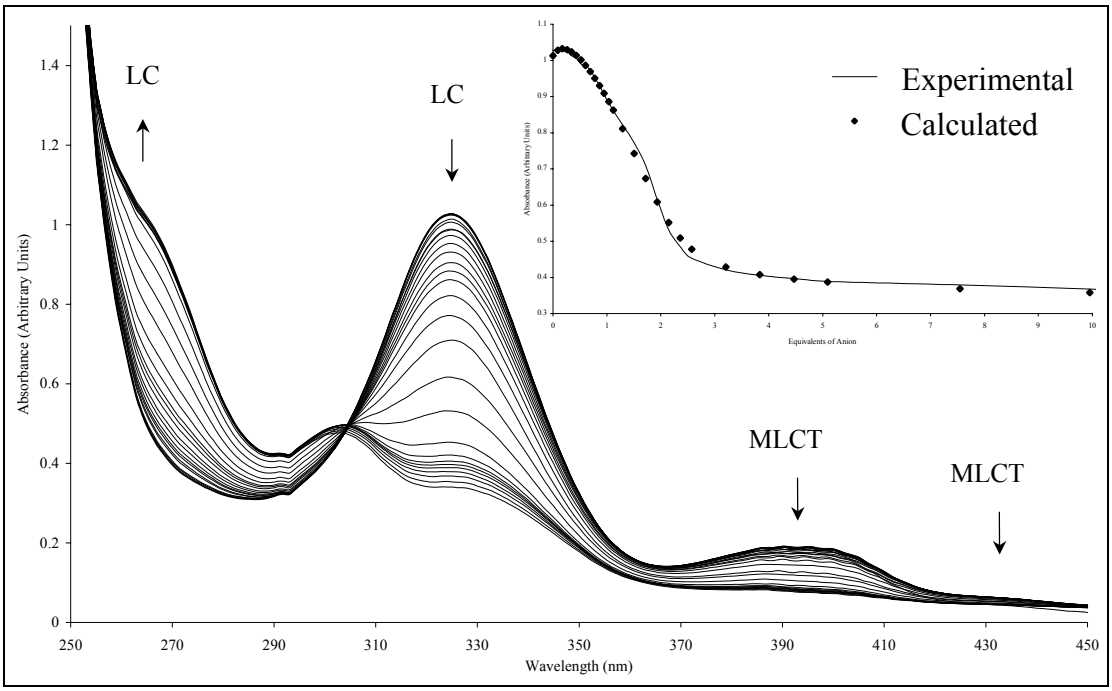

Figure 2.8 *UV/visible titration of **4** with TBA acetate in MeCN:DMSO (4:1) at 293K (Inset) The change in absorption at 325nm*

Stability Constants	Log β_1	Log β_2
4 & TBA Acetate	5.95 ± 0.12	11.71 ± 0.11

Table 2.4 *Stability constants with errors determined by UV/visible spectroscopy in MeCN:DMSO (4:1) at 293K*

A Job plot confirmed the 2:1, anion:receptor binding stoichiometry.[26] **Table 2.4** shows the stability constants for receptor **4** with acetate are very high for a neutral amide receptor.

Surprisingly, after the addition of an aliquot of benzoate and dihydrogen phosphate anions the UV/visible spectrum displayed a time delay before the absorption reached a constant value. To investigate this time delay, two equivalents of anion were added to a solution of the receptor and the spectrum recorded at one-minute intervals until the absorption reached a constant value. **Table 2.5** displays the time taken for the absorption to reach a constant value.

Anion	Equilibration time (minutes)
Benzoate	10
Dihydrogen Phosphate	15
Chloride	-

Table 2.5 *Time taken for the absorbance to reach a steady value after the addition of two equivalents of anion*

Interestingly, when chloride was added, very small changes in the spectrum were observed. However, **Table 2.5** shows that benzoate and dihydrogen phosphate require different amount of time for the absorption to reach a constant value. This kinetic effect was not observed in the NMR binding studies. Taking into account that no anion complexation has been reported that showed slow complexation kinetics, it seems likely that the anion is bound and then another process is occurring. This may be either a conformational change in the molecule or possibly the formation of a new coordination complex. This is discussed further in **Chapter 3 Section 3.2.2**.

2.2.3 Copper(II) Electrochemistry

The electrochemical properties of copper(II) dithiocarbamates have been well studied.[28,29,30] They undergo two metal based, one electron redox processes corresponding to a copper(II)/copper(III) oxidation and a copper(II)/copper(I) reduction. The properties of copper(II) dithiocarbamates can be studied by both cyclic and square wave voltammetry (**Appendix 3**).

If the rate of electron transfer from the electrode to the redox active species is fast compared to the diffusion of the electroactive molecule to the electrode, then the process is said to be reversible. A reversible electrochemical process satisfies the four criteria below.[31] The system is said to be quasi-reversible if only some of these criteria are satisfied.

i) the anodic and cathodic peak currents are the same,

ii) the separation between the anodic and cathodic wave potentials is approximately 59/n mV (n = the number of electrons transferred),

iii) wave potentials are independent of scan rate,

iv) current is proportional to the square root of the scan rate.

The electrochemical properties of receptor **5** were studied in a $CHCl_3$:MeCN (4:1) solvent mixture. The electrochemical properties of copper(II) bis(*N*,*N*-diethyl dithiocarbamate) ($Cu(DTCEt_2)_2$)[25] were also studied in the same solvent mixture for comparison purposes. **Table 2.6** shows the electrochemical data for receptor **5** and $Cu(DTCEt_2)_2$.

	Cu(II)/Cu(III)		Cu(II)/Cu(I)	
	$Cu(DTCEt_2)_2$	**5**	**$Cu(DTCEt_2)_2$**	**5**
E_{pa} (V)	0.260	0.350	-0.900	-
E_{pc} (V)	0.135	0.220	-1.050	-0.735
ΔE_p (V)	0.125	0.130	0.150	-
I_{pa}/I_{pc}	1.0	1.3	0.8	-
E_p (V)	0.205	0.290	-0.805	-0.630

Table 2.6 *Electrochemical data of the $Cu(DTCEt_2)_2$ compound and **5** in $CHCl_3$:MeCN (4:1) containing 0.1M $TBABF_4$, potentials given with reference to Ag/Ag^+ at 293K, scan rate = 100mVs^{-1}, E_p - peak potential in square wave voltammogram*

The potential of the oxidation and reduction waves of both $Cu(DTCEt_2)_2$ and **5** did not vary with scan rate and the peak current was found to be proportional to square root of the scan rate, thus both compounds displayed quasi-reversible electrochemical characteristics for the copper(II)/copper(III) couple. However, only $Cu(DTCEt_2)_2$ displayed quasi-reversibility of the copper(II)/copper(I) couple. The irreversible reduction behaviour shown by **5** maybe due to the stereochemical change that occurs from square planar copper(II) to tetrahedral copper(I).[28] The potential of the oxidation and reduction of **5** were anodically shifted, compared to $Cu(DTCEt_2)_2$, possibly due to the neighbouring electron withdrawing amide group.

The response of $Cu(DTCEt_2)_2$ and receptor **5** to the addition of anions was investigated using square wave voltammetry. The magnitudes of the cathodic shifts observed upon the addition of five equivalents of anion are displayed in **Table 2.7**.

Anion	ΔE Cu(II)/Cu(III) (mV)	
	$Cu(DTCEt_2)_2$	**5**
Acetate	25	80
Benzoate	15	100
Dihydrogen Phosphate	5	-[a]
Chloride	-	-[a]

Table 2.7 *Cathodic shifts in the square wave voltammogram upon the addition of 5 equivalents of anion to the $Cu(DTCEt_2)_2$ and **5** in $CHCl_3$:MeCN (4:1) containing 0.1M $TBABF_4$, potentials given with reference to Ag/Ag^+ at 293K (a - extra peaks observed)*

Small cathodic shifts of the copper(II)/copper(III) peak were observed upon the addition of five equivalents of acetate, benzoate and dihydrogen phosphate anions to $Cu(DTCEt_2)_2$. In contrast, **5** displayed a much larger shift upon the addition of acetate and benzoate anions. This is due to the proximity of the bound anion stabilising the charged copper(III) dithiocarbamate species.[7]

Interestingly, addition of dihydrogen phosphate and chloride anions caused the appearance of more than one redox wave in the voltammogram. In the case of dihydrogen phosphate both waves were at a more negative potential than the original, shifted by 40mV and 100mV respectively. Whereas, with chloride an extra peak was seen at a 75mV more positive potential and one at a 105mV more negative potential than the original wave. It is possible that a chemical reaction may be occurring.

Upon the addition of five equivalents of the four anions to $Cu(DTCEt_2)_2$ very small cathodic shifts of the copper(II)/copper(I) couple were observed. Receptor **5** also only displayed similar small shifts in the presence of excess amounts of all four anions.

2.2.4 Nickel(II) Electrochemistry

The electrochemical properties of the nickel(II) dithiocarbamates have previously been studied.[29,30,32] An irreversible two electron metal based oxidation occurs at a large positive potential corresponding to a metal based nickel(II)/nickel(IV) process. The nickel(IV) cation

shows two successive metal centred one-electron reduction steps, which are both metal based, and correspond to a nickel(IV)/nickel(III) and a nickel(III)/nickel(II) reduction respectively. Nickel(II) dithiocarbamates can also be reduced at fairly negative potential in a metal centred one-electron reduction to a nickel(I) species.

Receptor **4** and $Ni(DTCEt_2)_2$[25] were studied in DMF by cyclic and square wave voltammetry and the electrochemical data is shown in **Table 2.8**. DMF was used due to the low solubility of receptor **4**.

	Ni(II)/Ni(IV)			**Ni(II)/Ni(I)**	
	$Ni(DTCEt_2)_2$	**4**		**$Ni(DTCEt_2)_2$**	**4**
E_{pa} (V)	0.630	0.355	**E_{pa} (V)**	-1.800	-
E_p (V)	0.505	0.370	**E_{pc} (V)**	-1.980	-1.900
	Ni(IV)/Ni(III)		**ΔE (V)**	-0.180	-
	$Ni(DTCEt_2)_2$	**4**	**I_{pa}/I_{pc}**	0.9	-
E_{pa} (V)	-0.225	-0.150	**E_p (V)**	-1.870	-1.850
	Ni(III)/Ni(II)				
	$Ni(DTCEt_2)_2$	**4**			
E_{pa} (V)	-0.770	-0.655			

Table 2.8 *Electrochemical data of the $Ni(DTCEt_2)_2$ and **4** in $CHCl_3$:MeCN (4:1) containing 0.1M $TBABF_4$, potentials given with reference to Ag/Ag^+ at 293K, scan rate = 100mVs^{-1}, E_p - peak potential in square wave voltammogram*

Receptor **4** displayed typical redox characteristics for a nickel(II) dithiocarbamate compound except that the nickel(II)/nickel(I) couple was irreversible.

Five equivalents of acetate, benzoate, dihydrogen phosphate and chloride were added to a solution of **4** and the changes in the square wave voltammogram recorded. The response of $Ni(DTCEt_2)_2$[25] to the addition of anions was also studied.

The control compound showed very small cathodic shifts upon addition of five equivalents of the four anions. Disappointingly, **4** also showed very little shift of the

nickel(II)/nickel(I) square wave upon anion addition. This may be due to the very competitive nature of DMF as a solvent.

3 Thiourea Dithiocarbamate Anion Receptor

Thiourea groups are effective hydrogen bond donors and as such are capable of binding anions (see **Chapter 1 Sections 3.4**). In general, thiourea derivatives show stronger anion binding ability than that of the corresponding ureas due to the greater acidity of the thiourea protons.[33]

The target receptor **11** was designed to contain a thiourea anion binding site in close proximity to a metal dithiocarbamate centre.

3.1 Synthesis and Characterisation

The synthesis of the receptor molecule **11** is shown below in **Scheme 2.3**.

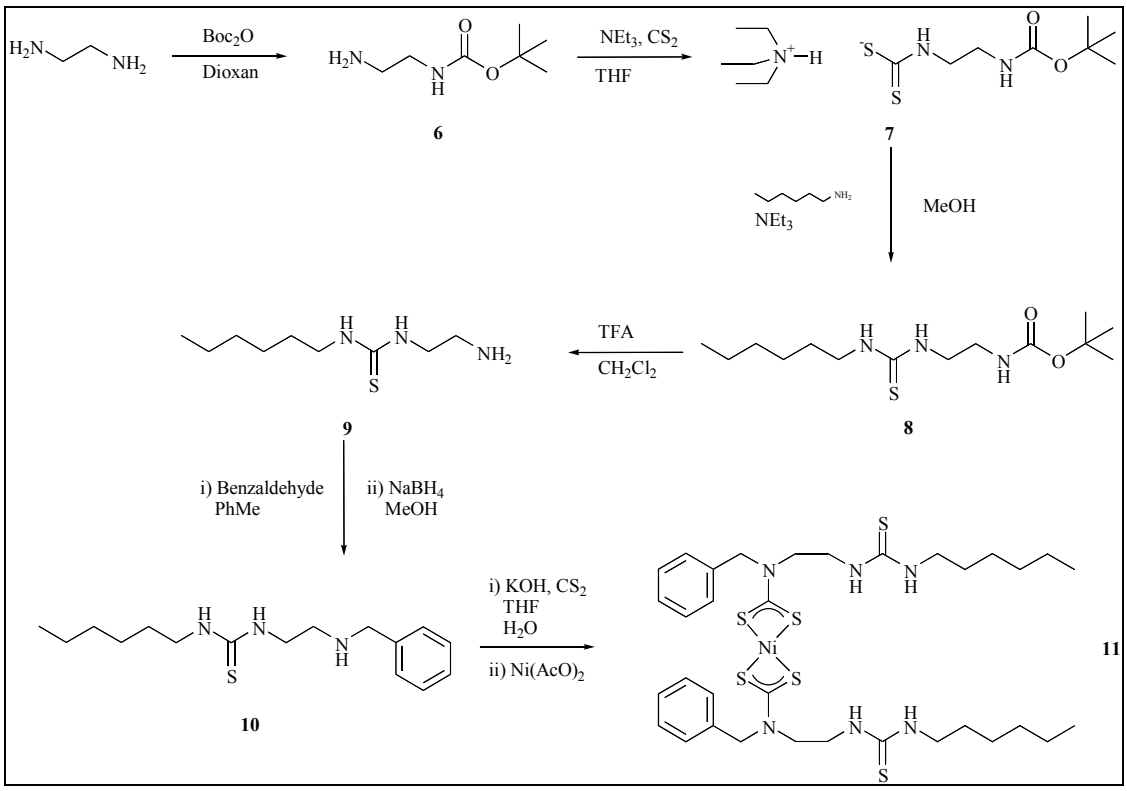

Scheme 2.3 *Synthesis of receptor **11***

Ethylene diamine was mono protected in 80% yield by using bis(*tert*-butoxycarbonyl)anhydride (Boc_2O) in 1,4-dioxane.[34]

The conversion of amine **6** to the corresponding isothiocyanate was attempted using thiophosgene,[35] carbon disulphide and hydrogen peroxide,[36] carbon disulphide and cyanamide,[37] carbon disulphide and dicyclocarbimide,[38] and 1,1'-thiocarbonyl-2,2'-pyridone.[39] Unfortunately, all of these methods produced a complex mixture of products.

An alternative route to form the thiourea group was employed in a method similar to that of Robbins.[40] One equivalent of carbon disulphide and one equivalent of triethylamine were added to the mono-protected amine dissolved in tetrahydrofuran producing the dithiocarbamate triethylamine salt **7** in quantitative yield. This was dissolved in methanol, and one equivalent of hexylamine was added to the mixture and refluxed for fifteen hours. After work up, the unsymmetrical thiourea **8** was isolated with the ^1H NMR spectrum revealing characteristically broad resonances at 6.24ppm and 6.94ppm.

The protecting group was removed quantitatively using trifluoroacetic acid in dichloromethane[41] and the resulting primary amine **9** condensed with benzaldehyde. The formation of the imine was driven by using toluene as solvent and Dean-Stark apparatus to azeotropically remove water from the reaction.[42] The imine was reduced using sodium borohydride in methanol[43] that gave the secondary amine **10** in 90% yield. All of the intermediates **6 - 10** were characterised by ^1H, ^1H-^1H COSY NMR and ESMS.

The secondary amine **10** was dissolved in a tetrahydrofuran:water (5:1) mixture and one equivalent of carbon disulphide and one equivalent of potassium hydroxide were added to create the potassium dithiocarbamate salt. Conversion of this salt to receptor **11** was achieved by addition of nickel(II) acetate.[4] After workup, the crude product was recrystallised from dichloromethane/diethyl ether yielding the corresponding transition metal dithiocarbamate salt as a light green powder in 27% yield.

The ^{13}C NMR spectrum of receptor **11** is shown below in **Figure 2.9** together with peak assignments.

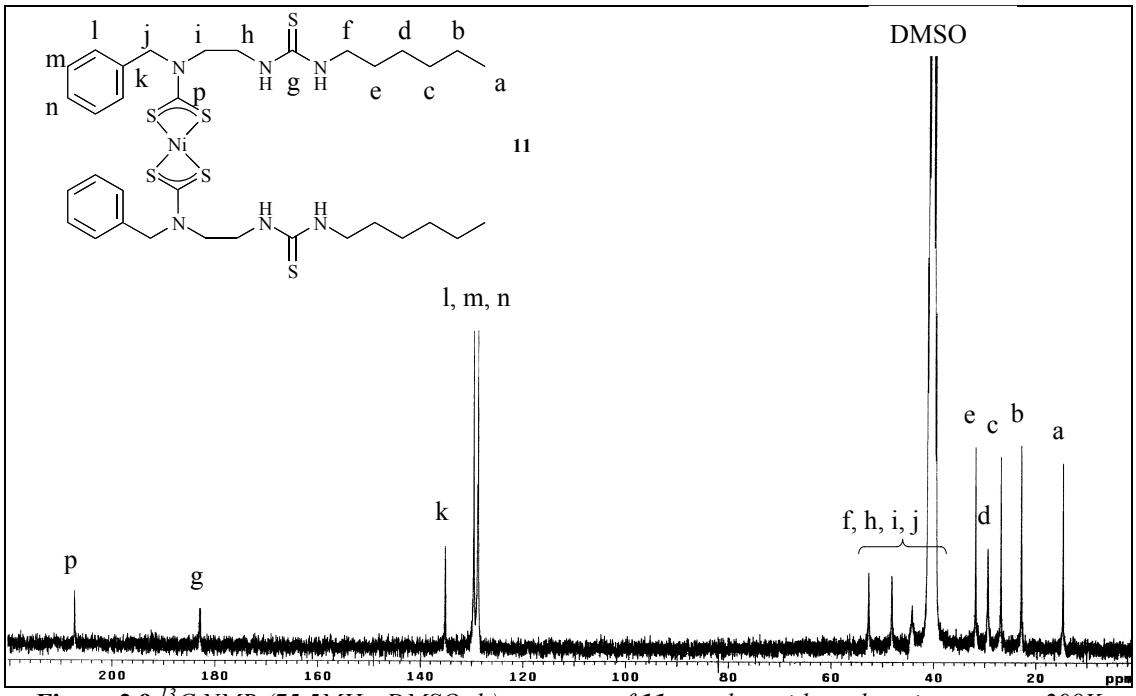

11

Figure 2.9 *^{13}C NMR (75.5MHz, DMSO-d_6) spectrum of **11** together with peak assignments at 298K*

The peak at 207.3ppm is characteristic of dithiocarbamate carbon[44] and the resonance at 183.2ppm is assigned to the thiocarbonyl carbon.[45]

The infrared spectrum showed absorptions at 3332cm^{-1} and 3242cm^{-1} characteristic of thiourea NH stretches.[46] The ESMS revealed good agreement between calculated and observed isotopic clusters for [**11** + Na^+]$^+$. **11** was also characterised by ^{1}H, ^{1}H-^{1}H COSY NMR, UV/visible and elemental analysis.

Attempts to synthesise the analogous copper(II) dithiocarbamate complex resulted in characteristically brown products. However, despite repeated recrystallisations the compound could not be obtained in a pure form.

3.2 Anion Binding Studies

The anion binding properties of receptor **11** were studied using ^{1}H NMR, UV/visible spectroscopy and electrochemical techniques as described below.

3.2.1 ^{1}H NMR spectroscopy

Receptor **11** was titrated with four different anions in DMSO-d_6 solution. This solvent was used due to the low solubility of the receptor. Upon the addition of ten equivalents of acetate, benzoate and dihydrogen phosphate anions, a large downfield shift of the thiourea resonances was observed (**Figure 2.10**). These downfield shifts imply the anion was binding to the thiourea's protons.[47]

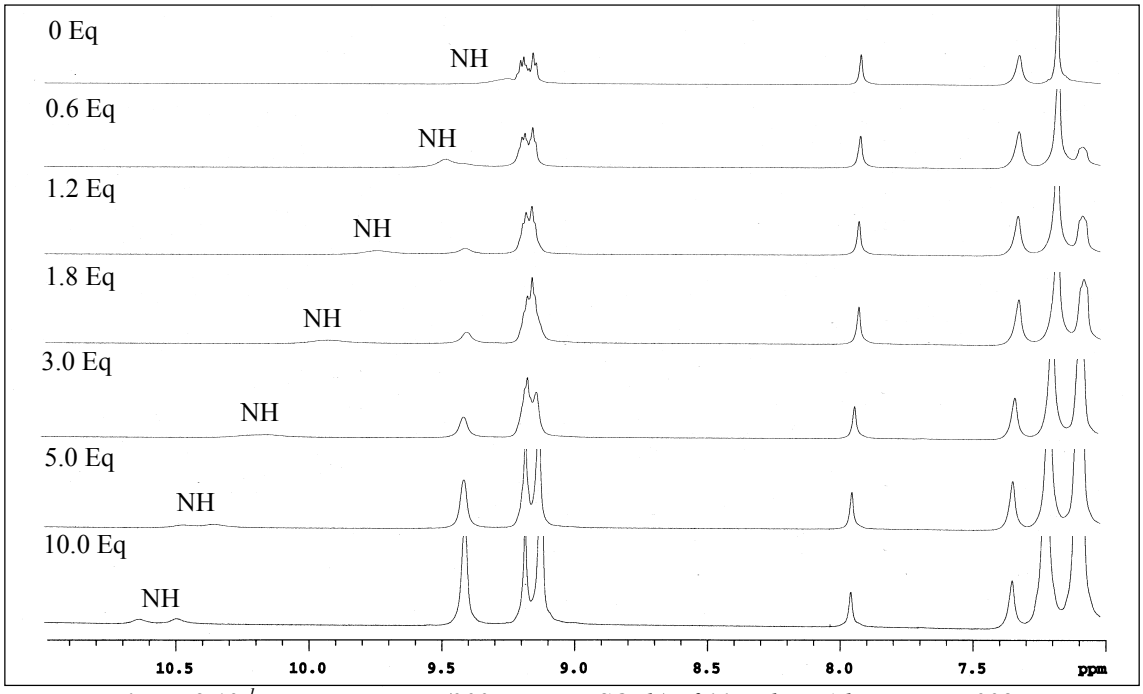

Figure 2.10 *^{1}H NMR titration (300MHz, DMSO-d_6) of **11** with TBA benzoate at 298K*

Figure 2.11 displays the variation of the thiourea resonance of receptor **11** upon addition of equivalents of acetate, benzoate and dihydrogen phosphate anions, together with the calculated binding curves.

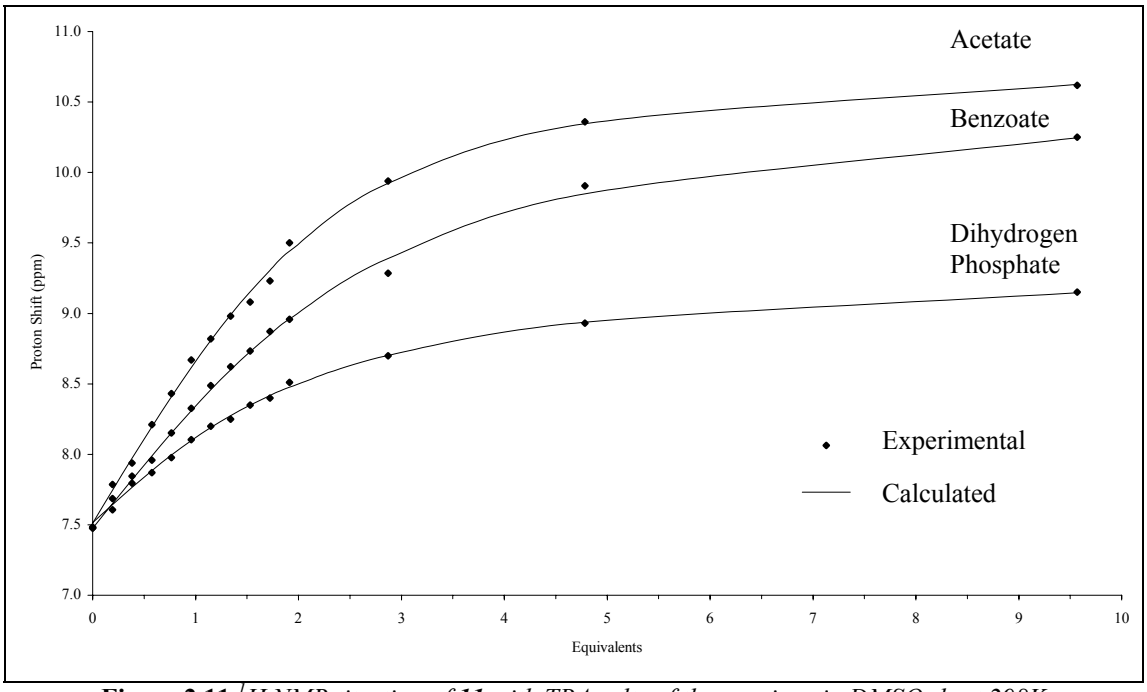

Figure 2.11 *^{1}H NMR titration of **11** with TBA salts of three anions in DMSO-d_6 at 298K*

EQNMR,[48] a least squares fitting computer program, was used to calculate stability constants for the anion binding as displayed in **Table 2.9**. Unfortunately, it was not possible to calculate the binding constant with chloride as the thiourea protons resonance only shifted very slightly, indicative of very weak binding in this competitive solvent.

Stability Constant (M^{-1})	Acetate	Benzoate	Dihydrogen Phosphate
K_1	530	410	740
K_2	100	55	60

Table 2.9 *Stability constants for **11** with three different anions as guests in DMSO-d_6 at 298K (Errors <10%)*

Acetate, benzoate and dihydrogen phosphate anions bound to receptor **11** in 2:1 (anion:receptor) stoichiometry. Unfortunately, Job plot analysis could not be used to confirm this as the thiourea resonances broadened into the baseline at high concentration of anion. However, the host:guest ratio was confirmed, as a 1:1 model could not be fitted to the data.

The first stability constant with acetate is of similar magnitude to those of simple acyclic mono-thioureas in DMSO.[49] Benzoate displayed a slightly lower stability constant due to its lower basicity.[20] For both anions, the second stability constant is much smaller, as would be expected from electrostatic and statistical considerations.

The first stability constant with dihydrogen phosphate is remarkably large, especially as the basicity of dihydrogen phosphate is very much less than both acetate and benzoate.[20] This may indicate that receptor **11** has the correct geometry so that both thiourea groups in the receptor molecule can bind to the anion co-operatively. The second binding constant is very much smaller as would be expected.

3.2.2 UV/visible spectroscopy

The anion binding characteristics of **11** were studied by UV/visible spectroscopy. The spectrum showed three intense bands characteristic of a nickel(II) dithiocarbamate species between 250nm - 500nm (see **Section 2.2.2**). **Table 2.10** displays the wavelengths and molar extinction coefficients of $Ni(DTCEt_2)_2$ and receptor **11** in MeCN:DMSO (4:1) solution.

Assignment	$Ni(DTCEt_2)_2$	11
LC	327 (36.9)	326 (31.8)
MLCT	399 (5.8)	390 (6.7)
MLCT	427 sh (1.6)	428 sh (1.6)

Table 2.10 *Wavelength λ/nm (molar extinction coefficient ε/10^3 $M^{-1}cm^{-1}$) of $Ni(DTCEt_2)_2$ and **11***

Anion titrations were performed with **11** in the same solvent mixture. Upon addition of acetate, benzoate and dihydrogen phosphate very large changes of the charge transfer bands were observed together with an isosbestic point at 304nm. Addition of chloride produced only a very small decrease in absorption due to dilution.

Similarly to receptor **4**, after the addition of the anions to the receptor solution there was a delay before the absorption reached a steady value. Thus, it was not possible to calculate stability constants from this titration data. Time delay experiments were performed by the addition of two equivalents of anion and the spectrum recorded at one-minute intervals until the absorption reached a constant value. The time taken for the systems to reach equilibrium is shown in **Table 2.11**.

Receptor	Equilibration time (minutes)		
	Acetate	Benzoate	Dihydrogen Phosphate
11	2	2	7.5

Table 2.11 *Time taken for the absorbance to reach a steady value after the addition of two equivalents of anion*

This kinetic effect was not observed in the NMR titrations. As noted previously, it may be due to either a conformation change upon anion complexation or a reaction. The reason for this effect is discussed further in **Chapter 3 Section 3.2.2**.

4 Crown Ether Dithiocarbamate Cation Receptor

Receptors containing crown ethers show a high affinity for the complexation of cationic metal ions (see **Chapter 1 Section 2.2**).[50] Crown ether groups have previously been combined with a transition metal dithiocarbamate linkage to create a cation receptor (**Figure 2.12**).[51]

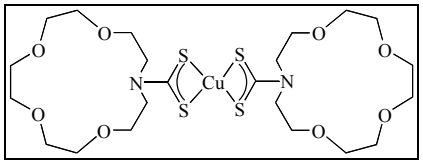

Figure 2.12 *Crown ether dithiocarbamate cation receptor*

This receptor sensed the presence of sodium cation by modest a 10mV anodic shift of its electrochemical couple. The magnitude of the shift was probably due to the partial positive charge that exists on the nitrogen atoms, which would not favour cation binding.[4]

A receptor was designed to have a crown ether group in close proximity to the transition metal dithiocarbamate group. The sections below detail how a benzo-[15]crown-5 moiety was incorporated into the structure of a dithiocarbamate receptor molecule. This particular size of crown ether was chosen because of its well known ability to form an intramolecular sandwich compound with potassium cations, in which the potassium cation is bound in between two crown ether rings.[52]

4.1 Synthesis and Characterisation

In order to synthesise the receptor it was necessary to create a secondary amine that was covalently attached to a crown ether group. Secondary amine crown ether **14** was prepared as shown in **Scheme 2.4**.

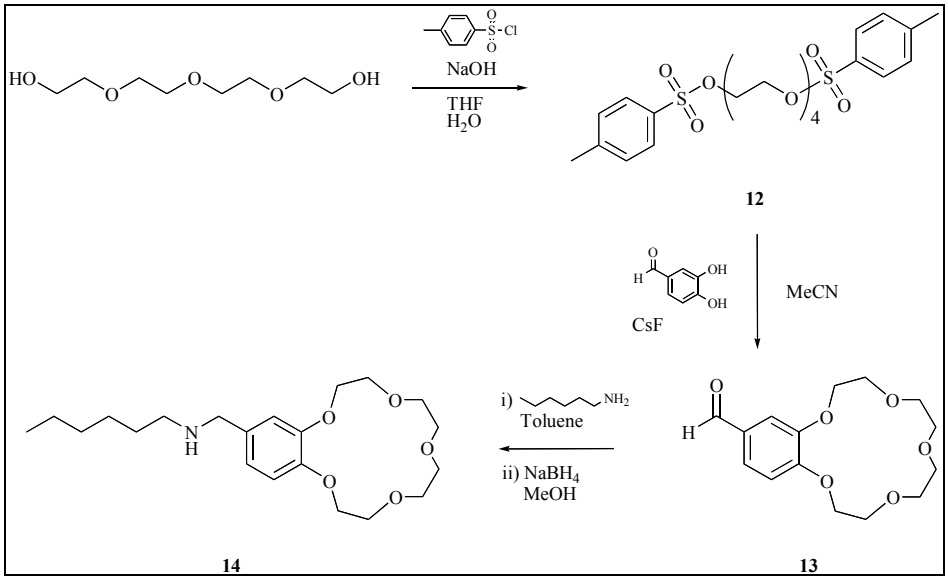

Scheme 2.4 *Synthesis of amine crown ether **14***

Commercially available tetraethyleneglycol was reacted with *p*-toluenesulphonylchloride using an excess of sodium hydroxide in a tetrahydrofuran:water (1:1) mixture forming the ditosylate **12** as a clear oil in a 98% yield.[53] Reaction of **12** with 3,4-dihydroxybenzaldehyde using caesium fluoride gave, after recrystallisation from isopropyl ether, the crown ether **13** in 30% yield.[54] Condensation of hexylamine with this aldehyde was accomplished using Dean Stark apparatus and toluene as the solvent.[42] The resulting imine was reduced in methanol using sodium borohydride.[43] ^{1}H NMR revealed that the peak at 9.80ppm, due to the aldehyde proton had disappeared indicating that the reaction was successful. Compounds **12** - **14** were characterised by ^{1}H, ^{1}H-^{1}H COSY NMR and ESMS.

Receptor **15** was synthesised using the usual conditions for dithiocarbamate formation, with the variation that tetrabutylammonium hydroxide was used as base instead of potassium hydroxide (**Scheme 2.5**). This was to prevent alkali metal cations associating with the crown ether groups.[55]

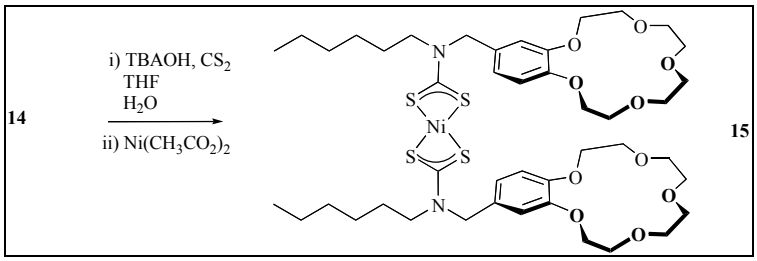

Scheme 2.5 *Synthesis of receptor **15***

Receptor **15** precipitated from solution and was isolated in 41% yield as a green solid which was thoroughly dried in *vacuo* and characterised by ^{1}H-^{1}H COSY NMR as shown in **Figure 2.13**.

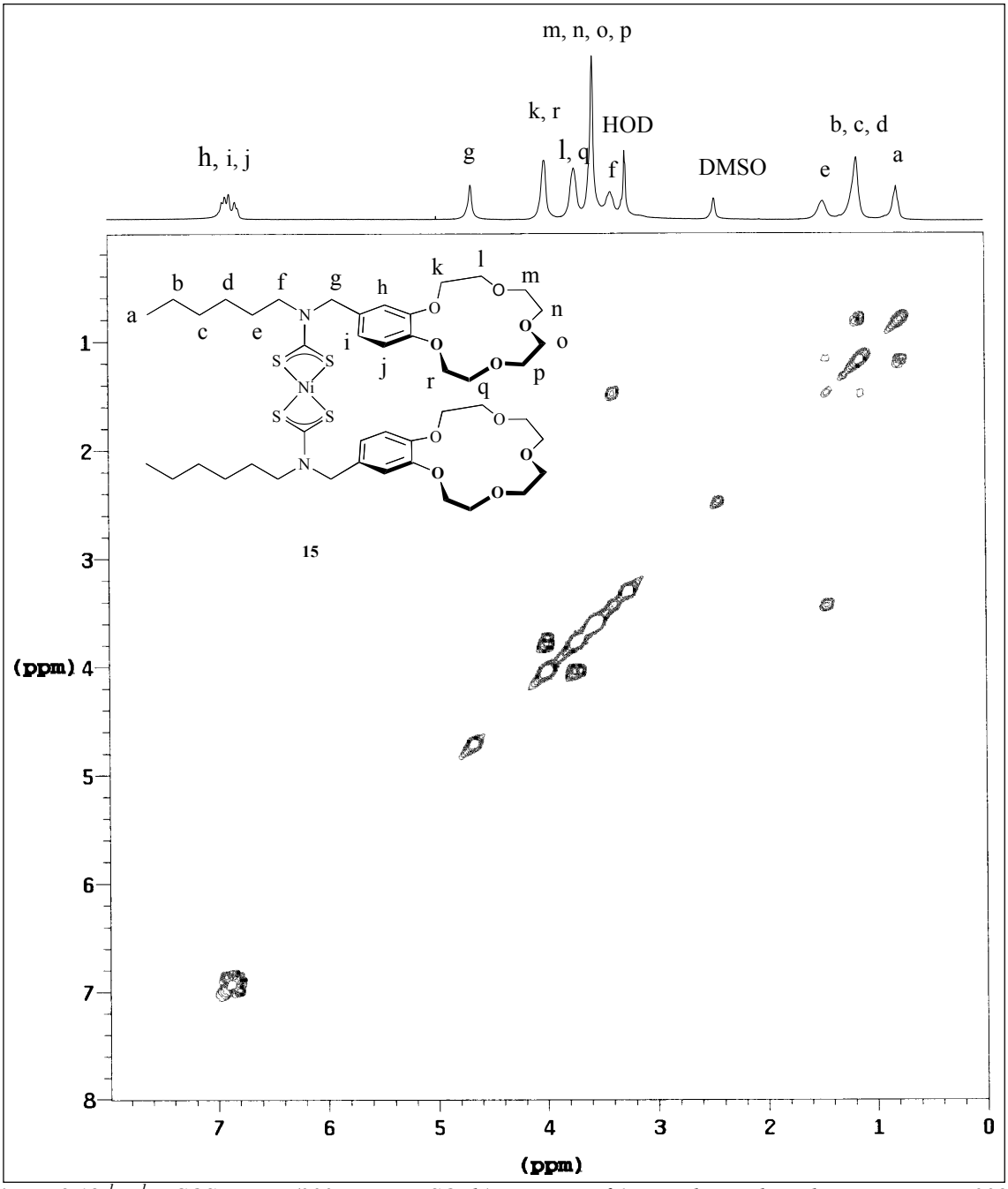

Figure 2.13 *^{1}H-^{1}H COSY NMR (300MHz, DMSO-d_6) spectrum of **15** together with peak assignments at 298K*

Three-bond coupling can be seen between adjacent protons k and l, r and q and along the hexyl chain.

^{13}C NMR, UV/visible, ESMS, infrared spectroscopies and elemental analysis also confirmed the structure of **15**. The infrared spectrum revealed absorptions at 1002cm^{-1} and 656cm^{-1} due to antisymmetric[16] and symmetric stretches of the CS group.[18]

Disappointingly, an analogous synthetic route to obtain the copper(II) based receptor proved much more troublesome. Repeated, attempts to purify the crude product using silica columns and recrystallisation from acetonitrile/water produced only a very small amount of the desired product. The ESMS confirmed the presence of the copper(II) based receptor however not enough could be isolated to enable binding studies to be performed.

4.2 Cation Binding Studies

The cation binding properties of receptor **15** were studied using ESMS, ^{1}H NMR, UV/visible spectroscopies and electrochemical techniques. The cations studied were sodium, potassium, rubidium and caesium either as their hexafluorophosphate (PF_6) or perchlorate (ClO_4) salts. These counter-anions were used as they are large and non-coordinating.

4.2.1 Electrospray Mass Spectrometry

Electrospray mass Spectrometry (ESMS) has been used to assess Group 1 cation binding with crown ether complexes.[56] Characterisation of receptor **15** using ESMS showed not only the expected [**15** + Na^+]$^+$and [**15** + 2Na^+]$^{2+}$ isotopic clusters but also a cluster corresponding to [**15** + K^+]$^+$. The Group 1 metal cations originate from alkali metal salts, which are used to calibrate the spectrometer.[57]

The cation binding capability of **15** was investigated further using ESMS cation competition experiments (**Appendix 4**). Two equivalents of Na^+, K^+, Rb^+ and Cs^+ were added to **15** in MeOH as their PF_6 salts (**Figure 2.14**).

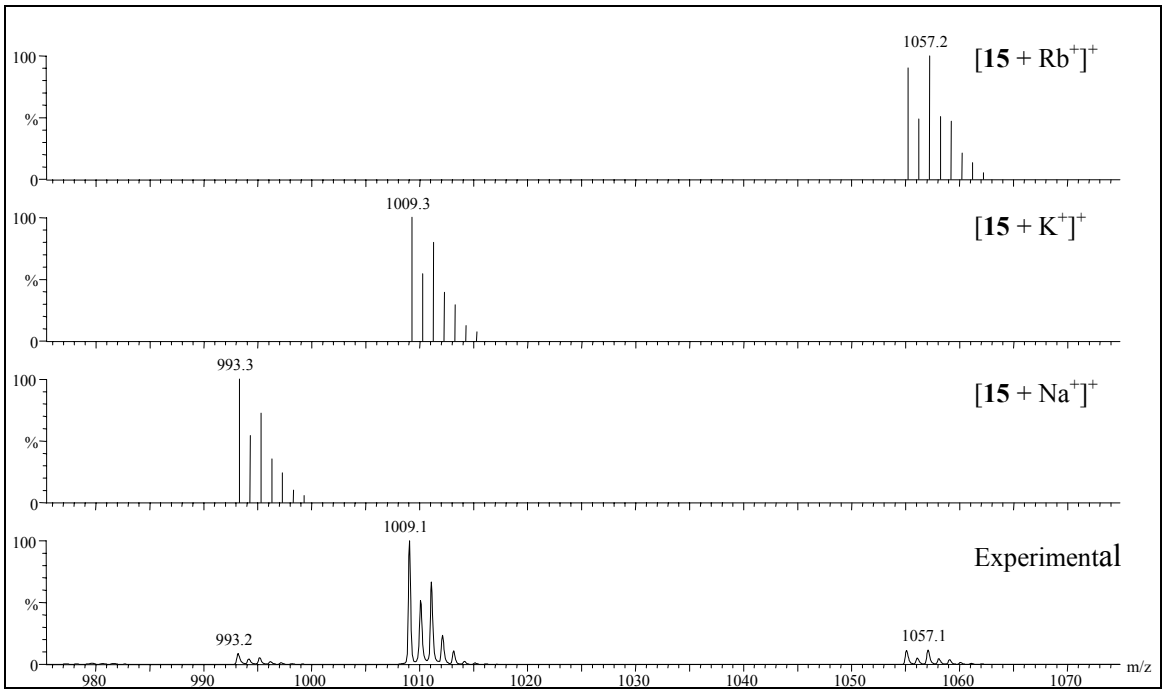

Figure 2.14 *ESMS competition experiment with Group 1 hexafluorophosphate salts*

Peaks due to [**15** + Na^+]$^+$, [**15** + K^+]$^+$ and [**15** + Rb^+]$^+$ were observed with the signal intensity increasing $Na^+ < Rb^+ < K^+$ indicating a preference for binding K^+. No [**15** + Cs^+]$^+$ peak was observed indicative of weak binding.

A biased competition experiment was also performed where one equivalent of K^+ was added along with ten equivalents of the other three cations. The ESMS spectra still showed a preference of the receptor to bind K^+ in 1:1 stoichiometry. It is likely that the K^+ was bound via the two crowns in an intramolecular sandwich complex.[58]

4.2.2 ^{1}H NMR Spectroscopy

^{1}H NMR titration experiments were conducted with KPF_6 in DMSO-d_6:CD_2Cl_2 (4:1) in order to investigate the cation binding of **15**. The ideal peaks to follow during the titration are the crown-ether methylene protons. Unfortunately, it was not possible to monitor these reliably as these peaks merged with each other as they were shifted upfield. However, the NC*H*$_2$Ar protons could be followed. The chemical shift of these protons increased up to 1 equivalent of KPF_6, and no further perturbation was seen upon further guest addition. This is indicative of a 1:1 binding stoichiometry. This agrees with the ESMS studies and is highly suggestive of the formation of an intramolecular sandwich complex with one K^+ ion binding in between the [15]crown-5 ether

groups. Unfortunately, it was not possible to calculate the stability constant of the **15**:K^+ complex due to the overlapping of the peaks of interest upon cation addition

4.2.3 UV/visible Spectroscopy

The cation binding of receptor **15** was studied by UV/visible spectroscopy. The spectrum showed two MLCT bands and a LC absorption between 250nm and 500nm (see **Section 2.2.2**).

Table 2.12 displays the wavelengths and molar extinction coefficients of $Ni(DTCEt_2)_2$ and **15** in MeCN:DMSO (4:1) solution.

Assignment	$Ni(DTCEt_2)_2$	15
LC	327 (36.9)	326 (34.8)
MLCT	399 (5.8)	395 (6.0)
MLCT	427 sh (1.6)	424 (1.2)

Table 2.12 *Wavelength λ/nm (molar extinction coefficient $\varepsilon/10^3$ $M^{-1}cm^{-1}$) of $Ni(DTCEt_2)_2$ and **15***

Receptor **15** was titrated with aliquots of K^+, Rb^+ and Cs^+ as their PF_6 salts, and Na^+ as its ClO_4 salt, in the same solvent mixture. Unfortunately, the electronic spectra for all titrations displayed very little change upon cation addition. A small decrease in absorption was observed at all wavelengths due to dilution. This is possibly due to the large distance between the crown ether groups and the dithiocarbamate metal centre.

5 Ion-Pair Dithiocarbamate Receptors

Ditopic receptors containing both amide and crown ether groups have been shown to simultaneously bind anions and cations (see **Chapter 1 Section 4**).

Ion-pair receptors often exhibit co-operative effects, whereby the complexation of one ion alters the binding affinity of the counter ion. This co-operativity can be either positive or negative depending on whether the binding affinity is enhanced or reduced respectively.

Beer reported that the heteroditopic receptor shown in **Figure 2.15** displayed remarkable switching of selectivity in the presence of a cation.

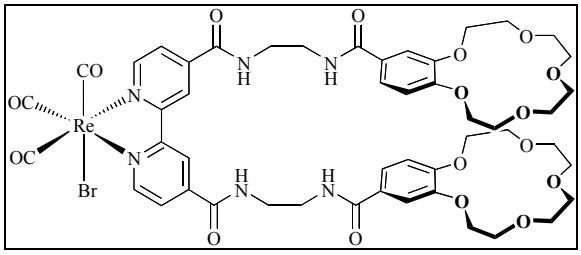

Figure 2.15 *Beer's rhenium(I) heteroditopic receptor*

In the absence of potassium cation the receptor is selective for dihydrogen phosphate over chloride, whereas following the formation of an intramolecular potassium bis-crown sandwich complex the reverse selectivity is exhibited.

The following sections detail the synthesis of a new type of self-assembled ion-pair receptor with the potential to display positive co-operativity between anion and cation binding sites.

5.1 Synthesis and Characterisation

Ion-pair receptors **19** and **20** were synthesised in four steps starting from the benzo-[15]crown-5 aldehyde, **13**. The ditopic amine **18** was prepared as shown in **Scheme 2.6**.

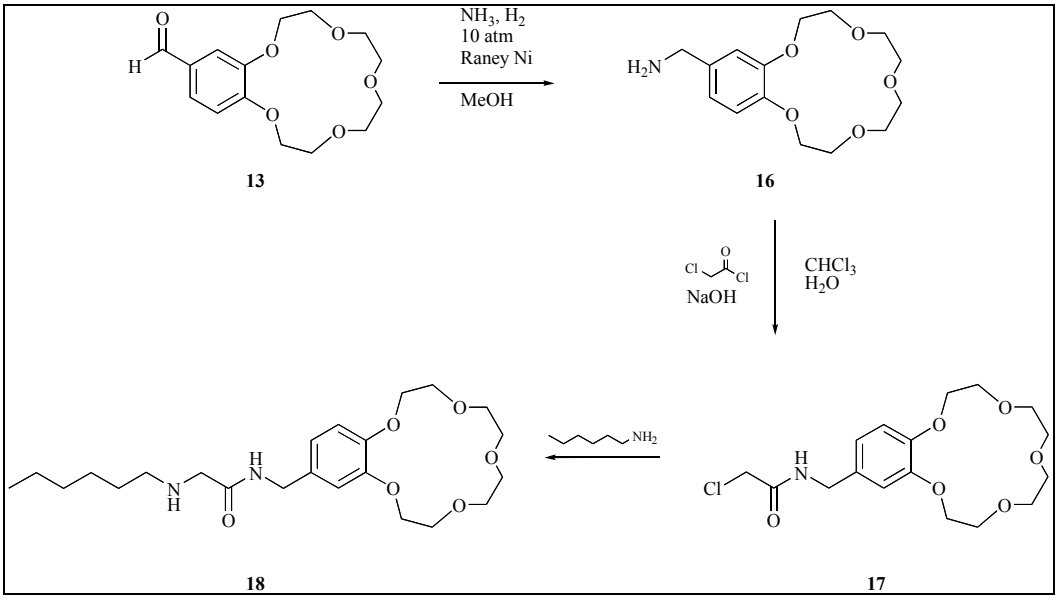

Scheme 2.6 *Synthesis of amide crown ether amine **18***

The crown aldehyde **13** was reductively aminated using a methanol solution saturated with ammonia using 10 bar of hydrogen with Raney-nickel catalyst, which gave **16** in 38% yield.[59] This was reacted with chloroacetyl chloride with sodium hydroxide as base to form the amide **17** in quantitative yield.[8] The secondary amine **18** was synthesised in 80% yield by the reaction of **17** with excess hexylamine.[60] Intermediates **16** - **18** were characterised by ^{1}H, ^{1}H-^{1}H COSY NMR and ESMS.

Standard synthetic conditions for dithiocarbamate formation were used to synthesise receptors **19** and **20** from **18** repectively,[4] as shown in **Scheme 2.7**.

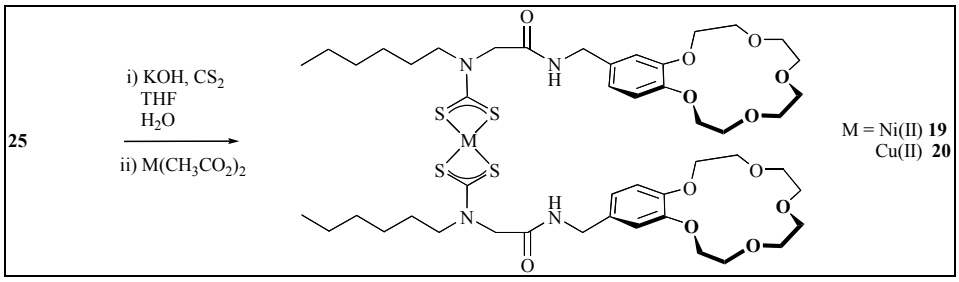

Scheme 2.7 *Synthesis of receptors **19** and **20***

Upon addition of water **19** and **20** precipitated out of the reaction mixture in 80% and 55% yields respectively. Both products analysed correctly for elemental composition.

Figure 2.16 shows the ^{13}C NMR of receptor **19** together with peak assignments.

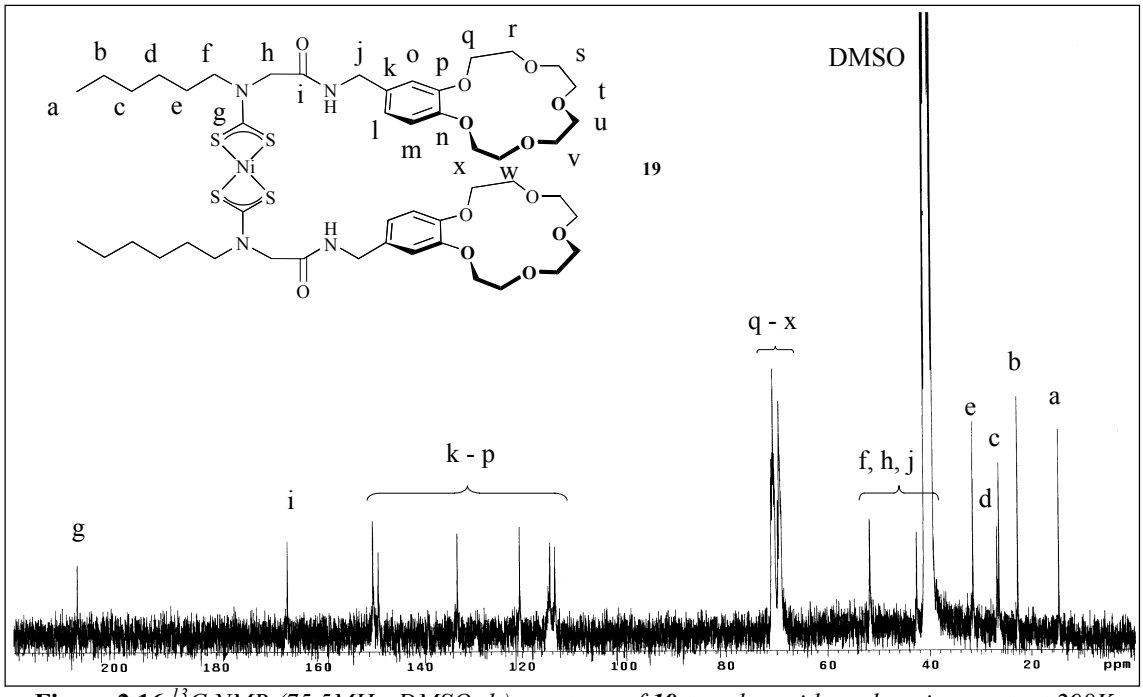

Figure 2.16 *^{13}C NMR (75.5MHz, DMSO-d_6) spectrum of **19** together with peak assignments at 298K*

The peak at 165.9 ppm is characteristic of a carbonyl resonance of an amide group.[10] Unfortunately, the peaks due to the solvent obscure one signal from the hexyl chain of the receptor molecule.

The ESMS of **19** and **20** showed peaks for both $[M + Na^+]^+$ and $[M + K^+]^+$ agreeing with calculated isotope patterns. The infrared spectrum of **20** showed a peak at 1558cm^{-1} due to a combination of a NH bend and CN stretch of the amide group.[15] ^{1}H, ^{1}H-^{1}H COSY NMR, UV/visible and electrochemistry were also used to confirm the structure of receptors **19** and **20**.

5.2 Ion-Pair Binding Studies

^{1}H NMR, UV/visible spectroscopies and electrochemistry were used to investigate the ion-pair binding properties of receptor **19**.

5.2.1 ^{1}H NMR Spectroscopy

^{1}H NMR titration experiments were conducted with acetate, benzoate, dihydrogen phosphate and chloride in DMSO-d_6:CD_2Cl_2 (4:1) solution. In order to investigate the ion-pair binding of receptor **19** the same four anions were titrated in the presence of one equivalent of KPF_6. **Table 2.13** highlights the change in chemical shift of the amide proton for these titrations.

Receptor	Anion	Change in amide proton shift (Δδ)				
		1 Eq	2 Eq	3 Eq	5 Eq	10 Eq
19	Acetate	0.31	0.57	0.76	1.09	1.54
	Benzoate	0.15	0.21	0.33	0.51	0.81
	Dihydrogen Phosphate	0.12	0.18	0.28	0.45	0.76
	Chloride	0.14	0.24	0.31	0.42	0.70
19·KPF_6	Acetate	0.56	0.97	1.20	1.38	1.65
	Benzoate	0.63	0.80	1.10	1.37	1.59
	Dihydrogen Phosphate	0.03	0.13	0.27	0.50	0.93
	Chloride	0.02	0.01	0.01	0.23	0.57

Table 2.13 *Change in chemical shift of the amide protons upon addition of anions as their TBA salts at 298K*

After the addition of ten equivalents of anion to **19** the magnitudes of downfield shifts of the amide proton were in the order acetate > benzoate > chloride ~ dihydrogen phosphate. This follows the basicities of acetate and benzoate,[20] however, dihydrogen phosphate is much more basic then chloride but this is not reflected in the NMR profiles. This maybe due to the specific design of the receptor.

A comparison of the titration curves between receptor **19** when titrated with acetate, in both the presence and absence of one equivalent of KPF_6, is shown in **Figure 2.17**.

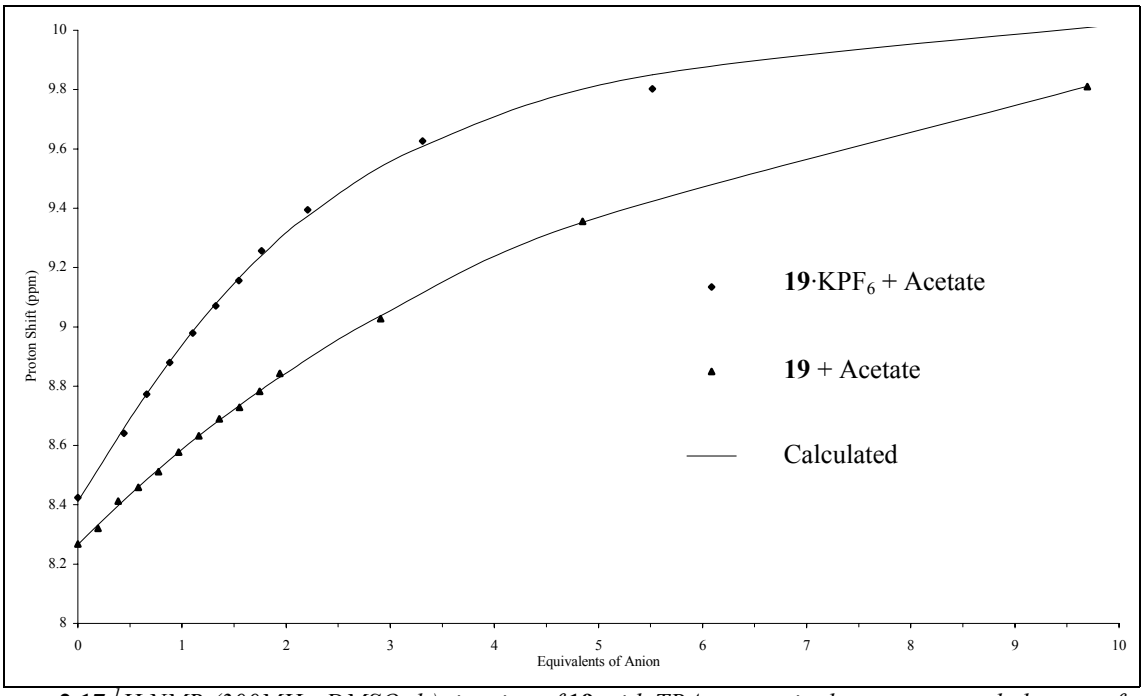

Figure 2.17 *^{1}H NMR (300MHz, DMSO-d_6) titration of* **19** *with TBA acetate in the presence and absence of one equivalent of KPF_6 at 298K*

The shape of the titration curve clearly indicates the increased strength in binding of the acetate anion when one equivalent of K^+ cation was present. EQNMR[48] analysis of this titration data gave stability constant values as shown in **Table 2.14**. Unfortunately, it was not possible to calculate stability constants by EQNMR[48] analysis of the resulting titration curves for chloride, benzoate and dihydrogen phosphate with or without one equivalent of K^+ present.

Stability Constant (M^{-1})	19 + Acetate	19·KPF_6 + Acetate
K_1	60	390
K_2	10	50

Table 2.14 *Stability constants for* ***19*** *with acetate in the presence and absence of potassium in DMSO-d_6 at 298K (Errors <10%)*

The stability constants of **19** with acetate are approximately six times larger in the presence of K^+. This is a demonstration of a positive cooperative effect where the bound metal ion enhances the anion binding due to electrostatic and pseudo-macrocyclic effects. The crown ether groups bind to the metal ion and the metal is coordinated in a 1:1 sandwich complex. Stronger binding is observed as the bound K^+ not only positions the positive ion in close

proximity to the anion binding site, but also preorganises the anion binding site thus combining ion-ion interactions with favourable entropic effects.

5.2.2. UV/visible Spectroscopy

The ion-pair binding capabilities of receptor **19** were studied by UV/visible spectroscopy. Three characteristic intense charge transfer bands were observed between 250nm and 500nm.[23] **Table 2.15** displays the wavelengths and molar extinction coefficients of **19** and $Ni(DTCEt_2)_2$ in MeCN:DMSO (4:1) solution.

Assignment	$Ni(DTCEt_2)_2$	19
LC	327 (36.9)	323 (25.0)
MLCT	399 (5.8)	382 (5.2)
MLCT	427 sh (1.6)	416 sh (1.7)

Table 2.15 *Wavelength λ/nm (molar extinction coefficient $\varepsilon/10^3$ $M^{-1}cm^{-1}$) of $Ni(DTCEt_2)_2$ and **19***

UV/visible spectroscopy was used to prove the number of copper(II) dithiocarbamate centres per receptor molecule by monitoring the oxidation of copper(II) to copper(III). **Figure 2.18** displays the change in UV/visible absorption spectrum when aliquots of copper(II) perchlorate were added to a $CHCl_3$:DMF (99:1) solution of receptor **20**.

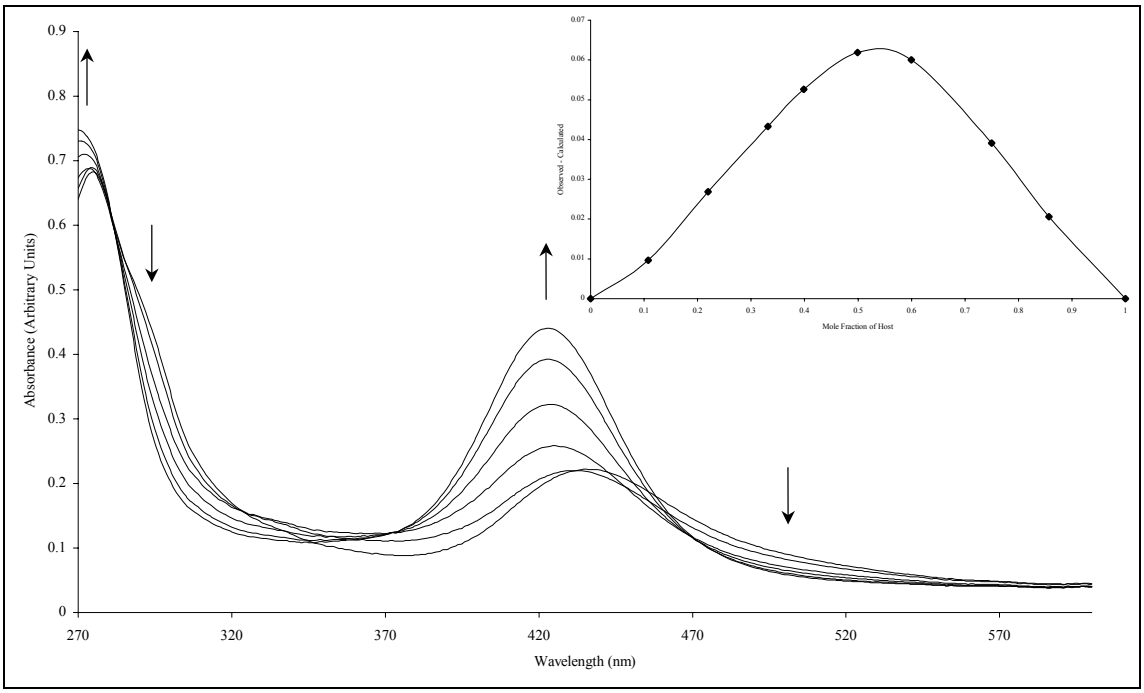

Figure 2.18 *UV/visible oxidation of **20** with copper(II) perchlorate in $CHCl_3$:DMF (99:1)*
*(Inset) Job Plot of **20** with copper(II) perchlorate in $CHCl_3$:DMF (99:1)*

The initial spectrum displays the characteristic peaks of a copper(II) dithiocarbamate spectrum. Upon oxidation a new peak was observed at 425nm corresponding to the copper(III) dithiocarbamate species.[7] The corresponding Job plot displayed a maximum at ~0.5 indicating that one equivalent of oxidant was required to carry out the oxidation,[26] confirming that receptor **20** contained one copper(II) dithiocarbamate centre.

Receptor **19** was titrated with acetate in the presence and absence of one equivalent of KPF_6. Large changes in the absorption spectrum were observed and Specfit™[27] was able to calculate stability constants.

Figure 2.19 shows the excellent calculated fit to the experimental data for receptor **19** with the acetate anion.

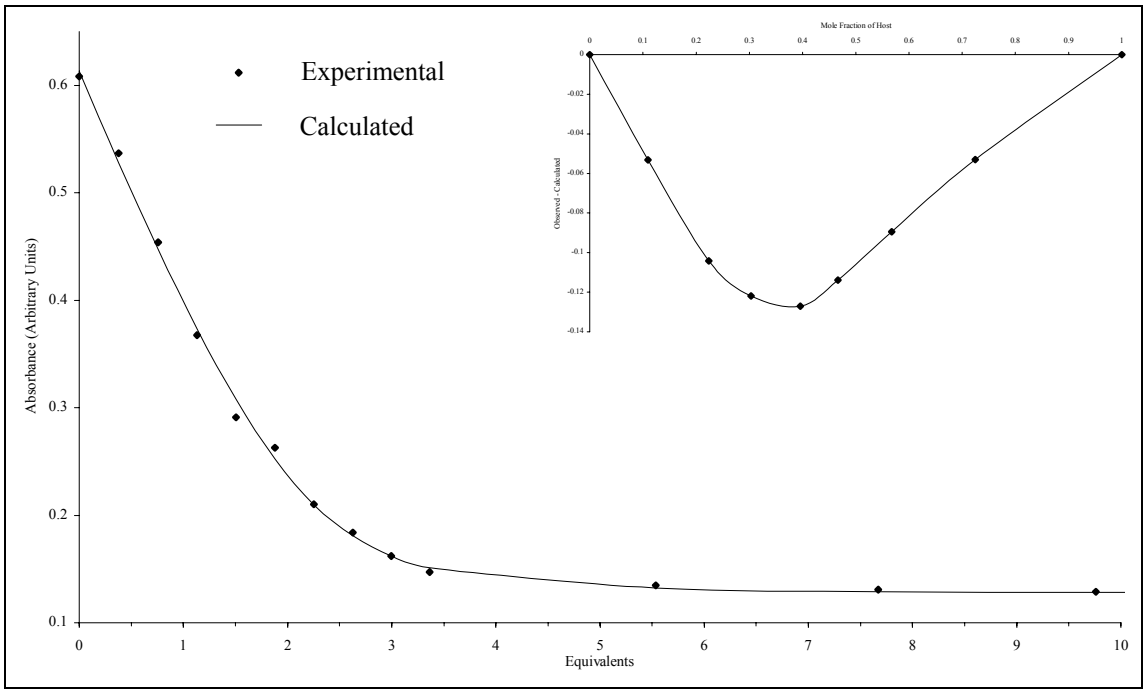

Figure 2.19 *UV/visible titration of **19** with TBA acetate in MeCN:DMSO (4:1) at 324 nm at 293K (Inset) Job Plot of **19** with TBA acetate in MeCN:DMSO (4:1)*

The Job plot shows a minimum at approximately 0.33 which indicates a 2:1, anion:receptor binding stoichiometry.[26] The calculated stability constants are displayed in **Table 2.16** together with that for receptor **4** for comparison.

Stability Constants	4 + Acetate	19 + Acetate	19.KPF_6 + Acetate
Log β_1	5.95 ± 0.12	4.72 ± 0.27	5.12 ± 0.14
Log β_2	11.71 ± 0.11	10.14 ± 0.15	10.74 ± 0.09

Table 2.16 *Stability constants with errors determined by UV/visible spectroscopy in MeCN:DMSO (4:1) at 293K*

The stability constants for receptor **19** are remarkably high for a neutral amide receptor. The stability constants are slightly lower than that of receptor **4** with the same anion. This is possibly due to a steric effect of the bulkier crown ether groups hindering anion binding. Pleasingly, when receptor **19** was titrated in the presence of one equivalent of K^+ the stability constants notably increased. This is in agreement with the NMR titration results and again demonstrates a cooperative ion-pair binding effect. The stability constants are higher from the UV/visible studies due to the less competitive solvent that was used.

Once again, upon the addition of an aliquot of benzoate and dihydrogen phosphate anions the UV/visible spectrum displayed a time delay before the absorption reached a constant value.

Two equivalents of anion were added to a solution of the receptor and the spectrum recorded at one-minute intervals until the absorption reached a constant value. **Table 2.17** displays the time taken for the absorption to reach a constant value.

Anion	Equilibration time (minutes)
Benzoate	6
Dihydrogen Phosphate	10

Table 2.17 *Time taken for the absorbance to reach a steady value after the addition of two equivalents of anion*

Interestingly, when chloride was added, very little change in the spectrum was observed. However, benzoate and dihydrogen phosphate required different amounts of time for the absorption to reach a constant value. Similar to **4**, this kinetic effect was not observed in the NMR binding studies. It may be either a conformational change in the molecule upon anion complexation or possibly the formation of a new complex. This is discussed further in **Chapter 3 Section 3.2.2**.

5.2.3 Copper(II) Electrochemistry

The redox properties of $Cu(DTCEt_2)_2$ and receptor **20** were studied by both cyclic and square wave voltammetry in $CHCl_3$:MeCN (4:1) solution.

Table 2.18 displays the electrochemical data for receptor **20** and $Cu(DTCEt_2)_2$.

	Cu(II)/Cu(III)		Cu(II)/Cu(I)	
	$Cu(DTCEt_2)_2$	**20**	**$Cu(DTCEt_2)_2$**	**20**
E_{pa} (V)	0.260	0.280	-0.900	-
E_{pc} (V)	0.135	0.180	-1.050	-0.740
ΔE_p (V)	0.125	0.100	0.150	-
I_{pa}/I_{pc}	1.0	1.1	0.8	-
E_p (V)	0.205	0.240	-0.805	-0.700

Table 2.18 *Electrochemical data of $Cu(DTCEt_2)_2$ and **20** in $CHCl_3$:MeCN (4:1) containing 0.1M $TBABF_4$, potentials given with reference to Ag/Ag^+ at 293K, scan rate = 100mVs^{-1}, E_p - peak potential in square wave voltammogram*

Receptor **20** displayed a quasi-reversible wave for the copper(II)/copper(III) couple. However, the copper(II)/copper(I) couple was irreversible which maybe due to the stereochemical change that occurs from square planar copper(II) to tetrahedral copper(I) upon reduction.[28] The oxidation and reduction waves of **20** were anodically shifted, compared to $Cu(DTCEt_2)_2$, due the neighbouring electron withdrawing amide group.

The response of $Cu(DTCEt_2)_2$ and **20** to the addition of anions was monitored by square wave voltammetry. The spectrum was recorded before and after the addition of five equivalents of both anions (as their TBA salts) and cations (as either their PF_6 or ClO_4 salts). The results are shown in **Table 2.19**.

Ion	ΔE Cu(II)/Cu(III) (mV)	
	$Cu(DTCEt_2)_2$	**20**
Acetate	25	60
Benzoate	15	70
Dihydrogen Phosphate	5	35
Chloride	-[a]	-[a]
Sodium	<5	-5[b]
Potassium	<5	-25[b]
Rubidium	<5	-15[b]

Table 2.19 *Cathodic shifts in the square wave voltammogram upon addition of 5 equivalents of anion or cation to $Cu(DTCEt_2)_2$ and **20** in $CHCl_3$:MeCN (4:1) containing 0.1M $TBABF_4$, potentials given with reference to Ag/Ag^+ at 293K (a - extra peaks observed, b – negative values indicate anodic shifts)*

Table 2.19 shows the cathodic shifts of the copper(II)/copper(III) couple were observed upon the addition of acetate, benzoate and dihydrogen phosphate anions to receptor **20**. These shifts were larger than those seen with $Cu(DTCEt_2)_2$. The shifts observed are indicative of anion complexation close to the copper(II) dithiocarbamate group.

Very small cathodic shifts were observed of the copper(II)/copper(I) couple both of the $Cu(DTCEt_2)_2$ compound and **20** when five equivalents of the anions were added to them. As noted previously, addition of five equivalents of chloride anion resulted two peaks being seen, one at higher potential and one a lower potential than that of the free receptor.

The control compound showed very little perturbation in either the copper(II)/copper(III) or copper(II)/copper(I) when Group 1 metal cations were added. However, when the same four cations were added to a solution of **20** small, but significant, anodic shifts were observed. This was because the crown ether groups coordinate the metal cation, decreasing the charge density near the redox centre and hence the oxidation process occurs at a more positive potential.[61]

Unfortunately due to solubility problems, it was not possible to carry out ion-pair electrochemical investigations.

5.2.4 Nickel(II) Electrochemistry

Receptor **19** and $Ni(DTCEt_2)_2$,[25] were studied in DMF by cyclic and square wave voltammetry (**Appendix 3**) and the data is shown in **Table 2.20**.

	Ni(II)/Ni(IV)			**Ni(II)/Ni(I)**	
	$Ni(DTCEt_2)_2$	**19**		**$Ni(DTCEt_2)_2$**	**19**
E_{pa} (V)	0.630	0.455	**E_{pa} (V)**	-1.800	-
E_p (V)	0.505	0.415	**E_{pc} (V)**	-1.980	-2.145
	Ni(IV)/Ni(III)		**ΔE (V)**	0.180	-
	$Ni(DTCEt_2)_2$	**19**	**I_{pa}/I_{pc}**	0.9	-
E_{pa} (V)	-0.225	0.245	**E_p (V)**	-1.870	-1.900
	Ni(IV)/Ni(III)				
	$Ni(DTCEt_2)_2$	**19**			
E_{pa} (V)	-0.770	-0.785			

Table 2.20 *Electrochemical data of the $Ni(DTCEt_2)_2$ and **21** in DMF containing 0.1M $TBABF_4$, potentials given with reference to Ag/Ag^+ at 293K, scan rate = 100mVs^{-1}, E_p - peak potential in square wave voltammogram*

Receptor **19** showed the normal electrochemical properties of a nickel(II) dithiocarbamate species.[29,32]

The effect on the nickel(II)/nickel(I) couple upon the addition of five equivalents of anion or cation to **19** was investigated using square wave voltammetry. The control compound displayed very small shifts upon addition of five equivalents of the four anions and Group 1 metal cations. Disappointingly **19** showed very little shift of the nickel(II)/nickel(I) redox couple upon the addition of either cationic of anionic guest species which maybe due to the competitive nature of this solvent.

6 Attempted Syntheses

Numerous attempts were made to synthesise variations of the molecules that have been discussed in the previous sections. The following sections outline the syntheses that were achieved and the problems encountered in isolating the receptor molecules.

6.1 Thiourea Receptors

Scheme 2.8 shows the synthesis of an acyclic thiourea precursor similar to the thiourea molecule **10**.

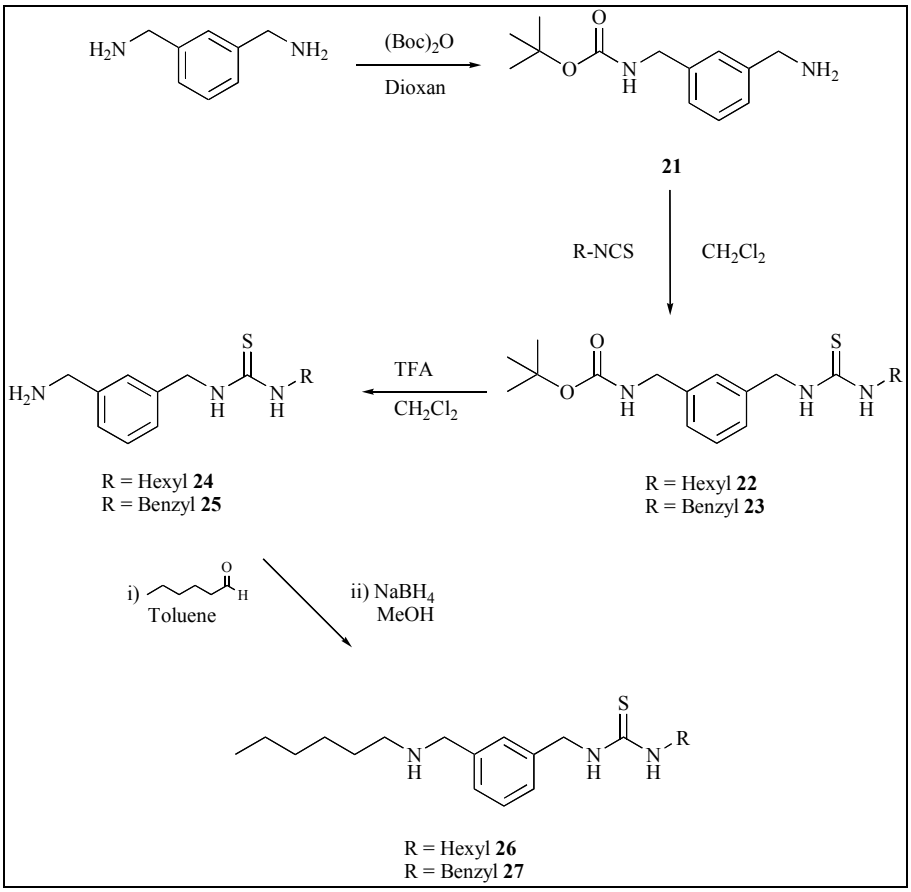

Scheme 2.8 *Synthesis of thiourea amines **26** and **27***

The commercially available *m*-xylene diamine was mono protected in 1,4-dioxane using a *tert*-butoxycarbonyl group (Boc) to form **21**.[34] This was condensed with either benzyl or hexyl isothiocyanate, to form corresponding thioureas[62] **22** and **23** in 88% and 95% yield respectively. The structures were confirmed by ^{1}H NMR spectroscopy showing characteristically broad resonances of the thiourea protons in the low field region. Interestingly, **22** displayed only one

thiourea peak at 6.30ppm, due to the similar proton environments, whereas **23** showed two peaks at 6.20ppm and 6.40ppm. These peaks disappeared when shaken with D_2O confirming that the protons were exchangable.[63] Treatment of **22** and **23** with trifluroacetic acid in dichloromethane removed the protecting group quantitatively.[41] The free amines were condensed with hexanal using Dean-Stark apparatus forming their respective imines,[42] which were reduced in methanol with sodium borohyride[43] forming **26** and **27**. Intermediates **21** - **27** were characterised by ^1H, ^1H-^1H COSY NMR and ESMS.

The conversion of these secondary amine precursors to receptor molecules is shown below in **Scheme 2.9**.

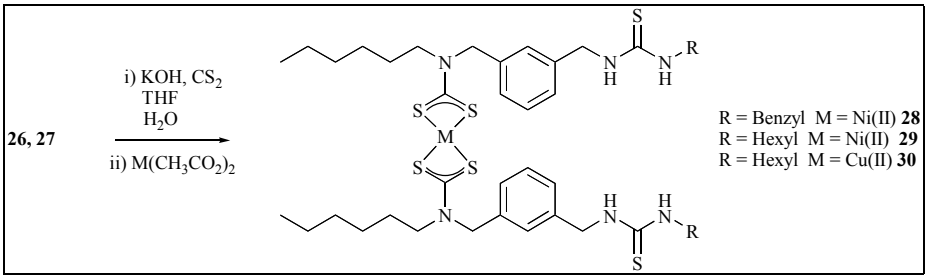

Scheme 2.9 *Attempted synthesis of receptor 28, 29 and **30***

The protocol for dithiocarbamate formation was the same as that used previously. Coloured powders were isolated and although ^1H NMR and ESMS of **28** revealed that although the target receptor had been formed, it was impure. Disappointingly, despite many attempts to purify by recrystallisation and running silica columns, it was not possible to isolate any of the desired receptors **28** - **30**.

6.2 Tris-Amide Receptor

Given the relative ease of synthesis of receptors **4** and **5**, syntheses of analogous receptors with iron (III) and cobalt (III) metal centres were attempted. This could potentially create an anion binding site with three convergent amide groups (**Scheme 2.10**).

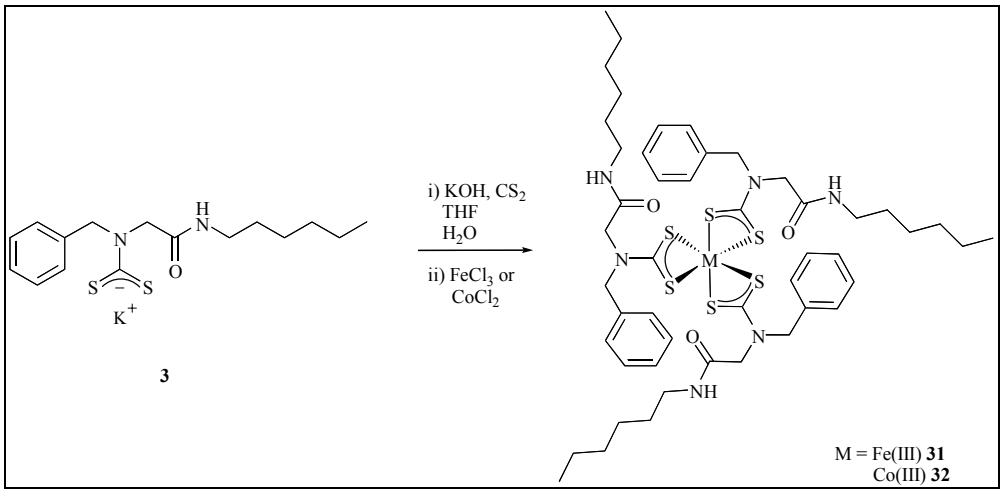

3

Scheme 2.10 *Potential tris-amide receptors **32** and **33***

Using the same method as described earlier, addition of either iron(III) chloride[4] or cobalt(II) chloride[4] to a solution of potassium dithiocarbamate salt **3** resulted in characteristic dark brown and dark green products respectively.

ESMS showed excellent match between calculated and experimental isotopic patterns of the iron(III) dithiocarbamate receptor **31**. Unfortunately the molecule was observed to decompose with time even when stored under vacuum. The cobalt(III) analogue was isolated by tituration from petroleum ether, however ESMS revealed no evidence of potential anion receptor **32**. This was surprising as both dithiocarbamate complexes of iron(III) and cobalt(III) are well known.[4]

7 Summary

A novel type of acyclic ion receptor has been developed based upon a transition metal dithiocarbamate moiety. The molecules were synthesised using simple organic chemistry and the final receptor assembled using base, carbon disulphide and a transition metal salt. Two anion receptors were prepared that contained amide and thiourea groups respectively, a cation receptor was synthesised that had a crown ether built into its architecture and an ion-pair receptor was synthesised that contained groups capable of binding both anions and cations.

The amide based anion receptor **4** reported anion binding via ^{1}H NMR and UV/visible spectroscopy. The latter technique was used to calculate a stability constant with acetate that was remarkably high for a neutral molecule in the competitive solvent mixture. Receptor **5** sensed the presence of anions in solution by electrochemical methods. Thiourea based receptor **11** displayed selectivity for binding dihydrogen phosphate over acetate, benzoate and chloride using ^{1}H NMR. Disappointingly, **11** did not recognise anions in electrochemical investigations, due to the competitive nature of the solvent DMF.

Cation receptor **15** displayed affinity for binding one potassium cation via an 'intramolecular sandwich' as shown by ESMS and ^{1}H NMR spectroscopy. Unfortunately, the cation binding was not reported by UV/visible spectroscopy, possibly due to the large distance between the cation binding site and the dithiocarbamate group.

Ion-pair receptor **19**, showed a six-fold enhancement of the stability constants upon binding acetate in the presence of a co-bound potassium ion, using ^{1}H NMR spectroscopy demonstrating a positive cooperative effect upon anion binding. UV/visible investigations confirmed the cooperative binding of potassium with acetate. Receptor **20** reported anion binding due by cathodic shifts in the square wave voltammogram of the copper(II)/copper(III) couple. The same receptor also sensed cations in solution by anodic shifts of the same redox couple.

In summary, the aim of this chapter was to develop a new type of acyclic ion receptor using a transition metal dithiocarbamate group to assemble the molecule and report the binding

phenomena. This goal has been achieved and ^{1}H NMR, UV/visible, ESMS spectroscopies and electrochemical methods have demonstrated that these receptors bind anions, cations and ion-pairs in a range of organic solvents.

8 References

[1] a) S. Leininger, B. Olenyuk, P. J. Stang, *Chem. Rev.*, 2000, **100**, 853; b) D. Philp, J. J. Stoddart, *Angew. Chem., Int. Ed. Engl.*, 1996, **35**, 1154; c) P. Tecilla, R. P. Dixon, G. Slobodkin, D. S. Alavi, D. H. Waldeck, A. D. Hamilton, *J. Am. Chem. Soc.*, 1990, **112**, 9408.
[2] M. Fujita, K. Umemoto, M. Yoshizawa, N. Fujita, T. Kusukawa, K. Biradha, *Chem. Commun.*, 2001, 509.
[3] M. Scherer, D. L. Caulder, D. W. Johnson, K. N. Raymond, *Angew. Chem., Int. Ed. Engl.*, 1999, **38**, 1588.
[4] a) D. Coucouvanis, *Prog. Inorg. Chem.*, 1979, **26**, 301; b) D. Coucouvanis, *Prog. Inorg. Chem.*, 1970, **11**, 233; c) D. J. Halls, *Mickro. Acta*, 1969, 62; d) J. Willemse, J. A. Cras, J. J. Steggerda, *Struct. Bonding*, 1976, **28**, 83; e) G. D. Thorn, R. A. Ludwig, *The Dithiocarbamates and Related Ligands*, Elsevier, 1962.
[5] O. D. Fox, M. G. B. Drew, E. J. S. Wilkinson, P. D. Beer, *Chem. Commun.*, 2000, 391.
[6] O. D. Fox, M. G. B. Drew, P. D. Beer, *Angew. Chem., Int. Ed. Engl.*, 2000, **39**, 136.
[7] P. D. Beer, N. G. Berry, M. G. B. Drew, O. D. Fox, M. E. Padilla-Tosta, S. Patell, *Chem. Commun.*, 2001, 199.
[8] A. J. Speziale, P. C. Hamm, *J. Am. Chem. Soc.*, 1956, **78**, 2556.
[9] L. M. Harwood, C. J. Moody, *Experimental Organic Chemistry Principles and Practice*, Blackwell Scientific Publishers, 1989, 750.
[10] L. M. Harwood, C. J. Moody, *Experimental Organic Chemistry Principles and Practice*, Blackwell Scientific Publishers, 1989, 330 & 751.
[11] L. M. Harwood, C. J. Moody, *Experimental Organic Chemistry Principles and Practice*, Blackwell Scientific Publishers, 1989, 292.
[12] G. Socrates, *Infrared Characteristic Group Frequencies*, 2nd Ed, J. Wiley & Sons, 104.
[13] G. Socrates, *Infrared Characteristic Group Frequencies*, 2nd Ed, J. Wiley & Sons, 32 & 119.
[14] L. M. Harwood, C. J. Moody, *Experimental Organic Chemistry Principles and Practice*, Blackwell Scientific Publishers, 1989, 286.
[15] G. Socrates, *Infrared Characteristic Group Frequencies*, 2nd Ed, J. Wiley & Sons, 105.
[16] R. Payne, R. J. Magee, J. Liesegang, *J. Elec. Spectr. Rel. Phen.*, 1985, **35**, 113.
[17] a) F. Bonati, R. Ugo, *J. Organomet. Chem.*, 1967, **10**, 257; b) H. C. Brinkhoff, A. M. Grotens, *Rec. Trav. Chim.*, 1971, **111**, 253.
[18] K. B. Pandeya, T. S. Waraich, R. C. Gaur, R. P. Singh, *J. Inorg. Nucl. Chem.*, 1981, 43, 3159.
[19] L. Radom, *J. Chem.*, 1976, **29**, 1635.
[20] a) S. Nishizawa, P. Buhlmann, M. Iwao, Y. Umeza, *Tetrahedron Lett.*, 1999, **36**, 6438; b) G. Aylward, T. Findlay, *SI Chemical Data*, 3rd Ed. J. Wiley & Sons, 136.
[21] C. S. Wilcox, *Frontiers of Supramolecular Organic Chemistry and Photochemistry*, Ed. H. J. Schneider, VCH, 1991, 129.
[22] L. Fielding, *Tetrahedron*, 2000, **56**, 6151.
[23] M. Castillo, J. J. Criado, B. Macias, M. V. Vaquero, *Trans. Met. Chem.*, 1986, **11**, 476.
[24] P. W. Atkins, *Physical Chemistry*, 4th Ed., 1990, 508.
[25] For synthesis and characterisation see the Experimental Chapter.
[26] K. A. Connors, *Binding Constants*, J. Wiley & Sons, 1987, 24.
[27] R. A. Binstead, A. D. Zuberbuhler, B. Jung, *Specfit 3.0.30*, Spectrum Software Associates, 2002.
[28] A. R. Hendrickson, R. L. Martin, N. M. Rohde, *Inorg. Chem.*, 1976, 15, 2115.
[29] A. M. Bond, R. L. Martin, *Coord. Chem. Rev.*, 1984, **54**, 23.
[30] R. Chant, A. R. Hendrickson, R. L. Martin, N. M. Rohde, *Aust. J. Chem.*, 1973, **26**, 2533.
[31] Southampton Electrochemical Group, *Instrumental Methods in Electrochemistry*, Ellis-Horwood, 1985, 185.
[32] A. R. Hendrickson, R. L. Martin, N. M. Rohde, *Inorg. Chem.*, 1975, **14**, 2980.
[33] F. G. Bordwell, D. J. Algrim, J. A. Harleson, *J. Am. Chem. Soc.*, 1988, **110**, 5903.

[34] A. P. Krapcho, C. S. Kuell, *Synth. Comm.*, 1990, **20**, 2559.
[35] G. M. Dyson, H. J. George, R. F. Hunter, *J. Chem. Soc.*, 1927, 436.
[36] G. Li, H. Tajima, T. Ohtani, *J. Org. Chem.*, 1997, **62**, 4539.
[37] T. Yamamoto, S. Sugiyama, K. Akimoto, K. Hayashi, *Org. Prep. Proc. Int.*, 1992, **24**, 346.
[38] D. M. Kneeland, K. Ariga, V. M. Lynch, C. Huang, E. V. Ansyln, *J. Am . Chem. Soc.*, 1993, **115**, 10042.
[39] S. Kim, K. Y. Yi, *J. Org. Chem.*, 1986, **51**, 2615.
[40] J. D. Robbins, J. R. Neal, *Syn. Comm.*, 1986, **16**, 891.
[41] M. Bodanszky, A. Bodanszky, *The Practice of Peptide Synthesis*, 2nd Ed., Springer Verlag, 1994.
[42] L. M. Harwood, C. J. Moody, *Experimental Organic Chemistry Principles and Practice*, Blackwell Scientific Publishers, 1989, 218.
[43] J. H. Billman, A. C. Diesing, *J. Org. Chem.*, 1957, **22**, 1068.
[44] H. L. M. van Gaal, J. W. Diesveld, F. W. Pijpers, J. G. M. van der Linden, *Inorg. Chem.*, 1979, **18**, 3251.
[45] H. Ie, S. Yi, S. Wu, *J. Chem. Soc. Perkin Trans. 2*, 1999, 2751.
[46] J. W. M. Nissink, H. Boerrigter, W. Verboom, D. N. Reinhoudt, J. H. van der Maas, *J. Chem. Soc. Perkin Trans. 2*, 1998, 2623.
[47] K. Hee. Lee, J. I. Hong, *Tetrahedron Lett.*, 2001, 6083.
[48] M. J. Hynes, *J. Chem. Soc. Dalton Trans.*, 1993, 311.
[49] E. Fan, S. A. Van Arman, S. Kincaid, A. D. Hamilton,, *J. Am. Chem. Soc.*, 1993, **115**, 369.
[50] C. J. Pedersen, *Angew. Chem., Int. Ed. Engl.*, 1988, **27**, 1021.
[51] J. Granell, M. L. H. Green, V. J. Lowe, S. R. Marder, P. Mountford, G. C. Saunders, N. M. Walker, *J. Chem. Soc. Dalton Trans.*, 1990, 605.
[52] P. R. Mallinson, M. R. Truter, *J. Chem. Soc. Perkin Trans. 2*, 1972, **12**, 1818.
[53] M. Ouchi, Y. Inone, Y. Liu, S. Nagamune, S. Nakamura, K.Wada, T. Hakushi, *Bull. Chem. Soc. Jpn.*, 1990, **63**, 1260.
[54] F. Camps, J. Coll, S. Ricart, *J. Heterocycl. Chem.*, 1983, **20**, 249.
[55] C. J. Pedersen, *Angew. Chem., Int. Ed. Engl.*, 1988, **27**, 1021.
[56] E. Leize, A. Jaffrezic, A. van Dorsselaer, *J. Mass. Spectrom.*, 1996, **31**, 537.
[57] F. E. Lyte, L. M. Petrosky, L. R. Carlson, *Anal. Chim. Acta*, 1971, **57**, 239.
[58] P. R. Mallinson, M. R. Truter, *J. Chem. Soc. Perkin Trans. 2*, 1972, **12**, 1818.
[59] J. Cookson, *Part II Thesis*, Oxford University, 2000, 21.
[60] R. N. Salvatore, C. H. Yoon, K. W. Jung, *Tetrahedron*, 2001, **57**, 7785.
[61] P. D. Beer, P. A. Gale, G. Z. Chen, *Coord. Chem. Rev.*, 1999, **185**, 3.
[62] C. Raposo, M. Martin, V. Weinrich, M. L. Mussons, V. Alcazar, M. C. Caballero, J. R. Moran, *Chem. Lett.*, 1995, 759.
[63] L. M. Harwood, C. J. Moody, *Experimental Organic Chemistry Principles and Practice*, Blackwell Scientific Publishers, 1989, 357.

Chapter Three

Macrocyclic Anion and Cation Dithiocarbamate Receptors

1 Introduction

The previous chapter described the use of transition metal dithiocarbamates to create acyclic receptors capable of binding anionic, cationic or ion-pair guest species. The work described in this chapter uses similar metal directed self-assembly methods to construct novel macrocyclic receptor molecules for anionic guest species.

Creating macrocyclic receptors using traditional covalent synthesis is synthetically challenging. However, macrocyclic receptor molecules that have been synthesised often possess remarkable selectivity in their binding. For example, [15]crown-5 displays remarkable selectivity for sodium cation over other Group 1 metal cations (see **Chapter 1 Section 2.2**).

In contrast to cation receptors, there are only a limited number of macrocyclic receptors for anions, however one example has been reported by Beer (**Figure 3.1**).[1]

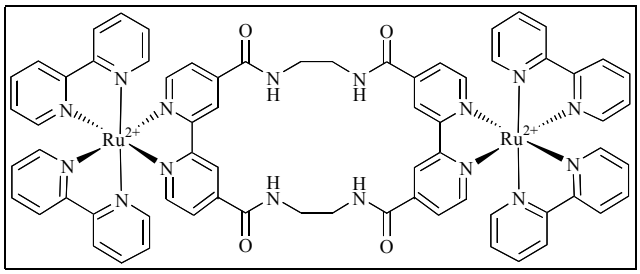

Figure 3.1 *Beer's macrocyclic receptor*

This receptor forms extremely stable 1:1 complexes with chloride even in competitive solvents such as DMSO while no evidence of binding dihydrogen phosphate was seen. This remarkable selectivity maybe attributed to the rigid structure of the macrocycle, as the acyclic analogue of this receptor displayed stronger binding of dihydrogen phosphate over chloride. The larger size and tetrahedral shape of dihydrogen phosphate made this anion non-complementary for the macrocyclic receptor's cavity.

The dithiocarbamate group has been successfully employed to create the macrocyclic compound shown in **Figure 3.2**.[2]

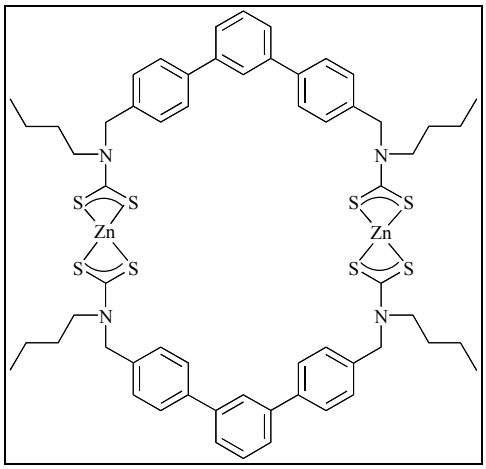

Figure 3.2 *Self-assembled terphenyl macrocycle*

This self-assembled macrocycle was shown to form 1:1 inclusion complexes with 4,4'-bipyridyl by NMR and mass spectrometry techniques. The formation of the complex was driven by the coordination of the pyridyl nitrogens to the zinc(II) metal centres.

The work in the first part of this chapter uses the dithiocarbamate group to create macrocyclic complexes using metal directed self-assembly of simple organic fragments. These fragments possess anion binding units to enable the target macrocycle to complex negatively charged guest species.

A schematic of the receptor's design is illustrated in **Figure 3.3**.

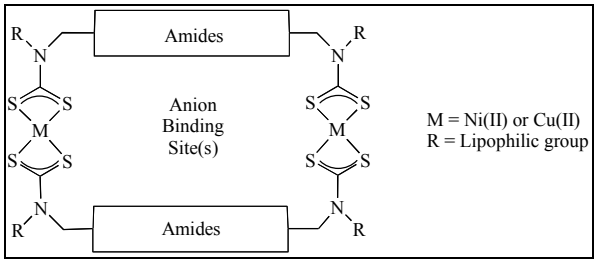

Figure 3.3 *Schematic of target receptors*

The anion receptors possess multiple amide groups for anion binding (see **Chapter 1 Section 3.4**) and incorporation of a lipophilic group (R) may confer solubility in a range of organic solvents. The choice of transition metal centre allows various techniques to be employed for monitoring the anion binding.

2 Macrocyclic Anion Dithiocarbamate Receptors

The following sections detail the synthesis and characterisation of a new type of macrocyclic anion receptor. The synthesis has incorporated four amide functionalities into the structure of the metal directed self-assembled macrocyclic receptor. A series of related macrocycles were synthesised by varying the 'spacer' group between the amide groups.

2.1 Synthesis and Characterisation

The synthesis of the desired receptors required that amide groups to be incorporated into a rigid hydrocarbon backbone. **Scheme 3.1** shows the synthesis of bis-amide molecules **33 - 37**.

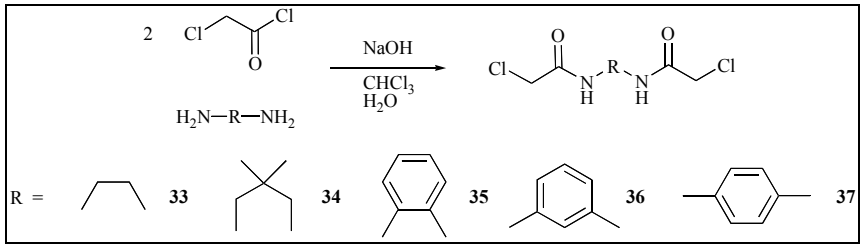

Scheme 3.1 *Synthesis of bis-amide precursors 33 - 37*

The bis-amide molecules **33 - 36** were synthesised using the same literature procedure.[3] One equivalent of diamine was dissolved in chloroform and excess aqueous sodium hydroxide was added. Two equivalents of chloroacetyl chloride was added drop wise to the mixture and the bis-amide product precipitated in ~80% yield.

In contrast, **37** was synthesised by adding an eight-fold excess of the diamine to a chloroform solution of the acid chloride. The product was isolated as a white powder in quantitative yield. The ^{1}H NMR revealed a singlet at 10.39ppm characteristic of an aromatic amide group.[4]

These bis-amide molecules needed to be transformed into secondary amines to enable the transition metal macrocycle to be synthesised. The alkyl chlorides were converted into corresponding secondary amines via **Scheme 3.2**.

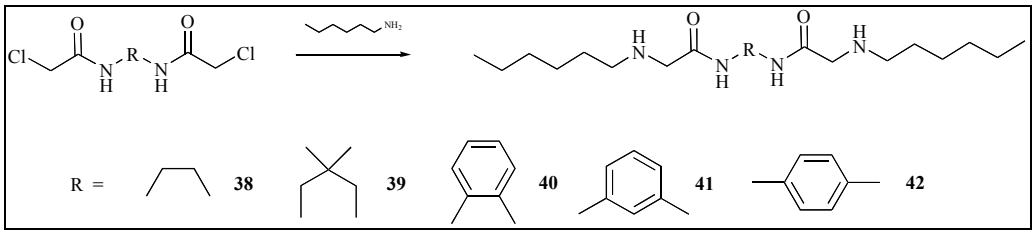

Scheme 3.2 *Synthesis of bis-amine precursors **40 - 44***

Portion wise addition of **33 - 36** to an excess of hexylamine and subsequent heating for 15 hours gave the bis-amine ligands **39 - 42** in ~60% yield.[5] Molecule **38** was highly insoluble in hexylamine and so a small amount *N*,*N*-dimethyl formamide was added to solubilise the bis-amide, resulting in the desired secondary amine being synthesised in a 38% yield. The diamines **38 - 42** were characterised by ^{1}H, ^{1}H-^{1}H COSY NMR and electrospray mass spectrometry (ESMS).

The receptor molecules were synthesised using the standard transition metal dithiocarbamate formation protocol as shown in **Scheme 3.3**.

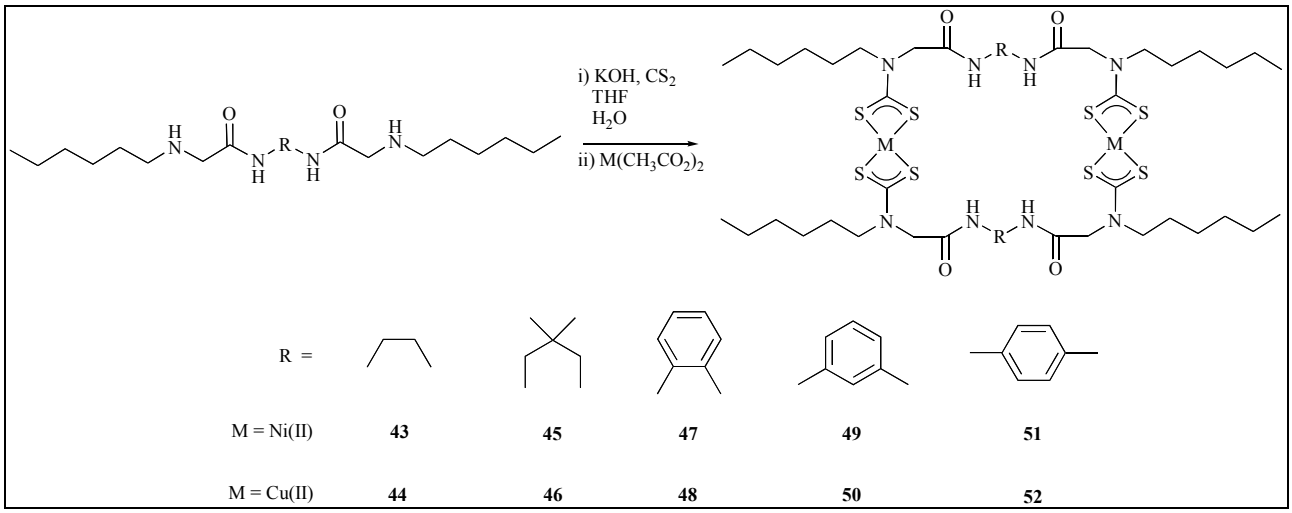

Scheme 3.3 *Synthesis of receptors **43 - 52***

Two equivalents of potassium hydroxide and two equivalents of carbon disulphide were added to one equivalent of the secondary amine, in a tetrahydrofuran:water mixture, forming the potassium dithiocarbamate salt. The respective dinuclear dinuclear transition metal dithiocarbamate macrocycle was synthesised by addition of one equivalent of nickel(II) or copper(II) acetate and stirring for 15 hours.[6] Upon the addition of water, the products precipitated and were isolated in yields of 20% - 70%.

Receptors **43** - **52** were characterised by ^{1}H, ^{1}H-^{1}H COSY, ^{1}H-^{13}C HSQC, ^{13}C NMR, ESMS, UV/visible, electrochemistry, infrared, magnetism, electron paramagnetic resonance and elemental analysis. A summary of the receptors is shown in **Appendix 11**.

2.1.1 ^{1}H NMR Spectroscopy

The ^{1}H and ^{1}H-^{1}H COSY NMR spectra of receptor **47** together with assignments are shown in **Figure 3.4**.

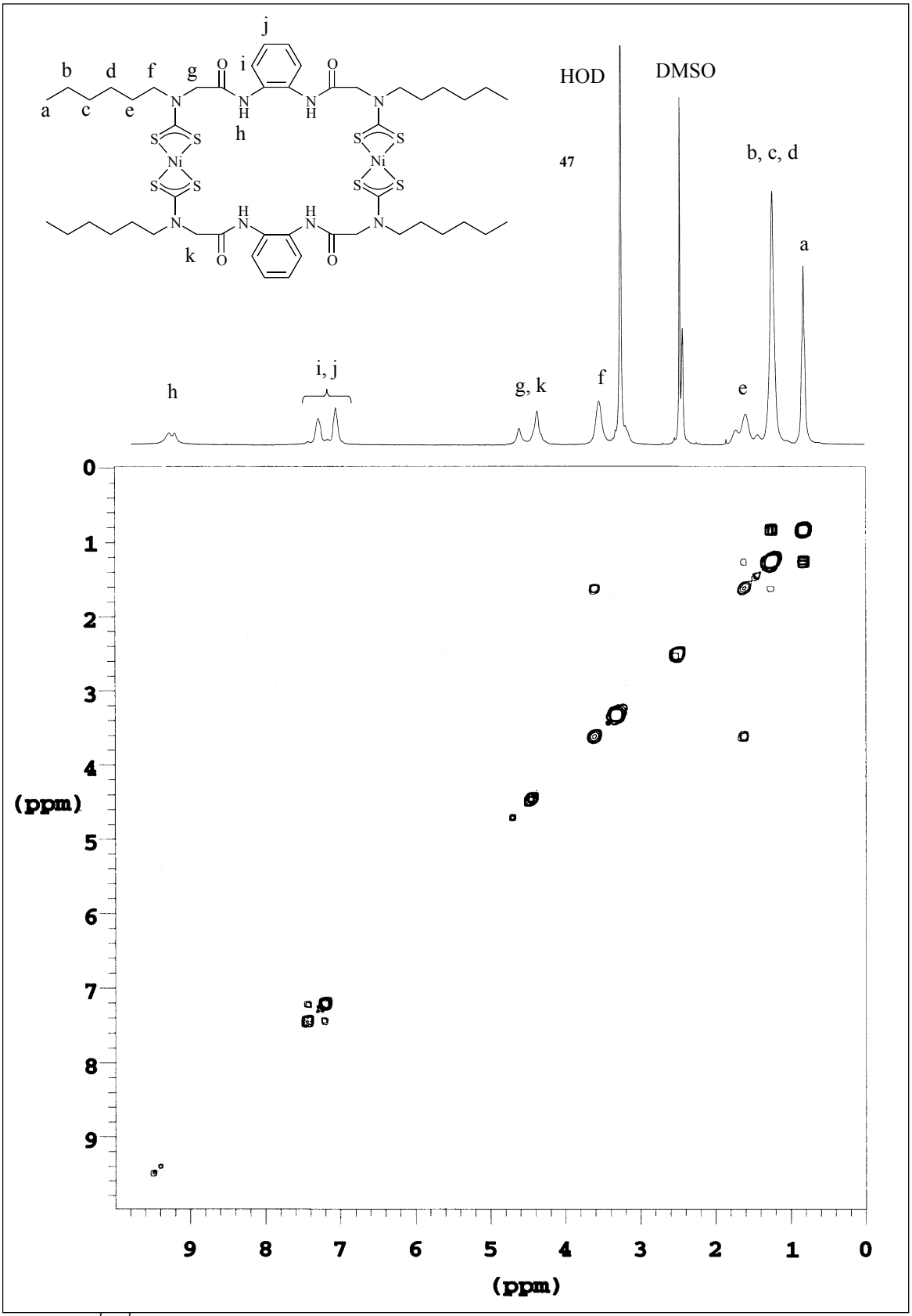

Figure 3.4 *^{1}H-^{1}H COSY NMR (300MHz, DMSO-d_6) spectrum of **47** together with peak assignments at 298K*

Surprisingly, the protons adjacent to the amide group (g & k) appeared as two broad peaks of equal intensity. This is because the receptor is in a conformation that positions these protons in inequivalent environments. Consequently, the hexyl protons are in slightly different

environments and so broadness was observed in all resonances. This phenomena was observed for all the nickel(II) dithiocarbamate receptors **43**, **45**, **47**, **49** and **51**. The ^{1}H-^{1}H COSY spectrum clearly shows the coupling of protons along the hexyl chain (a - f) and the coupling of the two sets of protons on the aromatic ring (i + j).

2.1.2 Variable Temperature ^{1}H NMR Spectroscopy

Variable temperature NMR can be used to investigate the dynamics of molecules in solution.[7] The temperature dependence of the ^{1}H NMR spectrum of receptor **47**, in DMSO-d_6, was studied between 298K and 373K. **Figure 3.5** shows the ^{1}H NMR spectra at various temperatures.

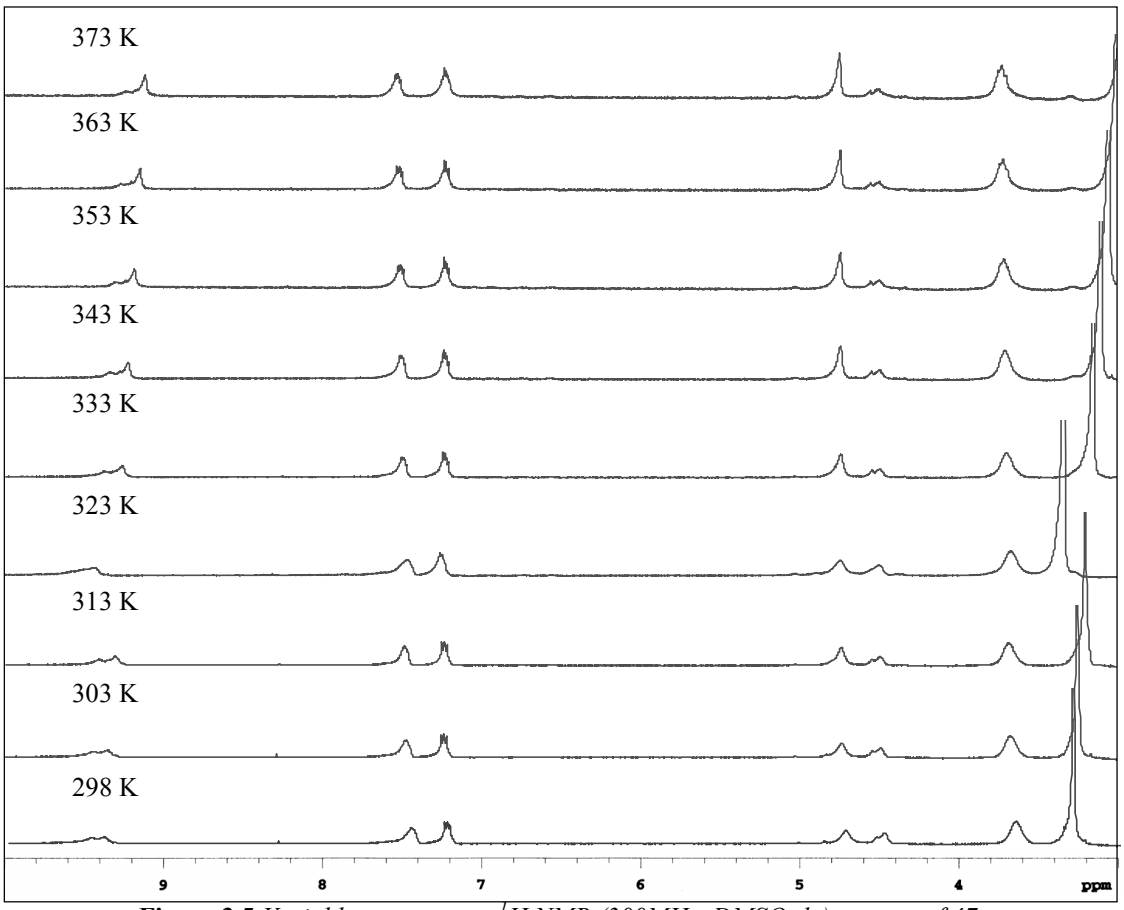

Figure 3.5 *Variable temperature ^{1}H NMR (300MHz, DMSO-d_6) spectra of **47***

The peaks corresponding to the protons adjacent to the amide unit were observed between 4ppm and 5ppm. Two resonances of roughly equal intensity were detected at 298K. As the temperature was elevated, the intensity of the peak at higher ppm increased while the other peak decreased proportionally. However, even at 398K there was still a small peak seen at

4.47ppm. After cooling to 298K an identical set of signals was observed as at the start of the experiment.

If the structure was conformationally mobile then it was expected that a single signal would be observed at high temperatures. This was not observed thus the structure did not have easily inter-convertible conformers. It was not possible to investigate the effect of lowering the temperature as the macrocycle was only soluble in DMSO which freezes at 291K.

2.1.3 ^{13}C NMR Spectroscopy

Figure 3.6 shows the ^{13}C NMR spectrum in DMSO-d_6 of **47** together with peak assignments.

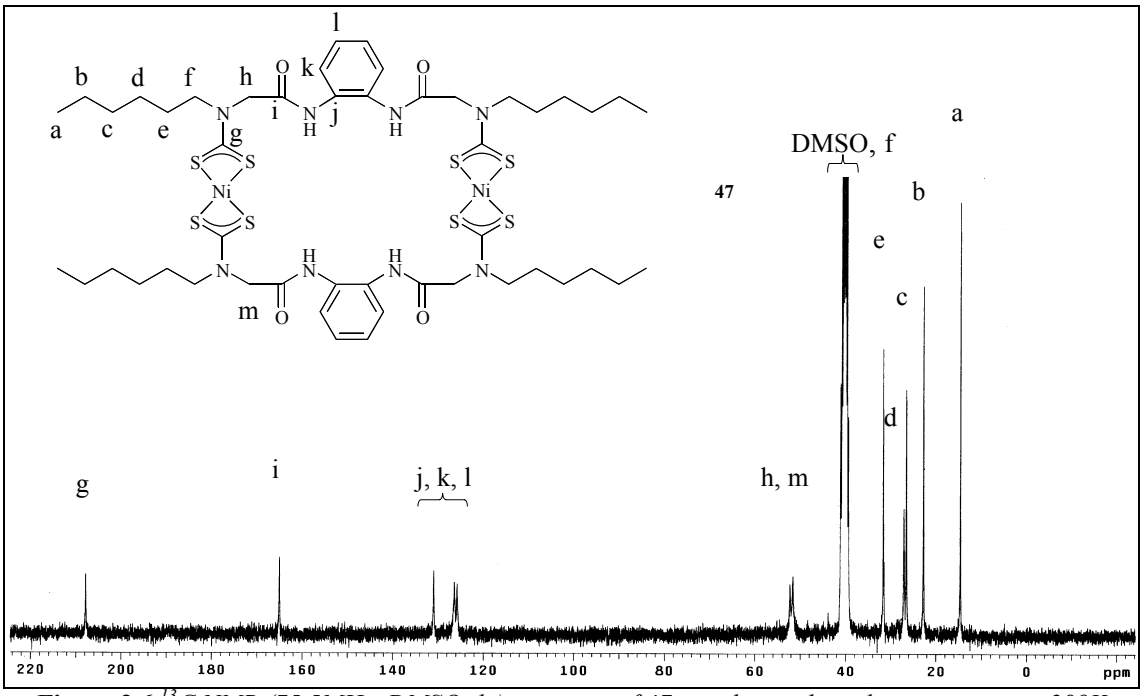

Figure 3.6 *^{13}C NMR (75.5MHz, DMSO-d_6) spectrum of **47** together with peak assignments at 298K*

The peak at 207.8ppm was characteristic of a nickel(II) dithiocarbamate species.[8] Two distinct signals were observed at 52.2ppm and 51.5ppm are due to the carbon atoms adjacent to the amide groups (h and m). The presence of two peaks confirms that that the carbon atoms are in different environments. Analogous acyclic receptors display just one signal in this region (see **Chapter 2 Section 3.1**). The presence of two peaks agreed with the ^{1}H NMR evidence that the CH_2 groups next to the amides are in non-equivalent environments.

The effect on the ^{13}C NMR spectrum upon increasing the temperature was also studied and the spectrum at 373K displayed very little difference to that displayed at 298K. Thus at high temperature these atoms do not experience equivalent magnetic environments agreeing with the ^{1}H NMR variable temperature study.

2.1.4 Crystal Structure of Receptor 47

Crystals of **47** suitable for X-ray analysis were grown from a chloroform/acetonitrile solution and the structure solved by Dr. A. Cowley, Oxford University (**Appendix 5**). The solid-state crystal structure is shown in **Figure 3.7**.

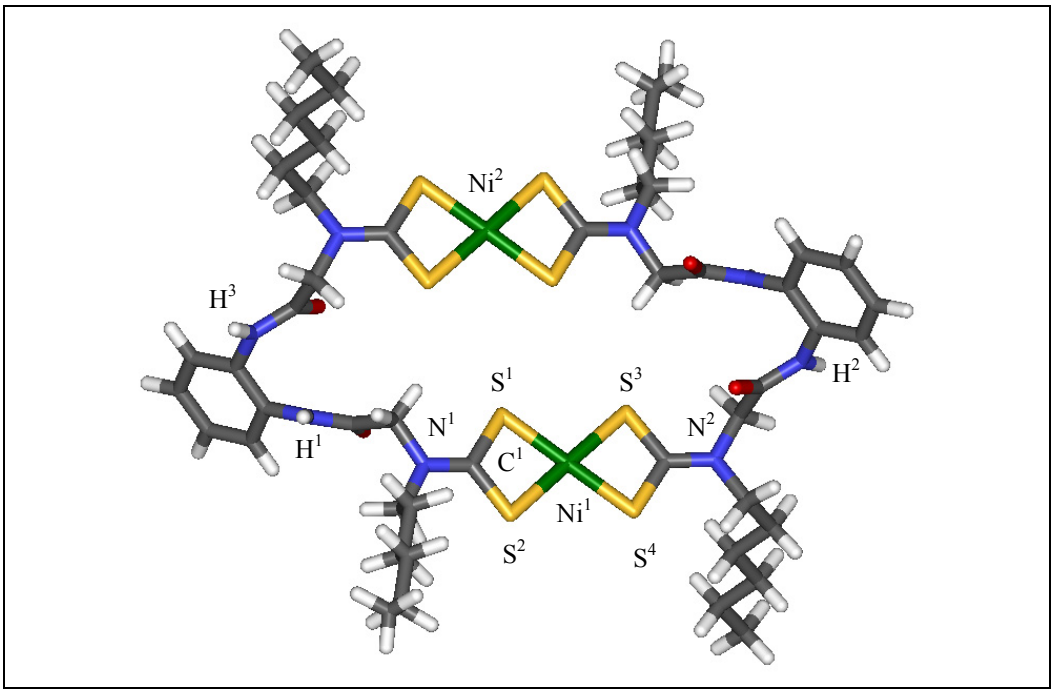

Figure 3.7 *Crystal structure of **47** (C - grey, N - blue, O - red, S - yellow, Ni - green)*

The structure displayed a crystallographic centre of symmetry and selected structural parameters are given in **Table 3.1**.

Distance (Å)				Angle (°)	
Ni^1-Ni^2	6.70	**H^1-H^2**	14.11	**S^1-Ni^1-S^2**	79.5
Ni-S^1	2.21	**H^1-H^3**	3.02	**S^3-Ni^1-S^4**	79.4
Ni-S^2	2.20	**N^1-C^1**	1.33	**N^1-Ni^1-N^2**	3.2
Ni-S^3	2.21				
Ni-S^4	2.20				

Table 3.1 *Selected structural parameters of **47***

As expected the nickel(II) dithiocarbamate group forms an almost square planar linkage[9] with the nickel atom lying only 3.2° out of the plane. The nickel-nickel distance is quite large (6.70Å) and the alkyl chains attached to N^1 and N^2 are disposed on opposite sides of the molecule. The distance between N^1 and C^1 is significantly less than that of a single carbon nitrogen bond (~1.47Å[10]) but more than a double carbon nitrogen bond (~1.30Å[10]). This is due to the considerable double bond character between these two atoms.[6]

Importantly, the distance from H^1 to H^2 is too large for simple anions (e.g, acetate, benzoate, chloride, dihydrogen phosphate) to cooperatively bind with both sets of amide groups at either end of the molecule simultaneously. However, the H^1-H^3 distance is small enough that bidentate anions, such as acetate and benzoate, may bind to the proximate amide groups cooperatively.

The X-ray data confirmed what was inferred from the ^1H and ^{13}C NMR evidence; the CH_2 groups adjacent to the amide groups were in similar, but not identical, environments. It is difficult for these CH_2s to adopt the same environment, as any rotation in the macrocycle would impart a strain upon the system that would be energetically unfavourable. This explains the presence of two signals observed in the ^1H and ^{13}C NMR spectra and their small changes upon raising the temperature.

Interestingly, the crystal packing of **47** revealed the formation of intermolecular hydrogen bonding interactions between adjacent macrocycles (**Figure 3.8**).

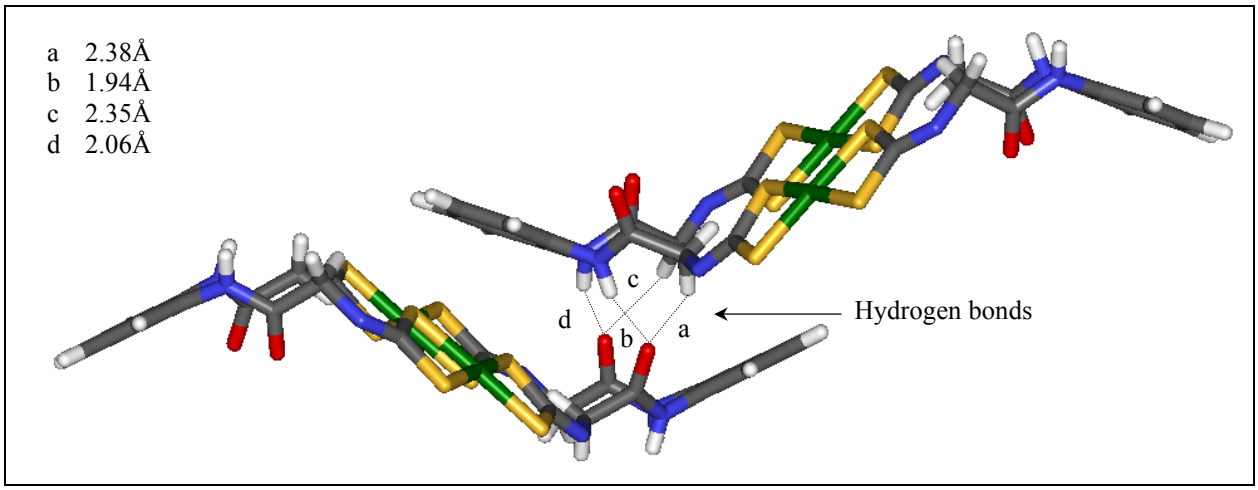

Figure 3.8 *Crystal structure of two molecules of* ***47*** *showing intramolecular hydrogen bonding (C - grey, N - blue, O - red, S - yellow, Ni – green, hexyl chains omitted for clarity)*

Hydrogen bonds are seen between the amide protons of one macrocycle to the carbonyl oxygens of the neighbouring macrocycle. In addition, there are hydrogen bonds between the carbonyl oxygen and one of the hydrogens attached to the carbon α to the dithiocarbamate nitrogen. This is due to the double bond character between the nitrogen and carbon atoms of the dithiocarbamate moiety producing a slight positive charge on the nitrogen atom. This in turn draws electron density away from the carbon atoms α to it, leaving the hydrogens slightly electron deficient and able to form hydrogen bonds with the carbonyl oxygen of the neighbouring molecule.

The hydrogen bonding manifested itself throughout the whole crystal structure and an extended view of the crystal packing is shown in **Figure 3.9**.

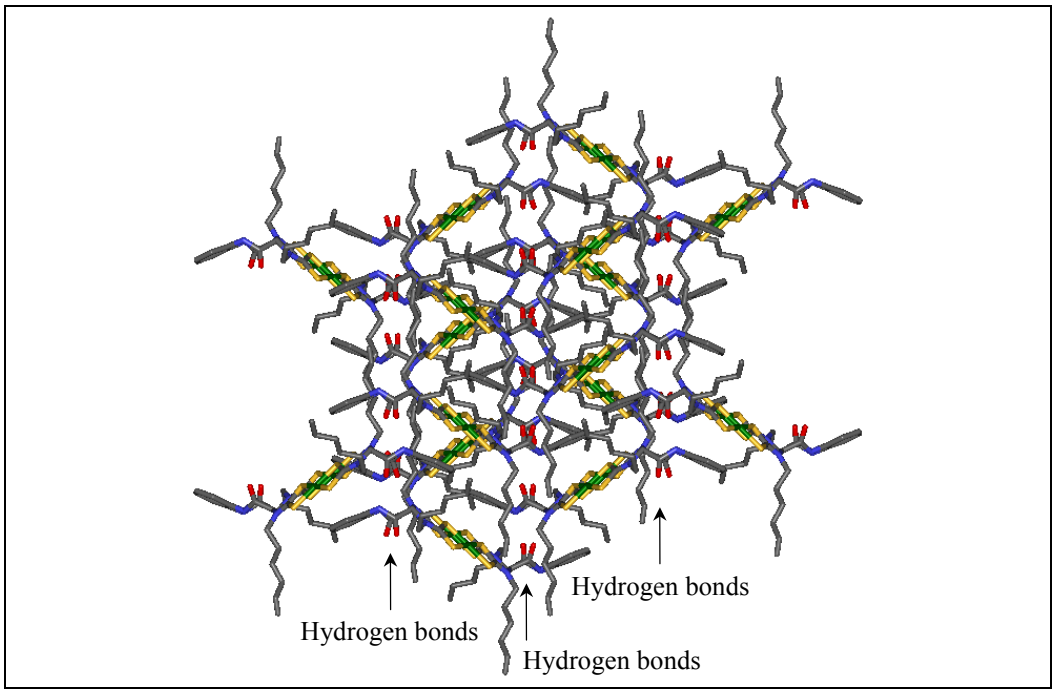

Figure 3.9 *Hydrogen bonding network of receptor **47***
(C - grey, N - blue, O - red, S - yellow, Ni – green, hydrogens omitted for clarity)

The 'lines' of hydrogen bond donor-acceptor interactions can be clearly seen running throughout the entire structure.

2.1.5 Electrospray Mass Spectrometry

Receptors **43** - **52** were further characterised by electrospray mass spectrometry (ESMS) (**Appendix 4**). It was possible to observe peaks due to the copper(II) dithiocarbamate receptors due to the inherent oxidation properties of the ionisation process.[11] This oxidises the transition metal centre creating a positive charge on the molecule enabling the species to be observed. However, the intensity of the peaks of both the nickel(II) and copper(II) receptors were greatly increased when a small amount of potassium hexafluorophosphate (KPF_6) was co-injected into the spectrometer.

Figure 3.10 reveals excellent agreement between calculated and experimental isotope patterns of receptor **47** with an associated potassium ion. Similar spectra were recorded for all receptors **43** - **52**.

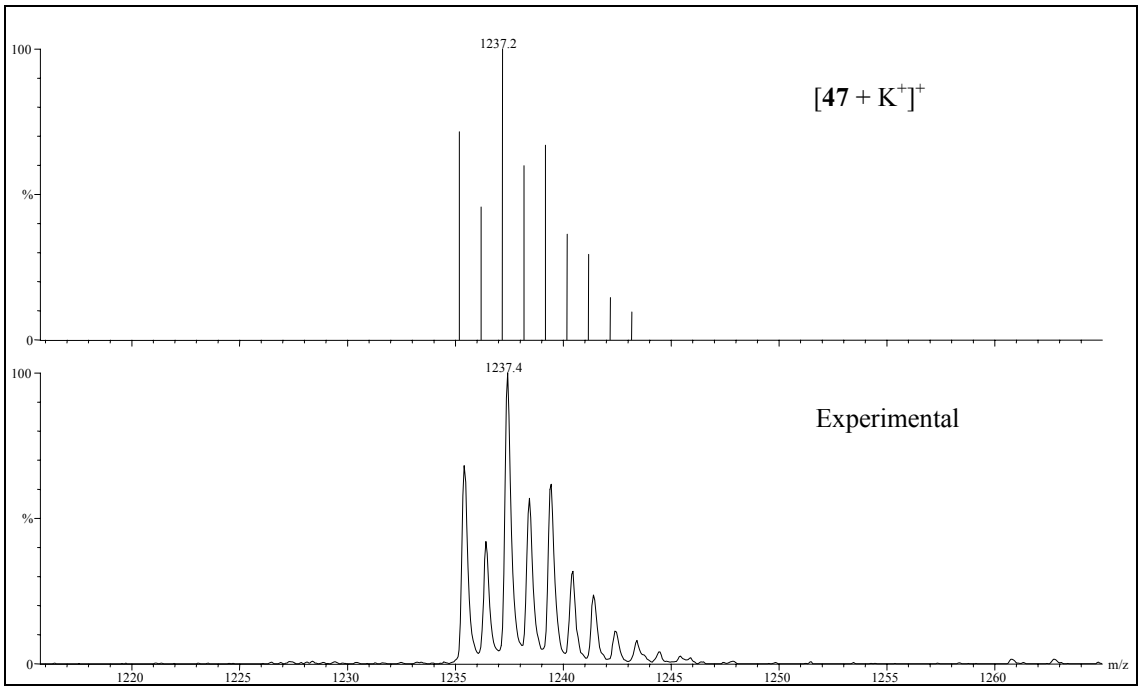

Figure 3.10 *ESMS of 47 together with the isotope model*

ESMS can also be performed using negative ionisation mode. **Figure 3.11** shows the match between the calculated and experimental spectra for receptor **47**. One proton is lost from each receptor molecule leaving a negative charge on the macrocycle.

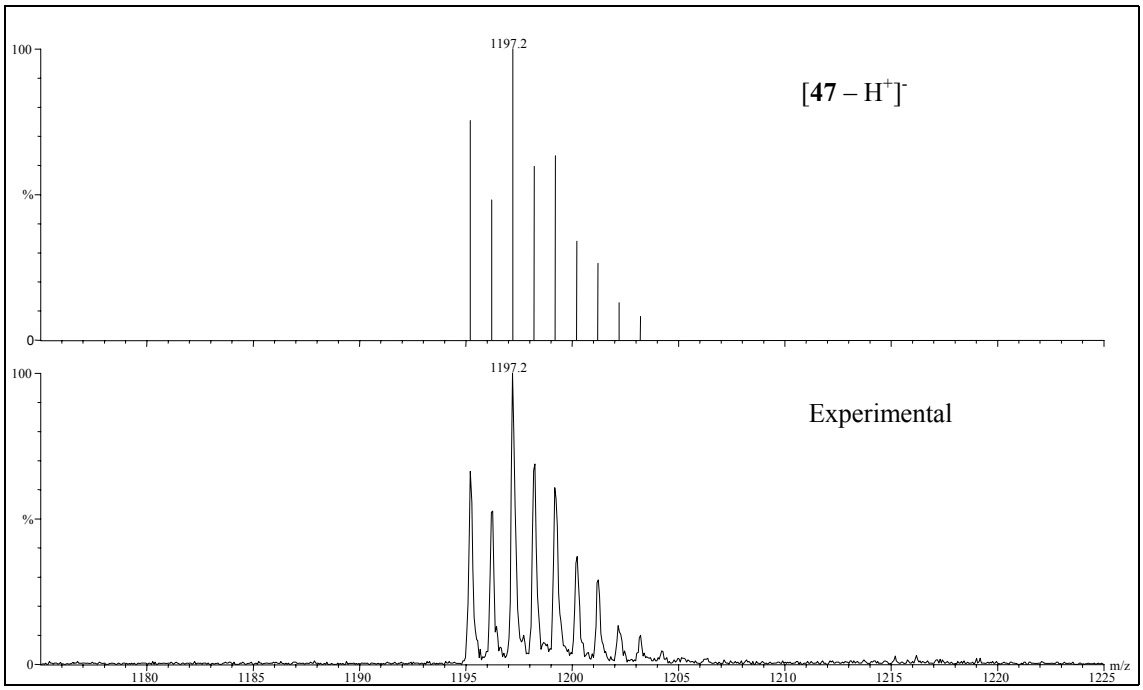

Figure 3.11 *ESMS of 47 together with the isotope model*

All the macrocycles were also observed in the mass spectrum by oxidising the transition metal centres.[12] Nitrosonium tetrafluoroborate ($NOBF_4$) was used with the copper(II) based macrocycles to oxidise the metal centres from copper(II) to copper(III). The observed spectrum of **48** after treatment with excess $NOBF_4$ is displayed in **Figure 3.12**.

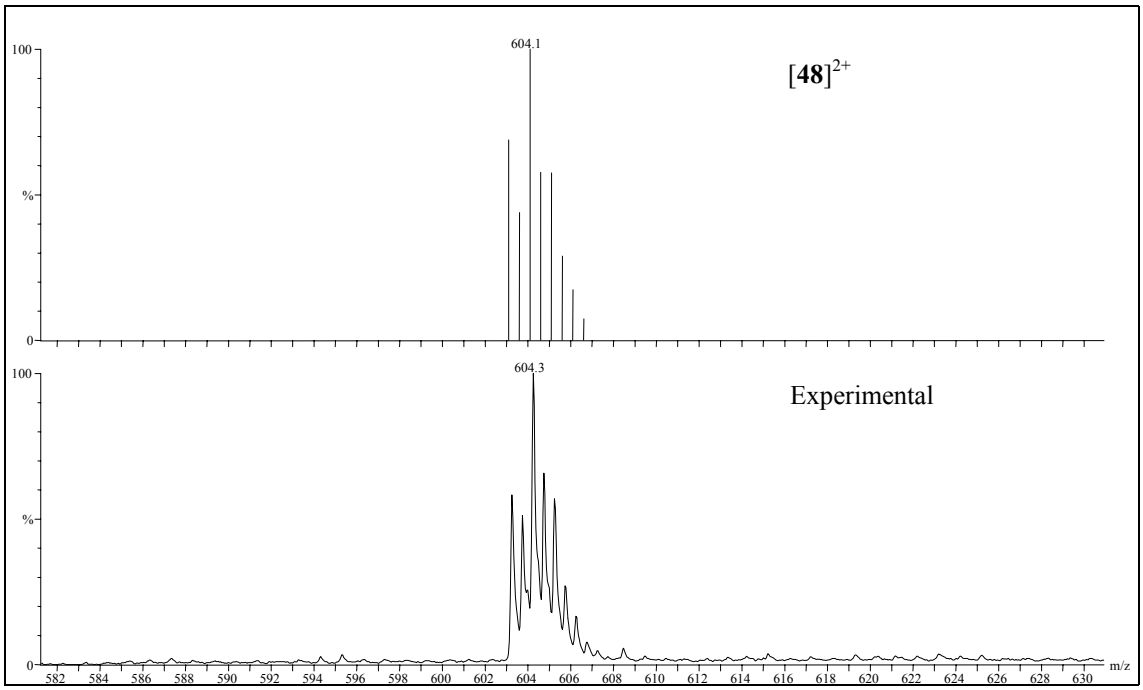

Figure 3.12 *ESMS of **48** together with the isotope model*

The spectrum showed a peak spacing of half a mass unit. This is consistent with the formation of a dicationic species, proving that each macrocycle contains two copper(II) dithiocarbamate centres.

Similar experiments were performed with the nickel(II) macrocycles using $NOBF_4$ as oxidant. This will be discussed further in **Chapter 5 Section 2**. The observed spectra displayed excellent agreement with the isotopic models, again confirming the presence of two metal centres for all the nickel(II) dithiocarbamate macrocycles.

2.1.6 UV/visible Spectroscopy

Nickel(II) dithiocarbamate ligands display absorptions in the UV region at ~230nm and ~320nm due to ligand centred (LC) π-π^* transitions.[13] Metal to ligand charge transfer (MLCT) peaks are also seen at ~400nm and ~430nm, while at ~490nm and ~650nm d-d, Laporte forbidden, spin allowed transitions occur.

All the nickel(II) receptors showed three characteristic peaks between 250nm and 500nm. **Table 3.2** shows the UV/visible spectroscopic data for the receptors and the control compound, nickel(II) bis(*N*,*N*-diethyl dithiocarbamate) ($Ni(DTCEt_2)_2$),[14] in MeCN:DMSO (4:1) solution

(**Appendix 2**). The higher energy LC transition was obscured by absorption of the DMSO and the d-d transitions were not observed due to their very low intensity.[15]

Assignment	$Ni(DTCEt_2)_2$	43	45	47	49	51
LC	327 (36.9)	324 (16.0)	322 (68.7)	323 (53.8)	322 (72.7)	323 (53.5)
MLCT	399 (5.8)	385 (2.81)	388 (12.6)	383 (10.6)	386 (13.5)	388 (9.1)
MLCT	427 sh (1.6)	423 sh (0.8)	422 sh (4.5)	425 sh (4.0)	422 sh (5.6)	472 sh (2.6)

Table 3.2 *Wavelength λ/nm (molar extinction coefficient $\varepsilon/10^3$ $M^{-1}cm^{-1}$) of $Ni(DTCEt_2)_2$ and the nickel(II) dithiocarbamate receptors*

The UV/visible spectrum of copper(II) dithiocarbamates usually display a ligand to metal (LMCT) charge transfer bands at ~430nm[16] together with two LC π-π^* bands observed ~275nm and ~290nm.[17]

Table 3.3 shows the UV/visible spectroscopic data for the receptors in MeCN:DMSO (4:1) solution and that of $Cu(DTCEt_2)_2$.[14] All the copper(II) receptors display typical spectra, although some of the receptors have the LC band at the longer wavelength obscured by the tail of the band at ~270nm.

Assignment	$Cu(DTCEt_2)_2$	44	46	48	50	52
LC	269 (32.9)	274 (48.36)	272 (48.2)	272 (42.0)	270 (64.8)	270 (64.8)
LC	287 sh (18.0)	-	291 sh (36.4)	-	286 sh (38.8)	286 sh (38.8)
LMCT	433 (11.8)	443 (13.7)	439 (11.3)	443 (8.8)	438 (17.8)	438 (17.8)

Table 3.3 *Wavelength λ/nm (molar extinction coefficient $\varepsilon/10^3$ $M^{-1}cm^{-1}$) of $Cu(DTCEt_2)_2$ and the copper(II) dithiocarbamate receptors*

UV/visible spectroscopy was used to prove the number of copper(II) dithiocarbamate centres per receptor molecule by monitoring the oxidation of copper(II) to copper(III). **Figure 3.13** displays the change in UV/visible absorption spectrum when aliquots of copper(II) triflate were added to a $CHCl_3$:DMF (99:1) solution of receptor **50**.

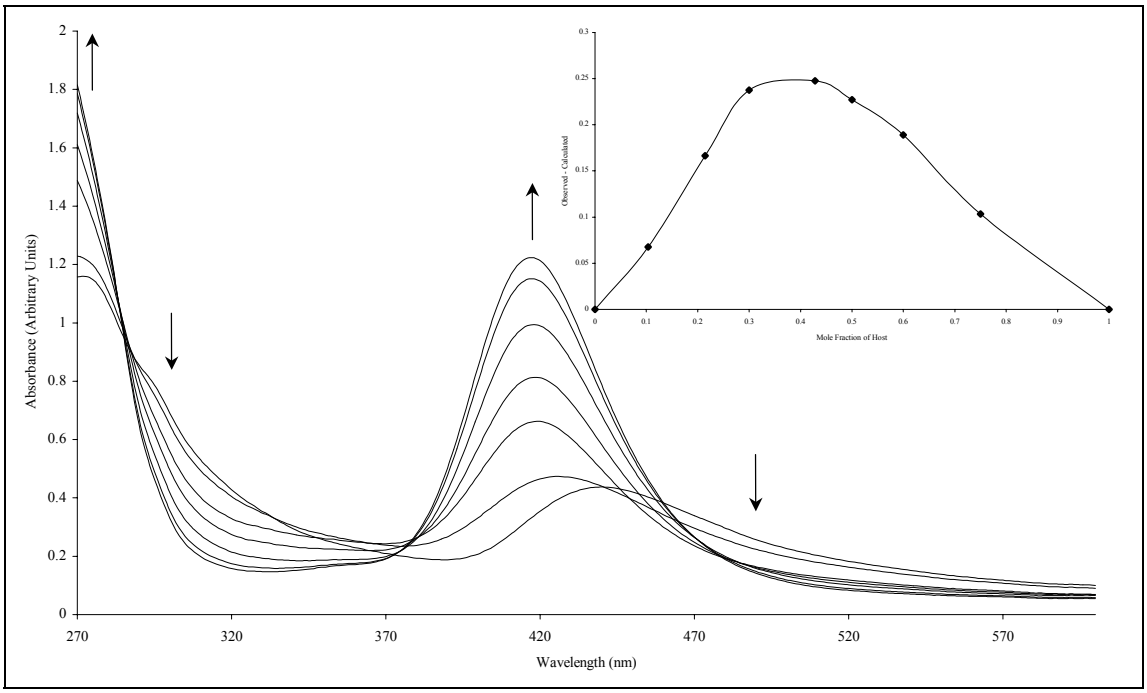

Figure 3.13 *UV/visible oxidation of **50** with copper(II) triflate in $CHCl_3$:DMF (99:1)*
*(Inset) Job Plot of **50** with copper(II) triflate in $CHCl_3$:DMF (99:1)*

The initial spectrum displays the characteristic peaks of a copper(II) dithiocarbamate spectrum. Upon oxidation, a new peak was observed at 417nm corresponding to the copper(III) dithiocarbamate species.[18] The Job plot displayed a maximum at ~0.33 indicating that two equivalents of oxidant were required to carry out the oxidation,[19] confirming that receptor **50** contained two copper(II) centres.

A corresponding oxidation was performed on receptor **47** and proved that the macrocycle contained two nickel(II) dithiocarbamate moieties. This will be discussed further in **Chapter 5 Section 2**.

2.1.7 Copper(II) Electrochemistry

Copper(II) dithiocarbamates complexes can undergo a relatively facile metal based one electron oxidation and reduction processes.[20,21,22] Due to the low solubility of the receptors the electrochemical characteristics of the receptors were studied in DMF solution (**Appendix 3**). The electrochemistry of $Cu(DTCEt_2)_2$[14] was also investigated to act as a reference.

Figure 3.14 shows the copper(II)/copper(III) and copper(II)/copper(I) cyclic voltammograms of receptor **50** at varying scan rates.

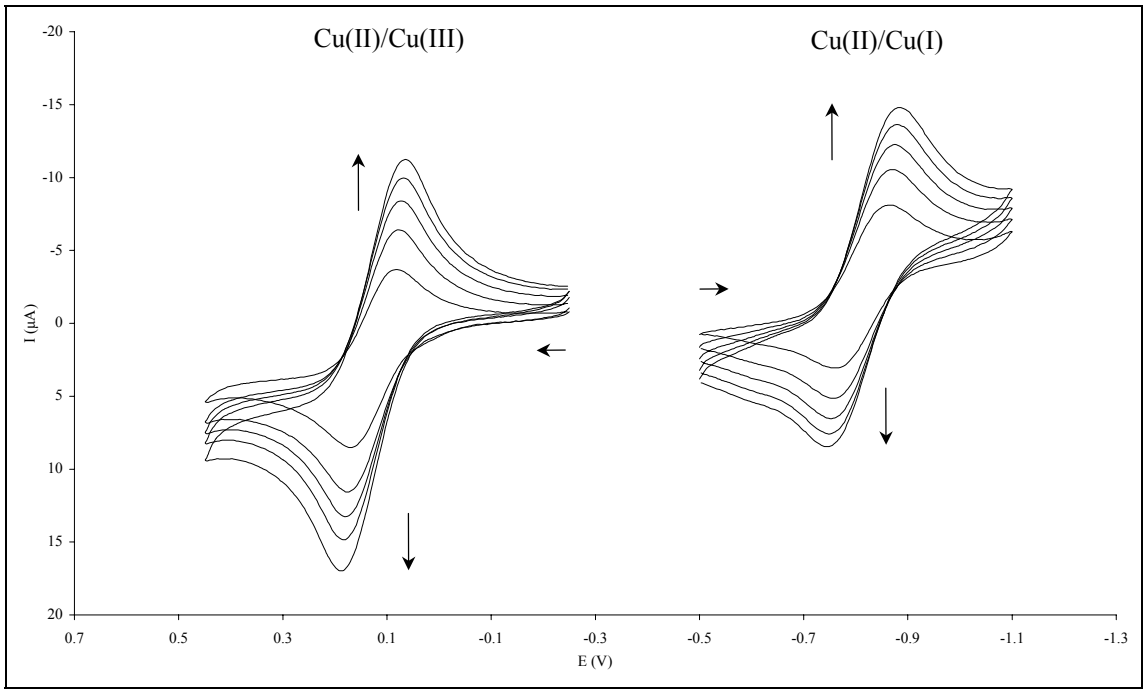

Figure 3.14 *Cyclic voltammetry electrochemical oxidation and reduction waves of **50** at varying scan rates together with assignments of electrochemical processes in DMF containing 0.1M $TBABF_4$, potentials given with reference to Ag/Ag^+ at 293K*

The potential of both the oxidation and reduction waves of both redox processes did not vary with scan rate. It was also found that the maximum peak current was proportional to the square root of the scan rate thus the **50** displayed quasi-reversible electrochemical behaviour.[23]

Interestingly, the oxidation and reduction waves represent a two electron oxidation with the copper(II) centres acting independently of each other. Similar results were obtained for all receptors as well as $Cu(DTCEt_2)_2$ and the data is presented in **Table 3.4**.

	Cu(II)/Cu(III)					
	$Cu(DTCEt_2)_2$	**44**	**46**	**48**	**50**	**52**
E_{pa} (V)	0.180	0.160	0.150	0.225	0.190	0.210
E_{pc} (V)	0.075	0.060	-0.010	0.050	0.060	0.105
ΔE (V)	0.105	0.100	0.160	0.175	0.130	0.105
I_{pa}/I_{pc}	1.2	1.0	0.9	1.1	1.1	1.0
E_p (V)	0.120	0.125	0.130	0.160	0.140	0.145

	Cu(II)/Cu(I)					
	$Cu(DTCEt_2)_2$	**44**	**46**	**48**	**50**	**52**
E_{pa} (V)	-0.800	-	-	-	-0.745	-0.715
E_{pc} (V)	-0.930	-0.930	-0.985	-0.850	-0.890	-0.930
ΔE (V)	0.130	-	-	-	0.145	0.220
I_{pa}/I_{pc}	0.9	-	-	-	0.9	0.7
E_p (V)	-0.860	-0.800	-0.810	-0.735	-0.790	-0.785

Table 3.4 *Electrochemical data of $Cu(DTCEt_2)_2$ and the copper(II) dithiocarbamate receptors in DMF containing 0.1M $TBABF_4$, potentials given with reference to Ag/Ag^+ at 293K, scan rate = $100mVs^{-1}$, E_p - peak potential in square wave voltammogram*

All of the receptors displayed a quasi-reversible copper(II)/copper(III) couple. However, only **50** and **52** showed a quasi reversible copper(II)/copper(I) couple. This is in contrast to the $Cu(DTCEt_2)_2$ that displayed quasi-reversible oxidation and reduction processes. The irreversible reduction behaviour shown by some of the receptors maybe due to the stereochemical change that occurs from square planar copper(II) to tetrahedral copper(I).[21] Interestingly, the peak potential of both the oxidation and reduction were shifted to more positive values for all the receptors than in $Cu(DTCEt_2)_2$ possibly due the proximity of the electron withdrawing amide group.

2.1.8 Thin Layer Coulometry

The number of electrons transferred to a compound in solution can be measured by thin layer coulometry (**Appendix 6**).[24] Within a thin layer the effect of diffusion can be considered insignificant, hence when the electrode is placed into the solution, the electro-active species is effectively locked in the layer. The volume of the thin layer can be calculated using a solution of ferrocene at a known concentration using the equation shown below (**Figure 3.15**).

$$Q = nFCV$$

Q - Charge transferred to the thin layer
n - Number of electrons per molecule
F - Faraday constant
C - Concentration of electro-active species
V - Volume of solution in the thin layer

Figure 3.15 *Formula relating charge to number of electrons transferred and volume of solution*

It was found that at the potential required to oxidise from copper(II) to copper(III) two electrons were removed from each molecule of **50**. This showed that each receptor contained two copper(II) centres that each underwent a one electron oxidation. A similar experiment, performed at a potential able to reduce copper(II) to copper(I), showed that each molecule of receptor required two electrons to carry out the reduction. This again confirmed the presence of two copper(II) centres in the molecule.

2.1.9 Rotating Disk Voltammetry

The electrochemical characteristics of receptor **50** were also studied by rotating disk electrode voltammetry (**Appendix 7**).[25] This technique allows the study of the heterogeneous electron transfer process from the electrode to the electro-active species in solution.

The electrode is spun at a known rate and this motion draws fresh solution towards the electrode surface. Thus, the solution in the electroactive layer is constantly being replenished with un-oxidised species. The limiting current observed for a reversible process is defined by the Levich equation (**Figure 3.16**).

$$i = 0.620nFAD_o^{3/2}\nu^{-1/6}C_o^*\sqrt{\omega}$$

i - current, n - number of electrons per molecule, F- Faraday constant,
A - area, $D^{3/2}$ - diffusion coefficent, ν - kinematic viscosity,
C - concentration, ω - rate of rotation

Figure 3.16 *Levich equation*

The limiting current is proportional to the square root of the rate of rotation of the electrode, thus, for a reversible process, a plot of I_{pa} against √ω should be linear.

Figure 3.17 shows the variation of peak current with angular velocity of the electrode for receptor **50** in DMF.

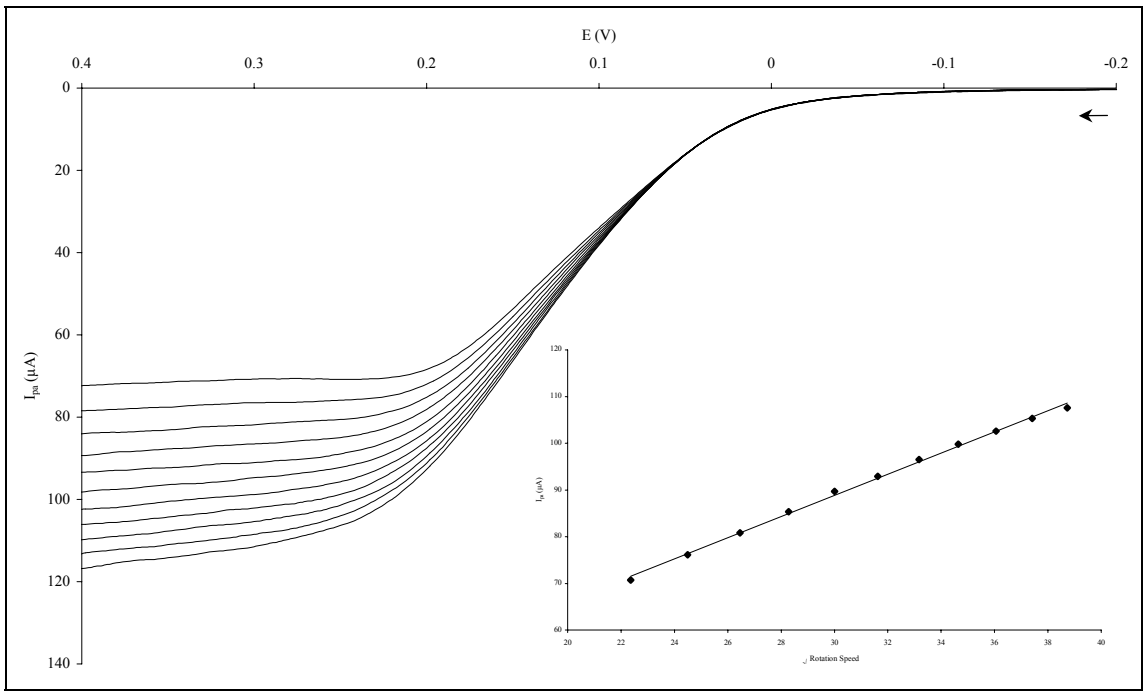

Figure 3.17 *Rotating disk linear voltammetry electrochemical oxidation waves of **50** in DMF at varying scan rates containing 0.1M $TBABF_4$, potentials given with reference to Ag/Ag^+ at 293K, scan rate = 100mVs^{-1}*
*(Inset) Plot of I_{pa} against √ω of **50** in DMF*

The plot of I_{pa} against square root of the rotation rate is linear, indicative of a quasi-reversible electrochemical process.

2.1.10 Nickel(II) Electrochemistry

Nickel(II) dithiocarbamate compounds can undergo many electrochemical processes.[20,22,26] The electrochemistry of the nickel(II) macrocycles was investigated using cyclic and square wave voltammetry in DMF due to the low solubility of the receptors.

Figure 3.18 shows a portion of the cyclic voltammogram of receptor **43** with assignments of the redox processes occurring.

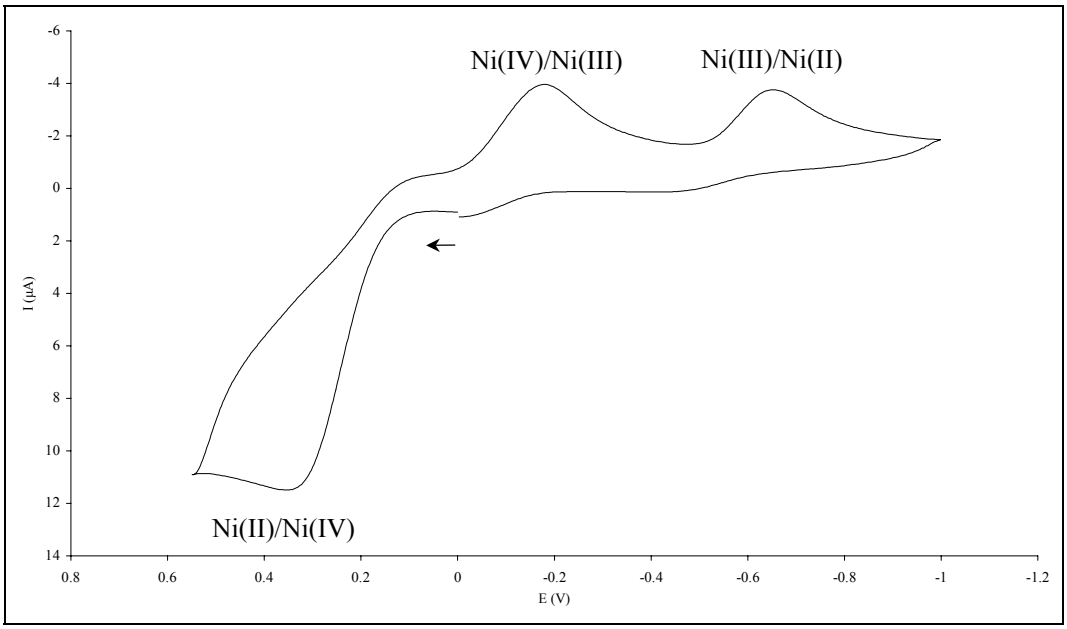

Figure 3.18 *Cyclic voltammetry electrochemical oxidation and reduction waves of **43** together with assignments of the electrochemical processes in DMF containing 0.1M $TBABF_4$, potentials given with reference to Ag/Ag^+ at 293K, scan rate = 500mVs^{-1}*

An irreversible oxidation occurs at a fairly positive potential. The electrogenerated nickel(IV) dithiocarbamate species can subsequently undergo two reductions of nickel(IV) to nickel(III) and nickel(III) to nickel(II) respectively. The nickel(IV)/nickel(III) and nickel(III)/nickel(II) waves are only observable at high scan rates as the electrogenerated nickel(IV) diffuses into bulk solution and subsequent reductions were not observed at low scan rates. **Table 3.5** displays the corresponding data for all the nickel(II) based receptors.

	Ni(II)/Ni(IV)					
	$Ni(DTCEt_2)_2$	**43**	**45**	**47**	**49**	**51**
E_{pa} (V)	0.630	0.490	0.565	0.460	0.575	0.400
E_p (V)	0.505	0.370	0.380	0.400	0.330	0.230
	Ni(IV)/Ni(III)					
E_{pc} (V)	-0.225	-0.165	-0.230	-0.180	-0.170	-0.165
	Ni(III)/Ni(II)					
E_{pc} (V)	-0.770	-0.650	-0.790	-0.684	-0.735	-0.710

Table 3.5 *Electrochemical data of $Ni(DTCEt_2)_2$ and the nickel(II) dithiocarbamate receptors in DMF containing 0.1M $TBABF_4$, potentials given with reference to Ag/Ag^+ at 293K, scan rate = 100mVs^{-1}, E_p - peak potential in square wave voltammogram*

All the receptors display typical electrochemical oxidation characteristics for a nickel(II) dithiocarbamate species.

Nickel(II) dithiocarbamates can also undergo a one electron, metal based reduction at fairly negative potential. **Figure 3.19** displays the nickel(II)/nickel(I) reduction wave of receptor **51** as the scan rate is varied.

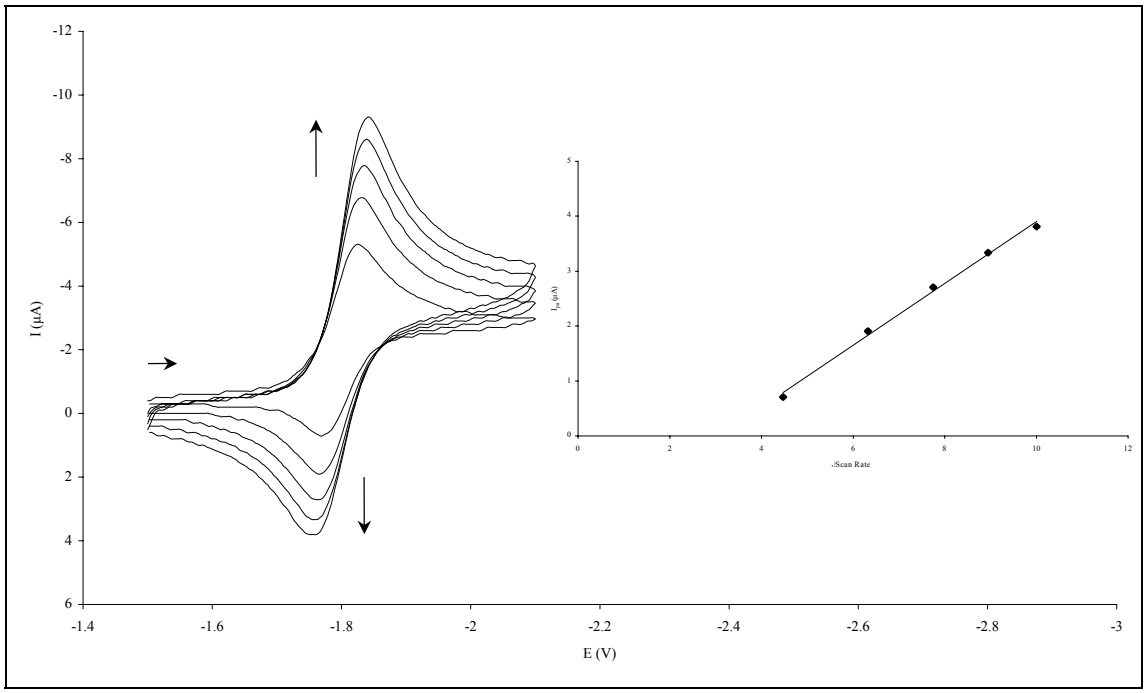

Figure 3.19 *Cyclic voltammetry electrochemical reduction waves of **51** at varying scan rates in DMF containing 0.1M $TBABF_4$, potentials given with reference to Ag/Ag^+ at 293K*
*(Inset) Plot of I_{pa} against √scan rate of **51** in DMF*

The plot of I_{pa} against the square root of scan rate was a straight line indicating quasi-reversibility. **Table 3.6** shows the data for the nickel(II)/nickel(I) reduction for all the receptors and the corresponding data of $Ni(DTCEt_2)_2$.

	Ni(II)/Ni(I)					
	$Ni(DTCEt_2)_2$	**43**	**45**	**47**	**49**	**50**
E_{pa} (V)	-1.800	-	-	-	-1.720	-1.750
E_{pc} (V)	-1.980	-1.900	-1.940	-1.910	-1.930	-1.845
ΔE (V)	0.180	-	-	-	0.210	-0.095
I_{pa}/I_{pc}	0.9	-	-	-	0.8	1.0
E_p (V)	-1.870	-1.765	-1.755	-1.810	-1.800	-1.770

Table 3.6 *Electrochemical data of $Ni(DTCEt_2)_2$ and the nickel(II) dithiocarbamate receptors in DMF containing 0.1M $TBABF_4$, potentials given with reference to Ag/Ag^+ at 293K*

Only receptors **49** and **51** showed quasi-reversible characteristics of nickel(II)/nickel(I) couple.

The number of electrons transferred to receptor **47** in solution was measured by thin layer coulometry (see **Section 2.1.8**). It was found that at the potential needed to oxidise nickel(II) to nickel(IV) four electrons were removed from each molecule of **47**. This proved that each receptor contains two nickel(II) dithiocarbamate centres and they each underwent a two electron oxidation. A similar experiment, performed at a potential able to reduce nickel(II) to nickel(I), showed that each molecule of receptor required two electrons to perform the reduction. This also confirmed the presence of two nickel(II) dithiocarbamate centres in the molecule.

2.1.11 Infrared Spectroscopy

Table 3.7 presents the infrared data of $Ni(DTCEt_2)_2$, $Cu(DTCEt_2)_2$ and receptors **43** - **52** in a Nujol® mull.[27]

ν (cm^{-1})	**Ni(DTCEt$_2$)$_2$**	**43**	**45**	**47**	**49**	**51**
ν (NH)	-	3284	3176	3252	3248	3264
Amide I	-	1662	1674	1678	1668	1660
Amide II	-	1530	1536	1537	1538	1554
ν (CN)	1516	1488	1484	1500	1486	1488
ν (CS$_{as}$)	992	962	956	962	958	958
ν (CS$_s$)	636	660	644	-	650	649

ν (cm^{-1})	**Cu(DTCEt$_2$)$_2$**	**44**	**46**	**47**	**50**	**52**
ν (NH)	-	3266	3174	3224	3282	3252
Amide I	-	1650	1650	1664	1698	1678
Amide II	-	1552	1534	1532	1536	1558
ν (CN)	1508	1482	1460	1486	1484	1494
ν (CS$_{as}$)	996	956	944	960	958	946
ν (CS$_s$)	-	648	650	648	650	646

Table 3.7 *Infrared data of Ni(DTCEt$_2$)$_2$, Cu(DTCEt$_2$)$_2$ and **43** – **52** (Nujol® mull) together with band assignments*

The band observed at ~3250cm^{-1} is characteristic of a NH stretch of an amide group.[28] The amide I band is due to the stretch of the CO bond in the amide group and all the receptors displayed absorption typical for an aromatic amide group.[29] The amide II band is due to a combination of NH bend and CN stretch of the amide group and the receptors exhibited absorptions for secondary amide moiety.

The dithiocarbamate group contains several characteristic absorptions in their infrared spectrum. The dithiocarbamate CN stretch ~1500cm^{-1} confirmed the partial double bond character between these two atoms.[30] The presence of a single absorption at ~1000cm^{-1} is due to a anti-symmetric CS stretch and has been used as evidence for the bidentate nature of the coordination of the metal atom by two sulphur atoms.[31] The symmetric stretch of the CS group is observed at ~650cm^{-1} and was sometimes too weak to be seen.[32]

2.1.12 Magnetic Measurements

Magnetic susceptibility data of receptor **48** and $Cu(DTCEt_2)_2$[14] were collected over the temperature range 5K - 300K using a superconducting quantum interference device (SQUID) (**Appendix 8**).

Two different procedures were used:

i) zero-field cooling (ZFC), where the sample was cooled from 300K to 5K under zero external field, then a static magnetic field was applied and the magnetisation was measured under the field as a function of temperature,

ii) field cooling (FC), where an external static magnetic field was applied to the sample at 300K and the sample was cooled to 5K in the presence of the field, then the magnetisation was measured under the field as a function of temperature.

Diamagnetic corrections ($\chi_m = -1.57 \times 10^{-4}$) were applied to the measured susceptibilities of $Cu(DTCEt_2)_2$ using Pascal's constants[33] and the magnetic moment calculated using the equation shown in **Figure 3.20**.[34]

$$\mu_{eff} = 2.828\sqrt{\chi_m T}$$

Figure 3.20 *Formula of the effective magnetic moment*
(χ_m - corrected molar susceptibility, T - absolute temperature)

The variable temperature data was fitted using the Curie-Weiss law allowing for a contribution from temperature independent paramagnetism (**Figure 3.21**).[35]

$$\chi_m = \frac{C}{(T - \theta)} + N\alpha$$

Figure 3.21 *Formula of the Curie-Weiss law with temperature independent paramagnetism*
(χ_m - corrected molar susceptibility, T - absolute temperature, θ – Weiss constant, $N\alpha$ – temperature independent paramagnetism)

A Curie-Weiss paramagnet displays, in addition to the interaction of the magnetic moments with the applied magnetic field, an interaction between the magnetic moments on different atoms.[36] This 'exchange interaction' can help align moments in the same direction (θ positive, a ferromagnetic interaction) or help align neighbouring moments in opposite direction (θ negative, an antiferromagnetic interaction).

Temperature independent paramagnetism reflects the mixing of excited states with that of the ground state, which alters the magnetic characteristics of the molecule.

Figure 3.22 shows the variation of observed magnetic moment with temperature of $Cu(DTCEt_2)_2$ together with the calculated best fit using the equation in **Figure 3.21** where R is the reliability factor defined as $R = \Sigma(\chi_m^{obs} - \chi_m^{calc})^2 / \Sigma(\chi_m^{obs})^2$.[37]

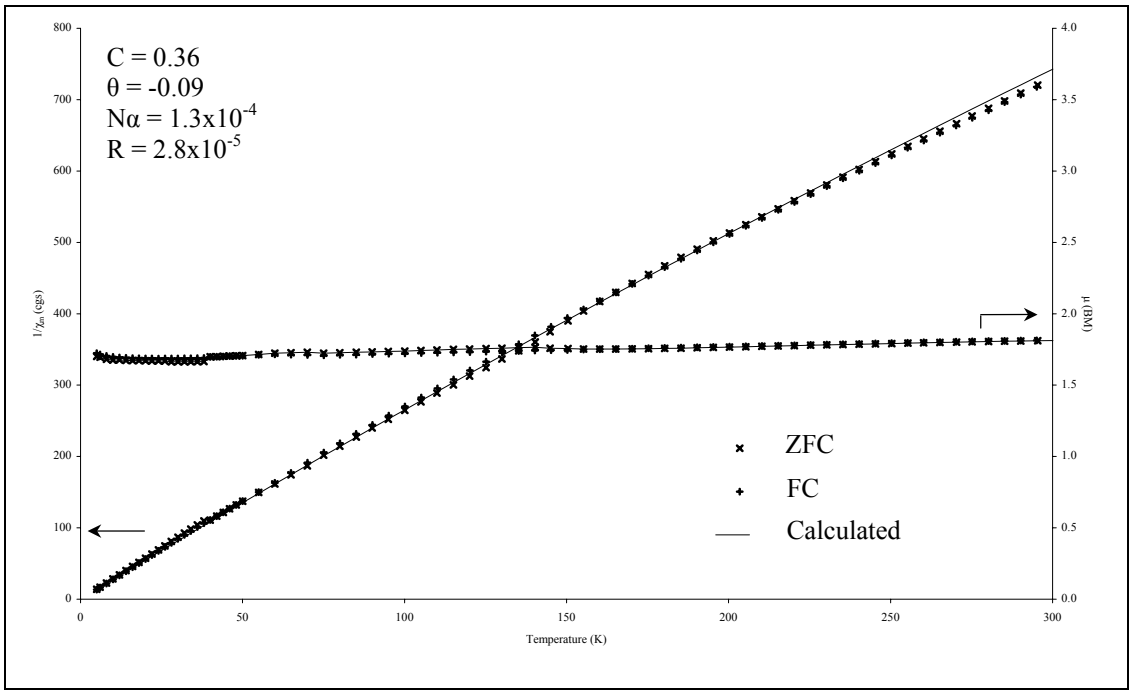

Figure 3.22 *Variable temperature magnetic susceptibility and magnetic moment of $Cu(DTCEt_2)_2$*

The value of the magnetic moment of $Cu(DTCEt_2)_2$ varied between 1.70BM at 5K to 1.80BM at 300K. This value is in good agreement with the spin only value for a molecule with one unpaired electron[38] and as the calculated value of θ is small, there is little interaction between adjacent copper(II) centres.[39] As the FC and ZFC curves lie on top of one another, no hysteresis was occurring.[40] This data is consistent with the presence of one copper(II) dithiocarbamate centre.

Figure 3.23 shows variation of the observed magnetic moment with temperature for receptor **48** after diamagnetic corrections ($\chi_m = -3.72x10^{-4}$) have been applied and the data was fitted using the equation in **Figure 3.21**.

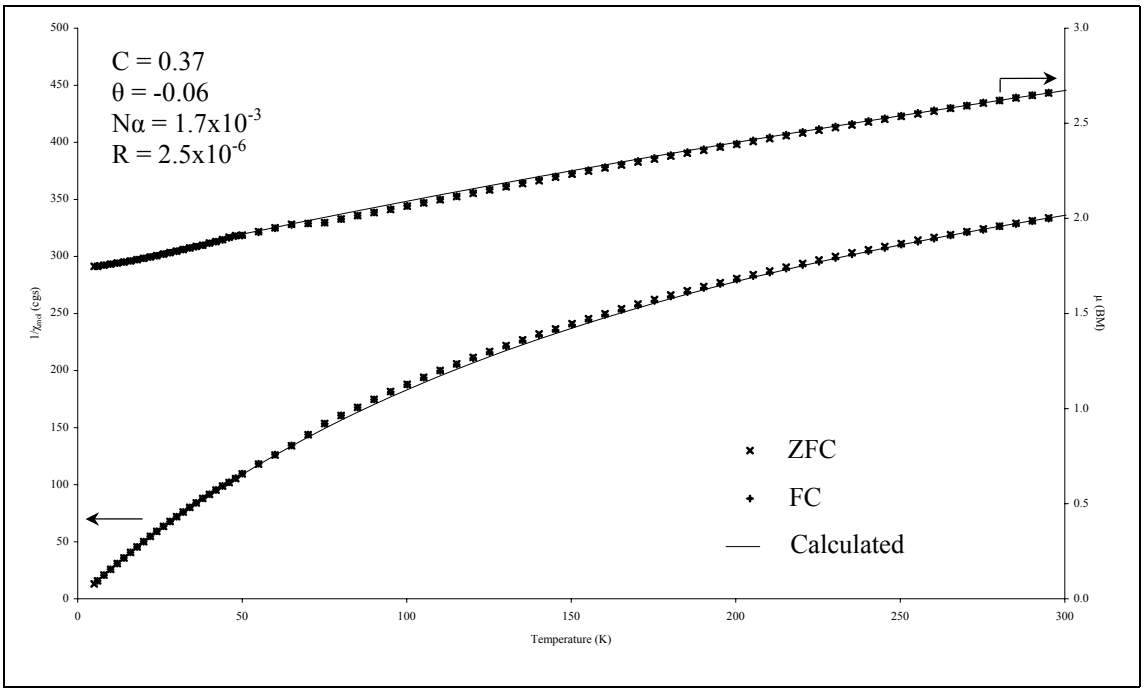

Figure 3.23 *Variable temperature magnetic susceptibility and magnetic moment of **48***

The magnetic moment varied linearly between 5K and 300K from 1.75BM to 2.66BM respectively. As the calculated value of θ is small, there is little interaction between adjacent copper(II) centres.[39] If the distance between metals is similar to that of **47** (see **Section 2.1.4**), the metal-metal distance would be large and any potential intramolecular copper-copper interactions would be small.[41] Thus it is likely that any small exchange interactions are predominately due to intermolecular communication between copper(II) centres. The contribution from temperature independent paramagnetism is one order of magnitude larger in receptor **48** than for $Cu(DTCEt_2)_2$ which accounts for the curvature of the data away from pure Curie-Weiss behaviour. As the FC and ZFC curves lie on top of one another, no hysteresis was occurring.[40]

It was hoped that by isolating a copper(II) dithiocarbamate receptor in the presence of anionic guest species it would be possible to see if the presence of the guest had altered the magnetic properties of the receptor. Unfortunately, it was not possible to isolate the **48**·$TBAH_2PO_4$ complex as a powder, possibly due to the hygroscopic nature of the TBA dihydrogen phosphate. Thus, it was not possible to study the affect the anion had on the magnetic properties of **48**.

2.1.13 Electron Paramagnetic Resonance

Electron paramagnetic resonance (EPR) has been of great value for the study of the bonding of transition metal ions. Copper has probably been the most studied transition metal due to the relative simple spectra it shows and the g-values and hyperfine coupling constants yield information about the nature of the bonding of the metal ion.[42] These studies were performed in collaboration with Dr. J. Maher at Bristol University.

Figure 3.24 shows the EPR spectrum of $Cu(DTCEt_2)_2$[14] in CH_2Cl_2.

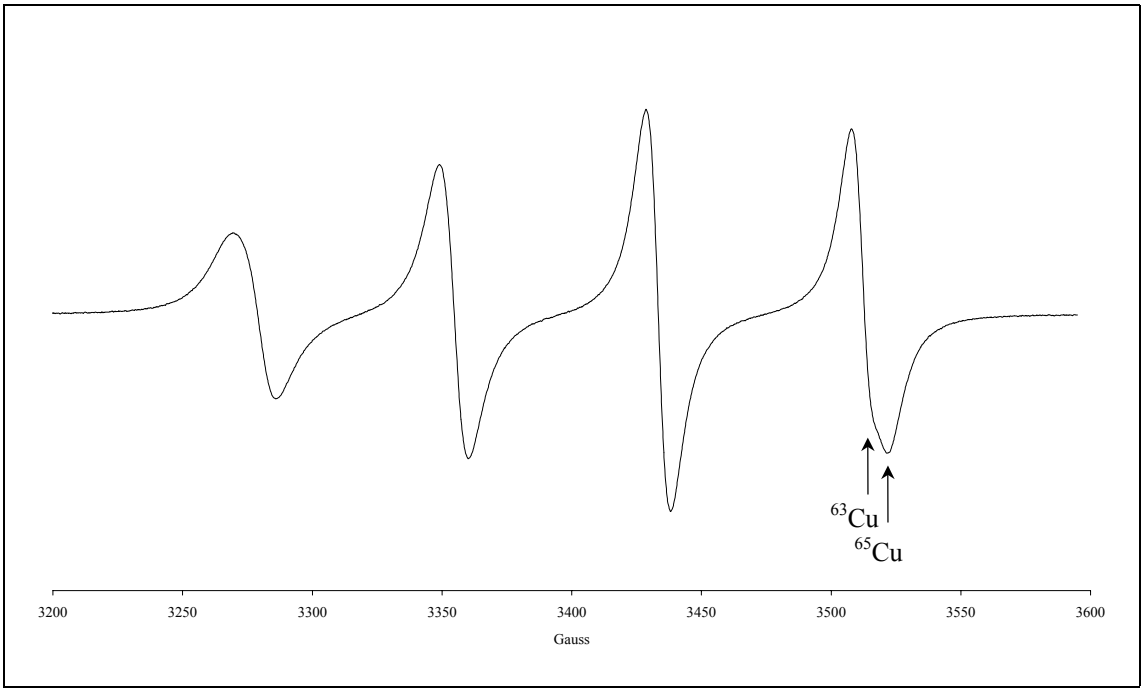

Figure 3.24 *EPR spectrum of $Cu(DTCEt_2)_2$ in CH_2Cl_2 at 296K*

The spectrum shows four hyperfine lines of varying widths. Four lines occur due to hyperfine interaction between the unpaired electron and the copper nucleus (I=3/2).[43] There is a shoulder observed on the high field peak due relative abundance of isotopes of ^{63}Cu (69.2%) and ^{65}Cu (30.8%).

It has been shown that the metal sulphur bond in $Cu(DTCEt_2)_2$ is quite covalent,[42] as was confirmed by its g-value being close to that of a free electron (2.002). This compound displayed an A(Cu) value of 78G, as expected for a simple copper(II) dithiocarbamate molecule (**Table 3.8**).

	$Cu(DTCEt_2)_2$
g	2.047
A(Cu) (G)	78

Table 3.8 *EPR data of $Cu(DTCEt_2)_2$ in CH_2Cl_2 at 296K*

Figure 3.25 shows the EPR spectrum of receptor **48** in CH_2Cl_2 and **Table 3.9** displays the EPR data of receptor **48**.

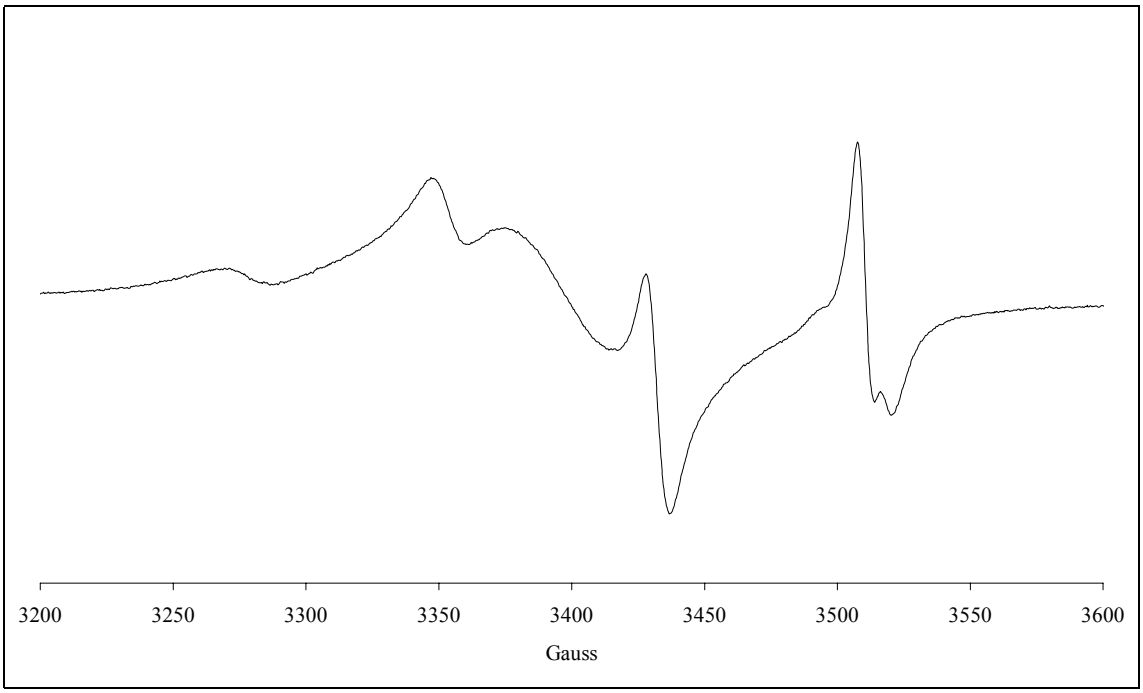

Figure 3.25 *EPR spectrum of **48** in CH_2Cl_2 at 296K*

	48
g	2.047
A(Cu) (G)	79

Table 3.9 *EPR data of **48** in CH_2Cl_2 at 296K*

The spectrum of **48** shows a broad line in the middle of the spectrum at g=2.047 with a typical A(Cu) value of 79G. This is super-imposed on a four line spectrum, which shows a clear $^{63}Cu/^{65}Cu$ splitting in the high field peak. This could be due to two conformations existing in solution, one with little copper-copper interaction and the other with a coupling between the copper centres.

2.2 Anion Binding Studies

The receptors anion binding properties were investigated using electrochemical techniques, UV/visible, infrared, ^{1}H and ^{13}C NMR spectroscopies.

2.2.1 Copper(II) Electrochemistry

The effect upon the addition of five equivalents of anion to the copper(II) dithiocarbamate receptors and $Cu(DTCEt_2)_2$ was monitored using square wave voltammetry. The magnitudes of the cathodic shift observed in DMF solution are presented in **Table 3.10**.

Anion	ΔE Cu(II)/Cu(III) (mV)					
	$Cu(DTCEt_2)_2$	**44**	**46**	**48**	**50**	**52**
Acetate	60	100	35	-[a]	70	100
Benzoate	10	30	15	-[a]	50	55
Dihydrogen Phosphate	30	130	20	-[a]	ppt	ppt

Anion	ΔE Cu(II)/Cu(I) (mV)					
	$Cu(DTCEt_2)_2$	**44**	**46**	**48**	**50**	**52**
Acetate	<5	50	45	25	30	25
Benzoate	<5	<5	20	35	20	5
Dihydrogen Phosphate	<5	40	20	-[b]	30	5
Chloride	<5	<5	<5	<5	<5	<5

Table 3.10 *Cathodic shifts in the square wave voltammogram upon the addition of 5 equivalents of anion to $Cu(DTCEt_2)_2$ and the copper(II) dithiocarbamate receptors in $CHCl_3$:MeCN (4:1) containing 0.1M $TBABF_4$, potentials given with reference to Ag/Ag^+ at 293K (a - extra peaks observed, b - no peak observed)*

In general, addition of excess acetate, benzoate and dihydrogen phosphate anions to a solution of the receptors produced small to moderate cathodic shifts of the oxidation wave. The magnitudes of these shifts are generally larger than that observed with $Cu(DTCEt_2)_2$ due to the

anion binding to the amide group in close proximity to the copper(II) dithiocarbamate and hence stabilising the copper(III) dithiocarbamate species.[18]

When dihydrogen phosphate was added to **50** and **52** a precipitate formed hindering further electrochemical investigations. Addition of excess acetate to both **44** and **52** produced cathodic shifts of the oxidation wave that were significantly larger than when benzoate was added. This is interesting as acetate and benzoate anions have a similar basicity.[44] Receptor **46** displayed no preference for a particular anion as small but significant shifts was seen upon the addition of all three anions.

Addition of five equivalents of all three anions to receptor **48** resulted in extra peaks being observed in the spectrum. One of the peaks was at a higher potential than the original wave and one at a lower potential. These peak maybe due to a chemical reaction occurring.

Upon the addition of five equivalents of the anions to $Cu(DTCEt_2)_2$ very small cathodic shifts were observed of the copper(II)/copper(I) couple. The receptors displayed small to moderate cathodic shifts of the reduction wave. The negatively charged guest species binds to the amide increasing charge density near the transition metal dithiocarbamate centre and so a greater negative potential is required to perform the reduction process.[45] For acetate, benzoate and dihydrogen phosphate **Table 3.10** shows there was little trend in the magnitudes of cathodic shifts observed. However, all three show significantly greater shifts than those observed when excess chloride was added. This follows the trend in basicity of the anions. Unfortunately, when dihydrogen phosphate was added to a solution of receptor **48** no peak in the square wave voltammogram could be observed. This unusual behaviour is hard to explain but another process could be occurring which significantly changes the potential at which the electrochemical process occurs.

2.2.2 Nickel(II) Electrochemistry

Table 3.11 shows the cathodic shift observed in the square wave voltammogram of the nickel(II)/nickel(I) couple when five equivalents of various anions were added to the nickel(II) receptors and $Ni(DTCEt_2)_2$[14] in DMF.

Anion	ΔE Ni(II)/Ni(I) (mV)					
	$Ni(DTCEt_2)_2$	**43**	**45**	**47**	**49**	**50**
Acetate	<5	35	40	60	40	15
Benzoate	<5	10	40	40	20	<5
Dihydrogen Phosphate	<5	40	50	50	40	<5
Chloride	<5	<5	<5	<5	<5	<5

Table 3.11 *Cathodic shifts in the square wave voltammogram upon the addition of 5 equivalents of anion to $Ni(DTCEt_2)_2$ and the nickel(II) dithiocarbamate receptors in $CHCl_3$:MeCN (4:1) containing 0.1M $TBABF_4$, potentials given with reference to Ag/Ag^+ at 293K*

The control compound shows very small shifts in the nickel(II)/nickel(I) couple upon the addition of excess anion. In contrast, the receptors showed moderate cathodic shifts of the square wave upon the addition of five equivalents of acetate, benzoate and dihydrogen phosphate.

Cathodic shifts were observed as the bound anion increased the negative charge density adjacent to the transition metal centre, inhibiting the reduction of the redox centre.[45] However, there was little trend in the magnitude of the anion induced shifts observed, which may be due to the competitive nature of the solvent.

2.2.3 UV/visible Spectroscopy

Large changes were observed in of the absorption bands between 250nm and 500nm upon the addition of acetate, benzoate and dihydrogen phosphate anions to MeCN:DMSO (4:1) solutions of the nickel(II) receptors.

Unfortunately, it was not possible to calculate stability constants from this data due to a kinetic effect between the addition of an aliquot of anion and the absorption reaching a steady

value. In order to investigate this time, two equivalents of a specific anion was added to a solution of the receptors and the spectrum recorded every minute until a constant absorption value was reached as shown in **Table 3.12**.

Anion	Equilibration time (minutes)				
	43	**45**	**47**	**49**	**51**
Acetate	8	6	1	6	1
Benzoate	11	18	16	12	11
Dihydrogen Phosphate	40	10	6	4	20

Table 3.12 *Time taken for the absorbance to reach a steady value after the addition of two equivalents of anion*

The data in **Table 3.12** shows that the time taken to reach a steady absorption value depends not only on the nature of the anion added, but also on the receptor. Upon the addition of two equivalents of chloride anion, all of the receptors showed very little change in absorption spectra. The percentage decrease in the absorption maximum ~323nm, after the addition of two equivalents of anion, are shown in **Table 3.13**.

Anion	Percentage decrease				
	43	**45**	**47**	**49**	**51**
Acetate	70	20	15	25	15
Benzoate	30	10	15	25	10
Dihydrogen Phosphate	15	5	5	5	5

Table 3.13 *Percentage decrease in the UV/visible absorption ~323nm for the nickel(II) receptors*

The percentage decrease in absorption follows the trend acetate > benzoate > dihydrogen phosphate. This order mirrors the basicity of the anions acetate > benzoate >> dihydrogen phosphate >> chloride.[44] Receptor **44** shows a large difference of the magnitude of the decrease of absorption depending on the anion added. This is in contrast to the all of the other receptors, which show much less variation in decrease of absorption with anion. This kinetic effect is discussed further in **Section 3.2.2**.

Titrations were performed using receptors **47** and **51** with acetate where the equilibration time was one minute. **Figure 3.26** shows the changes in spectra seen together with band assignments when aliquots of TBA acetate were added to receptor **47**.

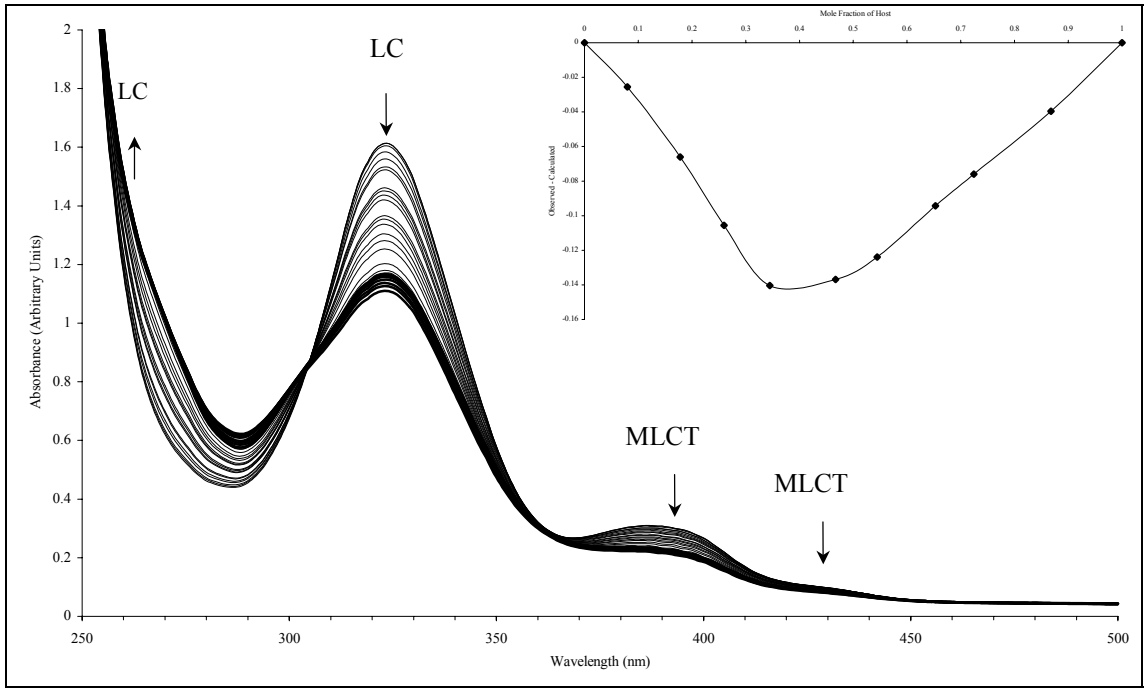

Figure 3.26 *UV/visible titration of **47** with TBA acetate in MeCN:DMSO (4:1) at 293K (Inset) Job Plot of **47** with TBA acetate in MeCN:DMSO (4:1)*

The Job plot shows a minimum at ~0.33 indicating that the two acetate anions bound to each receptor molecule[19] and an isosbestic point was observed at 305nm. Specfit™ was used to calculate the stability constants for the receptor:anion complex and the values are displayed in **Table 3.14**.[46]

Stability Constants	Log β_1	Log β_2
48 & TBA Acetate	5.1 ± 0.12	8.1 ± 0.13

Table 3.14 *Stability constants with errors determined by UV/visible spectroscopy in MeCN:DMSO (4:1) at 293K*

The stability constant for **47** with acetate is very large indicating a high thermodynamic stability of the complex that is formed, in a relatively competitive solvent. Unfortunately, Specfit™ could not calculate stability constants for **51** with acetate.

2.2.4 Infrared Spectroscopy

Infrared spectroscopy has had only limited use in molecular recognition possibly due to the complexity of the spectra obtained.[47] In order to investigate the effect of anion addition on the amide macrocyclic receptor **47**, two equivalents of acetate, benzoate, dihydrogen phosphate and chloride were added to a $CHCl_3$ solution of receptor **47** and stirred for 12 hours. The solvent was removed and the product thoroughly dried. The Nujol® mull infrared spectrum was recorded[27] and the shift of the NH stretch was recorded.

Table 3.15 reveals the shifts observed to a lower wavenumber of this band with four different anions.

	Acetate	**Benzoate**	**Dihydrogen Phosphate**	**Chloride**
Δν (NH) (cm^{-1})	55	60	80	60

Table 3.15 *Shifts of NH stretch of **47** upon the addition of two equivalents of anion in Nujol® mull*

The shift to a lower wavenumber of the NH stretch is characteristic of anion binding to the amide proton. Interestingly there is little discrepancy between the four anions and the magnitude of the shift observed.

2.2.5 ^{1}H NMR Spectroscopy

The anion binding properties of receptors **43**, **45**, **47**, **49** and **51** were studied using ^{1}H NMR spectroscopy (**Appendix 1**). The spectrum was recorded after additions of aliquots of the four anions in DMSO-d_6 solution. Initially, in all cases, the peak due to the amide proton was seen to shift further downfield indicating that the amide group was forming a favourable receptor:anion interaction.[48] For example, **47** displayed a shift of ~0.80ppm of the amide resonance after the addition of one equivalent of acetate anion. However, as the titration proceeded the amide peaks often changed multiplicity and new peaks were observed. This maybe due to a new species being formed in solution, however these could not be identified by ^{1}H NMR or ESMS.

2.2.6 ^{13}C NMR Spectroscopy

To investigate the anion binding by receptor **47** the ^{13}C NMR spectrum was recorded before and after the addition of 10 equivalents of each of the four anions. The observed shifts of the carbon peaks are shown in **Table 3.16**.

Anion	Change in carbon shift (Δδ)						
	CS_2	**CO**	**Ar-C**	**Ar-C**	**Ar-C**	**$\underline{C}H_2CO$**	**$\underline{C}H_2CO$**
Acetate	-0.5	-0.2	+0.3	Two peaks merge		-1.0	-1.1
Benzoate	-0.3	-0.2	-0.5	Hidden	-0.5	-0.7	-0.8
Dihydrogen Phosphate	-0.4	-0.1	-0.4	Two peaks merge		+0.1	-0.2
Chloride	-0.3	-0.3	-0.8	-0.6	-0.6	-0.5	-0.5

Table 3.16 *Change in chemical shift of carbon resonances of the nickel(II) dithiocarbamate receptors upon the addition of ten equivalents of anions as their TBA salts in DMSO-d_6 at 298K*

Shifts of the resonances that were observed upon the addition of all four anions were, in general, upfield. Interestingly, the magnitudes of the shifts are similar for all of the four anions studied even though the basicities of the anions vary greatly.[44]

2.2.7 Electrospray Mass Spectrometry

Electrospray mass spectrometry (ESMS) has been previously been employed to assess cation binding strength,[49] however little literature exists for analysing anion binding.[50]

It was hoped that negative ion mode ESMS could be used to qualitatively assess the anion binding strength of the receptors. In order to investigate this a $CHCl_3$ solution of **48** and a ten-fold excess of TBACl was injected into the spectrometer. A peak was observed in the spectrum corresponding with [**47** + Cl^-]$^-$. Unfortunately similar experiments with acetate, benzoate and dihydrogen phosphate displayed no peaks corresponding to [**47** + $Anion^-$]$^-$. Thus, it was not possible to assess the relative anion binding strengths of the receptors.

2.2.8 Electron Paramagnetic Studies

Rarely has EPR been used to monitor the binding of anions. One example is an octaaza cascade complex that displayed an unusual EPR spectrum in the presence of the azide anion.[51]

Figure 3.27 shows the EPR spectrum of receptor **48** in CH_2Cl_2 before and after the addition of excess TBA dihydrogen phosphate.

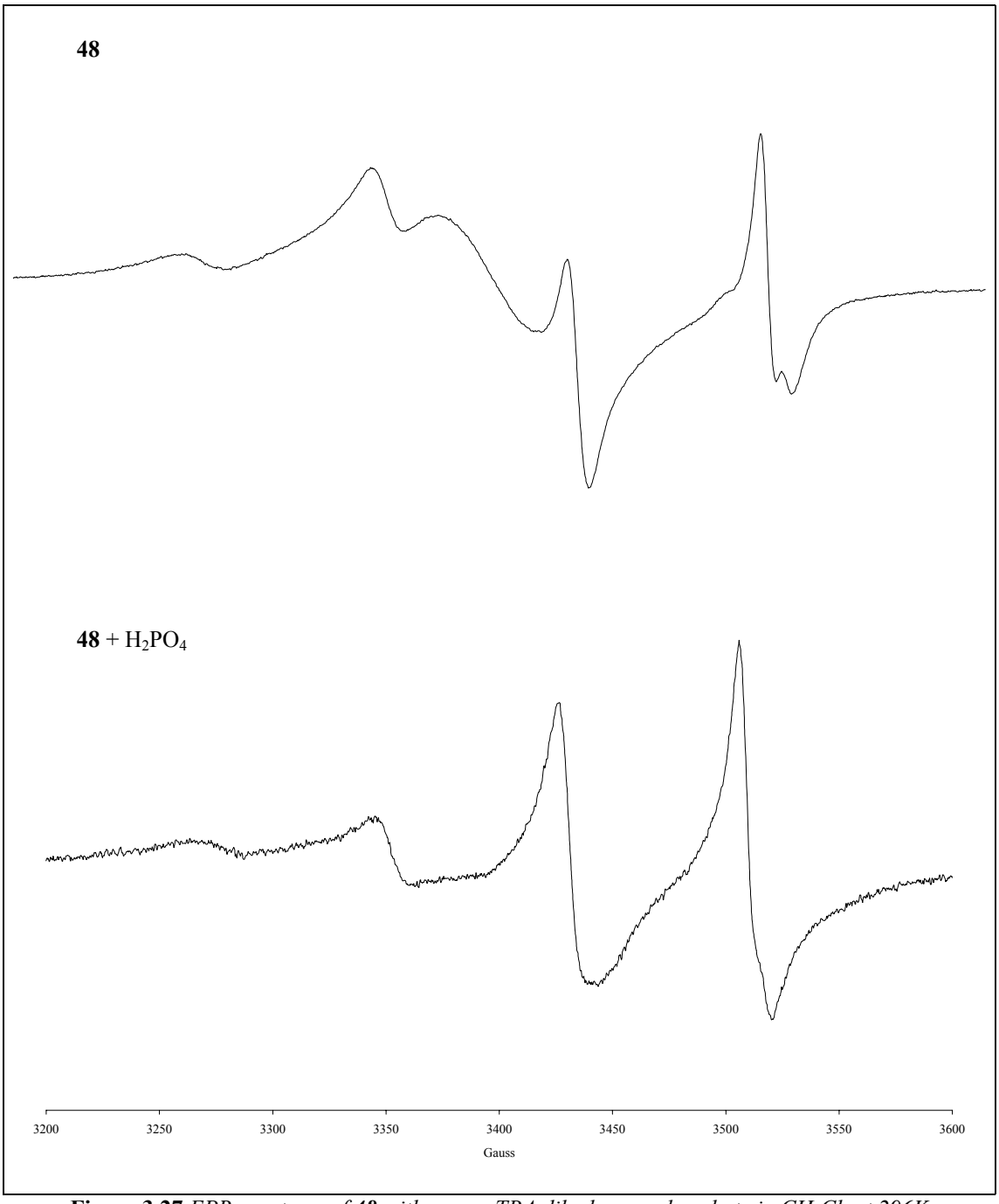

Figure 3.27 *EPR spectrum of **48** with excess TBA dihydrogen phosphate in CH_2Cl_2 at 296K*

Addition of dihydrogen phosphate to receptor **48** caused the broad centre line to disappear and a four line spectrum to be observed. The broadness of the lines are due to anisotropic effects. This spectrum has the same g and A(Cu) values as receptor **48** (**Table 3.17**).

	48	**48 & TBA Dihydrogen Phosphate**
G	2.047	2.047
A(Cu) (G)	79	79

Table 3.17 *EPR data of **48** and **48** with excess TBA dihydrogen phosphate in CH_2Cl_2 at 296K*

The EPR spectrum of receptor **48** had been perturbed by the presence of the dihydrogen phosphate anion in solution. It is possible that the anion is bound inside the cavity of **48** and so disfavours any interaction between the two copper(II) centres of the receptor. The spectrum after anion addition resembled that of a simple copper(II) dithiocarbamate species, and was very similar to that of the $Cu(DTCEt_2)_2$, consistent with non-interacting copper(II) centres.

3 Transmetallation of a Nickel(II) Receptor

Having observed the time dependent behaviour upon the addition of anion in the UV/visible spectrum of the nickel(II) receptors, it was decided to investigate this further by studying the properties of an analogous palladium(II) receptor.

It is known that nickel(II) dithiocarbamate complexes, although thermodynamically stable, undergo rapid ligand exchange.[52] In contrast, palladium(II) dithiocarbamates undergo much slower ligand exchange.[53] Thus, an analogous palladium(II) receptor could be studied using UV/visible and ^{1}H NMR spectroscopy techniques and the effect of slow anion complexation might be elucidated.

3.1 Synthesis and Characterisation

There were two potential routes to forming the palladium(II) analogue of receptor **47**. Firstly, to react potassium tetrachloropalladate(II) with the potassium dithiocarbamate salt of **40**, or secondly, to perform a transmetallation reaction with **47**.

Unfortunately, attempts to synthesise the palladium(II) dithiocarbamate receptor directly from the potassium dithiocarbamate salt of **40** gave a complex mixture of products. However,

when two equivalents of tetrachloropalladate(II) were added to a tetrahydrofuran:water solution of **47** an immediate colour change, from green to orange, was observed. The solution was stirred for 10 minutes, the tetrahydrofuran was removed under reduced pressure and the product extracted into chloroform. Drying and solvent removal gave the product **53** in 77% yield.

Receptor **53** was characterised by ^{1}H, ^{1}H-^{1}H COSY, ^{13}C NMR, UV/visible, infrared, ESMS and elemental analysis. For example, ESMS showed an excellent match between calculated and experimental isotopic patterns for [**53** + K^{+}]$^{+}$ when a solution of the receptor was co-injected with KPF_6 into the mass spectrometer.

3.2 Anion Binding Studies

The palladium(II) receptor's anion binding properties were investigated using UV/visible and ^{1}H NMR spectroscopies. The anions studied were acetate, benzoate, dihydrogen phosphate and chloride as their TBA salts.

3.2.1 UV/visible Spectroscopy

Palladium(II) dithiocarbamate complexes display absorptions in the UV region ~240nm and ~300nm due to LC π-π^{*} transitions from molecular orbitals in the NCS and SCS moieties respectively.[54] Another LC n-π^{*} transition occurs ~350nm due to transitions between energy levels originated from the sulphur atoms. A weak MLCT charge transfer peak occurs at ~460nm.

Table 3.18 displays the wavelengths and molar extinction coefficients of receptor **53** in MeCN:DMSO (4:1) solution between 250nm and 500nm. The LC peak ~240nm was masked by absorption of the DMSO and the MLCT absorption was hidden underneath the tail of the absorption at 348nm.

Assignment	53
LC	302 (70.0)
LC	348 sh (16.2)

Table 3.18 *Wavelength λ/nm (molar extinction coefficient ε/10^3 $M^{-1}cm^{-1}$) of* ***53***

Two equivalents of the four anions were added to a solution of **53** and the spectrum recorded every minute until a constant absorption value was reached. **Table 3.19** shows the time for the absorption to reach a steady value for **53** and the analogous nickel(II) receptor, **47**.

Anion	Equilibration time (minutes)	
	47	53
Acetate	1	>45
Benzoate	16	25
Dihydrogen Phosphate	6	20

Table 3.19 *Time taken for the absorbance to reach a steady value after the addition of two equivalents of anion*

Receptor **53** took considerably longer for the absorption to reach a constant value for each anion. It is important to note that similar experiments with $Ni(DTCEt_2)_2$[14] showed no change in absorption when ten equivalents of anion were added to the solution. Thus, the time dependent behaviour seen must be due to the specific properties of the macrocyclic receptors rather than the dithiocarbamate group.

3.2.2 ^{1}H NMR Spectroscopy

The anion binding properties of receptor **53** were studied using ^{1}H NMR spectroscopy. The spectrum was recorded after additions of aliquots of the four anions in DMSO-d_6 solution. In all cases, the peak due to the amide proton was seen to shift further downfield indicating that the amide group was forming a favourable receptor:anion interaction.[55] **Table 3.20** illustrates the change in chemical shift of the amide proton upon the addition of equivalents of the four anions.

Anion	Change in amide proton shift (Δδ)				
	1 Eq	2 Eq	3 Eq	5 Eq	10 Eq
Acetate	0.32	-[a]	-[a]	-[a]	-[a]
Benzoate	0.35	1.06	1.72	2.38	2.68
Dihydrogen Phosphate	0.42	1.40	1.94	2.23	2.42
Chloride	0.05	0.12	0.21	0.42	0.86

Table 3.20 *Change in chemical shift of the amide protons upon addition of anions as their TBA salts at 298K (a - discussed in the text)*

Disappointingly, upon addition of aliquots of acetate anion, the amide peak became increasingly broad and could not be observed above one equivalent of anion. When aliquots of chloride were added to receptor **53** very little perturbation of the amide peak was observed even after the addition of 10 equivalents.

Addition of dihydrogen phosphate and benzoate anions produced large changes in the chemical shift of the amide proton. Unfortunately, the titration data could not be fitted using EQNMR[56] as the shape of the binding profile was complex, indicating the existence of multiple equilibria in solution.

The behaviour of this palladium(II) receptor is very different to that of the analogous nickel(II) receptor **47**. The palladium(II) receptor did not display extra peaks in the spectrum in the presence of any anions whereas with **47** new resonances were noted (see **Section 2.2.5**). When 10 equivalents of the four anions were added to the model compound $Ni(DTCEt_2)_2$[14] in DMSO-d_6 the spectrum was not altered. The extra peaks observed with **47** must arise due to the specific properties of the macrocycle **47**.

Receptor **53** is identical to that of **47** except that the metal centre has been altered to a second row transition metal. Thus, it must be the properties of the metal affected the anion binding behaviour of the macrocyclic receptor in solution. It is likely that the amide groups coordinate to the anionic guest, and due to the proximity of the amide to the transition metal dithiocarbamate centre a subsequent competing reaction occurs which gives rise to new products.

The second row transition metal, palladium(II), is known to exhibit much slower ligand kinetics of dithiocarbamate ligand exchange than nickel(II) dithiocarbamate complexes.[53] Taking this into account together with the UV/visible and ^{1}H NMR titration results, the rate of this anion induced complexation reaction does appear to correlate with transition metal dithiocarbamate ligand exchange rates. Unfortunately, the identity of the species formed could not be determined by ^{1}H NMR or ESMS experiments, but addition of anion changed the spectrum obtained in both techniques.

4 Macrocyclic Anion Dithiocarbamate Receptors with Increased Solubility

The receptors described above (**43** – **52**) were, in general, only soluble in highly polar solvents, such as DMF and DMSO, which compete with anion binding.

By replacing the alkyl chains on the receptor molecules with a more lipophilic group, the solubility of the receptors may be increased in less competitive solvent such as chloroform. Anion binding studies may yield information about the any selectivity, as the magnitude of binding will be much greater in this solvent.

4.1 Synthesis and Characterisation

Scheme 3.4 shows the synthesis of macrocyclic bis-amide receptor **55** starting from bis amide **33**.

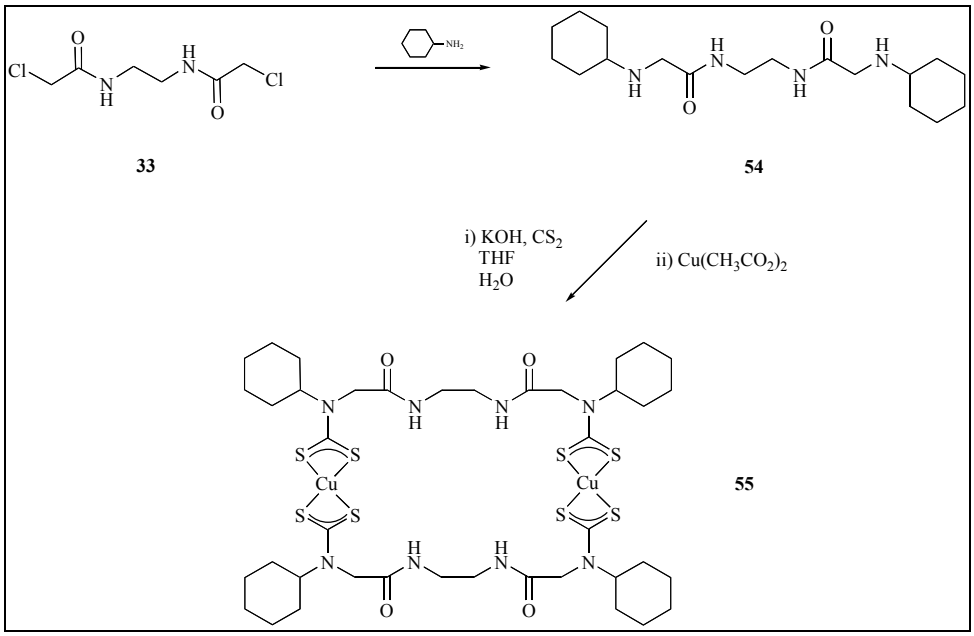

Scheme 3.4 *Synthesis of receptor **55***

The bis-chloro precursor **33** was synthesised as described in **Section 2.1**. This alkyl chloride was converted to secondary amine **54** by portion wise addition of **33** to an excess of cyclohexylamine and heating for 15 hours.[5] After washing with water, and removal of excess cyclohexylamine under reduced pressure, the bis-amine was isolated in 60% yield and was characterised by ^{1}H, ^{1}H-^{1}H COSY NMR and ESMS.

The secondary amine was converted to the final product using two equivalents of potassium hydroxide and two equivalents of carbon disulphide in a tetrahydrofuran:water (2:1) mixture followed by the addition of one equivalent of copper(II) acetate[6] to give **55** as a brown powder. The inclusion of the bulkier cyclohexyl groups had resulted in this receptor being soluble in the non-competitive solvent chloroform. The analogous receptor **43** was insoluble in chloroform.

Receptor **55** was characterised by UV/visible, infrared, ESMS spectroscopies, electrochemistry and elemental analysis. For example, when **55** was coinjected with $NOBF_4$ into the electrospray mass spectrometer, the spectrum showed isotopic clusters agreed with calculated values for $[\mathbf{55}]^{2+}$. The peaks were separated by 0.5 mass units consistent with **55** carrying a plus two charge, showing that each macrocycle had two copper(II) dithiocarbamate centres which had each been oxidised to copper(III).

Disappointingly, the synthesis of the analogous nickel(II) receptor gave a characteristically green product, however it proved to be insoluble in any common organic solvent.

4.2 Anion Binding Studies

4.2.1 Copper(II) Electrochemistry

The electrochemical properties of receptor **55** were studied in a $CHCl_3$:MeCN (4:1) solvent mixture. The electrochemical properties of $Cu(DTCEt_2)_2$[14] were also studied and the data displayed as in **Table 3.21**.

	Cu(II)/Cu(III)		**Cu(II)/Cu(I)**	
	$Cu(DTCEt_2)_2$	**55**	**$Cu(DTCEt_2)_2$**	**55**
E_{pa} (V)	0.260	0.335	-0.900	-
E_{pc} (V)	0.135	0.155	-1.050	-0.860
ΔE_p (V)	0.125	0.170	0.150	-
I_{pa}/I_{pc}	1.0	1.1	0.8	-
E_p (V)	0.205	0.255	-0.805	-

Table 3.21 *Electrochemical data of $Cu(DTCEt_2)_2$ and **55** in $CHCl_3$:MeCN (4:1) containing 0.1M $TBABF_4$, potentials given with reference to Ag/Ag^+ at 293K, scan rate = 100mVs^{-1}, E_p - peak potential in square wave voltammogram*

The potential of the oxidation and reduction waves of both $Cu(DTCEt_2)_2$ and **55** did not vary with scan rate and the peak current was found to be proportional to square root of the scan rate. Thus, both complexes displayed quasi-reversible electrochemical characteristics for the copper(II)/copper(III) couple.[23] However, only $Cu(DTCEt_2)_2$ displayed quasi-reversibility of the copper(II)/copper(I) couple. The oxidation of **55** was observed at a larger potential than that of $Cu(DTCEt_2)_2$ due to the neighbouring electron withdrawing amide group.

The response of $Cu(DTCEt_2)_2$ and receptor **55** to the addition of anions was investigated using square wave voltammetry. The magnitudes of the cathodic shifts observed upon the addition

of five equivalents of anion are displayed in **Table 3.22** together with the shifts observed with the analogous receptor **44** in DMF. Unfortunately, the copper(II)/copper(I) couple was not observed in the square wave voltammogram of **55**, thus no anion binding studies could be carried out. This may be due to the stereochemical change from copper(II) square planar to copper(I) tetrahedral.[21]

Anion	ΔE Cu(II)/Cu(III) (mV)		
	$Cu(DTCEt_2)_2$	**44[a]**	**55**
Acetate	25	100	55
Benzoate	15	30	75
Dihydrogen Phosphate	5	130	180

Table 3.22 *Cathodic shifts in the square wave voltammogram upon the addition of 5 equivalents of anion to $Cu(DTCEt_2)_2$ and **44** and **55** in $CHCl_3$:MeCN (4:1) containing 0.1M $TBABF_4$, potentials given with reference to Ag/Ag^+ at 293K (a - in DMF)*

Small cathodic shifts of the copper(II)/copper(III) peak were observed upon the addition of five equivalents acetate, benzoate and dihydrogen phosphate anions to $Cu(DTCEt_2)_2$. In contrast, **55** displayed much larger shifts upon the addition of excess acetate, benzoate and dihydrogen phosphate anions. Cathodic shifts were observed as the anion bound to the amide groups of the macrocycle stabilised the charged copper(III) dithiocarbamate species.[18]

The magnitudes of the shifts of benzoate and dihydrogen phosphate are much larger than those observed with the analogous receptor **44** in the more competitive solvent, DMF. The use of the less competitive solvent mixture has enhanced the cathodic shifts observed. This is because the strength of anion binding with the receptor is larger in this solvent.

When chloride was added to **55** two peaks were observed in the voltammogram, one at a higher potential and one at a lower potential possibly due to a reaction occurring.

5 Monometallic Macrocyclic Dithiocarbamate Anion Receptors

The dithiocarbamate moiety was used to synthesise monometallic macrocyclic structures. The synthesis depends upon flexibility of the hydrocarbon backbone and the distance between the two secondary amine moieties being large enough to enable cyclisation, but not too large so that polymerisation would be a competing side reaction. The following section details the synthesis and study of two such compounds.

5.1 Synthesis and Characterisation

Scheme 3.5 shows the synthesis of macrocyclic bis-amide receptors **58** and **59** from acyclic precursor molecules.

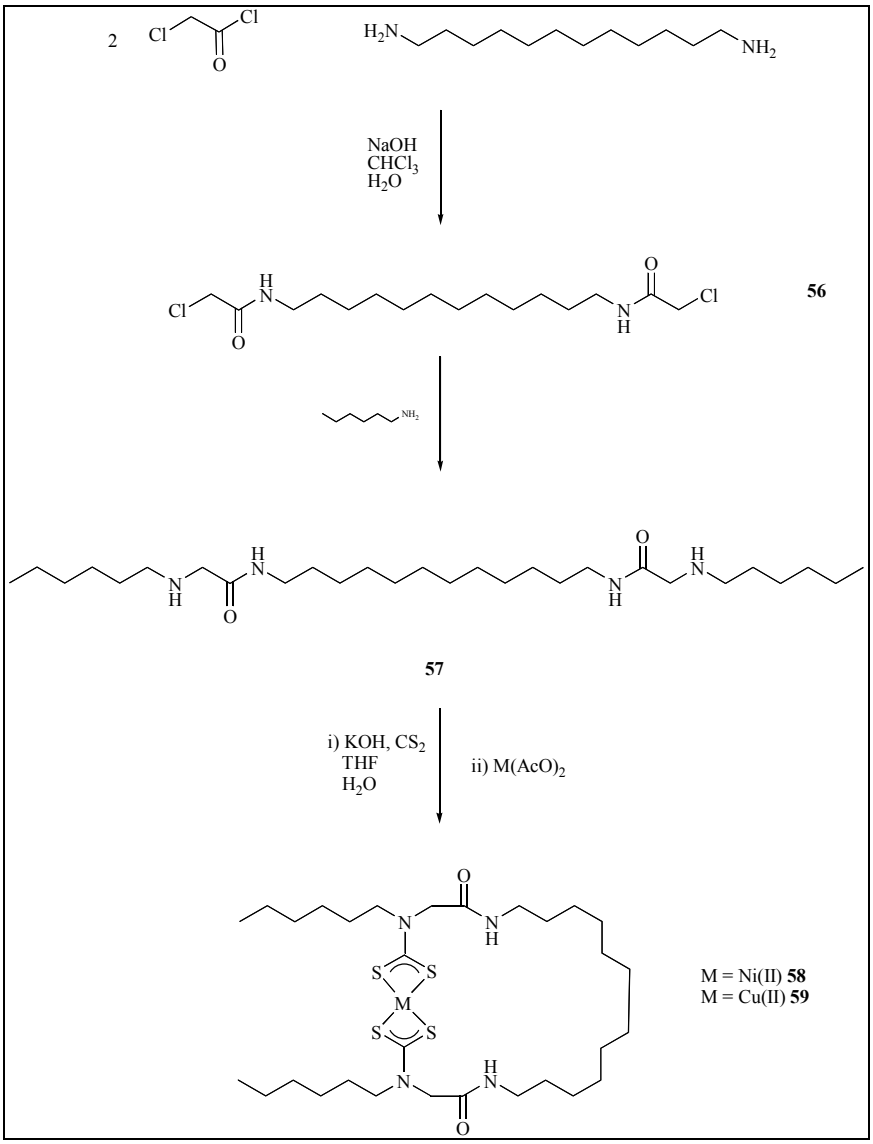

Scheme 3.5 *Synthesis of receptors **58** and **59***

The bis-amide molecule **56** was synthesised in ~80% yield using the same method described ealier[3] (see **Section 2.1**) and its structure was confirmed by ESMS and the ^{1}H NMR spectrum revealed a peak at 7.26ppm due to the amide proton.[4] The alkyl chloride was converted to the corresponding secondary amine by the portion wise addition of the bis-amide to an excess of hexylamine.[5] After heating for 15 hours and washing with water, excess hexylamine was removed under reduced pressure giving the bis-amine **57** in 58% yield. This diamine was characterised by ^{1}H, ^{1}H-^{1}H COSY NMR and ESMS.

The macrocyclic receptors were formed in the usual way using two equivalents of potassium hydroxide and two equivalents of carbon disulphide in a tetrahydrofuran:water (5:1) mixture followed by the addition of one equivalent of nickel(II) or copper(II) acetate and stirring for 15 hours.[6] Receptors **58** and **59** were isolated as green and brown powders in yields of 73%

and 91% respectively and were characterised by ^{1}H, ^{1}H-^{1}H COSY NMR, ^{13}C NMR, UV/visible, infrared, ESMS spectroscopies, electrochemistry and elemental analysis.

5.2 Anion Binding Studies

^{1}H NMR, UV/visible spectroscopy and electrochemical techniques were used to investigate the anion binding properties of receptors **58** and **59**.

5.2.1 Copper(II) Electrochemistry

The electrochemical properties of receptor **59** and $Cu(DTCEt_2)_2$[14] were studied by both cyclic and square wave voltammetry in a $CHCl_3$:MeCN (4:1) solvent mixture. **Table 3.23** presents the electrochemical data for receptor **59** and $Cu(DTCEt_2)_2$.

	Cu(II)/Cu(III)		**Cu(II)/Cu(I)**	
	$Cu(DTCEt_2)_2$	**59**	**$Cu(DTCEt_2)_2$**	**59**
E_{pa} (V)	0.260	0.285	-0.900	-
E_{pc} (V)	0.135	0.175	-1.050	-0.735
ΔE_p (V)	0.125	0.110	0.150	-
I_{pa}/I_{pc}	1.0	1.3	0.8	-
E_p (V)	0.205	0.235	-0.805	-0.650

Table 3.23 *Electrochemical data of $Cu(DTCEt_2)_2$ and **59** in $CHCl_3$:MeCN (4:1) containing 0.1M $TBABF_4$, potentials given with reference to Ag/Ag^+ at 293K, scan rate = 100mVs^{-1}, E_p - peak potential in square wave voltammogram*

Receptor **59** displayed typical electrochemical characteristics for a copper(II) dithiocarbamate species.

The response of $Cu(DTCEt_2)_2$ and **59** to the addition of anions was monitored by square wave voltammetry. The cathodic shifts observed upon the addition of five equivalents of anion are displayed in **Table 3.24**.

Anion	ΔE Cu(II)/Cu(III) (mV)		ΔE Cu(II)/Cu(I) (mV)	
	$Cu(DTCEt_2)_2$	**59**	$Cu(DTCEt_2)_2$	**59**
Acetate	25	45	<5	<5
Benzoate	15	10	<5	<5
Dihydrogen Phosphate	5	45	<5	<5

Table 3.24 *Cathodic shifts in the square wave voltammogram upon the addition of 5 equivalents of anion to $Cu(DTCEt_2)_2$ and **59** in $CHCl_3$:MeCN (4:1) containing 0.1M $TBABF_4$, potentials given with reference to Ag/Ag^+ at 293K*

In contrast to $Cu(DTCEt_2)_2$, receptor **59** displayed larger shifts of the oxidation couple when excess acetate anion was added, and a much larger shift upon the addition of dihydrogen phosphate. Cathodic shifts were observed as the proximity of the bound anion stabilises the copper(III) state.[18] However, addition of benzoate only produced a small cathodic shift.

This is of note as benzoate is much more basic than dihydrogen phosphate.[44] It is possible that dihydrogen phosphate maybe able to be bound by both amide groups cooperatively, thus holding the anion close to the metal centre so perturbing the copper(II) dithiocarbamate centre to a greater extent than benzoate.

When chloride was added two peaks were seen in the voltammogram, one anodically shifted by 120mV and the other cathodically shifted by 30mV, possibly due to a reaction occurring.

Similarly to $Cu(DTCEt_2)_2$, receptor **59** displayed very small cathodic shifts of the reduction wave upon anion addition.

5.2.2 Nickel(II) Electrochemistry

Receptor **58** and the $Ni(DTCEt_2)_2$[14] were studied in DMF by cyclic and square wave voltammetry and the data is shown in **Table 3.25**.

	Ni(II)/Ni(IV)			Ni(II)/Ni(I)	
	$Ni(DTCEt_2)_2$	**58**		**$Ni(DTCEt_2)_2$**	**58**
E_{pa} (V)	0.630	0.355	**E_{pa} (V)**	-1.800	-
E_p (V)	0.505	0.220	**E_{pc} (V)**	-1.980	-1.920
	Ni(IV)/Ni(III)		**ΔE (V)**	0.180	-
	$Ni(DTCEt_2)_2$	**58**	**I_{pa}/I_{pc}**	0.9	-
E_{pa} (V)	-0.225	-0.215	**E_p (V)**	-1.870	-1.795
	Ni(IV)/Ni(III)				
	$Ni(DTCEt_2)_2$	**58**			
E_{pa} (V)	-0.770	-0.700			

Table 3.25 *Electrochemical data of $Ni(DTCEt_2)_2$ and the **58** in DMF containing 0.1M $TBABF_4$, potentials given with reference to Ag/Ag^+ at 293K, scan rate = 100mVs^{-1}, E_p - peak potential in square wave voltammogram*

Receptor **58** displayed the redox characteristics typical of a nickel(II) dithiocarbamate compound except that the nickel(II)/nickel(I) couple was irreversible.

Table 3.26 presents the cathodic shift of the nickel(II)/nickel(I) couple in the square wave when five equivalents of various anions were added to receptor **58**.

Anion	**ΔE Ni(II)Ni(I) (mV)**	
	$Ni(DTCEt_2)_2$	**58**
Acetate	<5	15
Benzoate	<5	5
Dihydrogen Phosphate	<5	15
Chloride	<5	<5

Table 3.26 *Cathodic shifts in the square wave voltammogram upon the addition of 5 equivalents of anion $Ni(DTCEt_2)_2$ and **58** in DMF containing 0.1M $TBABF_4$, potentials given with reference to Ag/Ag^+ at 293K*

Receptor **58** showed small but significant cathodic shifts of the nickel(II)/nickel(I) redox couple, consistent with anion binding in the proximity of the dithiocarbamate centre, inhibiting the reduction of the redox centre, so a greater potential is required to perform the reduction.[45]

The magnitude of the shifts observed were small and could be due to the competitive nature of DMF as a solvent.

5.2.3 ^{1}H NMR Spectroscopy

Receptor **58** was titrated with TBA salts of the four different anions in DMSO-d_6 solution. Upon the addition of anion, the amide proton resonance was observed to move downfield, indicating the anion was binding to the amide group.[48] **Table 3.27** shows qualitatively the change in chemical shift of the amide proton upon the addition of equivalents of the four anions.

Anion	Change in amide proton shift (Δδ)				
	1 Eq	2 Eq	3 Eq	5 Eq	10 Eq
Acetate	0.05	0.14	0.20	0.35	0.64
Benzoate	0.09	0.17	0.24	0.36	0.60
Dihydrogen Phosphate	0.07	0.13	0.18	0.26	0.45
Chloride	0.04	0.07	0.09	0.14	0.25

Table 3.27 *Change in chemical shift of the amide protons of **58** upon addition of anions as their TBA salts at 298K*

There was a marked downfield shift of the amide peak after the addition of ten equivalents of all four anions however there was little movement of the proton resonance up to two equivalents of anion added. If anion binding was strong, the amide peak would be expected to significantly shift between zero and two equivalents followed by only small changes upon further anion addition. Unfortunately, it was not possible to accurately calculate stability constants from the data as the titration curve was very shallow, indicative of weak binding.

5.2.4 UV/visible Spectroscopy

The anion binding characteristics of receptor **58** was studied by UV/visible spectroscopy. Nickel(II) dithiocarbamates typically display three charge transfer absorption bands between 250nm and 500 nm.[13]

Table 3.28 displays the wavelengths and molar extinction coefficients of receptors **58** and $Ni(DTCEt_2)_2$ in MeCN:DMSO (4:1) solution.

Assignment	$Ni(DTCEt_2)_2$	58
LC	327 (36.9)	324 (35.0)
MLCT	399 (5.8)	388 (6.2)
MLCT	427 sh (1.6)	428 sh (2.0)

Table 3.28 *Wavelength λ/nm (molar extinction coefficient $\varepsilon/10^3$ $M^{-1}cm^{-1}$) of $Cu(DTCEt_2)_2$ and **58***

Upon addition of the four anions small changes in all the absorption bands were observed. The LC band at 257nm increased in intensity while the charge transfer bands at longer wavelengths decreased in intensity. Unfortunately, it was not possible to calculate stability constants from the titration data due to the changes in spectra being so small, indicating weak binding.

6 Attempted Syntheses

Several efforts were made to synthesise transition metal dithiocarbamate thiourea macrocyclic analogues. The following sections outline the syntheses that were attempted and the problems encountered.

6.1 Thiourea Macrocycles

A macrocyclic dithiocarbamate molecule containing thiourea groups could possess interesting anion binding properties due to the increased acidity of the thiourea protons (see **Chpater 2 Section 3**). Two different synthetic routes were attempted to produce such a receptor.

The first method initially synthesised the protected thiourea **60**, as shown in **Scheme 3.6**.

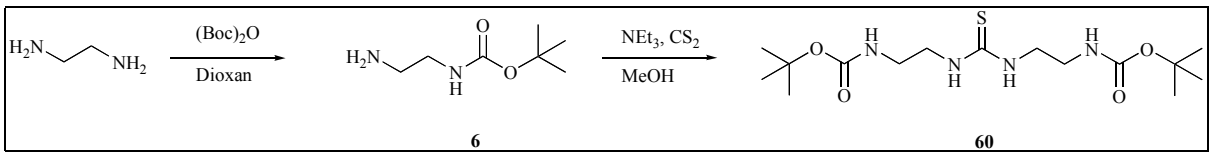

6 **60**

Scheme 3.6 *Synthesis of thiourea **60***

Commercially available ethylene diamine was mono protected in 1,4-dioxane using a *tert*-butoxycarbonyl group to form **6** in 80% yield.[57] This was dissolved in methanol, one equivalent of triethylamine and half an equivalent of carbon disulphide were added, and the mixture refluxed for fifteen hours.[58] After work up, the symmetrical thiourea was isolated as a yellow oil.

The next step of the reaction was to remove the protecting groups. Unfortunately, this was not possible either by using trifluoroacetic acid or hydrogen chloride gas in dichloromethane or aqueous hydrochloric acid.[59] Thus, an alternative route was tried to create a macrocyclic thiourea dithiocarbamate receptor.

Scheme 3.7 outlines the synthesis of a macrocyclic thiourea precursor.

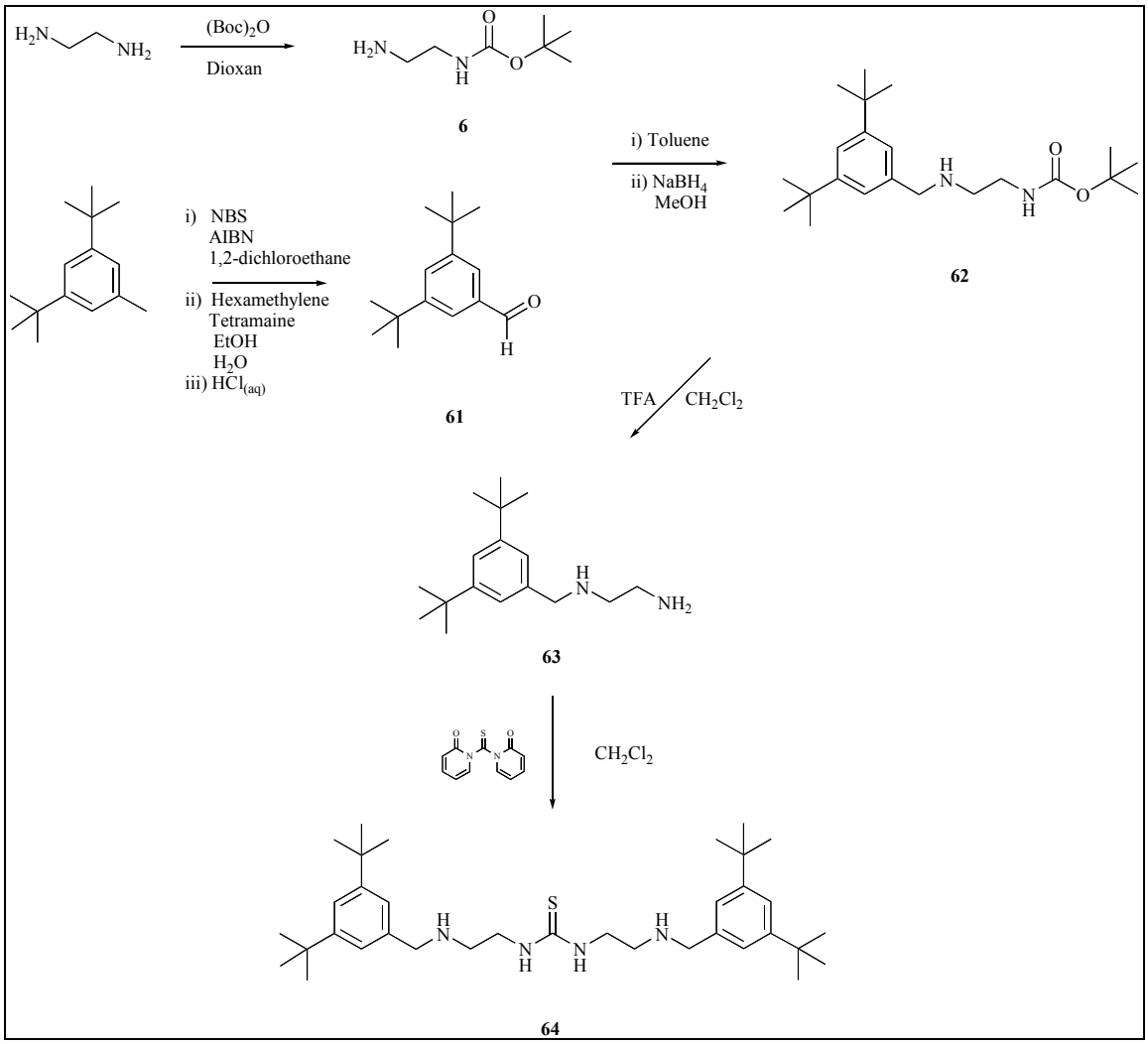

Scheme 3.7 *Synthesis of bis-amine thiourea precursor **64***

In light of the relative insolubility of the amide receptors reported earlier in this chapter (see **Section 2**) a highly lipophilic aldehyde **61** was used.[60] This was synthesised from 3,5-di-*tert*-butyl toluene using *N*-bromosuccinimide (NBS) and 2,2'-azobis(2-methyl-propionitrile) (AIBN) in 1,2-dichloroethane and refluxing for four hours. The solvent was removed and the products redissolved in an ethanol:water (1:1) mixture and refluxed with hexmethylenetetramine. The product, **61**, was subsequently isolated in 82% yield and its ^{1}H NMR spectrum revealed a peak at 10.0ppm, characteristic of an aldehyde proton.

One equivalent of the monoprotected amine **6** was condensed with the one equivalent of **73** in toluene. The formation of the imine was driven by using toluene as solvent and Dean-Stark apparatus to azeotropically remove water from the reaction.[61] The imine was reduced using sodium borohydride in methanol[62] to afford the secondary amine **62** in 86% yield. The protecting group was then removed using trifluoroacetic acid in dichloromethane.[59] The thiourea group was

synthesised by mixing half an equivalent of dichloromethane 1,1'-thiocarbonyldi-2(1H)-pyridone together with the primary amine and refluxing for one hour.[63] The ^{1}H NMR spectrum revealed a typically broad resonance at 5.70ppm due to the thiourea protons. All the molecules **6**, **61** - **64** were characterised by ^{1}H, ^{1}H-^{1}H COSY NMR and ESMS.

Attempted conversion of **64** into an anion receptor molecule is illustrated below in **Scheme 3.8**.

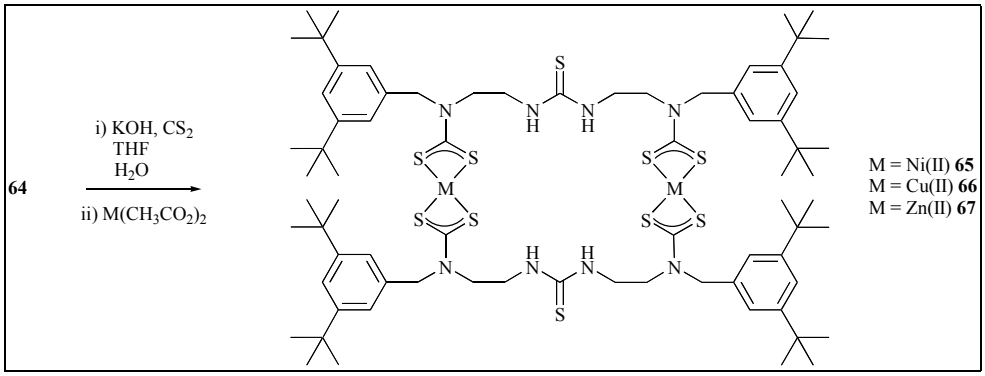

Scheme 3.8 *Attempted synthesis of receptor **65**, **66** and **67***

The dithiocarbamate formation was the same as that used previously described (see **Section 2.1**). Disappointingly, the isolated powders were not characteristically coloured and no evidence of the macrocyclic products **65** - **67** was found using NMR or ESMS.

7 Summary

Two novel types of transition metal dithiocarbamate macrocyclic anion receptors have been prepared using metal directed self-assembly which contain amide moieties linked by a variety of alkyl or aryl spacer groups.

The first type of receptor (**43** - **52**) contained amide groups and were characterised by a wide range of techniques including a single crystal X-ray structure of **47**. The macrocycles reported anion binding via electrochemical techniques, UV/visible, infrared, ^{1}H and ^{13}C NMR spectroscopies and EPR. UV/visible studies revealed that receptor **48** bound acetate very strongly in a relatively competitive solvent mixture. However, for some of the receptors the strength of anion binding could not be determined by UV/visible or ^{1}H NMR, due to a kinetic effect upon anion complexation. This unusual behaviour was due to the nature of the macrocycle, as the acyclic control compounds did not display changes in their spectra upon anion addition.

The palladium(II) based receptor **53** was synthesised via a transmetallation reaction. This compound showed very different behaviour upon anion addition compared to its nickel(II) analogue, **47**. It is likely that the anion is bound by the amide groups and a competing reaction subsequently occurs. The difference between **47** and **53** upon anion addition is due to the slower kinetics of reorganisation of the dithiocarbamate group of palladium(II) compared to nickel(II). It was not possible to identify the new products by ^{1}H NMR or ESMS experiments.

A more lipophilic anion receptor, **55**, was synthesised by employing cyclohexyl groups. Electrochemical studies, in a relatively non-competitive solvent, revealed much larger cathodic shifts in the square wave than the analogous receptor, **33**, in DMF. There was, however, little discrimination shown for a particular anion.

The second type of macrocycle formed used the dithiocarbamate group to self-assemble receptors that contained one metal centre. Receptors **58** and **59** reported anion binding by ^{1}H

NMR and UV/visible spectroscopies together with electrochemical techniques. All four anions were bound weakly by these receptors.

In summary, the aim of this chapter was to develop new types of macrocyclic anion receptors using the dithiocarbamate group to assemble the molecule and to report the guest binding. This goal has been achieved and ^{1}H NMR, UV/visible, infrared, electron paramagnetic spectroscopies and electrochemical methods have demonstrated that these receptors bind and sense anions in various organic solvents.

8 References

[1] P. D. Beer, F. Szemes, V. Balzani, C. M. Sala, M. G. B. Drew, S. W. Dent, M. Maestri, *J. Am. Chem. Soc.*, 1997, **119**, 11864.
[2] L. H. Uppadine, J. M. Weeks, P. D. Beer, *J. Chem. Soc. Dalton Trans.*, 2001, 3367.
[3] A. J. Speziale, P. C. Hamm, *J. Am. Chem. Soc.*, 1956, **78**, 2556.
[4] L. M. Harwood, C. J. Moody, *Experimental Organic Chemistry Principles and Practice*, Blackwell Scientific Publishers, 1989, 750.
[5] R. N. Salvatore, C. H. Yoon, K. W. Jung, *Tetrahedron*, 2001, **57**, 7785.
[6] a) D. Coucouvanis, *Prog. Inorg. Chem.*, 1979, **26**, 301; b) D. Coucouvanis, *Prog. Inorg. Chem.*, 1970, **11**, 233; c) D. J. Halls, *Mickro. Acta*, 1969, 62; d) J. Willemse, J. A. Cras, J. J. Steggerda, *Struct. Bonding*, 1976, **28**, 83; e) G. D. Thorn, R. A. Ludwig, *The Dithiocarbamates and Related Ligands*, Elsevier, 1962.
[7] L. M. Harwood, C. J. Moody, *Experimental Organic Chemistry Principles and Practice*, Blackwell Scientific Publishers, 1989, 354.
[8] H. L. M. van Gaal, J. W. Diesveld, F. W. Pijpers, J. G. M. van der Linden, *Inorg. Chem.*, 1979, **18**, 3251.
[9] a) M. Bonamico, G. Dessy, C. Mariani, A. Vaciago, L. Zambonelli, *Acta Crystallogr.*, 1965, **19**, 619; b) M. N. I. Khan, J. P. Fackler Jr., H. H. Murray, D. D. Heinrich, C. Campana, *Acta Crystallogr., Sect. C (Cr. Str. Comm.),* 1987, **43**, 1917.
[10] G. Aylward, T. Findlay, S.I. Chemical Data, 3rd Edition, 1994, J. Wiley & Sons, 114.
[11] D. F. Schoener, M. A. Olsen, P. G. Cummings, C. Basic, *J. Mass. Spectrom.*, 1999, **34**, 1069.
[12] A. M. Bond, R. Colton, A. D'Agostino, J. Harvey, J. J. Traeger, *Inorg. Chem.*, 1993, **32**, 3952.
[13] M. Castillo, J. J. Criado, B. Macias, M. V. Vaquero, *Trans. Met. Chem.*, 1986, **11**, 476.
[14] For synthesis and characterisation see the Experimental Chapter.
[15] P. W. Atkins, *Physical Chemistry*, 4th Ed., 1990, 508.
[16] G. H. Sarova, B. G. Jeliazkova, *Transition Met. Chem.*, 2001, **26**, 388.
[17] D. Oktavec, J. Stefanec, B. Siles, E. Beinrohr, V. Konecy, J. Garaj, *Coll. Czech. Chem. Comm.*, 1982, **47**, 2867.
[18] P. D. Beer, N. Berry, M. G. B. Drew, O. D. Fox, M. E. Padilla-Tosta, S. Patell, *Chem. Commun.*, 2001, 199.
[19] K. A. Connors, *Binding Constants*, J. Wiley & Sons, 1987, 24.
[20] A. M. Bond, R. L. Martin, *Coord. Chem. Rev.*, 1984, **54**, 23.
[21] A. R. Hendrickson, R. L. Martin, N. M. Rohde, *Inorg. Chem.*, 1976, 15, 2115.
[22] R. Chant, A. R. Hendrickson, R. L. Martin, N. M. Rhode, *Aust. J. Chem.*, 1973, **26**, 2533.
[23] Southampton Electrochemical Group*, Instrumental Methods in Electrochemistry*, Ellis-Horwood, 1985, 183.
[24] A. J. Bard, L. R. Faulkner, *Electrochemical Methods Fundamentals and Applications*, J. Wiley & Sons, 406.
[25] A. J. Bard, L. R. Faulkner, *Electrochemical Methods Fundamentals and Applications*, J. Wiley & Sons, 283.
[26] A. R. Hendrickson, R. L. Martin, N. M. Rohde, *Inorg. Chem.*, 1975, **14**, 2980.
[27] L. M. Harwood, C. J. Moody, *Experimental Organic Chemistry Principles and Practice*, Blackwell Scientific Publishers, 1989, 294.
[28] G. Socrates, *Infrared Characteristic Group Frequencies*, 2nd Ed, J. Wiley & Sons, 104.
[29] G. Socrates, *Infrared Characteristic Group Frequencies*, 2nd Ed, J. Wiley & Sons, 105.
[30] R. Payne, R. J. Magee, J. Liesegang, *J. Elec. Spectr. Rel. Phen.*, 1985, **35**, 113.
[31] a) F. Bonati, R. Ugo, *J. Organomet. Chem.*, 1967, **10**, 257; b) H. C. Brinkhoff, A. M. Grotens, *Rec. Trav, Chim.*, 1971, **111**, 253.
[32] K. B. Pandeya, T. S. Waraich, R. C. Gaur, R. P. Singh, *J. Inorg. Nucl. Chem.*, 1981, 43, 3159.

[33] a) F. E. Mabbs, D. J. Machin, *Magnetism and Transition Metal Complexes*, Chapman and Hall, 1973, 5; b) E. A. Bordreaux, L. N. Mulay, *Theory and Applications of Molecular Paramagnetism*, J. Wiley & Sons, 491; c) O. Kahn, *Molecular Magnetism*, VCH, 1993, 3.
[34] F. E. Mabbs, D. J. Machin, *Magnetism and Transition Metal Complexes*, Chapman and Hall, 1973, 7.
[35] F. E. Mabbs, D. J. Machin, *Magnetism and Transition Metal Complexes*, Chapman and Hall, 1973, 22.
[36] M. McElfresh, *Fundamentals of Magnetism and Magnetic Measurements Featuring* Q*uantum Design's Magnetic Property Measurement System*, 1994, 19.
[37] P. S. Mukherjee, S. Dalai, G. Mostafa, T. H. Lu, E. Rentschler, N. R. Chaudhuri, *New J. Chem.*, 2001, **25**, 1203.
[38] F. E. Mabbs, D. J. Machin, *Magnetism and Transition Metal Complexes*, Chapman and Hall, 1973, 20.
[39] A. C. Fabretti C. Preti, L. Tassi, G. Tosi, P. Zannini, *Aust. J. Chem.*, 1986, **39**, 605.
[40] M. McElfresh, *Fundamentals of Magnetism and Magnetic Measurements Featuring Quantum Design's Magnetic Property Measurement System*, 1994, 23.
[41] W. E. Hatfield, P. Singh, F. Nepveu, *Inorg. Chem.*, 1990, **29**, 4214.
[42] R. Petterson, T. Vanngard, *Arkiv fur Chemie*, 1960, Bd 17 nr 21, 249.
[43] http://www.webelements.com/webelements/elements/text/Cu/isot.html
[44] a) S. Nishizawa, P. Buhlmann, M. Iwao, Y. Umeza, *Tetrahedron Lett.*, 1999, **36**, 6438; b) G. Aylward, T. Findlay, *SI Chemical Data*, 3rd Ed. J. Wiley & Sons, 136.
[45] P. D. Beer, P. A. Gale, G. Z. Chen, *Coord. Chem. Rev.*, 1999, **185**, 3.
[46] R. A. Binstead, A. D. Zuberbuhler, B. Jung, *Specfit 3.0.30*, Spectrum Software Associates, 2002.
[47] a) K. Kavallieratos, C. M. Bertao, R. H. Carbtree, *J. Org. Chem.*, 1999, **64**, 1675; b) J. W. M. Nissink, H. Boerrigter, W. Verboom, D. N. Reinhoudt, J. H. van der Maas, *J. Chem. Soc. Perkins Trans. 2*, 1998, 2623.
[48] C. S. Wilcox, *Frontiers of Supramolecular Organic Chemistry and Photochemistry*, Ed. H. J. Schneider, VCH, 1991, 129.
[49] E. Leize, A. Jaffrezic, A. van Dorsselaer, *J. Mass Spectrom.*, 1996, **31**, 537.
[50] A. Szumna, J. Jurczak, *Eur. J. Org. Chem.*, 2001, 4031.
[51] M. G. B. Drew, J. Hunter, D. J. Marrs, J. Nelson, C. Harding, *J. Chem. Soc. Dalton Trans.*, 1992, 3235.
[52] M. Moriyasu, Y. Hasimoto, *Bull. Chem. Soc. Jpn.*, 1981, **54**, 2470.
[53] M. Moriyasu, Y. Hashimoto, M. Endo, *Bull. Chem. Soc. Jpn.*, 1983, **56**, 1972.
[54] J. J. Craido, I. Fernandez, B. Macias, J. M. Salas, M. Medarde, *Inorg. Chim. Acta*, 1990, **174**, 67.
[55] C. S. Wilcox, *Frontiers of Supramolecular Organic Chemistry and Photochemistry*, Ed. H. J. Schneider, VCH, 1991, 129.
[56] M. J. Hynes, *J. Chem. Soc. Dalton Trans.*, 1993, 311.
[57] A. P. Krapcho, C. S. Kuell, *Synth. Comm.*, 1990, **20**, 2559.
[58] J. D. Robbins, J. R. Neal, *Syn. Comm.*, 1986, **16**, 891.
[59] M. Bodanszky, A. Bodanszky, *The Practice of Peptide Synthesis*, 2nd Ed., Springer Verlag, 1994.
[60] M. S. Newman, L. F. Lee, *J. Org. Chem.*, 1972, **26**, 4460.
[61] L. M. Harwood, C. J. Moody, *Experimental Organic Chemistry Principles and Practice*, Blackwell Scientific Publishers, 1989, 218.
[62] J. H. Billman, A. C. Diesing, *J. Org. Chem.*, 1957, **22**, 1068.
[63] S. Kim, K. Y. Yi, *J. Org. Chem.*, 1986, **51**, 2615.

Chapter Four

Macrocyclic Dithiocarbamate Receptors

1 Introduction

Chapter 3 described the use of transition metal dithiocarbamates to create macrocyclic receptors capable of binding anionic guest species. The work described in this chapter uses a similar self-assembly strategy to create novel macrocyclic molecules with the potential to bind cationic guest species.

As described in **Chapter 2 Section 1**, electron deficient C_{60} binds to polymetallic zinc(II) or cadmium(II) dithiocarbamate resorcarene loop shaped complexes in organic media via favourable charge transfer interactions between electron rich transition metal dithiocarbamate moieties and electron deficient C_{60}.[1] Taking this into account, novel macrocyclic compounds based upon meta substituted aryl groups may possess interesting coordination properties with cationic guest species.

A schematic of the receptor's design is illustrated in **Figure 4.1**.

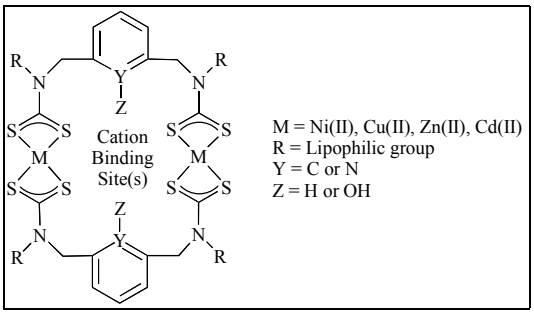

Figure 4.1 *Schematic of target receptors*

The nature of the aromatic groups in the macrocycles has been varied by the incorporation of a variety of donor groups such as pyridine and phenol into the molecular framework. A lipophilic group (R) confers solubility of the macrocycle in a range of organic solvents and the choice of transition metal centre allows various spectroscopic probes to be employed for monitoring the cation binding.

2 Macrocyclic Dithiocarbamate Receptors

The self-assembly of novel receptors containing aromatic groups was achieved using the dithiocarbamate group and the cation binding properties of the macrocycles were studied.

2.1 Synthesis and Characterisation

Scheme 4.1 outlines the synthesis of the amines **68**, **69** and **70**.

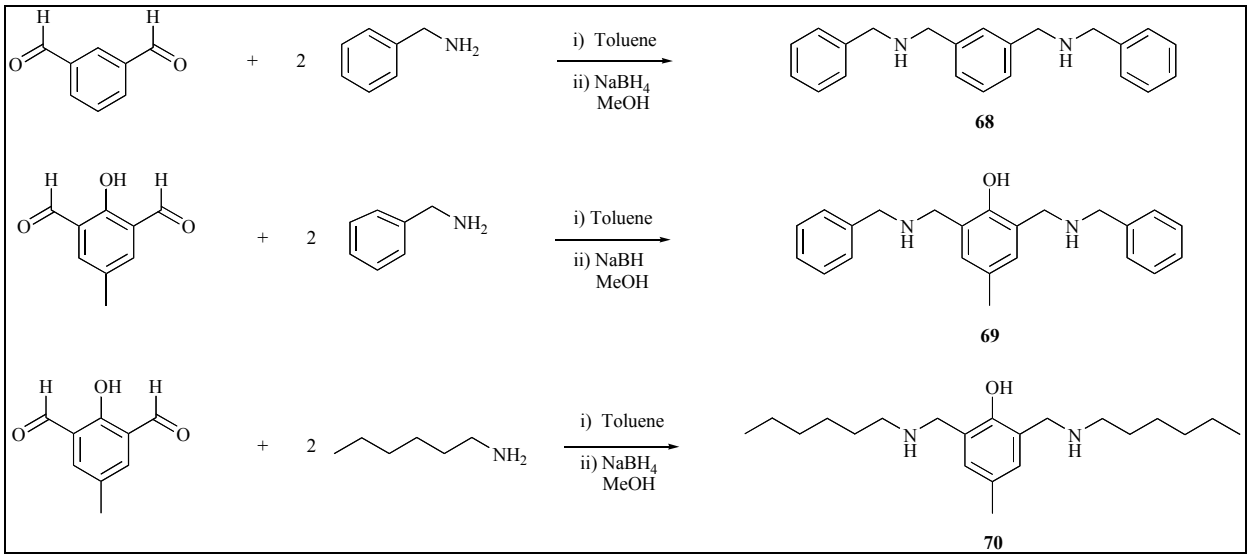

Scheme 4.1 *Synthesis of bis-amine precursors **68 - 70***

Compounds **68 - 70** were synthesised by the addition of two equivalents of a primary amine to one equivalent of a bis-substituted aldehyde. The Schiff base equilibrium is reversible and so imine formation was driven using toluene as solvent and Dean-Stark apparatus.[2] This azeotropically removed the water from the reaction mixture and the resulting imine was reduced to the secondary amine using sodium borohydride in methanol.[3] The amines were isolated in yields of 80% - 90% and characterised by ^{1}H, ^{1}H-^{1}H COSY NMR and electrospray mass spectrometry (ESMS).

The pyridine bis-amine derivative **72** was synthesised as shown in **Scheme 4.2**.

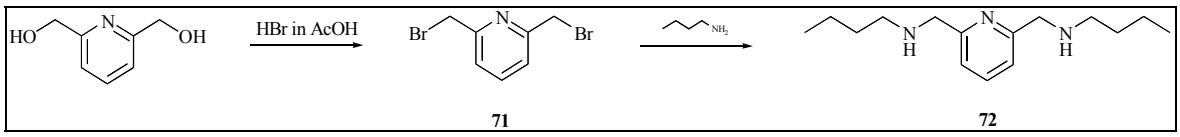

Scheme 4.2 *Synthesis of bis-amine precursor 72*

2,6-Bis-bromomethyl-pyridine was synthesised from 2,6-bis-hydroxymethyl-pyridine using hydrobromic acid in acetic acid.[4] Addition of aqueous sodium hydroxide precipitated the product as a white powder in 20% yield. The bis-brominated product was added portion wise to an excess butylamine, giving the secondary amine **72** in 96% yield.[5] This amine was characterised by ESMS, ^{1}H and ^{1}H-^{1}H COSY NMR spectroscopy that revealed three-bond coupling of adjacent protons on the butyl chain.

The macrocyclic receptors were synthesised as illustrated in **Scheme 4.3**.

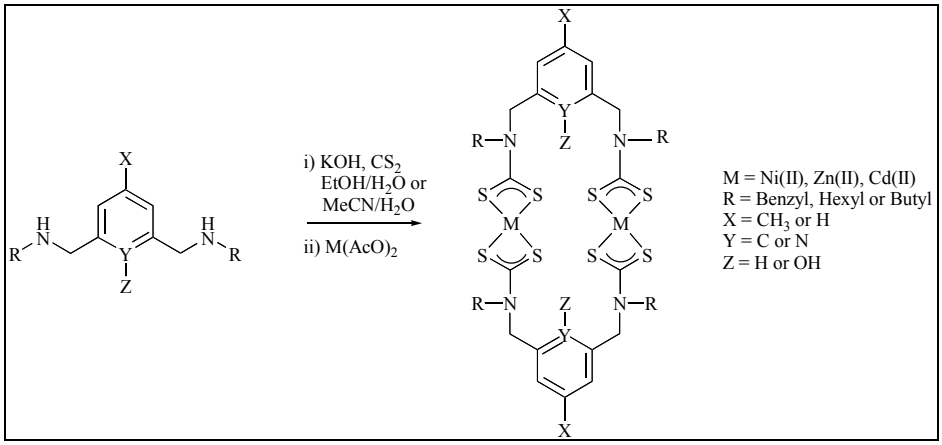

Scheme 4.3 *Synthesis of receptors **86 - 93***

The standard procedure for dithiocarbamate formation was used[6] and the crude product was filtered, extracted into dichloromethane which yielded characteristically coloured oils.

The macrocycles containing zinc(II) or cadmium(II) metal centres were redissolved in pyridine. The pyridine co-ordinated to the vacant fifth coordination site of the zinc(II) or cadmium(II) dithiocarbamate and increased the solubility of the macrocycles.[7] Excess pyridine was removed under reduced pressure.

All receptors (**73 - 80**) were recrystallised from dichloromethane/ethanol yielding the corresponding transition metal dithiocarbamate macrocycles as powders whose yields varied from 15% to 75%.

The synthesised receptors are shown below in **Figure 4.2** and a summary is displayed in **Appendix 12**.

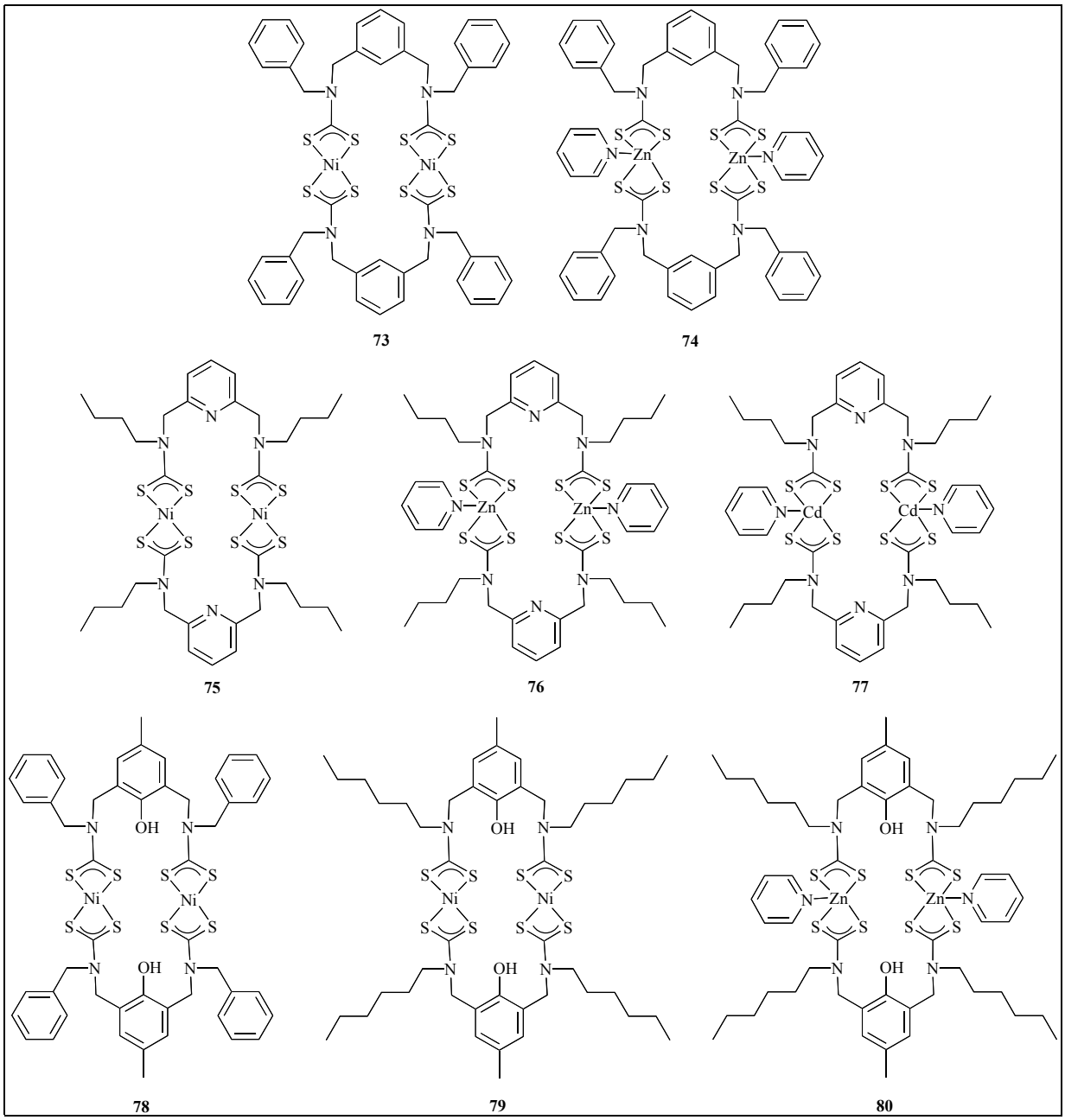

Figure 4.2 *Summary of receptors*

All the macrocycles were characterised by ^{1}H, ^{1}H-^{1}H COSY NMR and ^{13}C NMR, UV/visible, infrared, ESMS spectroscopies and elemental analysis.

At room temperature, the ^{1}H NMR spectrum of **79** revealed considerable broadness of all the peaks. To investigate this, a variable temperature ^{1}H NMR study of this macrocycle was undertaken. The observed spectra are shown below together with peak assignments (**Figure 4.3)**.

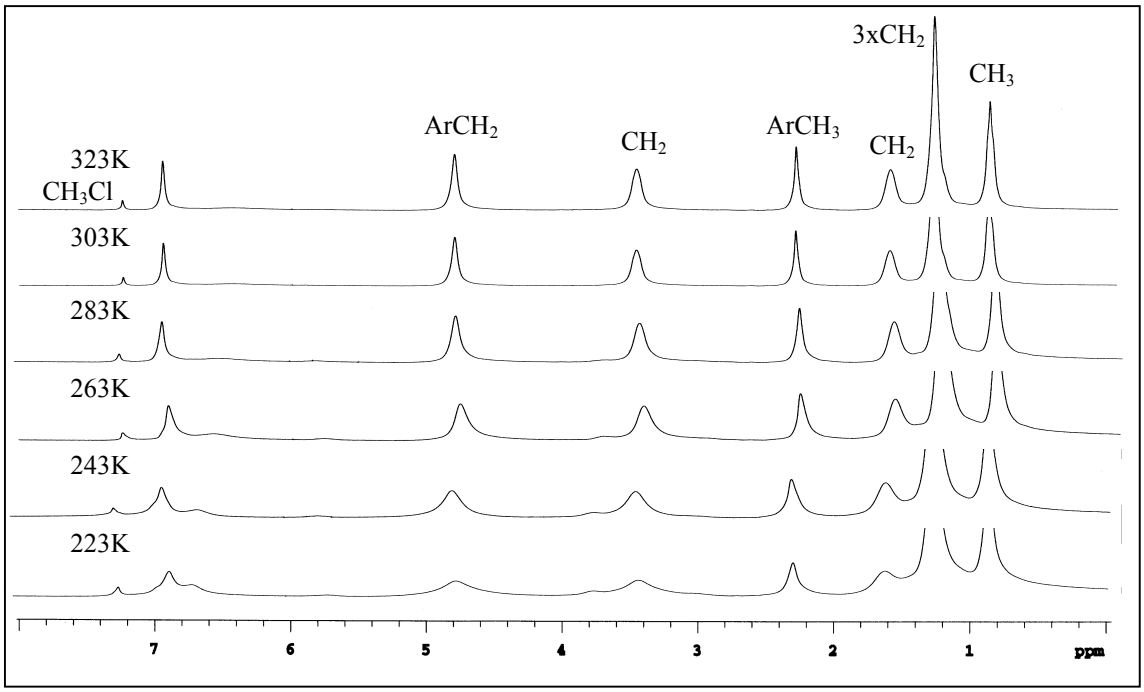

Figure 4.3 *Variable temperature ^{1}H NMR (300MHz, $CDCl_3$) spectra of* ***79***

The broad peaks observed at room temperature were probably due to restricted rotation around the carbon-nitrogen bond of the dithiocarbamate unit.[8] Upon cooling to 223K these peaks became even broader, and new peaks were observed due to aromatic protons and alkyl protons due to the various conformers of **79** being observed. However, at 323K these conformers inter-converted much faster and the peaks became much sharper than those at room temperature.

The ^{13}C NMR spectrum of receptor **79** is shown below together with peak assignments (**Figure 4.4**).

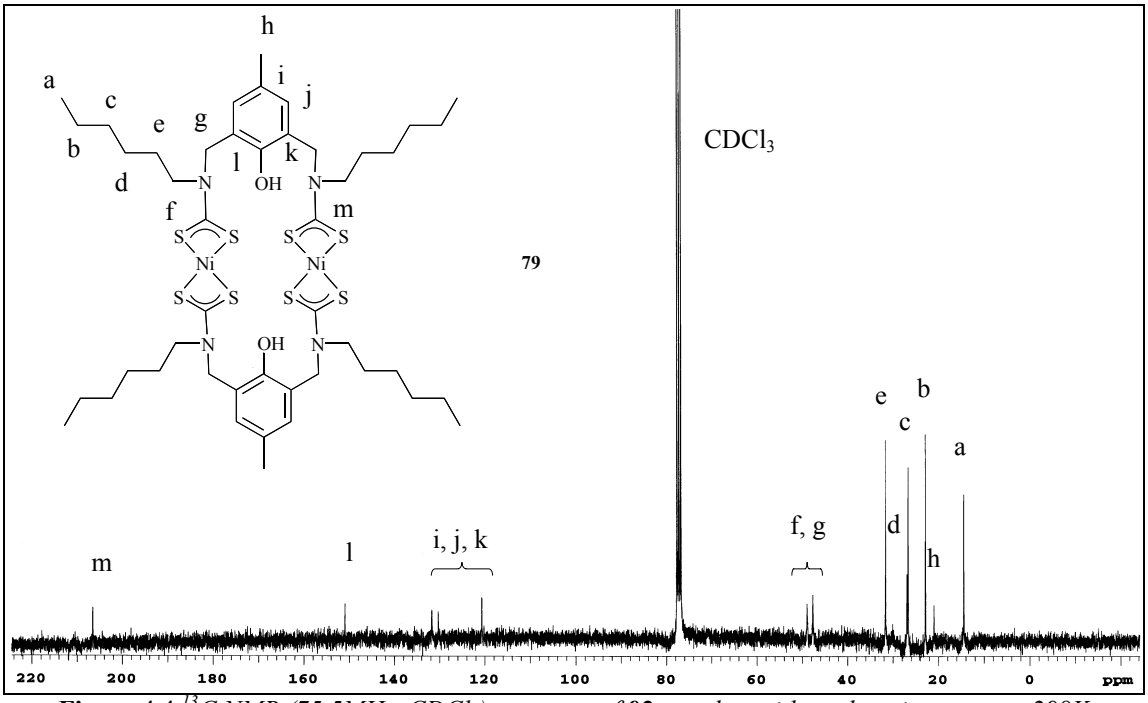

Figure 4.4 *^{13}C NMR (75.5MHz, $CDCl_3$) spectrum of* ***92*** *together with peak assignments at 298K*

The peak at 207.8ppm was characteristic of a nickel(II) dithiocarbamate species[9] and the phenolic carbon (l) was observed at 150.9ppm, typical for a carbon in that environment.[10]

Synthesis of copper(II) analogues of all the macrocycles resulted in characteristically brown powders, however, despite many attempts, they could not be isolated in a pure form.

2.2 Cation Binding studies

The cation binding properties **73 - 80** were investigated using ESMS, UV/visible, ^{1}H NMR spectroscopies and membrane transport studies. The cations studied were sodium, potassium, rubidium and caesium as their hexafluorophosphate (PF_6), triiodide (I_3) or perchlorate (ClO_4) salts. These counter anions were used as they are large, non-coordinating anions.

2.2.1 Electrospray Mass Spectrometry

Alkali metal competition experiments were performed using ESMS spectroscopy (**Appendix 4**). A ten-fold excess of $NaPF_6$, KPF_6, $RbPF_6$ and $CsPF_6$ were added to a methanol solution of each of the receptors in turn. The spectra revealed peaks in the mass spectrum corresponding to $[Receptor + M^+]^+$ for every cation.

In order to qualitatively assess the selective binding strengths of each receptor with each cation a competition experiment was performed. Ten equivalents of Na^+, K^+, Rb^+ and Cs^+ as their PF_6 salts were added to each of the receptors and the mass spectrum recorded. Peaks due to $[Receptor + Na^+]^+$, $[Receptor + K^+]^+$, $[Receptor + Rb^+]^+$ and $[Receptor + Cs^+]^+$were observed.

Figure 4.5 reveals the experimental data and the calculated isotope models for receptor **79** when a competition experiment was carried out.

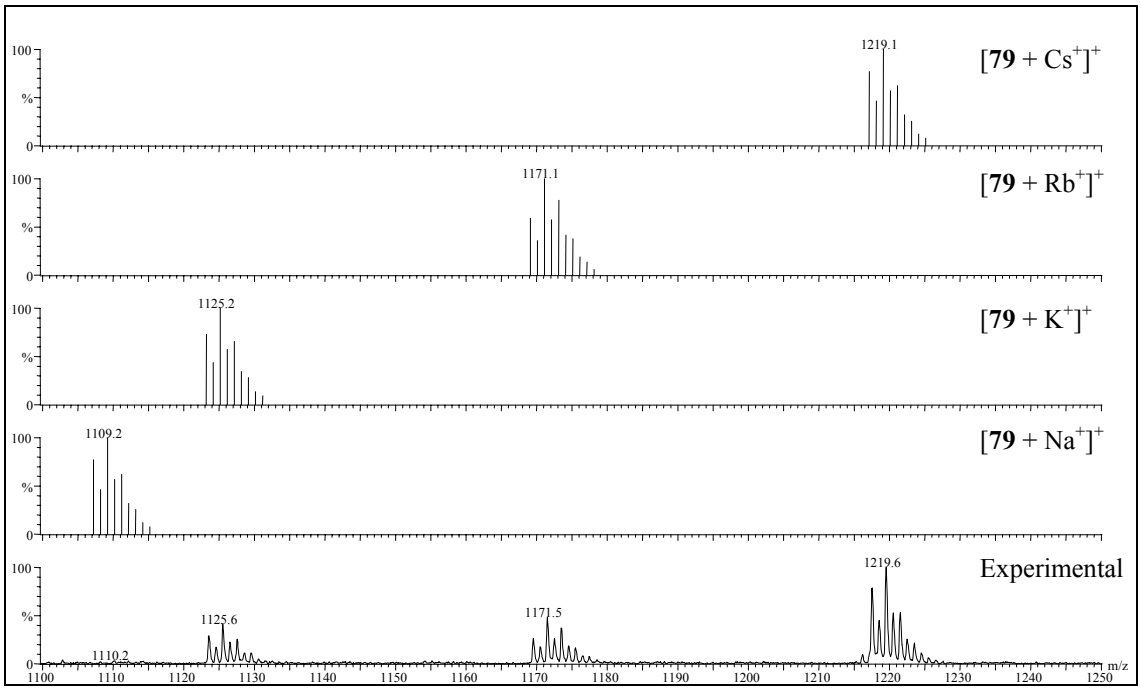

Figure 4.5 *ESMS competition experiment of **79** with Group 1 salts*

The largest peak was observed for receptor [**79** + Cs^+]$^+$, which indicates that this receptor preferentially forms an association with the caesium cation over the other Group 1 metal cations.

All of the receptors were studied in similar competition experiments and the relative intensities of the respective peaks are presented in **Table 4.1**. The respective control compounds, metal(II) bis(*N*,*N*-diethyl dithiocarbamate) (M(DTCEt_2)$_2$), were also studied.

Cation	$Ni(DTCEt_2)_2$	73	75	78	79
Na^+	5	75	5	5	5
K^+	20	75	60	35	35
Rb^+	20	50	60	55	40
Cs^+	100	100	100	100	100

Cation	$Zn(DTCEt_2)_2$	74	76	80
Na^+	5	15	50	10
K^+	10	20	60	75
Rb^+	20	25	60	90
Cs^+	100	100	100	100

Cation	$Cd(DTCEt_2)_2$	77
Na^+	5	5
K^+	30	75
Rb^+	30	80
Cs^+	100	100

Table 4.1 *Intensities of the peaks observed in the ESMS competition experiments*

All the receptors showed the most intense peak due to [Receptor + Cs^+]$^+$. This indicates a preference for binding Cs^+ cation over other Group 1 metal cations. Surprisingly ESMS also revealed the model compounds form selective adducts with the Cs^+ cation. Obviously, the ESMS technique does not discriminate between Group 1 cation complexation and adduct formation.

2.2.2 UV/visible Spectroscopy

In order to investigate the strength and selectivity of cation binding, studies were undertaken using UV/visible spectroscopy.

The nickel(II) dithiocarbamate receptors exhibits three characteristic absorptions in their spectrum between 250 and 500nm.[11] These bands are two metal to ligand charge transfer (MLCT) bands at ~390nm and ~430nm, and a ligand centred (LC) bands at ~330nm.

Table 4.2 displays the wavelengths and molar extinction coefficients of the nickel(II) based receptors and $Ni(DTCEt_2)_2$[12] in $CHCl_3$:MeCN (7:3) solution (**Appendix 2**).

Assignment	$Ni(DTCEt_2)_2$	73	75	78	79
LC	327 (36.9)	323 (42.0)	321 (81.4)	328 (67.3)	325 (77.2)
MLCT	399 (5.8)	402 (7.7)	396 (15.7)	399 (12.0)	392 (15.3)
MLCT	427 sh (1.6)	442 sh (0.2)	434 sh (5.6)	437 sh (2.8)	431 sh (5.1)

Table 4.2 *Wavelength λ/nm (molar extinction coefficient $\varepsilon/10^3$ $M^{-1}cm^{-1}$) of $Ni(DTCEt_2)_2$ and the nickel(II) dithiocarbamate receptors*

The oxidation of nickel(II) dithiocarbamate to nickel(IV) dithiocarbamate can be followed by UV/visible spectroscopy and used to calculated the number of transition metal centres in the molecule. The initial spectrum of **79** was typical of a nickel(II) dithiocarbamate and the final spectrum, on oxidation with *N*-bromosuccinimide (NBS) showed peaks characteristic of a nickel(IV) dithiocarbamate species (see **Chapter 5 Section 2**). The Job plot for the oxidation displayed a minimum ~0.33 NBS were added to perform the oxidation.[13] This confirmed that macrocycle **79** contained two nickel(II) dithiocarbamate centres.

In contrast, the zinc(II) dithiocarbamate receptors do not show any absorptions in the visible region due to their d^{10} electronic configuration.[14] However, at ~265nm and ~285nm there are two LC π-π^* transitions.[15]

Table 4.3 shows the wavelengths and molar extinction coefficients of the zinc(II) based receptors and $Zn(DTCEt_2)_2$[12] in $CHCl_3$:MeCN (7:3) solution.

Assignment	$Zn(DTCEt_2)_2$	74	76	80
LC	264 (31.6)	267 (72.6)	262 (25.7)	264 (114.8)
LC	287 sh (22.2)	287 sh (38.0)	-	279 sh (81.2)

Table 4.3 *Wavelength λ/nm (molar extinction coefficient $\varepsilon/10^3$ $M^{-1}cm^{-1}$) of $Zn(DTCEt_2)_2$ and the zinc(II) dithiocarbamate receptors*

Cadmium(II) dithiocarbamates display a similar LC absorptions as zinc(II) dithiocarbamates. An intra-ligand π-π^* transitions occur at ~240nm and ~300nm due to transitions between energy levels based in the CS_2 and NCS moieties respectively.[16] A n-π^* transition is seen ~465nm due to transition between energy levels on the sulphur atom and a weak band between 500nm and 540nm and is due a to MLCT absorption.

Table 4.4 reveals the wavelengths and molar extinction coefficients of the cadmium(II) based receptors and $Cd(DTCEt_2)_2$[12] in $CHCl_3$:MeCN (7:3) solution. In the case of receptor **77** the bands ~300nm, ~465nm and ~500nm were not discernable.

Assignment	$Cd(DTCEt_2)_2$	77
LC	264 (35.4)	262 (65.7)
LC	282 sh (15.3)	-

Table 4.4 *Wavelength λ/nm (molar extinction coefficient $\varepsilon/10^3$ $M^{-1}cm^{-1}$) of $Cd(DTCEt_2)_2$ and the cadmium(II) dithiocarbamate receptor*

The receptor:cation interaction was investigated using UV/visible absorption spectroscopy. Aliquots of MeCN solutions of $NaClO_4$, KPF_6, $RbPF_6$ and $CsPF_6$ were added to $CHCl_3$:MeCN (7:3) solutions of receptors **73** - **80** and the spectrum recorded.

Disappointingly, only very small changes of the electronic spectrum were observed in all cases. This is indicative of weak binding and it was not possible to calculate stability constants from the titration data.

2.2.3 Membrane Transport Studies

In an effort to assess the membrane transport ability of macrocycles **74**, **75**, **76**, **79** and **80** a series of bulk liquid membrane experiments were performed and compared with $Ni(DTCEt_2)_2$.[12] Unfortunately, macrocycles **73**, **77** and **78** were too insoluble to be studied.

The cell design was based on that of Rebek.[17] The transport of caesium picrate was investigated across a liquid membrane containing the appropriate receptor molecule as outlined in **Figure 4.6** (**Appendix 9**). At 24 hour intervals an aliquot of the receiving phase was

withdrawn and the amount of caesium picrate in the receiving phase was calculated using UV/visible spectroscopy by monitoring the picrate absorption maximum at 356nm.

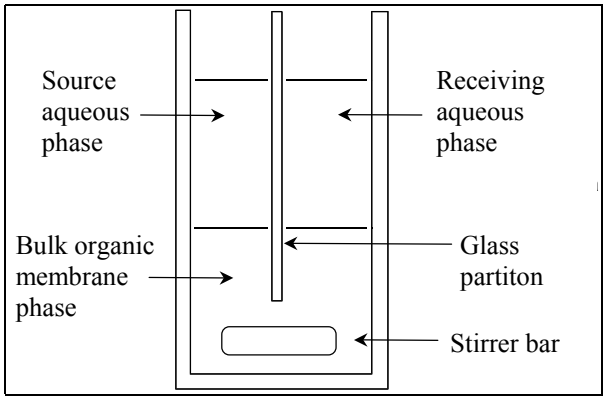

Figure 4.6 *Design of the cell used in transport experiments*

The percentage of caesium picrate transported into the receiving phase after each day is illustrated in **Figure 4.7**. The flux of the cation metal salt through the bulk membrane is shown in **Table 4.5**.

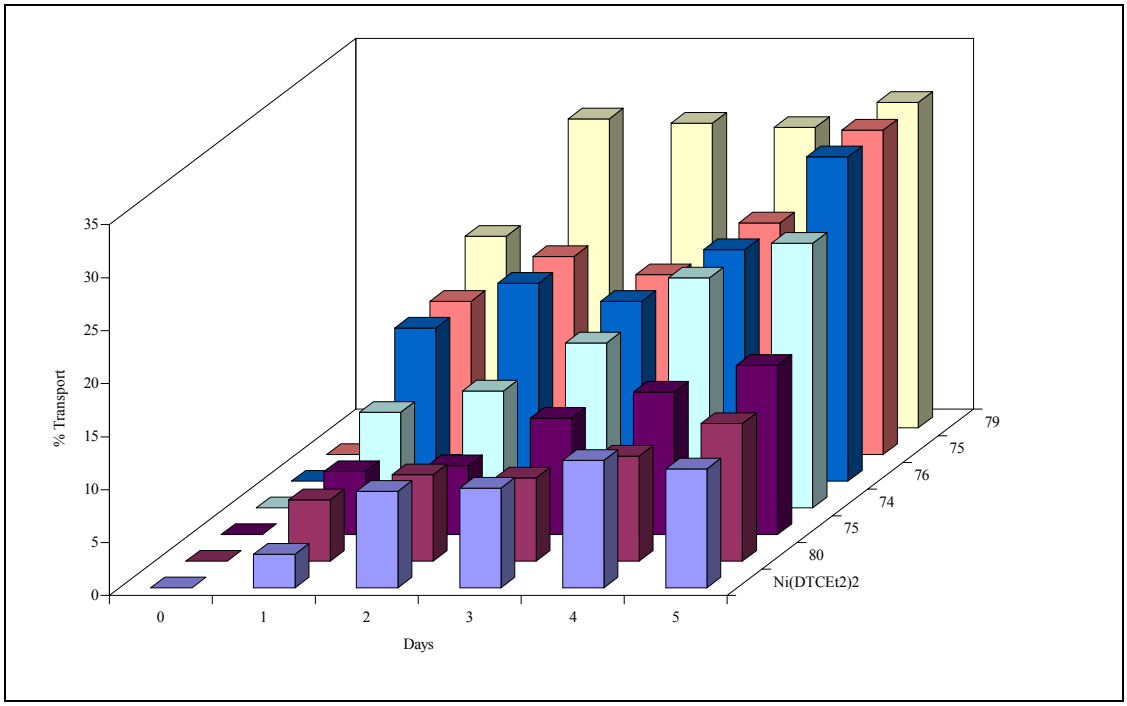

Figure 4.7 *Transport of caesium picrate through a bulk liquid membrane using **74**, **75**, **76**, **79** and **80** at 293K, stirring rate = 100 revsmin^{-1}*

	$Ni(DTCEt_2)_2$	**74**	**75**	**76**	**79**	**80**
Flux ($x10^{-10}$mol h^{-1} cm^{-2})	5.2	11.5	7.3	14.1	14.1	6.0

Table 4.5 *Flux of caesium picrate through bulk liquid membrane using $Ni(DTCEt_2)_2$, **86**, **87**, **88**, **91** and **92** at 293K, stirring rate = 100 revsmin^{-1}*

When the control compound was studied, a small amount of transport was observed. This is probably due to a slight leakage due to mechanical stirring as when no receptor was in the membrane a similar flux of caesium was observed.[18] When **79** was investigated, the amount of caesium picrate found in the receiving phase after 5 days was found to be 30%. In contrast, receptor **80** showed less then 10 percent of Cs^+ in the receiving phase after the same time period. Thus the nickel(II) receptor showed increased transport after 5 days than did the analogous zinc(II) receptor. Interestingly, the opposite trend was observed of the pyridyl receptors, with the zinc(II) macrocycle **76** transporting more caesium picrate than the analogous nickel(II) receptor **75** after 5 days. Receptor **74**, which contained no donor atom in the aromatic ring, showed almost as much transport as receptor **79**.

The results are hard to explain in terms of the donor atoms included in macrocycle, however there is a clear indication of a macrocyclic cation transport effect as receptors **74**, **76** and **79** show much higher transport and transport rate than $Ni(DTCEt_2)_2$.

2.2.4 Nickel(II) Electrochemistry

Nickel(II) dithiocarbamates posses rich electrochemical characteristics.[19,20,21] Receptors **73**, **75**, **78**, **79** and $Ni(DTCEt_2)_2$[12] were studied in DMF by cyclic and square wave voltammetry (**Appendix 3**) and the data is shown in **Table 4.6**. DMF was used as the receptors were insoluble in less competitive solvents.

	Ni(II)/Ni(IV)				
	$Ni(DTCEt_2)_2$	**73**	**75**	**78**	**79**
E_{pa} (V)	0.630	0.370	0.500	0.395	0.625
E_p (V)	0.505	0.260	0.230	0.206	0.290
	Ni(IV)/Ni(III)				
E_{pc} (V)	-0.225	-0.200	-0.165	-0.260	-0.200
	Ni(III)/Ni(II)				
E_{pc} (V)	-0.770	-0.690	-0.660	-0.790	-0.775
	Ni(II)/Ni(I)				
E_{pa} (V)	-1.800	-	-	-	-
E_{pc} (V)	-1.980	-1.930	-1.930	-1.930	-1.965
ΔE (V)	0.180	-	-	-	-
I_{pa}/I_{pc}	0.9	-	-	-	-
E_p (V)	-1.870	-1.790	-1.760	-1.810	-1.790

Table 4.6 *Electrochemical data of $Ni(DTCEt_2)_2$ and the nickel(II) dithiocarbamate receptors in DMF containing 0.1M $TBABF_4$, potentials given with reference to Ag/Ag^+ at 293K, scan rate = 100mVs^{-1}, E_p - peak potential in square wave voltammogram*

All the receptors showed the typical electrochemical characteristics of a nickel(II) dithiocarbamate species. For example an irreversible nickel(II)/nickel(IV) couple was observed together with successive reductions of the electro-generated nickel(IV) species. However, the nickel(II)/nickel(I) reduction showed irreversible characteristics for every receptor in contrast to the quasi-reversible wave observed with $Ni(DTCEt_2)_2$.

The effect on the nickel(II)/nickel(I) couple upon the addition of five equivalents of cation to the solutions of the receptors was investigated by square wave voltammetry. Unfortunately, none of the receptors showed any perturbation of the reduction wave upon the addition of five equivalents of any of the Group 1 metal cations.

2.2.5 ^{1}H NMR Spectroscopy

^{1}H NMR spectroscopy was also used to try to assess the cation binding ability of the receptors **73 - 80**. Unfortunately, the macrocycles were insoluble in solvents such as MeCN-d_3 and MeOH-d_4, which Group 1 salts are soluble in, hence DMSO-d_6 had to be used. When ten equivalents of $CsPF_6$ was added to a DMSO-d_6 solution of each of the receptors **73** – **80** no shifts in proton resonances was observed due to the competitive nature of the solvent.

3 Attempted Syntheses

Several efforts were made to synthesise various macrocycles and polymetallic ladders. The following sections outline the syntheses that were attempted and the problems encountered.

3.1 Alkyne Macrocycles

Scheme 4.4 outlines the synthesis of a bis-secondary amine containing an alkyne moiety.

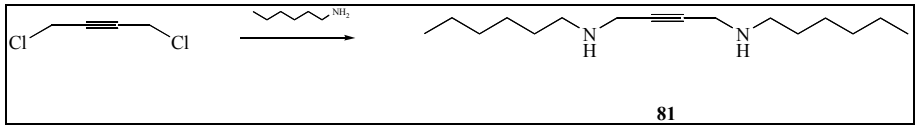

Scheme 4.4 *Synthesis of **94***

Portion wise addition of commercially available of 1,4-dichloro-2-butyne to an excess of hexylamine and heating for 15 hours gave the bis-amine ligand **81** in 82% yield.[22] The bis-amine was characterised by ^{1}H and ESMS. In addition, the ^{1}H-^{1}H COSY NMR spectrum revealed coupling between adjacent alkyl protons along the hexyl chain

Attempted conversion of **81** into a cation receptor molecule is shown below in **Scheme 4.5**.

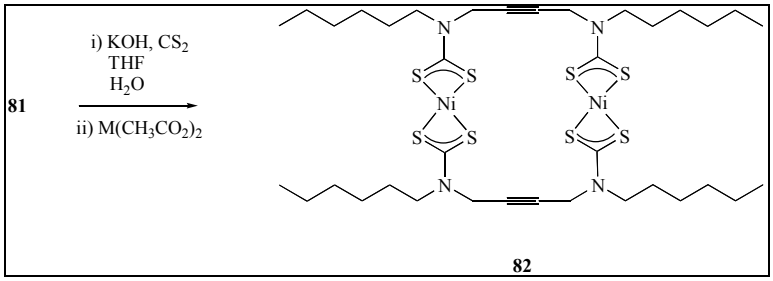

Scheme 4.5 *Attempted synthesis of receptor **82***

The dithiocarbamate formation was the same as that used previously described. Unfortunately, the ^{1}H, ^{1}H-^{1}H COSY NMR and ESMS revealed that the macrocyclic product was not formed. However, the isolated green powder was characterised as the structure shown in **Figure 4.8**.

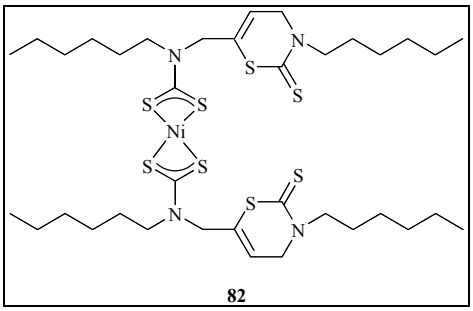

82

Figure 4.8 *Structure of* ***82***

3.2 Polydithiocarbamates

It was envisaged that by the careful design of an secondary amine the synthesis of molecules that contained more than two dithiocarbamate metal centres would be possible. These 'molecular ladders' may possess interesting structures and properties.

The tris-amine **88** was synthesised, as shown below in **Scheme 4.6**.[23] This amine could be used as a precursor to a novel tri-metallic structure if the dithiocarbamate moiety could be successfully applied to the three amine groups.

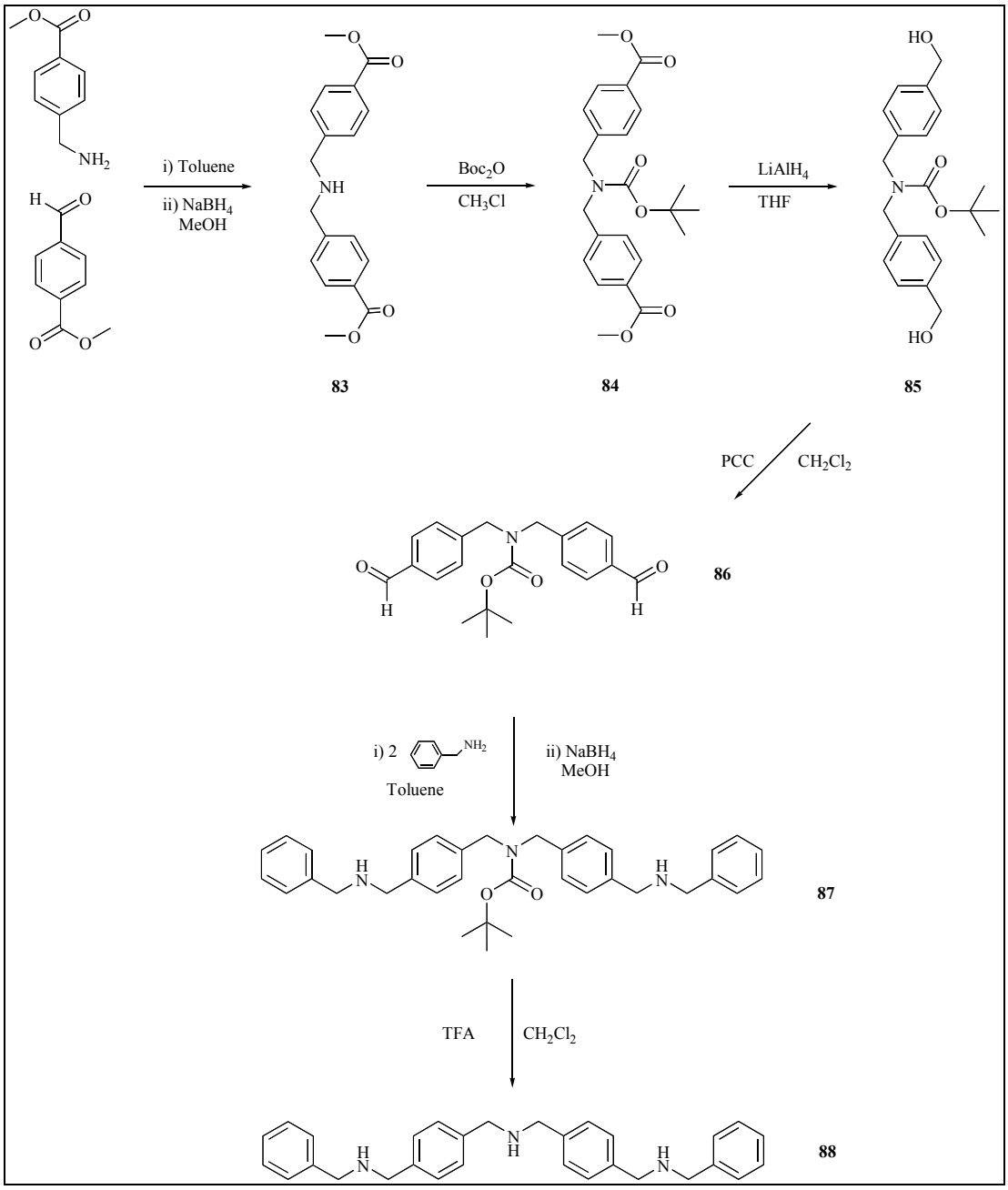

Scheme 4.6 *Synthesis of tris-amine **88***

The methyl-4-amino benzoate hydrochloride salt was converted to the free amine by the addition of sodium hydroxide in water. This amine was condensed with methyl-4-formyl-benzoate in toluene using Dean-Stark apparatus to produce the imine, which was reduced with sodium borohydride in methanol to give the secondary amine **83** in 81% yield. This amine was protected using the *tert*-butoxy carbonyl group in chloroform that gave the product, **84** in 97% yield. The ester functionalities were reduced to alcohols using lithium aluminium hydride in tetrahydrofuran and oxidation of the alcohol moieties to the corresponding aldehydes was achieved using pyridinium chlorochromate (PCC) in dichloromethane. The ^{1}H NMR of **86** revealed a singlet at 10.0ppm typical for an aldehyde. Two equivalents of benzylamine were

added to the bis-aldehyde in toluene, and the imine was reduced with sodium borohydride in methanol to give the bis secondary amine **87** in 88% yield. The protecting group was removed by the action of trifluoroacetic acid in dichloromethane, which gave the tris-amine **88** in an overall yield of 28%. All products were characterised by ^{1}H, ^{1}H-^{1}H COSY NMR and ESMS.

Attempted conversion of **88** into a tri-metallic dithiocarbamate molecule is shown below in **Scheme 4.7**.

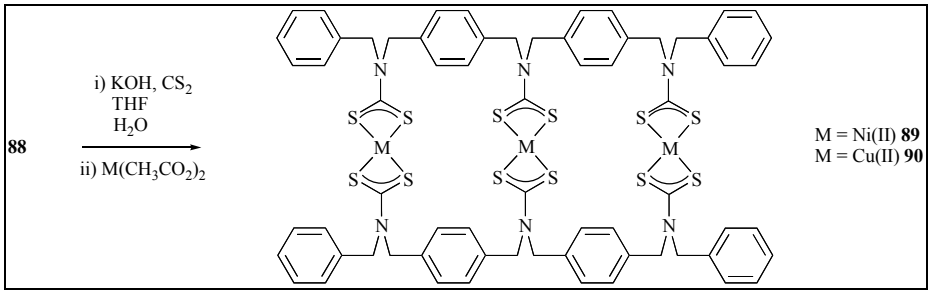

Scheme 4.7 *Attempted synthesis of **89** and **90***

Three equivalents of potassium hydroxide and carbon disulphide were added to a tetrahydrofuran:water solution of **88**. The resulting potassium dithiocarbamate salt was converted in situ by the addition of one and a half equivalents of nickel(II) or copper(II) acetate.[6] Unfortunately, the green and brown products that precipitated were highly insoluble and no evidence was found for the tri-metallic structure using ESMS or ^{1}H NMR.

An attempt to synthesise a tetra-metallic structure was undertaken using a molecule containing four amine functionalities. The precursor tetra-amine **93** was synthesised in four steps, as shown in **Scheme 4.8**.

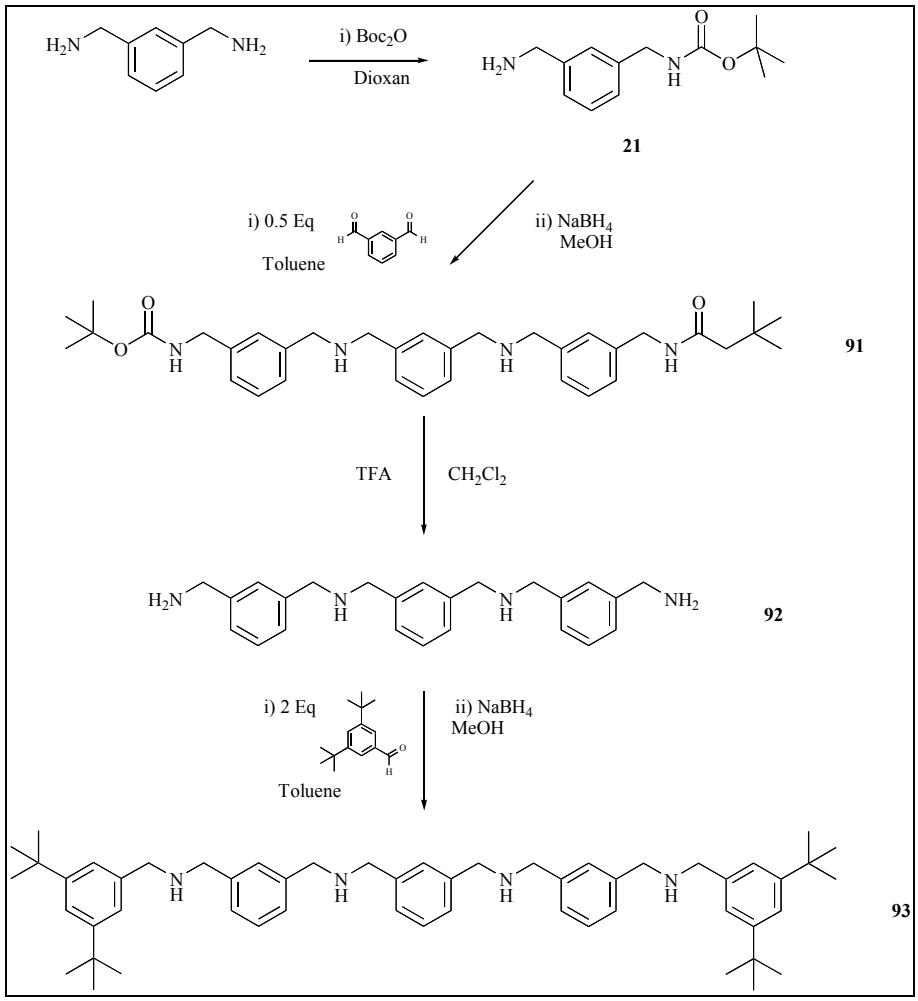

Scheme 4.8 *Synthesis of tetra-amine **93***

m-Xylene diamine was mono protected using bis(*tert*-butoxycarbonyl)anhydride in dioxane.[24] **21** was condensed with half an equivalent of isopthalic dicarboxaldehyde in toluene using Dean-Stark apparatus to form the imine.[25] Reduction of the imine was achieved in methanol using sodium borohydride giving the amine in 88% yield.[26] The protecting group was removed by trifluoroacetic acid and the free amine reacted with two equivalents of 3,5-di-*tert*-butyl-benzaldehyde[27] in toluene. The imine was reduced to the tetra-amine **93** using sodium borohydride in methanol.[26] All the products were characterised by ^{1}H, ^{1}H-^{1}H COSY NMR and ESMS.

Attempted conversion of **93** into a tetra-metallic dithiocarbamate molecule is displayed below in **Scheme 4.9**.

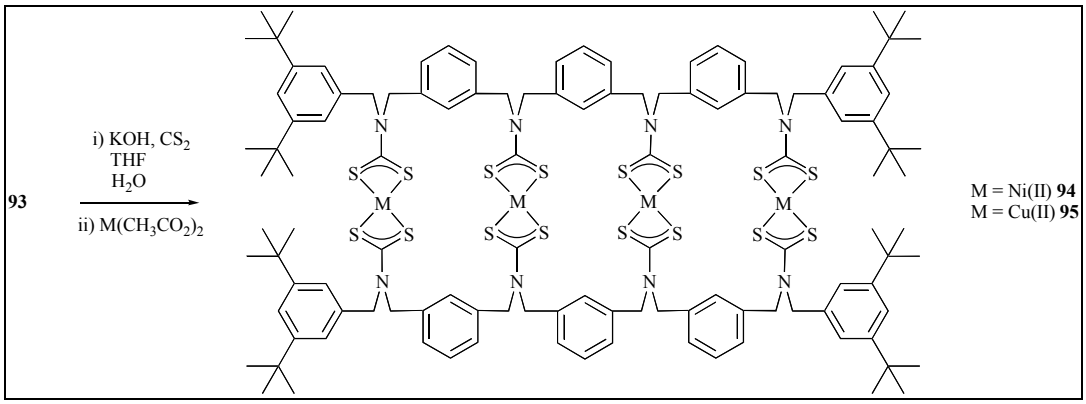

Scheme 4.9 *Attempted synthesis of **94** and **95***

Four equivalents of potassium hydroxide and carbon disulphide were added to a tetrahydrofuran:water solution of **93**. The potassium dithiocarbamate salt was converted to the transition metal product upon the addition of two equivalents of nickel(II) or copper(II) acetate.[6] Unfortunately, the green and brown products that precipitated were highly insoluble and ^{1}H NMR and ESMS found no evidence for the tetra-metallic structure.

The reaction was attempted again but the transition metal salt was added under high dilution conditions. A solution of the transition metal acetate salt was added drop wise to a dilute solution of the tetra-amine (~0.02M). It was hoped that this would favour the formation of discreet molecular complexes rather than polymer. Disappointingly, a highly insoluble complex was formed which did not agree with calculated elemental composition.

4 Summary

A novel type of macrocyclic receptor has been developed based upon a transition metal dithiocarbamate moiety. The molecules were synthesised using covalent synthesis and the final receptor assembled using base, carbon disulphide and a transition metal salt. The receptors contained two dithiocarbamate groups and two aromatic groups that created the macrocycles.

Receptors **73 - 80** were successfully synthesised in a small number of steps. The molecules were characterised by ^{1}H, ^{1}H-^{1}H COSY, ^{13}C NMR, UV/visible, infrared, ESMS and electrochemical techniques. **73 - 80** displayed an affinity for binding one caesium cation over the other Group 1 metals as shown by ESMS and transport studies. Unfortunately, the cation binding was not observed by UV/visible or ^{1}H NMR spectroscopy.

In summary, the aim of this chapter was to develop a new type of macrocyclic molecule using a transition metal dithiocarbamate group. This goal has been achieved and ESMS and transport studies have demonstrated that these receptors bind and transport caesium cations.

5 References

[1] O. D. Fox, M. G. B. Drew, E. J. S. Wilkinson, P. D. Beer, *Chem. Commun.*, 2000, 391.
[2] L. M. Harwood, C. J. Moody, *Experimental Organic Chemistry Principles and Practice*, Blackwell Scientific Publishers, 1989, 218.
[3] J. H. Billman, A. C. Diesing, *J. Org. Chem.*, 1957, **22**, 1068.
[4] M. A. Reppy, M. E. Cooper, J. L. Smithers, L. G. Douglas, *J.Org.Chem.*, 1999, **64**, 4191.
[5] R. N. Salvatore, C. H. Yoon, K. W. Jung, *Tetrahedron*, 2001, **57**, 7785.
[6] a) D. Coucouvanis, *Prog. Inorg. Chem.*, 1979, **26**, 301; b) D. Coucouvanis, *Prog. Inorg. Chem.*, 1970, **11**, 233; c) D. J. Halls, *Mickro. Acta*, 1969, 62; d) J. Willemse, J. A. Cras, J. J. Steggerda, *Struct. Bonding*, 1976, **28**, 83; e) G. D. Thorn, R. A. Ludwig, *The Dithiocarbamates and Related Ligands*, Elsevier, 1962.
[7] A. V. Ivanov, V. I. Mitrofanova, M. Kritikos, O. N. Antzukin, *Polyhedron*, 1999, **18**, 2069.
[8] B. M. Mattson, A. E. Madera, M. C. Palazzotto, *J. Coord. Chem.*, 1984, **13**, 321.
[9] H. L. M. van Gaal, J. W. Diesveld, F. W. Pijpers, J. G. M. van der Linden, *Inorg. Chem.*, 1979, **18**, 3251.
[10] O. Yamamoto, K. Someno, N. Wasada, J. Hiraishi, K. Hayamizu, K. Tanabe, T. Tamura, M. Yanagisawa, *Anal. Sci.*, 1988, **4**, 235. (http://www.aist.go.jp/RIODB/SDBS/menu-e.html)
[11] M. Castillo, J. J. Criado, B. Macias, M. V. Vaquero, *Trans. Met. Chem.*, 1986, **11**, 476.
[12] For synthesis and characterisation see the Experimental Chapter.
[13] K. A. Connors, *Binding Constants*, J. Wiley & Sons, 1987, 24.
[14] A. Manohar, K. Ramalingam, G. Bocelli, L. Righi, *Inorg. Chim. Acta*, 2001, **314**, 177.
[15] G. St. Nikolov, N. Jordanov, I. Havezov, *J. Inorg. Nucl. Chem.*, **33**, 1971, 1059.
[16] B. S. Garg, R. K. Garg, M. J. Reddy, *Indian J. Chem.*, 1993, **32A**, 697.
[17] J. Rebek, B. Askew, D. Nemeth, K. Parris, *J. Am. Chem. Soc.*, 1987, **109**, 2432.
[18] S. Patell, *Part II Thesis*, Oxford University, 2000, 46.
[19] A. M. Bond, R. L. Martin, *Coord. Chem. Rev.*, 1984, **54**, 23.
[20] A. R. Hendrickson, R. L. Martin, N. M. Rohde, *Inorg. Chem.*, 1975, **14**, 2980.
[21] R. Chant, A. R. Hendrickson, R. L. Martin, N. M. Rohde, *Aust. J. Chem.*, 1973, **26**, 2533.
[22] R. N. Salvatore, C. H. Yoon, K. W. Jung, *Tetrahedron*, 2001, **57**, 7785.
[23] P. R. Ashton, M. P. T Glink, S. Menzer, J. F. Stoddart, P. A. Tasker, A. J. P. White, D. J.Williams, *Chem. Eur. J.*, 1996, **2**, 729.
[24] A. P. Krapcho, C. S. Kuell, *Synth. Comm.*, 1990, **20**, 2559.
[25] L. M. Harwood, C. J. Moody, *Experimental Organic Chemistry Principles and Practice*, Blackwell Scientific Publishers, 1989, 218.
[26] J. H. Billman, A. C. Diesing, *J. Org. Chem.*, 1957, **22**, 1068.
[27] M. S. Newman, L. F. Lee, *J. Org. Chem.*, 1972, **26**, 4460.

Chapter Five

Macrobicyclic Anion Dithiocarbamate Receptors

1 Introduction

The receptors described in **Chapter 3** contained a macrocyclic cavity lined with amide functionalities to bind anions. The molecular cavity was formed due to the rigidity of the ligand and the planar stereochemistry of the transition metal that was employed.[1,2] It was hoped that it maybe possible to use the dithiocarbamate group to self-assemble novel macrobicyclic cryptand-like anion receptor molecules using related methodology.

Macrobicyclic anion receptors have previously been constructed using covalent synthetic chemistry. This route, however, possesses several drawbacks. For example, the synthesis can contain many steps and consequently the final product maybe formed in an overall poor yield.

Pascal's macrobicyclic anion receptor described in **Chapter 1 Section 3.4** was one of the first anion receptor to include amide groups for anion binding, however it was only synthesised in an overall yield of 11%. **Figure 5.1** shows a polyammonium macrobicyclic that was synthesised in eight steps and employed high dilution conditions.[3] Another drawback to this receptor is the limited pH window in which it can strongly bind anions (see **Chapter 1 Section 3.3.1**).[4]

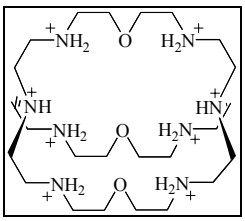

Figure 5.1 *Polyammonium macrobicyclic receptor*

With this in mind, it was hoped by using the same precursor molecules that were synthesised in **Chapter 3**, but altering either the metal ion or the oxidation state of the metal ion, it maybe possible to create novel macrobicyclic anion receptors using relatively simple synthetic procedures.

Beer reported that simple partial oxidation of a dinuclear copper(II) dithiocarbamate macrocycle produces a novel interlocked molecular structure in near quantitative yield (**Figure 5.2**).[5]

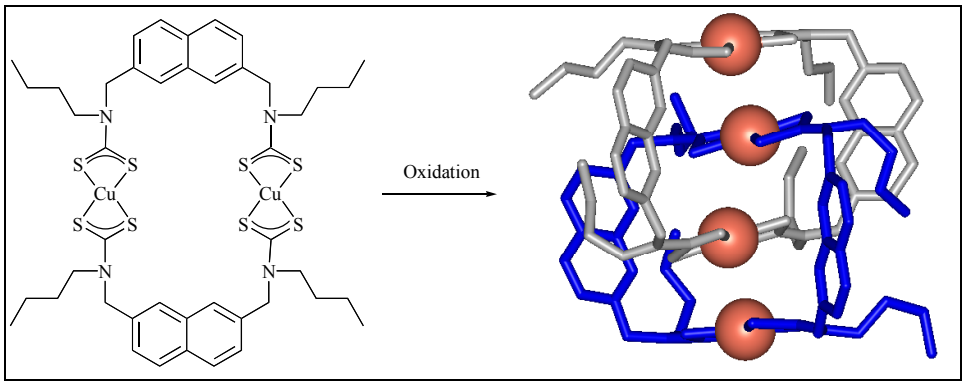

Figure 5.2 *Beer's catenane formation controlled by the oxidation state of the transition metal*

The catenane contained mixed valency metal centres which alternated in a copper(II)copper(III)copper(II)copper(III) fashion.

It was envisaged that anion receptors maybe synthesised by altering the oxidation state of the transition metal centre. The dinculear nickel(II) dithiocarbamate receptors discussed in the previous chapter possessed two dithiocarbamate ligands bound to each metal centre in a square planar arrangement.[1] In contrast, nickel(IV) dithiocarbamates have three ligands surrounding the nickel centre, creating an approximate D_3 symmetry.[6] Thus oxidation of the dinuclear nickel(II) macrocycle to the nickel(IV) analogue may create a cryptand like structure as shown in **Figure 5.3**.

It was also anticipated that novel macrobicyclic receptors could be synthesised by using a different transition metal ion that exhibits different stereochemical requirements. Iron(III) dithiocarbamates typically have D_3 symmetry around the metal centre,[7,8] therefore interesting cryptand-like molecules maybe synthesised which are capable of binding anions (**Figure 5.3**).

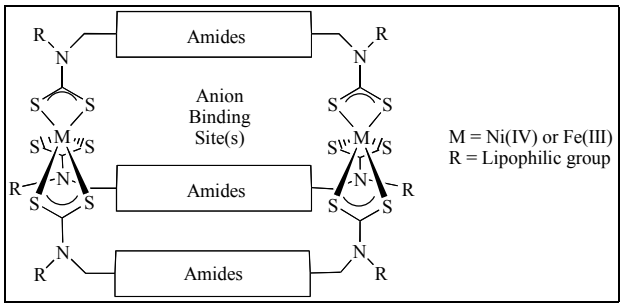

Figure 5.3 *Schematic of target receptors*

The target cryptand anion receptors possess multiple amide groups for anion binding (see **Chapter 1 Section 3.4**) and incorporation of a lipophilic group (R) may confer solubility in a

range of organic solvents. The choice of transition metal centre allows various spectroscopic probes to be employed for monitoring the anion binding.

The first part of the chapter describes the synthesis, characterisation and anion binding properties of macrobicyclic anion receptors, which incorporate a nickel(IV) dithiocarbamate group. The second section of this chapter discusses the formation and study of similar type of macrobicyclic structures but using iron(III) as the transition metal centre. Finally, the self-assembly of two tripodal ligands that forms a cryptand-like structure is described together with the anion binding properties of the resulting compounds.

2 Nickel(IV) Macrobicyclic Anion Receptors

It has been reported that that nickel(II) dithiocarbamate complexes can undergo a two electron oxidation to form a nickel(IV) species.[9] It was predicted that if such an oxidation was performed on the macrocycles described in **Chapter 3 Section 2**, a novel macrobicyclic structure could be formed (**Figure 5.4**).

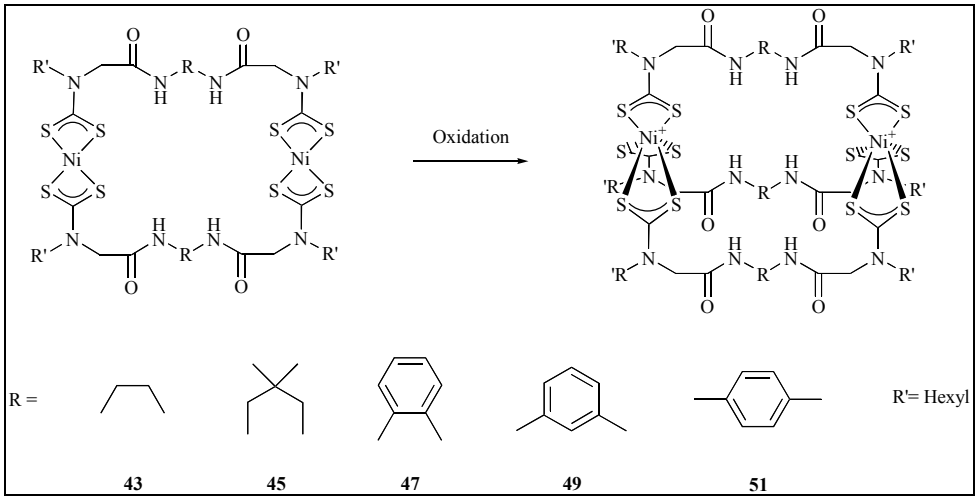

Figure 5.4 *Schematic of synthesis of macrobicyclic receptors*

This macrobicyclic molecule would not only possess hydrogen bond donors groups for anion complexation, but also a two positive charge which could would favour anion binding.

2.1 Synthesis and Characterisation

Receptor **96** was synthesised by an oxidation reaction as illustrated in **Scheme 5.1**.

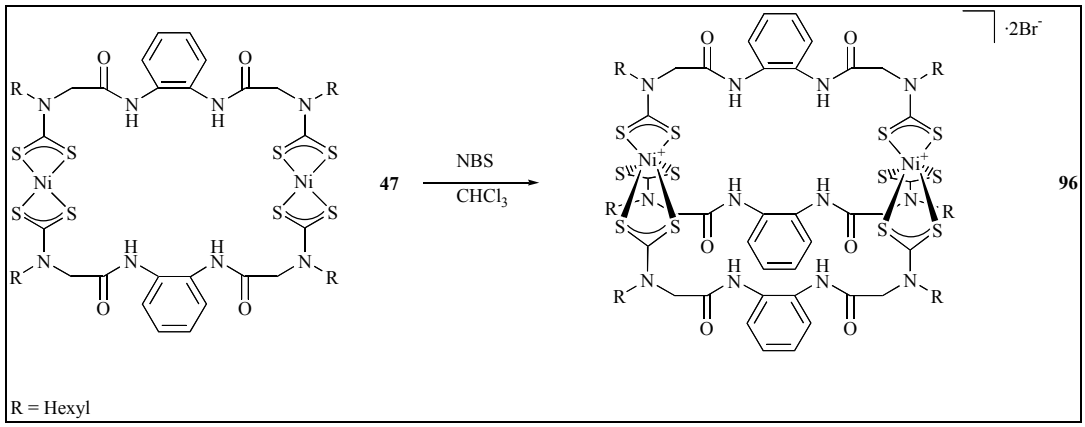

Scheme 5.1 *Synthesis of receptor **96***

Two equivalents of *N*-bromosuccinimide (NBS) were added to a chloroform solution of receptor **47**.[9] After one hour, water was added and the product was extracted into chloroform. Drying followed by solvent removal and recrystallisation from dichloromethane/ethanol yielded a dark brown solid in 70% yield.

Disappointingly, this was the only macrobicyclic structure that could be synthesised due to the very low solubility of receptors **43**, **45**, **49 a**nd **51** in chloroform. Other non-halogented solvents, such as dimethyl sulphoxide, could not be used as nickel(IV) dithiocarbamate compounds are photochemically irreversibly reduced to nickel(II) dithiocarbamates in such solvents.[10]

Receptor **96** displayed very broad resonances in the ^{1}H NMR spectrum in the expected chemical shift range. This maybe due to restricted rotation about the carbon nitrogen bond in the dithiocarbamate group.[11] Thus, NMR was not used for characterisation or anion binding studies. However, receptor **96** was characterised by UV/visible spectroscopy, electrochemistry, infrared, electrospray mass spectrometry (ESMS) and elemental analysis.

2.1.1 UV/visible Spectroscopy

The oxidation of nickel(II) to nickel(IV) can be followed by UV/visible spectroscopy. **Figure 5.5** shows the change in UV/visible absorption spectrum upon the addition of aliquots of a $CHCl_3$ solution of NBS to a $CHCl_3$ solution of receptor **47**.[9]

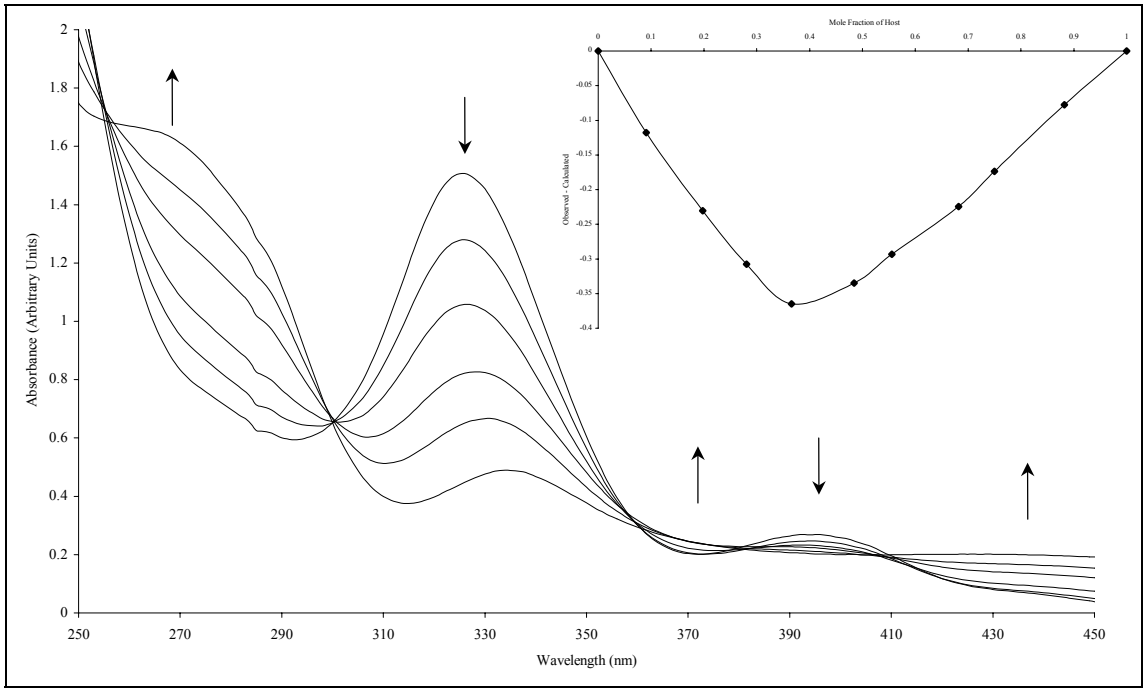

Figure 5.5 *UV/visible oxidation of **47** with NBS in $CHCl_3$*
*(Inset) Job Plot of **47** with with NBS in $CHCl_3$*

The initial spectrum is characteristic of a nickel(II) dithiocarbamate species (see **Chapter 3 Section 2.1.6**)[12] and the final spectrum shows peaks distinctive of a nickel(IV) dithiocarbamate moiety.

Nickel(IV) dithiocarbamate species typically show six bands in their UV/visible spectrum between 250nm and 600nm.[9] The similarity of the spectra of isoelectronic nickel(IV) and cobalt(III) dithiocarbamates has been previously reported[13] and tentative band assignments have been made with reference to a cobalt(III) dithiocarbamate.[14] At ~330nm and ~390nm two ligand to metal charge transfer (LMCT) bands are seen. A ligand centred (LC) transition is seen ~267nm and a d-d transition occurs at ~484nm. Peaks at ~430nm and ~560nm have been previously reported but remain unassigned.

Table 5.1 presents the UV/visible spectroscopic data for receptor **96** and nickel(IV)-tris(*N*,*N*-diethyl dithiocarbamate) bromide ($Ni(DTCEt_2)_3Br$)[15] recorded in $CHCl_3$ solution (**Appendix 2**).

Assignment	$Ni(DTCEt_2)_3Br$	96
LC	267 sh (30.4)	265 sh (80.0)
LMCT	331 (27.3)	335 (30.8)
LMCT	387 (7.0)	388 (13.8)
	425 (6.9)	435 (11.6)
d-d	484 sh (5.0)	495 sh (9.6)
	560 sh (3.0)	556 sh (6.0)

Table 5.1 *Wavelength, λ/ nm (molar extinction coefficient $\varepsilon/10^3$ M^{-1} cm^{-1}) of $Ni(DTCEt_2)_3Br$ and* ***96***

The Job plot of the oxidation displays a minimum ~0.33, clearly indicating that two equivalents of NBS were required to perform the oxidation,[16] confirming that the macrocycle **47** contained two nickel(II) dithiocarbamate centres.

The final spectrum was virtually identical to the spectrum seen when the nickel(IV) dithiocarbamate species was prepared synthetically. The very slight differences were due to low absorption of the by products of the oxidation.[9]

2.1.2 Nickel(IV) Electrochemistry

Nickel(IV) dithiocarbamate compounds can undergo a metal centred one electron reversible reduction.[17,18,19] The nickel(III) species that is produced is also electrochemically active with its reduction occurring at a more negative potential.

The electrochemistry of the receptor **96** was investigated using cyclic and square wave voltammetry in $CHCl_3$:MeCN (4:1) solvent mixture (**Appendix 3**). **Figure 5.6** shows a portion of the cyclic voltammogram of **96** with assignments of the redox processes occurring.

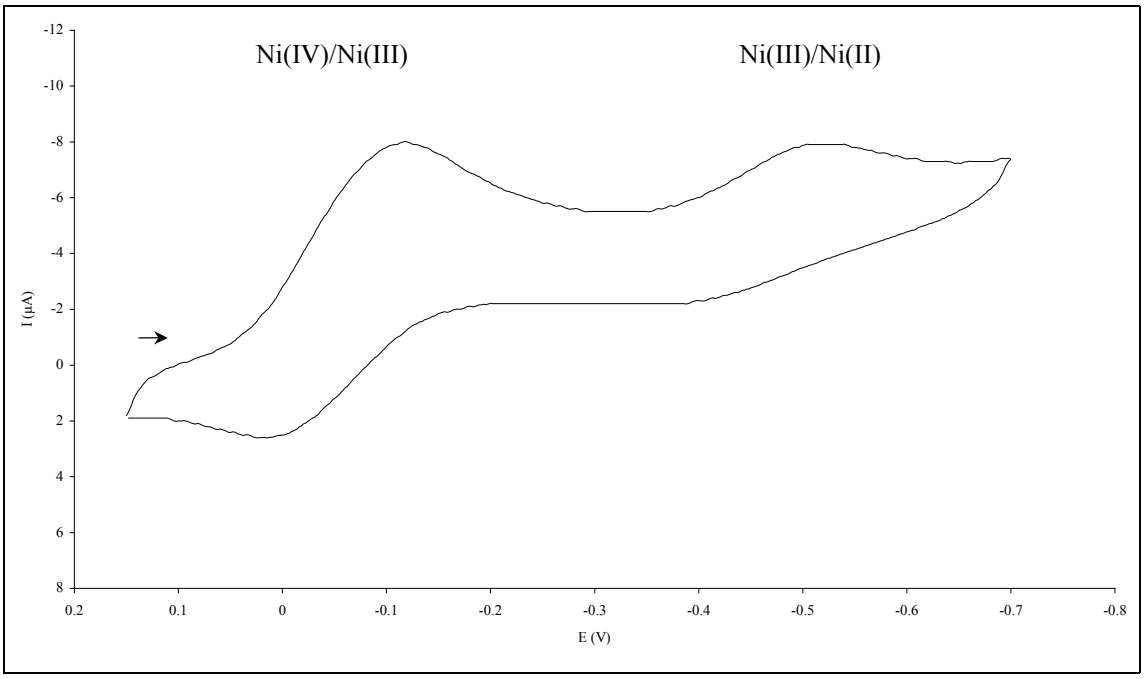

Figure 5.6 *Cyclic voltammetry electrochemical reduction waves of* ***96*** *together with assignments of electrochemical processes in $CHCl_3$:MeCN (4:1) containing 0.1M $TBABF_4$, potentials given with reference to Ag/Ag^+ at 293K, scan rate = 100mVs^{-1}*

The nickel(IV) compound **96** can be seen to undergo two reductions corresponding to nickel(IV)/nickel(III) and nickel(III)/nickel(II). The nickel(IV)/nickel(III) redox couple shows both reduction and oxidation waves whereas the nickel(III)/nickel(II) reduction only shows the reductive part of the peak. This was because the nickel(III) species, which was electrochemically generated, diffused away from the surface of the electrode and so was not observed on the reverse scan. Similar behaviour was seen for $Ni(DTCEt_2)_3Br$.[15]

Table 5.2 displays the data for the nickel(IV) receptor together with the data for $Ni(DTCEt_2)_3Br$.[15]

	Ni(IV)/Ni(III)			Ni(III)/Ni(II)	
	$Ni(DTCEt_2)_3Br$	**96**		$Ni(DTCEt_2)_3Br$	**96**
E_{pa} (V)	-0.065	0.070	E_{pc} (V)	-0.760	-0.525
E_{pc} (V)	-0.220	-0.110			
ΔE (V)	0.155	0.180			
I_{pa}/I_{pc}	0.7	1.0			
E_p (V)	-0.115	-0.065			

Table 5.2 *Electrochemical data of $Ni(DTCEt_2)_3Br$ and **96** in $CHCl_3$:MeCN (4:1) containing 0.1M $TBABF_4$, potentials given with reference to Ag/Ag^+ at 293K, scan rate = 100mVs^{-1}, E_p - peak potential in square wave voltammogram*

Receptor **96** displayed electrochemical reductions at potentials typical for nickel(IV)/nickel(III) and nickel(III)/nickel(II) processes. The potential of the nickel(IV)/nickel(III) reduction occurred at a less negative potential in **96** than for $Ni(DTCEt_2)_3Br$ possibly due to the electron withdrawing amide groups.

Figure 5.7 shows the nickel(IV)/nickel(III) reduction of receptor **96** as the scan rate is varied.

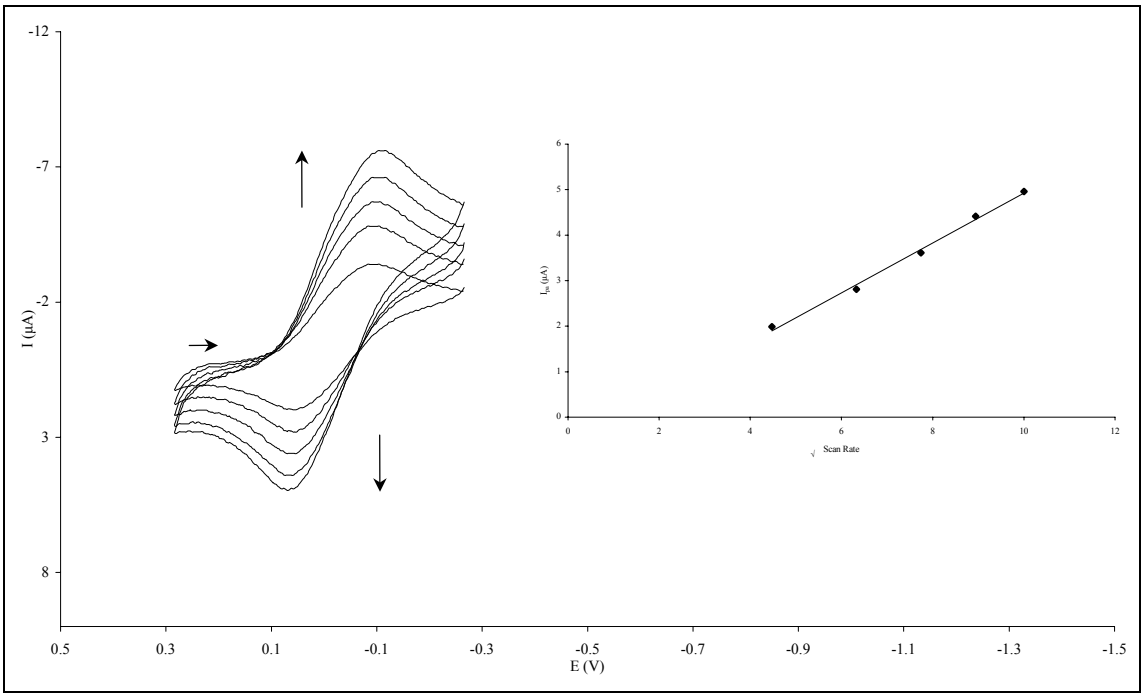

Figure 5.7 *Cyclic voltammetry electrochemical reduction waves of **96** in $CHCl_3$:MeCN (4:1) at varying scan rates (Inset) Plot of I_{pa} against √scan rate of **96** in $CHCl_3$:MeCN (4:1)*

The peak potential of both the anodic and cathodic peaks did not vary with scan rate and the plot of I_{pa} against the square root of scan rate was a straight line. Thus, **96** displayed quasi-reversible electrochemical behaviour.[20] Interestingly, the redox wave appeared only as one wave indicating that the two metal centres were acting independently.

2.1.3 Infrared Spectroscopy

Table 5.3 displays the infrared data for receptors **47**, **96** and $Ni(DTCEt_2)_3Br$ in a Nujol® mull.[21]

ν (cm^{-1})	**$Ni(DTCEt_2)_3$ Br**	**47**	**96**
ν (NH)	-	3252	3186
Amide I	-	1678	1660
Amide II	-	1537	1548
ν (CN)	1538	1500	1518
ν (CS_{as})	970	962	962
ν (CS_s)	672	-	652

Table 5.3 *Infrared data of $Ni(DTCEt_2)_3Br$, **47** and **96** (Nujol® mull) together with band assignments*

Both receptors **47** and **96** displayed a band ~3250cm^{-1} characteristic of an amide NH stretch.[22] Absorptions due to the amide I band occur ~1670cm^{-1} and the amide II band were seen ~1540cm^{-1}.[23] Both receptors display peaks consistent with a secondary amide moiety.

The CN stretch confirms the partial double bond character in the dithiocarbamate linkage.[24] This 'thioureide' band is observed at a higher wavenumber in the charged nickel(IV) species **96**, compared to the neutral nickel(II) receptor **47**. This is consistent with increased double bond character due to the electron withdrawing nature of the higher oxidation state metal centre.[25] The presence of a single absorption ~1000cm^{-1} is due to a anti-symmetric CS stretch and has been used as evidence for the bi-dentate nature of the coordination to the metal atom.[26] The symmetric stretch of the CS group is observed ~650cm^{-1} but was of too low intensity to be observed for **47**.[27]

2.1.4 Electrospray Mass Spectrometry

When excess $NOBF_4$ was added to a chloroform solution of the nickel(II) macrocyclic receptor **47** an immediate colour change from green to brown was observed.[28] When this solution was introduced into the electrospray mass spectrometer (**Appendix 4**) a cluster of peaks was observed which corresponded to the macrobicyclic structure.

Figure 5.8 illustrates the experimental spectrum and calculated isotopic distribution for receptor **96**.

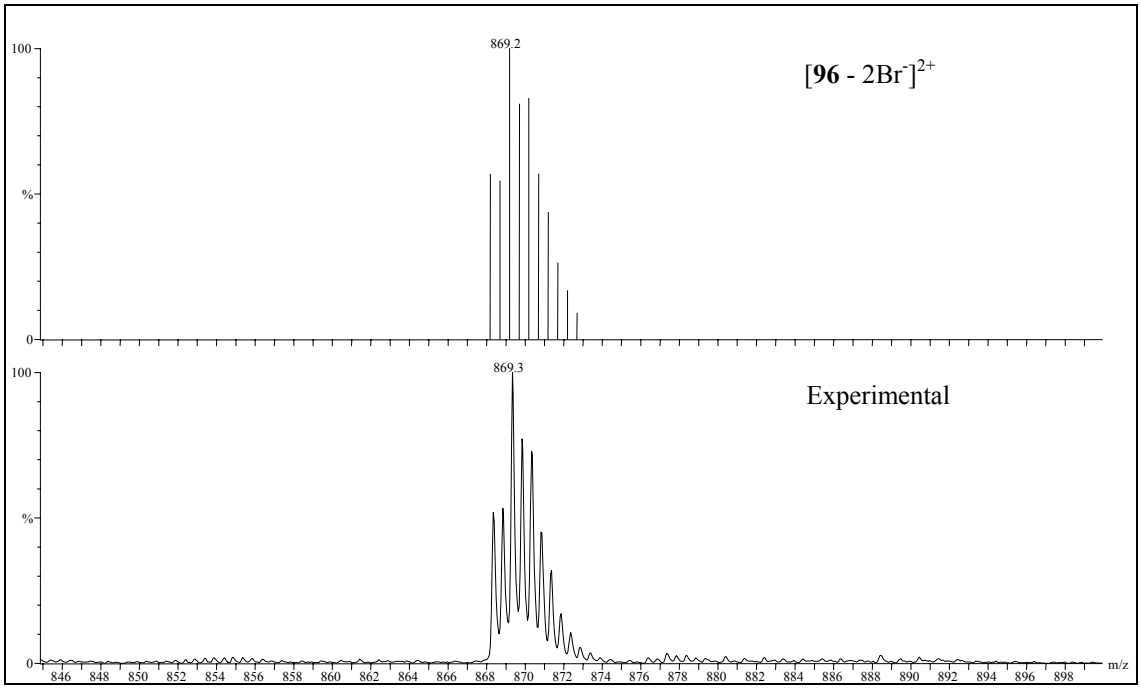

Figure 5.8 *ESMS of* ***96*** *and the isotope model*

Each peak was separated by half a mass unit consistent with a molecule carrying a plus two charge. This confirmed the presence of two nickel(II) centres each undergoing oxidation to a nickel(IV) species. This spectrum was identical to the one observed when the macrobicycle was synthesised on a preparative scale.

Macrocycles **43**, **45**, **49** and **51** displayed spectra consistent with analogous oxidation reactions when excess $NOBF_4$ was added to solutions of the receptors. Each spectrum showed excellent agreement between calculated isotopic patterns and experimental data.

2.2 Anion Binding Studies

The anion binding characteristics of **96** were investigated using electrochemical techniques and UV/visible spectroscopy. The anions studied were acetate, benzoate, dihydrogen phosphate, chloride, nitrate and perrhenate as their tetrabutyl ammonium (TBA) salts.

2.2.1 Nickel(IV) Electrochemistry

Disappointingly, when five equivalents of acetate, benzoate and dihydrogen phosphate anions were added to a $CHCl_3$:MeCN(4:1) solution of receptor **96**, a colour change was observed from dark red-brown to green. The presence of the anion was causing the reduction of the nickel(IV) dithiocarbamate to the nickel(II) species (see **Section 2.2.2**).

Table 5.4 presents the cathodic shift observed in the square wave voltammogram when five equivalents of various anions were added to the $Ni(DTCEt_2)_3Br$,[15] and **96**. These anions did not cause reduction of the nickel(IV) metal centres.

Anion	ΔE Ni(IV)/Ni(III) (mV)	
	$Ni(DTCEt_2)_3Br$	**96**
Chloride	15	70
Nitrate	<5	15
Perrhenate	<5	<5

Table 5.4 *Cathodic shifts in the square wave voltammogram upon the addition of 5 equivalents of anion to $Ni(DTCEt_2)_3Br$ and **96** in $CHCl_3$:MeCN (4:1) containing 0.1M $TBABF_4$, potentials given with reference to Ag/Ag^+ at 293K*

The control compound showed a small cathodic shift upon the addition of excess chloride anion however addition of five equivalents of nitrate and perrhenate anions resulted in negligible shifts of the nickel(IV)/nickel(III) couple. In contrast, **96** showed a moderately large cathodic shift upon the addition of chloride anion due to the bound chloride anion stabilising the nickel(IV) dithiocarbamate species. Five equivalents of nitrate produced a small cathodic shift, however addition of perrhenate showed virtually no change in the nickel(IV)/nickel(III) couple.

2.2.2 UV/visible Spectroscopy

The interaction of receptor **96** in $CHCl_3$ with various anions was investigated by recording the spectrum after the addition of aliquots of the TBA salts of acetate, dihydrogen phosphate, benzoate and chloride anions.

As noted earlier in the ecectrochemical studies, when acetate, dihydrogen phosphate and benzoate were added to **96** the receptor was reduced. This was shown by the characteristic nickel(IV) absorptions being replaced by nickel(II) dithiocarbamate absorptions. When aliquots of chloride were added very little change in the spectrum was observed.

3 Iron(III) Dithiocarbamate Macrobicyclic Anion Receptors

It was anticipated that novel macrobicyclic receptors could be synthesised by employing the same ligands that were utilised in **Chapter 3** but using a different transition metal ion with an octahedral stereochemical preference. For example iron(III) dithiocarbamates exhibit D_3 symmetry around the metal centre[7,8] so interesting cryptand-like molecules may be synthesised.

The dithiocarbamate moiety generates a ligand field which place iron(III) dithiocarbamates at an electronic crossover point such that high spin and low spin states are of similar energy.[7a] Thus, their magnetic and spectroscopic properties are exceptionally sensitive.[29] It was hoped that this sensitivity could be employed to monitor anion binding.

3.1 Synthesis and Characterisation

The target receptors were synthesised via a secondary amine-amide moiety, which was prepared as shown in **Scheme 5.2**.

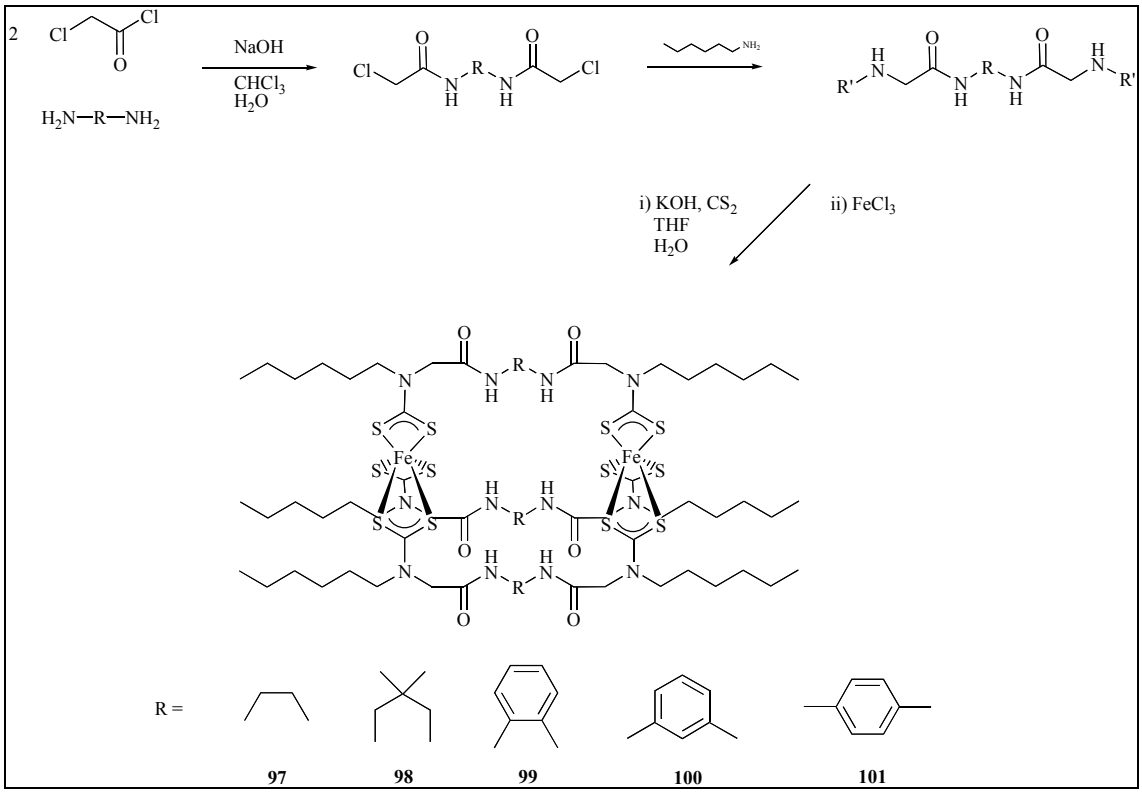

Scheme 5.2 *Synthesis of receptors **97** - **101***

The syntheses of the diamine precursors are described in **Chapter 3 Section 2.1**. Conversion of the amine ligands to the macrobicyclic structures was achieved by the addition of two equivalents of potassium hydroxide and carbon disulphide in a tetrahydrofuran:water mixture. After thirty minutes two thirds of an equivalent of iron(III) chloride was added and the mixture stirred for fifteen hours.[7] Addition of water precipitated the black products, which were filtered and thoroughly dried.

The NMR spectra of iron(III) dithiocarbamates can display peaks even though the complexes are paramagnetic in nature.[30] For example, iron(III) tris(*N*,*N*-diethyl dithiocarbamate)[15] displays relatively sharp, paramagnetically shifted peaks in its spectrum. Other complicating factors are the stereochemical non-rigidity of iron(III) dithiocarbamates[31] and the restricted rotation about the dithiocarbamate bond,[32] both of which cause increased broadness in the resonances. Unfortunately, **97** and **101** were too insoluble to obtain a spectrum while the other receptors displayed very broad peaks at room temperature in $CDCl_3$, which upon cooling became increasingly sharp. However, it was not possible to assign the individual peaks, thus, ^{1}H NMR was not used for characterisation or anion binding studies.

All the receptors **97** – **101** were characterised by UV/visible, electrochemistry, infrared, ESMS and magnetic measurements together with element analysis. A summary of the receptors is shown is **Appendix 13**.

3.1.1 UV/visible Spectroscopy

Iron(III) dithiocarbamate complexes exhibit many absorption bands between 250nm and 900nm. An intraligand π-π^* transition occurs ~250nm,[33] however in these studies this band was masked by absorption due to the solvent. At ~265nm, ~350nm, ~385nm and ~595nm there are LMCT absorptions and at ~285nm and ~510nm there are MLCT transitions.[34] Absorptions ~400nm and ~625nm have previously been ascribed to charge transfer processes.[33] However, in all cases the peak ~400nm was not discernable due to the overlap of the other transitions. In the region around 650nm, absorptions due to d-d electronic transitions are observed.[35] The low intensity and width of these bands are indicative of spin forbidden transitions, as expected of an iron(III) metal centre in an approximately octahedral environment. Extra broadness of these absorptions occur due to two overlapping bands; one associated with the low spin state and the other due to the high spin state.

Table 5.5 shows the UV/visible spectroscopic data for receptors **97** - **100** and the control compound, iron(III)-tris(*N*,*N*-diethyl dithiocarbamate) ($Fe(DTCEt_2)_3$)[15] in DMSO solution. Unfortunately, **101** was too insoluble to record a UV/visible spectrum and receptors **97** and **98** precipitated out of solution and so their extinction coefficients could not be calculated.

Assignment	$Fe(DTCEt_2)_3$	97	98	99	100
MLCT	-	281 sh	-	-	-
LMCT	343 (6.8)	351 sh	354 sh	354 sh (10.4)	345 (20.4)
LMCT	384 sh (4.4)	402	402 sh	389 sh (15.0)	394 sh (15.6)
MLCT	506 (1.8)	509 sh	505 sh	503 sh (4.3)	512 sh (4.9)
LMCT	593 sh (1.4)	597 sh	592 sh	602 sh (2.3)	586 sh (3.7)

Table 5.5 *Wavelength λ/nm (molar extinction coefficient $\varepsilon/10^3$ $M^{-1}cm^{-1}$) of $Fe(DTCEt_2)_3$ and the iron(III) dithiocarbamate receptors*

For all the iron(III) receptors it was not possible to assign the bands between 600nm and 800 nm due to the extreme broadness of the absorptions, and the absorptions ~280nm frequently did not show a clear maximum.

As seen previously, the oxidation of the transition metal centres in a molecule can be monitored by using UV/visible spectroscopy. **Figure 5.9** shows the changes in the UV/visible absorption spectrum upon addition of aliquots of an acetone solution of iron(III) perchlorate[25] to an acetone:DMF (99:1) solution of receptor **99**.

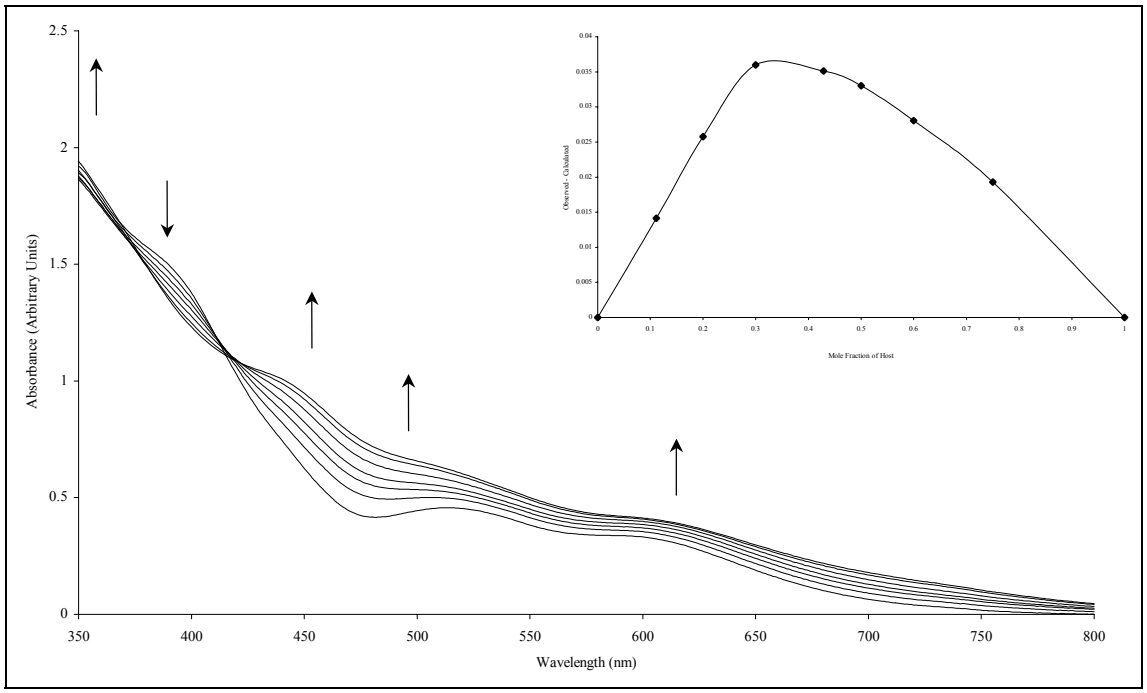

Figure 5.9 *UV/visible oxidation of **99** with iron(III) perchlorate in acetone:DMF (99:1)*
*(Inset) Job Plot of **99** with iron(III) perchlorate in acetone:DMF (99:1)*

The initial spectrum is typical of an iron(III) dithiocarbamate species and the final spectrum shows absorptions characteristic of a iron(IV) dithiocarbamate species.

In the regions ~360nm and ~450nm there are two LMCT transitions.[36] The shoulder ~490nm has previously been observed for a iron(IV) dithiocarbamate species but remains undefined,[37] and a weak shoulder at 650nm is due to a d-d transition.

The Job plot for the oxidation displayed a minimum ~0.33 clearly indicating that two equivalents of iron(III) perchlorate were needed to perform the oxidation.[16] This confirmed that the macrobicycle **71** contained two iron(III) dithiocarbamate centres.

3.1.2 Iron(III) Electrochemistry

Iron(III) dithiocarbamate complexes can undergo two relatively facile, metal based one electron reversible electrochemical processes corresponding to an iron(III)/iron(IV) oxidation and a iron(III)/iron(II) reduction.[17,19,38]

The electrochemistry of **97** - **101** was investigated using cyclic and square wave voltammetry in DMF. This solvent had to be used due to the low solubility of the receptors. **Figure 5.10** illustrates these redox waves of receptor **100** as the scan rate was varied.

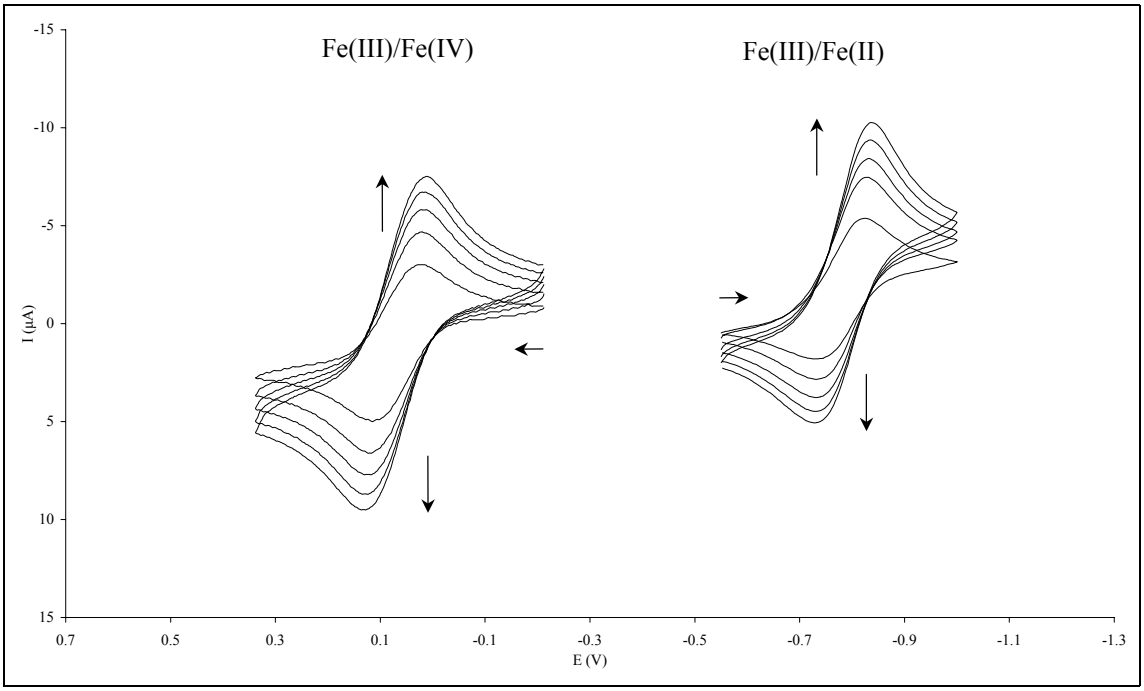

Figure 5.10 *Cyclic voltammetry electrochemical oxidation and reduction waves of **100** at varying scan rates together with assignments of electrochemical processes in DMF) containing 0.1M $TBABF_4$, potentials given with reference to Ag/Ag^+ at 293K*

The receptor **100** displayed typical electrochemical characteristics of iron(III)/iron(IV) and iron(III)/iron(II) processes. Both the oxidation and reduction processes appeared only as one

wave indicating that the two metal centres were independent of each other. A plot of I_{pa} against the square root of scan rate, for both oxidation and reduction processes, was a straight line, indicating quasi-reversibility.[20]

Similar results were obtained for all the iron(III) receptors and the data is presented in **Table 5.6** together with the data of $Fe(DTCEt_2)_3$.[15] Unfortunately, receptor **101** was insoluble in DMF and so could not be studied.

	Fe(III)/Fe(IV)				
	$Fe(DTCEt_2)_3$	**97**	**98**	**99**	**100**
E_{pa} (V)	0.070	0.205	0.120	0.140	0.135
E_{pc} (V)	-0.040	-	-0.030	0.030	0.010
ΔE (V)	0.110	-	0.150	0.110	0.125
I_{pa}/I_{pc}	1.0	-	1.2	1.0	1.0
E_p (V)	0.065	0.100	0.060	0.070	0.070

	Fe(III)/Fe(II)				
	$Fe(DTCEt_2)_3$	**97**	**98**	**99**	**100**
E_{pa} (V)	-0.800	-0.645	-	-	-0.730
E_{pc} (V)	-0.905	-0.780	-0.810	-0.855	-0.840
ΔE (V)	0.105	0.165	-	-	0.110
I_{pa}/I_{pc}	0.8	-	-	-	0.9
E_p (V)	-0.825	-0.690	-	-0.760	-0.765

Table 5.6 *Electrochemical data of $Fe(DTCEt_2)_3$ and the **97 – 100** in DMF containing 0.1M $TBABF_4$, potentials given with reference to Ag/Ag^+ at 293K, scan rate = 100mVs^{-1}, E_p - peak potential in square wave voltammogram*

Only the control compound and receptor **100** showed quasi-reversible characteristics of both the iron(III)/iron(IV) couple and iron(III)/iron(II) couple. Molecule **97** displayed an irreversible iron(III)/iron(IV) wave while receptors **98** and **99** showed an irreversible reduction of iron(III)/iron(II).

Thin layer coulometry was used to calculate the number of electrons transferred to receptor **100** (see **Chapter 3 Section 2.1.10**). It was found, that at the potential at which oxidation occurred, two electrons were removed from each molecule of the receptor. This showed that each receptor contained two iron(III) dithiocarbamate centres as each metal centre underwent a one electron oxidation. A similar experiment performed at a potential to reduce iron(III) to iron(II) showed that each molecule of receptor required two electrons to perform the reduction, again confirming the presence of two iron(III) dithiocarbamate centres.

3.1.3 Infrared Spectroscopy

Table 5.7 displays the infrared data for receptors **97 - 101** and $Fe(DTCEt_2)_3$ in a Nujol® mull.[21]

ν (cm^{-1})	**$Fe(DTCEt_2)_3$**	**97**	**98**	**99**	**100**	**101**
ν (NH)	-	3300	3268	3214	3284	3292
Amide I	-	1666	1660	1676	1686	1674
Amide II	-	1556	1530	1518	1532	1550
ν (CN)	1504	1486	1480	1482	1484	1484
ν (CS_{as})	992	962	960	960	964	966
ν (CS_s)	-	-	648	644	-	646

Table 5.7 *Infrared data of the $Fe(DTCEt_2)_3$ compound and **97 – 101** (Nujol® mull) together with band assignments*

All of the iron(III) receptors displayed bands ~3250cm^{-1}, ~1670cm^{-1} and ~1540cm^{-1} which are characteristic of an NH stretch, amide I and amide II absorptions respectively.[22,23]

The position of the CN stretch confirmed the partial double bond character in the dithiocarbamate linkage.[24] This stretch occurred at a lower wavenumber compared with the nickel(II) and copper(II) analogues due to the larger steric congestion around the iron(III) metal centre.[39] A single absorption ~1000cm^{-1} is due to a anti-symmetric CS stretch and has been used as evidence for the bi-dentate nature of the coordination to the metal atom[26] and the symmetric

stretch of the CS group was observed ~650cm^{-1}, which was occasionally too weak to be observed.[27]

3.1.4 Electrospray Mass Spectrosopy

When excess $NOBF_4$ was added to a solution of the iron(III) dithiocarbamate macrocyclic receptors **97 - 101** and this solution was injected into the ESMS, peaks were observed which corresponded to the macrobicyclic structure.[28]

Figure 5.11 displays the experimental spectrum and calculated isotopic distribution for receptor **99**.

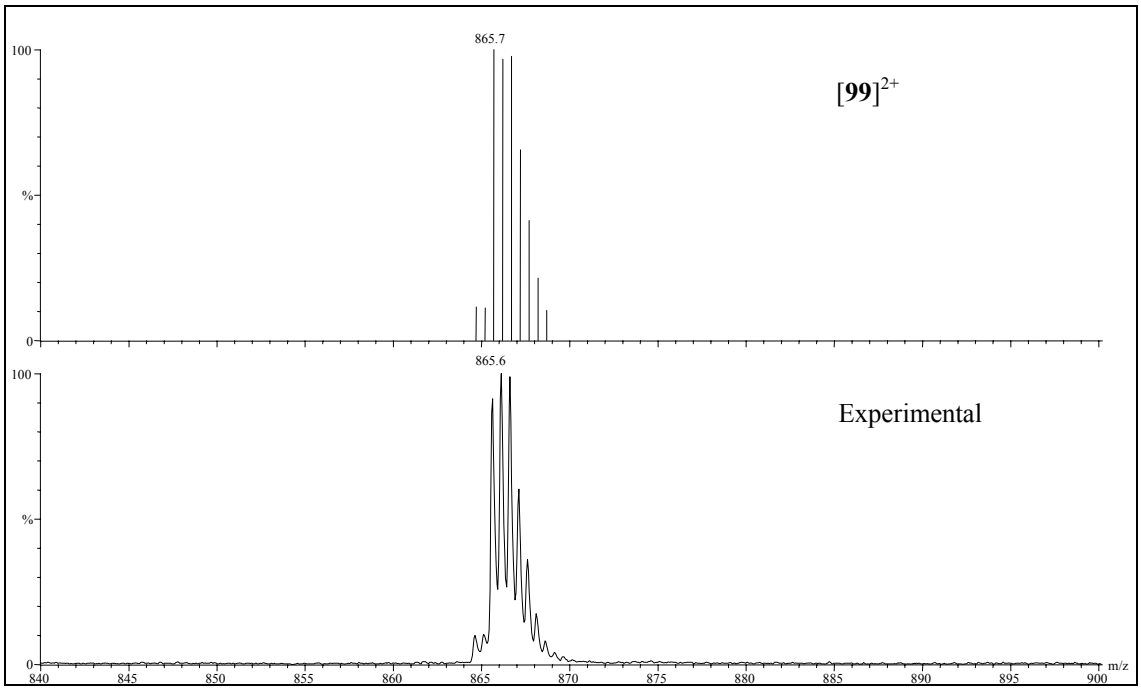

Figure 5.11 *ESMS of **99** together with the isotope model*

Excellent agreement between calculated isotopic distribution and experimental data was seen for every receptor. The peaks were separated by half a mass unit, indicating the molecule carried a dipositive charge confirming the presence of two iron centres per molecule of receptor.

3.1.5 Magnetic Studies

Magnetic susceptibility data for receptor **99** and the $Fe(DTCEt_2)_3$[15] were collected over the temperature range 5K - 300K using a super conducting quantum interference device (SQUID) (see **Chapter 3 Section 2.1.12**).

Iron(III) dithiocarbamate complexes exhibit magnetic moments which typically vary from ~2.2BM below 20K to 5.9BM at room temperature.[40] This anomalous behaviour is due to a thermal equilibrium between the two possible ground states, $^2T_2$ and $^6A_1$, which are separated by an energy ~kT. The low-spin $^2T_2$ usually lies lowest with the high-spin $^6A_1$ becoming increasingly populated according to the Boltzmann distribution.

Figure 5.12 shows the variation of the observed magnetic moment with temperature of $Fe(DTCEt_2)_3$.[15] Diamagnetic corrections (χ_m = -2.18x10^{-4}) were applied to the measured susceptibilities using Pascal's constants.[41]

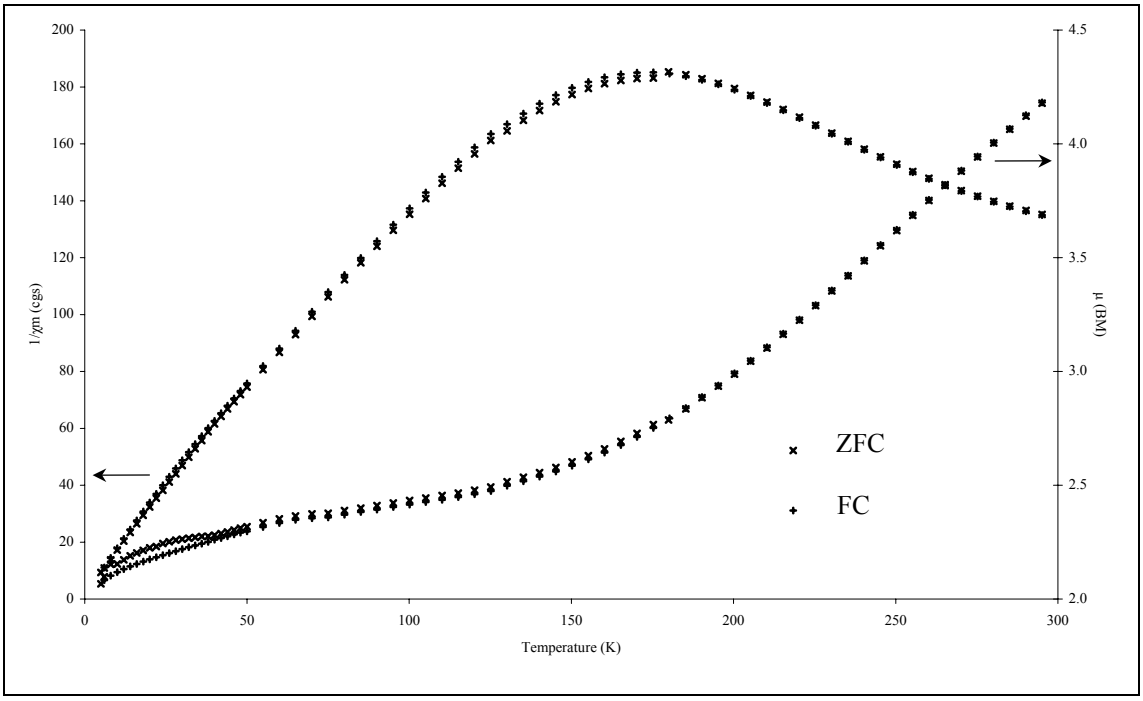

Figure 5.12 *Variable temperature magnetic susceptibility and magnetic moment of $Fe(DTCEt_2)_3$*

The magnetic moment of $Fe(DTCEt_2)_3$ varied smoothly from 2.08BM at 5K to 4.18BM at 300K. No hysteresis was observed as the FC and ZFC curves lay on top of each other.[42]

It has previously been shown that a good representation of magnetic behaviour of iron(III) *N*,*N*-dialkyldithiocarbamate compounds at atmospheric pressure maybe given by the equation in **Figure 5.13**.

$$\mu_{eff}^{\ 2} = \frac{0.75g^2 + 8x^{-1}(1 + e^{-3x/2}) + 105Ce^{-(1+(E/\xi))x}}{1 + 2e^{-3x/2} + 3Ce^{-(1+(E/\xi))x}}$$

$x = \xi/kT$

ξ - One electron spin-orbital coupling constant

g - Spectroscopic splitting factor of the $^2T_2$ state

E - Separation of the zero-point energies of the $^2T_2$ and $^6A_1$ states

$C = Q_a/Q_t$ - Ratio of molecular vibrational partition functions in $^2T_2$ and $^6A_1$

Figure 5.13 *Equation for the magnetic moment of simple iron(III) dithiocarbamate compounds*

Figure 5.14 shows the variation of observed ZFC magnetic moment between 100K and 300K for $Fe(DTCEt_2)_3$ together with the calculated best fit using the equation in **Figure 5.13**. The parameters were calculated assuming that $\xi = 370cm^{-1}$ and R is the reliability factor defined as $R = \Sigma(\chi_m^{obs} - \chi_m^{calc})^2 / \Sigma(\chi_m^{obs})^2$.[43]

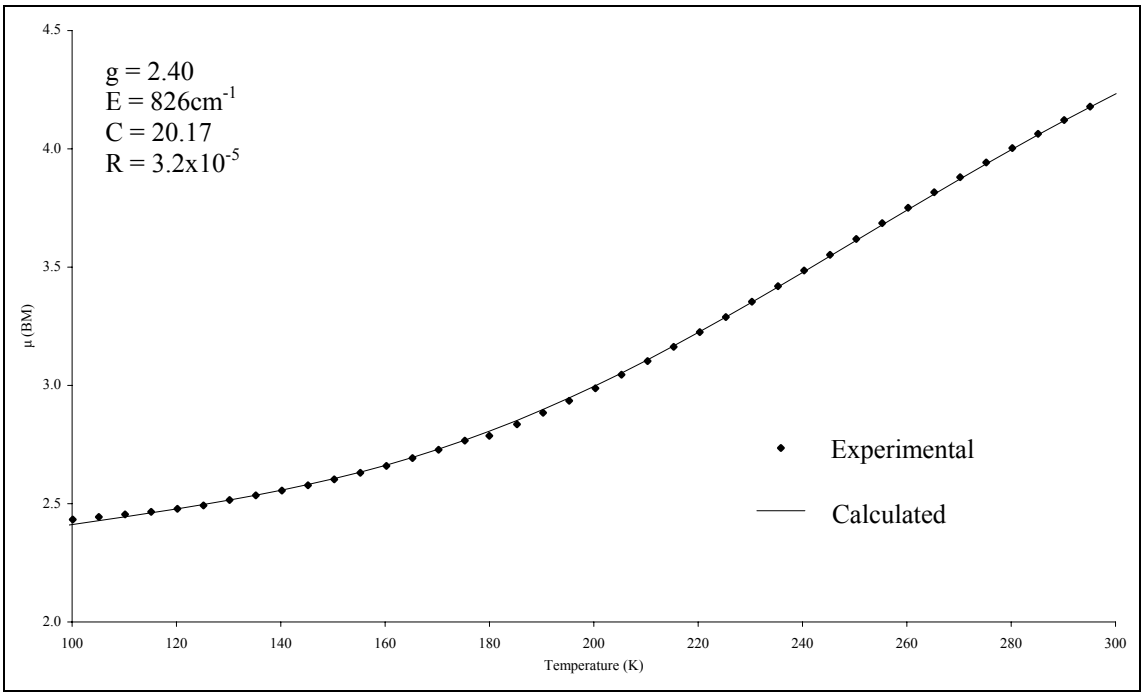

Figure 5.14 *Variable temperature magnetic moment of $Fe(DTCEt_2)_3$*

There is a very good fit between the experimental data and the calculated best fit line. The calculated values of g, E and C are very similar to those that have been reported previously.[40]

Figure 5.15 shows the observed magnetic moment of **99** varying with temperature, which has been corrected for diamagnetic contributions ($\chi_m = -7.78x10^{-4}$).[41]

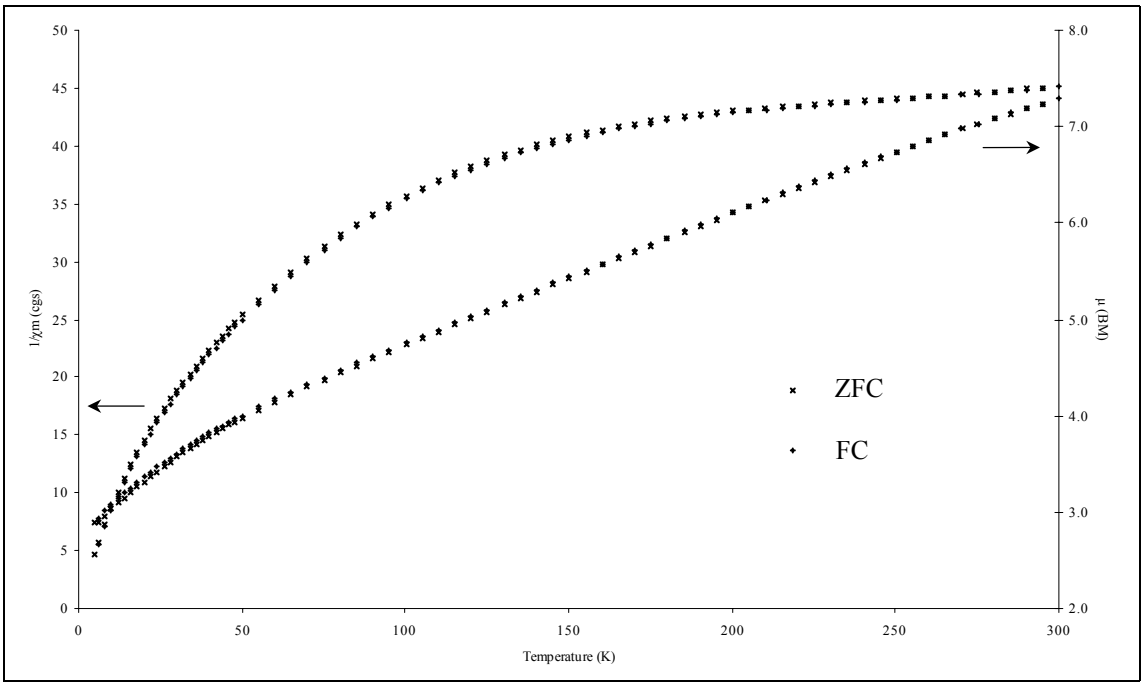

Figure 5.15 *Variable temperature magnetic susceptibility and magnetic moment of **99***

The observed magnetic moment of **99** varied smoothly from 2.94BM at 5K to 7.24BM at 300K and no hysteresis was observed. The μ values observed are consistent with the spin equilibrium described above. At low temperatures the majority of the sample is in a low spin state while at high temperature the sample has an increased population in a high spin state.

Unfortunately, it was not possible to fit this curve using the equation in **Figure 5.13**. This maybe due to exchange interactions[44] between the iron(III) dithiocarbamate centres either intra- or intermolecularly.

3.2 Anion Binding Studies

The anion binding characteristics of **97 - 101** were investigated using electrochemical techniques and UV/visible spectroscopy.

3.2.1 Iron(III) Electrochemistry

Five equivalents of acetate, benzoate and dihydrogen phosphate anions were added to DMF solutions of receptors **97 - 100**. Disappointingly, **101** was too insoluble to be studied.

Unfortunately, solutions of $Fe(DTCEt_2)_3$ and receptors **97** and **99** were seen to change colour from dark brown to orange upon anion addition. Iron(III) dithiocarbamates are known to undergo rapid ligand exchange.[45] It is possible that the anionic guest species displace one or more of the dithiocarbamate ligands from the metal centre creating a new species in solution. Attempts were made to identify the products using ESMS, however these peaks observed could not be assigned.

Table 5.8 reveals the cathodic shifts observed (when no colour change was seen) in the iron(III)/iron(IV) square wave voltammogram upon addition of five equivalents of the anions, together with the data for $Fe(DTCEt_2)_3$.

	ΔE Fe(III)/Fe(IV) (mV)		
	$Fe(DTCEt_2)_3$	**98**	**100**
Acetate	-[a]	-[a]	10
Benzoate	-[a]	-[a]	-[a]
Dihydrogen Phosphate	-[a]	-[a]	40
Chloride	10	30	25

Table 5.8 *Cathodic shifts in the square wave voltammogram upon the addition of 5 equivalents of anion to $Fe(DTCEt_2)_3$ and **98**, **100** in DMF containing 0.1M $TBABF_4$, potentials given with reference to Ag/Ag^+ at 293K (a - colour change observed)*

Moderate cathodic shifts was seen upon addition of chloride to both $Fe(DTCEt_2)_3$ and receptors **98** and **100**. The magnitude of this cathodic shift was larger than was observed with the $Fe(DTCEt_2)_3$. The shifts were to more negative potentials as the bound anion stabilised the charged iron(IV) dithiocarbamate species. In addition, **100** showed cathodic shifts when excess acetate and dihydrogen phosphate were added.

It proved impossible to monitor the effect of anion addition by following the iron(III)/iron(II) couple, because when the anion was added as the voltammogram showed no peak in the region where the redox process is usually observed.

3.2.2 UV/visible Spectroscopy

Large changes in the absorption bands were observed upon addition of acetate, benzoate and dihydrogen phosphate anions to MeCN:DMSO (4:1) solutions of the iron(III) based receptors **99** and **100**.

Unfortunately, it was not possible to calculate stability constants, as there was a time delay between addition of an aliquot of anion and the absorption reaching a steady value. In order to investigate the delay, two equivalents of anion were added to solutions of the receptors and the spectra recorded every minute until a constant absorption value was reached (**Table 5.9**).

Anion	Equilibration time (minutes)		
	$Fe(DTCEt_2)_3$	**99**	**100**
Acetate	8	2	8
Benzoate	25	2	7
Dihydrogen Phosphate	7	25	10
Chloride	2	-	-

Table 5.9 *Time taken for the absorbance to reach a steady value after the addition of two equivalents of anion*

The data in **Table 5.9** shows that the time to reach a constant absorption value depends not only on the anion added but also on the receptor's structure. Upon addition of chloride anion the spectrum showed a very small decrease in intensity at all wavelengths due to dilution effects.

The percentage increase in the absorption at 302nm after the addition of two equivalents of anion, are shown in **Table 5.10**.

Anion	Percentage change		
	$Fe(DTCEt_2)_3$	**99**	**100**
Acetate	40	25	25
Benzoate	20	30	25
Dihydrogen Phosphate	65	20	25
Chloride	30	-	-

Table 5.10 *Percentage increase in the UV/visible absorption ~301nm for **99** and **100***

The increase in absorption with $Fe(DTCEt_2)_3$ varies dependent upon the anion added. In contrast, the percentage increase in absorption of **99** and **100** is roughly equal irrespective of anion added or receptor design. This differs from the time delay effects observed for the nickel(II) macrocycles in **Chapter 3**.

As mentioned in **Section 3.2.1**, iron(III) dithiocarbamates undergo ligand exchange easily, thus it seems possible that the guest species could coordinate to the metal centre creating a new species in solution which may account for the unusual behaviour observed.

3.2.3 Magnetic Studies

Variable temperature magnetic studies have been employed in a cascade complex to assess anion binding (see **Chapter 1 Section 4.1**). It was hoped that iron(III) dithiocarbamate receptors in the presence of anionic guest species may possess different magnetic characteristics to that of the free receptor. In order to investigate the effect of the anion upon **99** one equivalent of dihydrogen phosphate was added to a DMF solution of the receptor and stirred for 1 hour. The solvent was removed and the product thoroughly dried. Elemental analysis of the isolated black solid confirmed that a 1:1 host:guest complex has been formed. Variable temperature magnetic susceptibility measurements were undertaken together with the analogous complex $Fe(DTCEt_2)_3 \cdot TBAH_2PO_4$. and the results are illustrated in **Figure 5.16**.

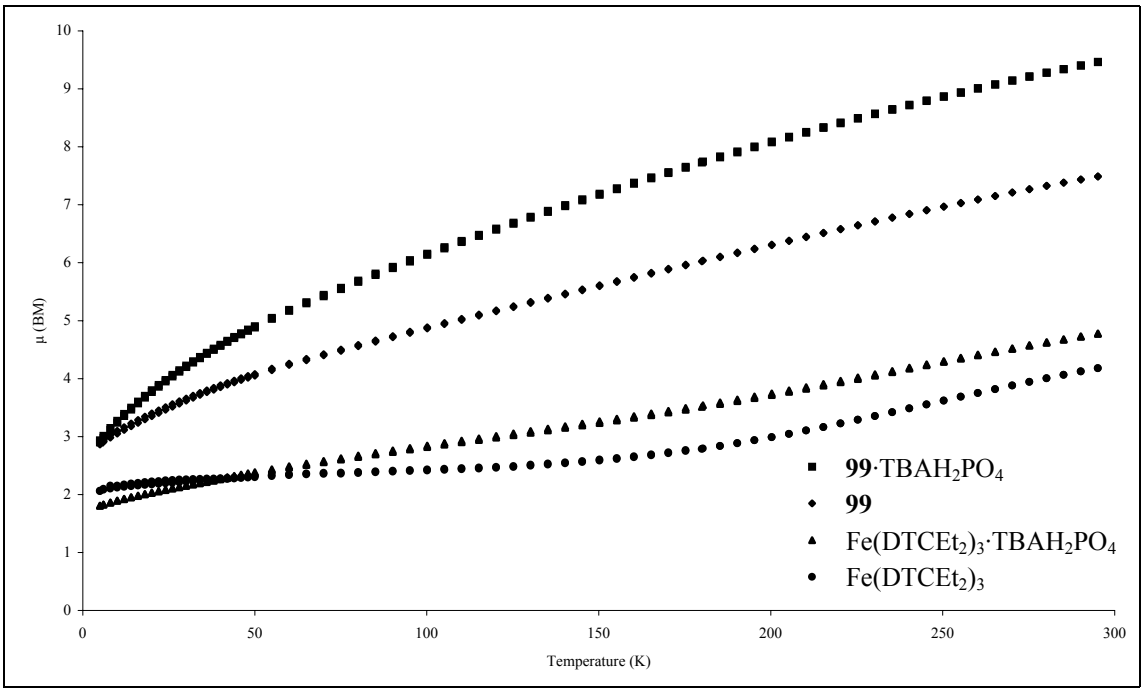

Figure 5.16 *Variation of magnetic moment of $Fe(DTCEt_2)_3.TBAH_2PO_4$ and **99**.$TBAH_2PO_4$ with temperature*

Both H_2PO_4 complexes showed larger magnetic moments, above 50K, than either of the iron(III) compounds on their own and the magnetic moment increased with temperature, as expected for the spin-crossover system. Additionally, the difference between the free and complexed species of **99** was twice that of $Fe(DTCEt_2)_3$ which may be due to the receptor possessing two dithiocarbamate centres whereas $Fe(DTCEt_2)_3$ only has one. However, the temperature dependence of the magnetic moment of the complexes was very different to that of the free compounds and so the presence of the anion is having an effect.

It was not possible to fit the data using the equation shown in **Figure 5.13** due to complexity of intra- and intermolecular magnetic interactions that may be occurring. For example, one can imagine the anion binding inside the macrobicyclic cavity which may either promote or prevent magnetic coupling between the two iron(III) dithiocarbamte centres in **99**.

4 Tripodal Macrobicyclic Anion Receptors

The previous sections in this chapter have been concerned with using octahedral stereochemistry around the metal centre to enable a macrobicyclic structure to be formed using the same secondary amine-amide ligands used in **Chapter 3 Section 2**. However, an alternative

route to macrobicyclic structures is to use a tripodal ligand with three linear connections to join two tripodal fragments together, creating a cryptand-like structure.

An example of a self-assembled macrobicycle that used a 1,3,5 substituted benzene molecule has been reported. This motif was used so that the ethyl groups and the thiol groups would be disposed on opposite sides of the molecule favouring potential self-assembly (**Figure 5.17**).[46]

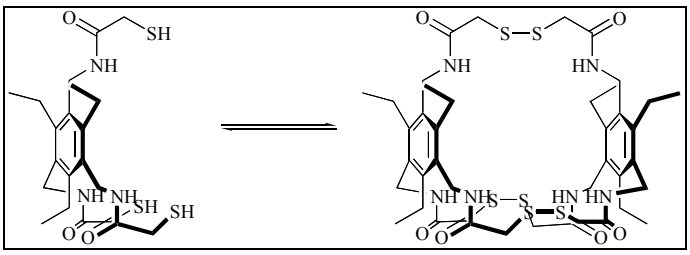

Figure 5.17 *Self-assembled macrobicyclic compound*

Preliminary reports have shown that the self-assembly of the macrobicyclic capsule in **Figure 5.17** was possible under certain conditions. However, this particular example displayed only moderate stability.

It was hoped that the dithiocarbamate group could be used to self-assemble novel anion cryptand-like receptors as shown in **Figure 5.18.**

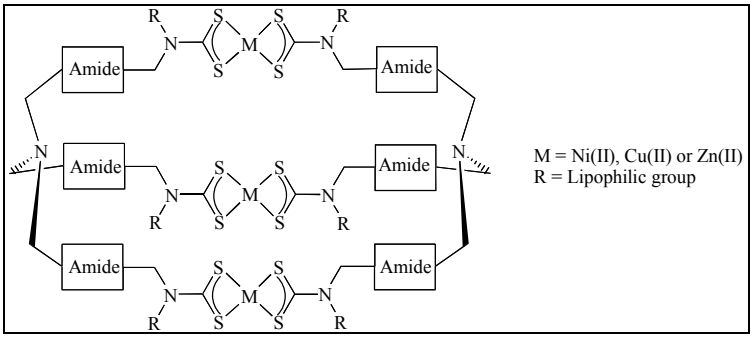

Figure 5.18 *Schematic of target receptors*

4.1 Synthesis and Characterisation

Macrobicyclic receptors **104** and **105** were synthesised from a secondary amide-amide molecule as illustrated in **Scheme 5.3**.

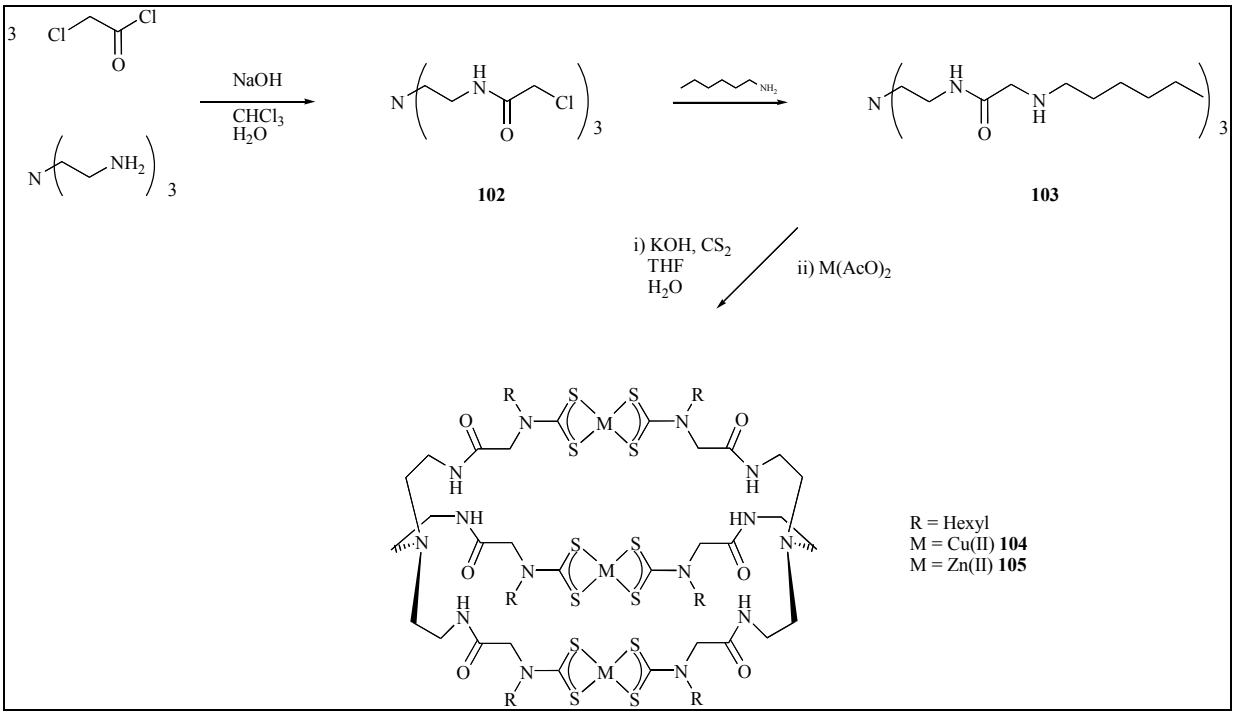

Scheme 5.3 *Synthesis of receptors **104** and **105***

One equivalent of tris-(2-aminoethyl) amine was dissolved in chloroform and excess aqueous sodium hydroxide was added. To this was added three equivalents of chloroacetyl chloride with stirring and the product precipitated in ~83% yield.[47] Portion wise addition of **102** to an excess of hexylamine and heating at 40°C for 15 hours gave the tris-amine ligand **103** in 87% yield.[48] Both of these precursors were characterised by ^{1}H, ^{1}H-^{1}H COSY NMR and ESMS.

Three equivalents of potassium hydroxide and three equivalents of carbon disulphide were added to one equivalent of the secondary amine in a tetrahydrofuran:water (5:1) mixture. The potassium dithiocarbamate salt was converted to the macrobicyclic product by the addition of one and a half equivalents of copper(II) or zinc(II) acetate with stirring for 15 hours.[7] Upon addition of water the white zinc(II) product was precipitated, isolated by filtration and thoroughly dried. The copper(II) product was isolated as a brown powder by the removal of tetrhydrofuran and extraction into chloroform followed by drying.

Receptors **104** and **105** were characterised by infrared, ESMS and elemental analysis. In addition, receptor **104** was characterised by ^{1}H and ^{1}H-^{1}H COSY NMR and receptor **105** analysed using UV/visible and electrochemical techniques.

The synthesis of an analogous nickel(II) dithiocarbamate receptor resulted in a green product and was characterised using ESMS. Disappointingly, despite recyrstallisations, the receptor could not be isolated in pure form to perform anion binding studies.

4.1.1 ^{1}H NMR Spectroscopy

The ^{1}H and ^{1}H-^{1}H COSY NMR spectra of receptor **105** together with peak assignments are shown in **Figure 5.19**.

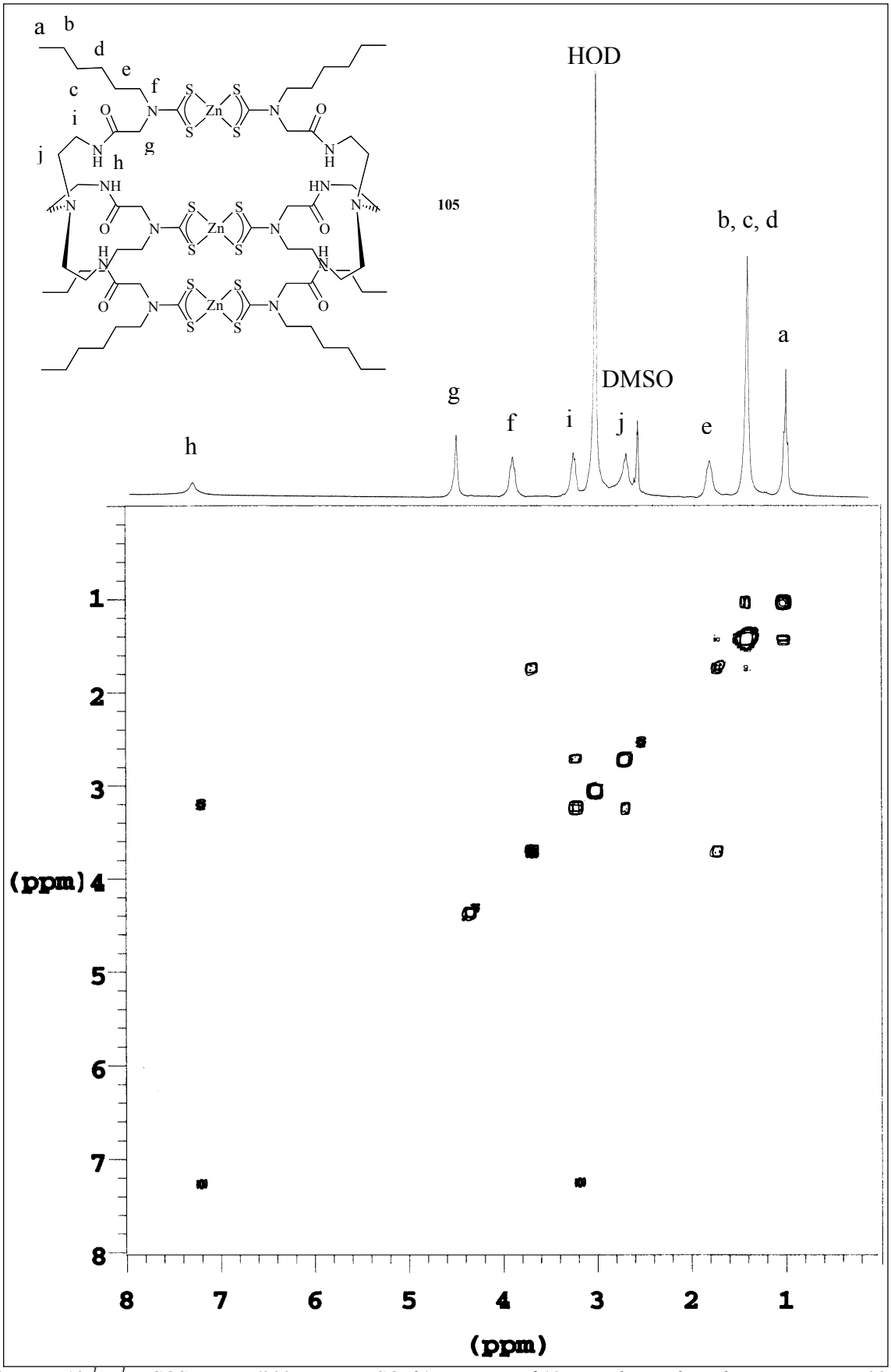

Figure 5.19 *^{1}H-^{1}H COSY NMR (300MHz, DMSO-d_6) spectrum of **105** together with peak assignments at 298K*

The ^{1}H NMR spectrum of receptor **105** is remarkably simple for a macrobicyclic system. The amide proton can be seen at 7.44ppm coupling to the protons on the adjacent carbon at

3.20ppm. The proton-proton coupling is also clearly visible along the hexyl chain. Unfortunately, this receptor was too insoluble for a ^{13}C NMR spectrum to be obtained.

4.1.2 UV/visible Spectroscopy

The UV/visible spectra of copper(II) dithiocarbamates typically display a LMCT charge transfer band at ~430nm[49] and two LC π-π^* bands at ~275nm and ~290nm.[50]

Table 5.11 presents the UV/visible spectroscopic data for receptor and $Cu(DTCEt_2)_2$ in $CHCl_3$ solution. In the case of receptor **104** the absorption ~290nm was hidden by the tail of the band at 275nm.

Assignment	$Cu(DTCEt_2)_2$	104
LC	269 (32.9)	275 (55.6)
LC	287 sh (18.0)	-
LMCT	433 (11.8)	439 (16.8)

Table 5.11 *Wavelength, λ/ nm (molar extinction coefficient ε/10^3 M^{-1} cm^{-1}) of $Cu(DTCEt_2)_2$ and **104***

Figure 5.20 shows the change in the UV/visible absorption spectrum upon addition of a MeCN solution of copper(II) triflate to a chloroform solution of receptor **104**.

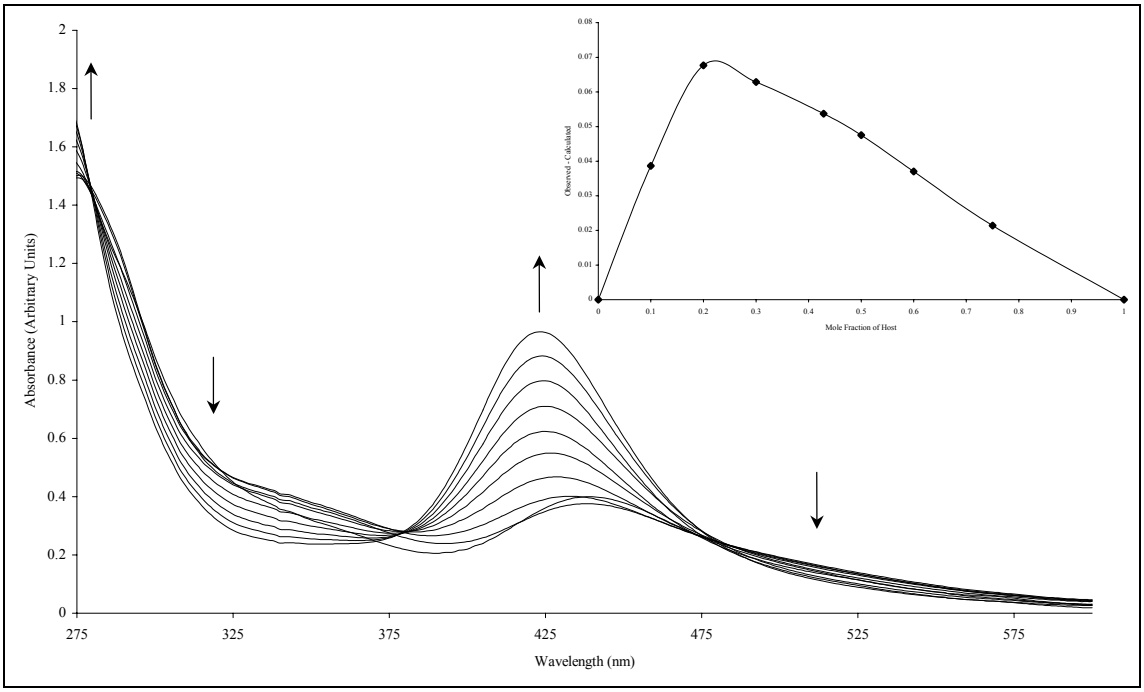

Figure 5.20 *UV/visible oxidation of **104** with copper(II) triflate in $CHCl_3$*
*(Inset) Job Plot of **104** with copper(II) triflate in $CHCl_3$*

The initial absorption spectrum is typical of a copper(II) dithiocarbamate. Upon oxidation, a new peak was observed at 426nm due to the copper(III) dithiocarbamate species.[51] The Job plot displayed a maximum at ~0.25 indicating that three equivalents of oxidant were required to oxidise the copper(II) dithiocarbamate metal centres.[16] This confirmed that receptor **76** contained three copper(II) dithiocarbamate centres.

4.1.3 Copper(II) Electrochemistry

Copper(II) dithiocarbamates can undergo a relatively facile one electron, metal centred oxidation and reduction.[17,19,52] The electrochemical characteristics of receptor **104** were studied in $CHCl_3$:MeCN(4:1) solution. The electrochemistry of $Cu(DTCEt_2)_2$[15] was also investigated to act as a reference.

The cyclic voltammogram displayed waves due to the copper(II)/copper(III) oxidation. These peaks were identified using square wave voltammetry as three separate redox processes with each peak being due to the oxidation of one copper(II) dithiocarbamate centre. Either this is due to communication between proximate dithiocarbamate centres or the redox active moieties are situated in three unique environments. This is in contrast to the macrocyclic receptors described in **Chapter 3 Section 2** and the macrobicyclic receptor **96** (see **Section 2.1.2**). Unfortunately, no copper(II)/copper(I) couple could be seen in the usual electrochemical window, possibly due to the structural rearrangement that occurs from square planar copper(II) to tetrahedral copper(I).[52] The electrochemical data is displayed in **Table 5.12**.

	Cu(II)/Cu(III)			
	$Cu(DTCEt_2)_2$	E_1	E_2	E_3
		104		
E_{pa} (V)	0.260	0.475	0.315	-[a]
E_{pc} (V)	0.135	0.375	0.225	0.095
ΔE (V)	0.125	0.100	0.090	-[a]
E_p (V)	0.205	0.405	0.288	0.170

Table 5.12 *Electrochemical data of $Cu(DTCEt_2)_2$ and **104** in $CHCl_3$:MeCN(4:1) containing 0.1M $TBABF_4$, potentials given with reference to Ag/Ag^+ at 293K, scan rate = 100mVs^{-1}, E_p - peak potential in square wave voltammogram (a - Peak could not be identified due to the broadness of the waves)*

Cyclic voltammetry revealed that the peak potential of E_1, E_2, and E_3 did not vary with scan rate and the maximum peak current was proportional to the square root of the scan rate indicating quasi-reversible electrochemical behaviour.[20]

4.1.4 Infrared Spectroscopy

Table 5.13 displays the infrared data for $Cu(DTCEt_2)_2$, $Zn(DTCEt_2)_2$ and receptors **104** and **105** in a Nujol® mull.[21]

ν (cm^{-1})	$Cu(DTCEt_2)_2$	104	$Zn(DTCEt_2)_2$	105
ν (NH)	-	3266	-	3286
Amide I	-	1662	-	1662
Amide II	-	1538	-	1540
ν (CN)	1508	1486	1504	1486
ν (CS_{as})	996	956	994	962
ν (CS_s)	-	650	666	-

Table 5.13 *Infrared data of $Cu(DTCEt_2)_2$, $Zn(DTCEt_2)_2$, **104** and **105** (Nujol® mull) together with band assignments*

104 and **105** displayed typical absorptions for a secondary amide.[22,23] The CN stretches of all the compounds were observed at the usual wavenumbers for a dithiocarbamate group

confirming the partial double bond character between these atoms.[24] A single absorption ~1000cm^{-1} confirmed the bi-dentate nature of nature of the coordination to the transition metal atom by two sulphur atoms.[26] The symmetric stretch of the CS group is observed ~650cm^{-1} although it was too low in intensity to be observed for **105**.[27]

4.1.5 Electrospray Mass Spectrometry

Excess $NOBF_4$ was added to a $CHCl_3$ solution of the tri-nuclear copper(II) macrobicyclic receptor **104** and was injected into the spectrometer.[28] Clusters of peaks were observed corresponding to the proposed macrobicyclic structure.

Figure 5.21 displays the experimental spectrum and calculated isotopic distribution for receptor **104**.

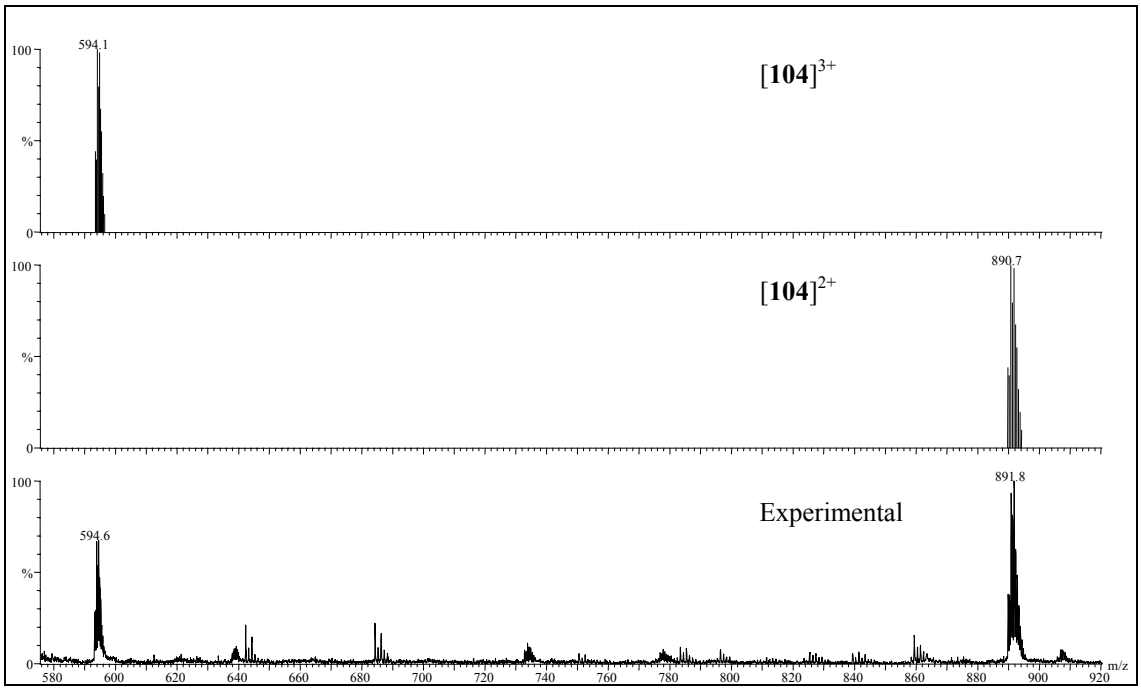

Figure 5.21 *ESMS of **104** and the isotope models*

The clusters at 891.8m/z and 594.6m/z were separated by half a mass unit and a third of a mass unit respectively. This was consistent with a molecule carrying a plus two and a plus three charge respectively, indicating that two and three copper(II) dithiocarbamate centres had been oxidised. There was excellent agreement between calculated isotopic patterns and experimental data for both species.

Receptor **105** was observed in the mass spectrum as the K^+ adduct when excess KPF_6 was co-injected with a solution of **105** into the spectrometer.

4.2 Anion Binding Studies

The anion binding characteristics of receptor **104** was investigated using electrochemical techniques and UV/visible spectroscopy. The anions studied were acetate, benzoate, dihydrogen phosphate, chloride and perrhenate as their TBA salts.

Disappointingly, **105** could not be investigated by UV/visible or ^{1}H NMR due to its insolubility.

4.2.1 Copper(II) Electrochemistry

The response of $Cu(DTCEt_2)_2$[15] and receptor **104** to the addition of five equivalents of anion was monitored by square wave voltammetry.

Receptor **104** displayed three separate oxidation waves due to the three copper(II) dithiocarbamate groups in the molecule, thus three peaks could be monitored upon anion addition. The cathodic shifts observed when five equivalents of anion were added to receptor **104** and $Cu(DTCEt_2)_2$ are displayed in **Table 5.14**.

Anion	ΔE Cu(II)/Cu(III) (mV)			
	$Cu(DTCEt_2)_2$	E_1	E_2	E_3
		104		
Acetate	25	15	35	20
Benzoate	5	60	75	40
Dihydrogen Phosphate	15	-[a]	-[a]	-[a]
Perrhenate	<5	<5	<5	<5

Table 5.14 *Cathodic shifts in the square wave voltammogram upon the addition of 5 equivalents of anion to $Cu(DTCEt_2)_2$ and **104** in $CHCl_3$:MeCN (4:1) containing 0.1M $TBABF_4$, potentials given with reference to Ag/Ag^+ at 293K (a – see text for discussion)*

As mentioned previously, small cathodic shifts of the copper(II)/copper(III) peak were observed upon the addition of all of the anions to a solution of $Cu(DTCEt_2)_2$. In contrast, **104** displayed much larger shifts in the square wave voltammograms when excess acetate, benzoate and dihydrogen phosphate were added.

However, addition of chloride resulted in two very broad peaks being seen in the volatmmogram. One was at a higher potential than the receptor and one at lower potential. It is possible that a reaction had occurred.

The magnitude of the shift of the square wave upon addition of excess dihydrogen phosphate was remarkably large. This maybe due to the shape complementarity of the tetrahedral anion coordinating with the tripodal array of amide groups on this receptor. A titration was carried out and the voltammograms displayed in **Figure 5.22**.

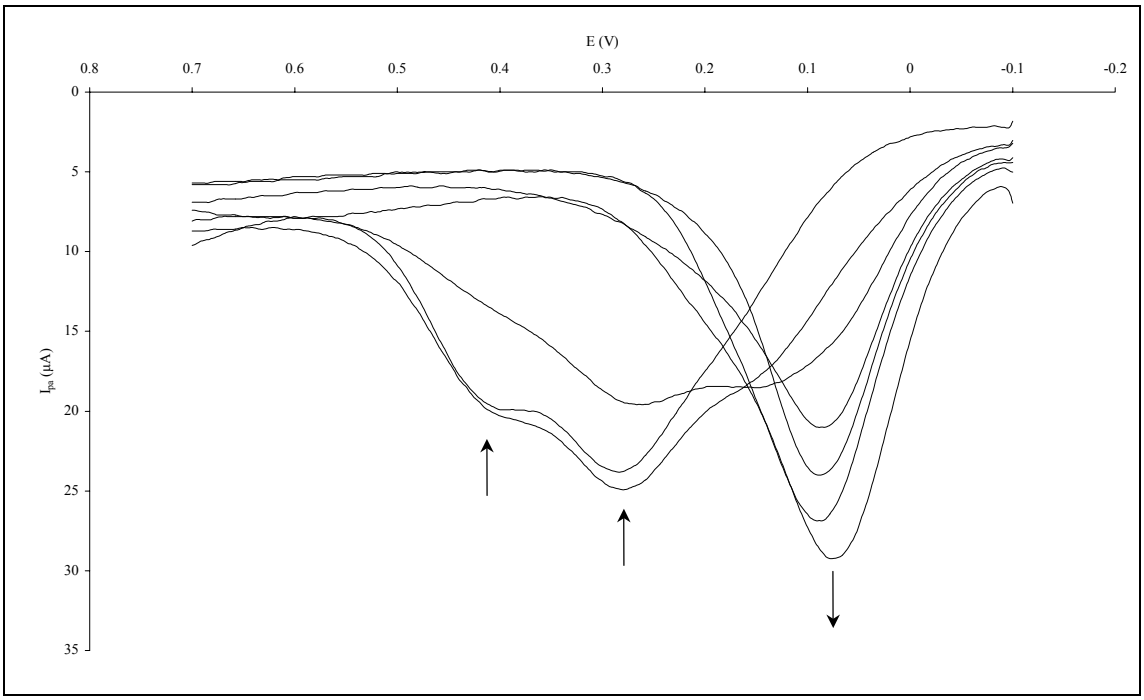

Figure 5.22 *Square wave voltammograms of **104** upon the addition of $TBAH_2PO_4$ in $CHCl_3$:MeCN (4:1) containing 0.1M $TBABF_4$, potentials given with reference to Ag/Ag^+ at 293K*

Upon addition of aliquots of dihydrogen phosphate to the receptor, dramatic shifts in peak potentials were seen ($\Delta E(E_1 - 0.078) = 325mV$). The peaks at 0.405V and 0.290V decreased in intensity and at the same time a new wave at 0.080V increased in intensity. This behaviour is due to the rate of anion complexation-decomplexation is slow on the timescale of the square wave experiment. Unfortunately, it was not possible to assess the binding stoichiometry as the

peak at 0.078V continued increasing in intensity up to ten equivalents of anion. Additionally, it was not possible to follow the peak potentials as the waves became extremely broad upon anion addition.

4.2.2 UV/visible Spectroscopy

Aliquots of acetate, dihydrogen phosphate, benzoate and chloride anions were added to a $CHCl_3$ solution of receptor **104**, unfortunately the spectrum changed very little for all of the anions.

5 Attempted Syntheses

Given the relative ease with which cryptand-like structures **104** and **105** were synthesised it was decided to try to make a macrobicyclic structure containing only one tris-chelated metal dithiocarbamate metal centre. Such a molecule would have three amide groups that could bind anions, which could be reported by the spectroscopic properties of the transition metal centre.

Scheme 5.4 illustrates the synthesis of the precursor tri-amide molecule **106**.

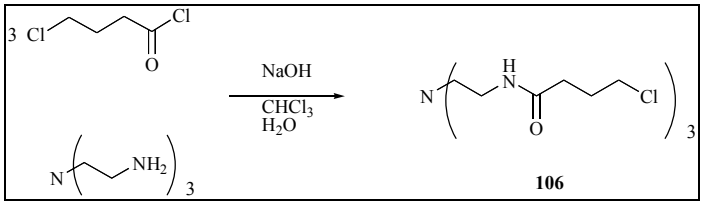

Scheme 5.4 *Synthesis of tris-amide **106***

One equivalent of tris-(2-aminoethyl) amine was dissolved in chloroform and excess aqueous potassium hydroxide was added and to this was added three equivalents of chlorobutyryl chloride with stirring.[47] The product was extracted into chloroform and after drying and solvent removal was isolated in 75% yield.

Several methods were employed to convert the alkyl chloride to the corresponding secondary amine; addition of excess hexylamine and heating, and the same method but in the presence of sodium iodide both proved unsuccessful. Unfortunately, the desired receptor molecule shown in **Figure 5.23** could not be synthesised.

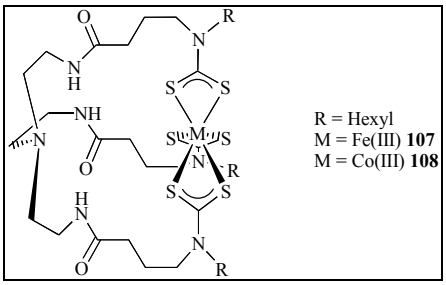

Figure 5.23 *Potential receptors **107** and **108***

6 Summary

Two novel types of macrobicyclic molecules have been developed based upon a transition metal dithiocarbamate moiety. The choice of transition metal ion dictated, via metal directed self-assembly, the type of cryptand-like structure formed by bringing either two or three tripodal or bipodal acyclic ligands together to compile the final receptor.

The nickel(IV) dithiocarbamate receptor **96** was synthesised by the oxidation of the analogous nickel(II) receptor **47**. Although **96** sensed chloride and nitrate anions electrochemically, acetate, benzoate and dihydrogen phosphate anions reduced the metal centre to nickel(II) as shown by UV/visible spectroscopy.

A range of anion receptors that employed the iron(III) dithiocarbamate moiety were successfully prepared. These receptors possessed amide moieties that were separated by a variety of spacer groups. Variable temperature magnetic susceptibility measurements of **98** revealed spin-crossover characteristics. Disappointingly, upon anion addition solutions of the receptors changed colour from dark brown to orange. It is thought that this maybe due to the ease with which iron(III) dithiocarbamates exchange their ligands, so the anionic guests maybe coordinating to the metal centre creating new species.

Two macrobicyclic tripodal anion receptors were successfully synthesised and characterised. Copper(II) receptor **104** sensed the presence of acetate and benzoate electrochemically and, in particular, displayed remarkably large cathodic shifts upon the addition of dihydrogen phosphate. This maybe due to the match in symmetry between the array of three amide groups and the tetrahedral anion. Unfortunately, **105** proved to be too insoluble to perform anion binding studies.

In summary, the aim of this chapter was to synthesise new types of macrobicyclic anion receptors using a transition metal dithiocarbamate group to assemble the molecule and to use the dithiocarbamate group to report the guest binding. This goal has been achieved and some of the receptors electrochemically sensed anions in organic solvents.

7 References

[1] a) M. Bonamico, G. Dessy, C. Mariani, A. Vaciago, L. Zambonelli, *Acta Crystallogr.*, 1965, **19**, 619; b) M. N. I. Khan, J. P. Fackler Jr., H. H. Murray, D. D. Heinrich, C. Campana, *Acta Crystallogr., Sect. C (Cr. Str. Comm.),* 1987, **43**, 1917.
[2] M. Bonamico, G. Dessy, C. Mariani, A. Vaciago, L. Zambonelli, *Acta Crystallogr.*, 1965, **19**, 886.
[3] J. M. Lehn, S. H. Pine, W. Watanabe, A. K. Willard, *J. Am. Chem. Soc.*, 1977, **99**, 6766.
[4] R. J. Motekaitis, A. E. Martell, J. M. Lehn, E. Watanabe, *Inorg. Chem.*, 1982, **21**, 4253.
[5] M. E. Padilla-Tosta, O. D. Fox, M. G. B. Drew, P. D. Beer, *Angew. Chem., Int. Ed. Engl.*, 2001, **40**, 4235.
[6] A. Avdeef, J. P. Fackler Jr., R. G. Fischer, *J. Am. Chem. Soc.*, 1970, **92**, 6972.
[7] a) D. Coucouvanis, *Prog. Inorg. Chem.*, 1979, **26**, 301; b) D. Coucouvanis, *Prog. Inorg. Chem.*, 1970, **11**, 233; c) D. J. Halls, *Mickro. Acta*, 1969, 62; d) J. Willemse, J. A. Cras, J. J. Steggerda, *Struct. Bonding*, 1976, **28**, 83; e) G. D. Thorn, R. A. Ludwig, *The Dithiocarbamates and Related Ligands*, Elsevier, 1962.
[8] J. G. Leipoldt, P. Coppens, *Inorg. Chem.*, 1973, **12**, 2269.
[9] J. P. Fackler Jr., A. Avdeef, R. G. Fischer Jr., *J. Am. Chem. Soc.*, 1973, **95**, 774.
[10] V. F. Plyusnin, V. P. Grivin, S. V. Larionov, *Coord. Chem. Rev.*, 1997, **159**, 121.
[11] B. M. Mattson, A. E. Madera, M. C. Palazzotto, *J. Coord. Chem.*, 1984, **13**, 321.
[12] M. Castillo, J. J. Criado, B. Macias, M. V. Vaquero, *Trans. Met. Chem.*, 1986, **11**, 476.
[13] H. C. Brinkhoff, J. A. Cras, J. J. Steggerda, J. Willemse, *Rec. Trav. Chim. Pays Bas*, 1969, **88**, 633.
[14] R. D. Webster, G. A. Heath, A. M. Bond, *J. Chem. Soc. Dalton Trans.*, 2001, 3189.
[15] For synthesis and characterisation see the Experimental Chapter.
[16] K. A. Connors, *Binding Constants*, J. Wiley & Sons, 1987, 24.
[17] A. M. Bond, R. L. Martin, *Coord. Chem. Rev.*, 1984, **54**, 23.
[18] A. R. Hendrickson, R. L. Martin, N. M. Rohde, *Inorg. Chem.*, 1975, **14**, 2980.
[19] R. Chant, A. R. Hendrickson, R. L. Martin, N. M. Rhode, *Aust. J. Chem.*, 1973, **26**, 2533.
[20] Southampton Electrochemical Group*, Instrumental Methods in Electrochemistry*, Ellis-Horwood, 1985, 183.
[21] L. M. Harwood, C. J. Moody, *Experimental Organic Chemistry Principles and Practice*, Blackwell Scientific Publishers, 1989, 294.
[22] G. Socrates, *Infrared Characteristic Group Frequencies*, 2nd Ed, J. Wiley & Sons, 104.
[23] G. Socrates, *Infrared Characteristic Group Frequencies*, 2nd Ed, J. Wiley & Sons, 105.
[24] R. Payne, R. J. Magee, J. Liesegang, *J. Elec. Spectr. Rel. Phen.*, 1985, **35**, 113.
[25] R. M. Golding, C. M. Harris, K. J. Jessop, W. C. Tennant, *Aust. J. Chem.*, 1972, **25**, 2567.
[26] a) F. Bonati, R. Ugo, *J. Organomet. Chem.*, 1967, **10**, 257; b) H. C. Brinkhoff, A. M. Grotens, *Rec. Trav, Chim.*, 1971, **111**, 253
[27] K. B. Pandeya, T. S. Waraich, R. C. Gaur, R. P. Singh, *J. Inorg. Nucl. Chem.*, 1981, **43**, 3159.
[28] A. M. Bond, R. Colton, A. D'Agostino, J. Harvey, J. J. Traeger, *Inorg. Chem.*, 1993, **32**, 3952.
[29] P. Ganguli, V. Marathe, *Inorg. Chem.*, 1978, **17**, 543.
[30] E. Beinrohr, J. Garaj, *Coll. Czech. Chem. Comm.*, 1980, **45**, 1785.
[31] L. H. Pignolet, *Top. Curr. Chem.*,1975, **56**, 91.
[32] B. L. Edgar, D. J. Duffy, M. C. Palazzotto, L. H. Pignolet, *J. Am. Chem. Soc.*, 1973, **95**, 1125.
[33] H. S. Sangari, G. S. Sodhi, *Indian J. Chem.*, 1993, **32A**, 730.
[34] G. St. Nikolov, *Inorg. Chim. Acta*, 1970, **4**, 610.
[35] C. A. Tsipis, C. C. Hadjikostas, G. E. Manoussaki, *Inorg. Chim. Acta*, 1977, **23**, 163.
[36] B. C. Verma, S. B. Kahlia, B. S. Manhas, *Indian J. Chem.*, 1997, **36A**, 160.
[37] L. I. Victoriano, J. A. Gnecco, H. V. Carbacho, *Polyhedron*, 1996, **15**, 1315.
[38] R. Chant, A. R. Hendrickson, R. L. Martin, N. M. Rohde, *Inorg. Chem.*, 1975, **14**, 1894.
[39] S. Thirumaran, V. Venkatachalam, K. Ramalingam, *Trans. Met. Chem.*, 1997, **22**, 89.

[40] A. H. Ewald, R. L. Martin, E. Sinn, A. H. White, *Inorg. Chem.*, 1969, **8**, 1837.
[41] a) F. E. Mabbs, D. J. Machin, *Magnetism and Transition Metal Complexes*, Chapman and Hall, 1973, 5; b) E. A. Bordreaux, L. N. Mulay, *Theory and Applications of Molecular Paramagnetism*, J. Wiley & Sons, 491; c) O. Kahn, *Molecular Magnetism*, VCH, 1993, 3.
[42] M. McElfresh, *Fundamentals of Magnetism and Magnetic Measurements Featuring Quantum Design's Magnetic Property Measurement System*, 1994, 23.
[43] P. S. Mukherjee, S. Dalai, G. Mostafa, T. H. Lu, E. Rentschler, N. R. Chaudhuri, *New J. Chem.*, 2001, **25**, 1203.
[44] M. McElfresh, *Fundamentals of Magnetism and Magnetic Measurements Featuring* Q*uantum Design's Magnetic Property Measurement System*, 1994, 19.
[45] N. H. Duffy, W. G. Mouvius, D. L. Uhrich, *Inorg. Chim. Acta*, 1982, **64**, L91.
[46] S. Tam-Chang, J. S. Stehouwer, A. Hao, *J. Org. Chem.*, 1999, **64**, 334.
[47] A. J. Speziale, P. C. Hamm, *J. Am. Chem. Soc.*, 1956, **78**, 2556.
[48] R. N. Salvatore, C. H. Yoon, K. W. Jung, *Tetrahedron*, 2001, **57**, 7785.
[49] G. H. Sarova, B. G. Jeliazkova, *Transition Met. Chem.*, 2001, **26**, 388.
[50] D. Oktavec, J. Stefanec, B. Siles, E. Beinrohr, V. Konecy, J. Garaj, *Coll. Czech. Chem. Comm.*, 1982, **47**, 2867.
[51] P. D. Beer, N. G. Berry, M. G. B. Drew, O. D. Fox, M. E. Padilla-Tosta, S. Patell, *Chem. Commun.*, 2001, 199.
[52] A. R. Hendrickson, R. L. Martin, N. M. Rohde, *Inorg. Chem.*, 1976, **15**, 2115.

Chapter Six

Experimental

1 Solvent and Reagent Pre-Treatment

Solvents were not pre-treated prior to use. Commercial grade chemicals were used without any further purification in all cases. De-ionised water was used in all cases.

2 Instrumental Techniques

NMR spectra were recorded on a Varian Mercury 300 or a Varian Unity Plus 500 instrument. UV/visible absorption spectra were acquired on a Perkin Elmer Lambda 6 Spectrometer. Mass spectrometry was carried using a Micromass LCT electrospray mass spectrometer. Infrared spectra were obtained in a Nujol® mull[1] on a Perkin Elmer 1600 series Fourier Transform Infrared Spectrometer controlled by Lab Control Spectacle software. Elemental analyses were performed by the Inorganic Chemistry Laboratory Microanalysis Service. Cyclic and square wave voltammetry were performed on a EG & G Princeton Applied Research Potentiostat/Galvanostat model 273 linked to a computer using a National Instruments GPIB-PCII/IIA interface and controlled by EG & G Princeton Applied Research Model 270/250 Research Electrochemistry Software.

3 Syntheses

2-Chloro-*N*-hexyl-acetamide 1

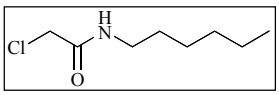

Hexylamine (2.07g, 20.0mmol) was dissolved in $CHCl_3$ (50mL) and $NaOH_{(aq)}$ (10mL, 40% w/w, excess) was added. Chloroacetyl chloride (2.44g, 20.0mmol) was dissolved in $CHCl_3$ (50mL) and added drop wise to the mixture with stirring. After 15 minutes, $HCl_{(aq)}$ (100mL, 1M) was added. The product was extracted into $CHCl_3$ (2x25mL) and dried over K_2CO_3. Filtration followed by solvent removal and drying in *vacuo* yielded a while solid.

Yield = 3.35g (93.4%)

^{1}H NMR (300MHz, $CDCl_3$) δ: 6.80 (s, 1H, N*H*), 3.93 (s, 2H, CH_2Cl), 3.18 (q, ^{3}J = 7Hz, 2H, NHCH_2), 1.43 (m, 2H, $NHCH_2CH_2$), 1.20 (m, 6H, $CH_2CH_2CH_2CH_3$), 0.78 (t, ^{3}J = 6Hz, 3H, CH_3)

ESMS m/z: 179.1 $[M + H^+]^+$

2-Benzylamino-*N*-hexylacetamide hydrochloride 2

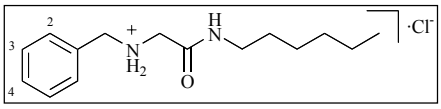

Benzylamine (1.81g, 16.9mmol) was heated to 70ºC and 2-chloro-*N*-hexyl-acetamide (3.00g, 16.9mmol) was added portion wise with stirring. The mixture was stirred for 2 hours and after cooling to room temperature Et_2O (50mL) was added. Filtration followed by drying in *vacuo* yielded a white solid.

Yield = 2.58g (53.8%)

^{1}H NMR (300MHz, $CDCl_3$) δ: 8.07 (m, 1H, CON*H*) 7.55 (m, 2H, ArH^2), 7.38 (m, 3H, ArH^3 & ArH^4), 4.19 (s, 2H, ArCH_2), 3.79 (s, 2H, NH_2CH_2CO), 3.17 (m, 2H, NHCH_2), 1.49 (m, 2H, $NHCH_2CH_2$), 1.25 (m, 6H, $CH_2CH_2CH_2CH_3$), 0.89 (t, ^{3}J = 7Hz, 3H, CH_3)

ESMS m/z: 249.2 $[M + H^+]^+$, 271.2 $[M + Na^+]^+$

Receptor 4

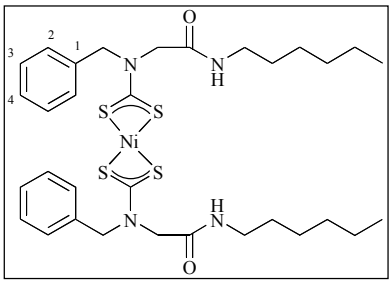

2-Benzylamino-*N*-hexylacetamide hydrochloride (1.5g, 6.0mmol) was dissolved in THF:H_2O (2:1 v/v, 60mL) and KOH (0.34g, 6.0mmol) was added and stirred under $N_{2(g)}$ until dissolved. CS_2 (0.46g, 6.0mmol) was then added and the solution stirred for 30 minutes. $Ni(CH_3CO_2)_2{\cdot}4H_2O$ (0.75g, 3.0mmol) was added to the yellow solution and the mixture stirred for 15 hours. H_2O (10mL) was added and filtration followed washing with EtOH (20mL) and Et_2O (20mL) yielded a light green powder, which was dried in *vacuo*.

Yield = 0.49g (23.2%)

^{1}H NMR (300MHz, $CDCl_3$) δ: 7.36 (m, 10H, Ar*H*), 5.75 (s, 2H, CON*H*), 4.89 (s, 4H, ArCH_2), 4.12 (s, 4H, COCH_2), 3.20 (m, 4H, NHCH_2), 1.46 (m, 4H, NHCH$_2$CH_2), 1.31 (m, 12H, CH_2CH_2CH_2CH$_3$), 0.91 (t, ^{3}J = 7Hz, 6H, CH_3)

^{13}C NMR (75.5MHz, $CDCl_3$) δ: 210.0 (*C*S$_2$), 165.4 (*C*O), 133.5 (Ar*C*^{1}), 129.4 (Ar*C*^{2}), 129.1 (Ar*C*^{3}), 129.0 (Ar*C*^{4}), 53.5 (Ar*C*H$_2$N), 51.4 (N*C*H$_2$CO), 40.1 (N*C*H$_2$), 31.6 (NCH$_2$CH$_2$*C*H$_2$), 29.5 (NCH$_2$*C*H$_2$), 26.7 (NCH$_2$CH$_2$CH$_2$*C*H$_2$), 22.8 (*C*H$_2$CH$_3$), 14.3 (*C*H$_3$)

UV/visible (MeCN:DMSO 4:1) λ/nm (ε/dm^3 mol^{-1} cm^{-1}): 331 (30.7), 399 (5.0), 434 (1.3)

IR (Nujol®) ν/cm^{-1}: 3296 (NH), 1662 (Amide I), 1566 (Amide II), 1484 (CN), 976 (CS$_{as}$)

ESMS m/z: 727.3 [M + Na$^+$]$^+$

Elemental Analysis %:	Calculated	C	54.5	H	6.6	N	8.3
	Experimental	C	54.5	H	6.6	N	7.8

Receptor 5

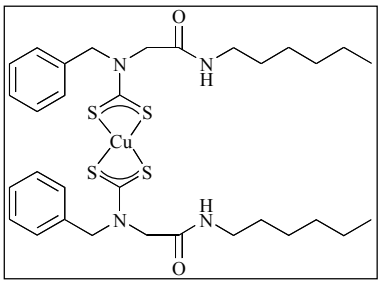

Method the same as that of **4**, except Cu(CH$_3$CO$_2$)$_2$·H$_2$O (0.60g, 3.0mmol) was used. After 15 hours stirring the THF was removed under reduced pressure and H$_2$O (100mL) was added and the product extracted into $CHCl_3$ (3x50mL). Drying over K_2CO_3 and filtration followed by solvent removal yielded a brown powder.

Yield = 0.46g (21.6%)

UV/visible (MeCN:DMSO 4:1) λ/nm (ε/dm^3 mol^{-1} cm^{-1}): 273 (45.1), 291 sh (31.1), 437 (12.4)

IR (Nujol®) ν/cm^{-1}: 3286 (NH), 1652 (Amide I), 1572 (Amide II), 1482 (CN), 1006 (CS$_{as}$), 676 (CS$_s$)

ESMS m/z: 732.3 [M + Na$^+$]$^+$

Elemental Analysis %:	Calculated	C	54.1	H	6.5	N	7.9
	Experimental	C	53.9	H	6.5	N	7.5

(2-Amino-ethyl)-carbamic acid *tert*-butyl ester 6[2]

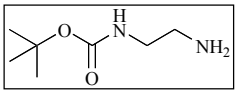

Di-*tert*-butoxy carbonyl (2.18g, 10.0mmol) was dissolved in 1,4-dioxane (50mL) and added drop wise over 1 hour to ethylenediamine (4.80g, 80mmol) dissolved in 1,4-dioxane (50mL). The mixture was stirred under $N_{2(g)}$ for 2 hours. The solvent was removed under reduced pressure and the white solid suspended in H_2O (50mL) and filtered to remove the insoluble bis substituted product. The filtrate was extracted into CH_2Cl_2 (3x50mL) then dried over K_2CO_3. Filtration followed by solvent removal and drying in *vacuo* yielded a yellow oil.

Yield = 1.28g (80.0%)

^{1}H NMR (300MHz, $CDCl_3$) δ: 5.04 (br, 1H, CON*H*), 3.12 (q, ^{3}J = 6Hz, 2H, CH_2NHCO), 2.74 (t, ^{3}J = 6Hz, 2H, CH_2NH$_2$), 1.39 (s, 9H, (CH_3)$_3$), 1.19 (s, 2H, NH_2)

ESMS m/z: 161.2 $[M + H^+]^+$

***N*-(*tert*-Butoxycarbonyl)ethylenediaminodithiocarbamate triethylamine 7**

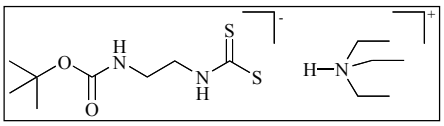

(2-Amino-ethyl)-carbamic acid *tert*-butyl ester (1.28g, 8.0mmol), triethylamine (0.81g, 8.0mmol) and CS_2 (0.61g, 8.0mmol) were dissolved in THF (50mL). The mixture was stirred under $N_{2(g)}$ for 10 minutes. Solvent removal under reduced pressure and drying in *vacuo* yielded a yellow solid.

Yield = 2.70g (Quantitative)

^{1}H NMR (300MHz, $CDCl_3$) δ: 7.92 (br, 1H, N*H*CS), 5.35 (br, 1H, CON*H*), 5.17 (br, 1H, *H*N (CH_2CH$_3$)$_3$), 3.69 (q, ^{3}J = 4Hz, 2H, CH_2NHCO), 3.28 (t, ^{3}J = 6Hz, 2H, CH_2NH$_2$), 3.22 (q, ^{3}J = 7Hz, 6H, HN (CH_2CH$_3$)$_3$), 1.39 (s, 9H, (CH_3)$_3$), 1.33 (t, ^{3}J = 7Hz, 9H, HN (CH$_2$CH_3)$_3$)

[2-(3-Hexyl-thioureido)-ethyl]-carbamic acid *tert*-butyl ester 8

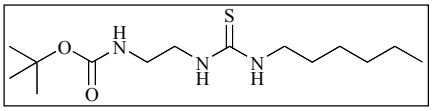

N-(*tert*-Butoxycarbonyl)ethylenediaminodithiocarbamate triethylamine (1.64g, 4.9mmol), hexylamine (0.49g, 4.9mmol) and triethylamine (0.49g, 4.9mmol) were dissolved in MeOH (50mL). The mixture was refluxed

under $N_{2(g)}$ for 12 hours. H_2O (100mL) and $HCl_{(aq)}$ (20mL, 2M) were added and the product was extracted into CH_2Cl_2 (4x50mL) and dried over K_2CO_3. Filtration followed by solvent removal and drying in *vacuo* yielded a yellow oil.

Yield = 1.23g (83.3%)

^{1}H NMR (300MHz, $CDCl_3$) δ: 6.95 (br, 1H, N*H*CS), 6.24 (br, 1H, N*H*CS), 5.18 (br, 1H, CON*H*), 3.60 (br, 2H, C*H*$_2$NHCO), 3.33 (br, 4H, C*H*$_2$NHCSNHC*H*$_2$), 1.57 (m, 2H, NHCH$_2$C*H*$_2$CH$_2$), 1.43 (s, 9H, (C*H*$_3$)$_3$), 1.30 (m, 6H, C*H*$_2$C*H*$_2$C*H*$_2$CH$_3$), 0.87 (t, ^{3}J = 5Hz, 3H, C*H*$_3$)

1-(2-Amino-ethyl)-3-hexyl-thiourea 9

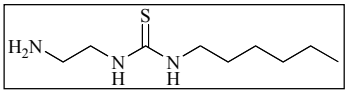

[2-(3-Hexyl-thioureido)-ethyl]-carbamic acid *tert*-butyl ester (1.23g 4.1mmol) was dissolved in CH_2Cl_2 (20mL) and TFA (5mL) was added and the mixture stirred for 3 hours under $N_{2(g)}$. $NaOH_{(aq)}$ (2M) was added carefully until pH = 11 and the product was extracted into CH_2Cl_2 (4x50mL) and dried over K_2CO_3. Filtration followed by solvent removal and drying in *vacuo* yielded a yellow oil.

Yield = 0.80g (76.3%)

^{1}H NMR (300MHz, $CDCl_3$) δ: 6.95 (br, 1H, N*H*CS), 6.48 (br, 1H, N*H*CS), 3.40 (br, 4H, C*H*$_2$NHCSNHC*H*$_2$), 2.92 (t, ^{3}J = 5Hz, 2H, NH$_2$C*H*$_2$), 1.58 (m, 2H, NHCH$_2$C*H*$_2$CH$_2$), 1.30 (m, 6H, C*H*$_2$C*H*$_2$C*H*$_2$CH$_3$), 0.87 (t, ^{3}J = 6Hz, 3H, C*H*$_3$)

1-(2-Benzylamino-ethyl)-3-hexyl-thiourea 10

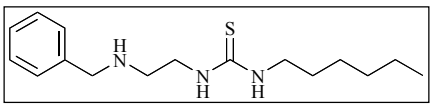

1-(2-Amino-ethyl)-3-hexyl-thiourea (0.8g, 3.9mmol) and benzaldehyde (0.40mL, 3.9mmol) were dissolved in toluene (100mL). The mixture was refluxed under $N_{2(g)}$ for 45 minutes using Dean-Stark apparatus and then the solvent was removed to yield an orange oil. This was dissolved in MeOH (100mL) and $NaBH_4$ (1g, excess) was added cautiously and stirred for 1 hour under $N_{2(g)}$. $HCl_{(aq)}$ (2M) was added carefully until pH = 1 and then $NaOH_{(aq)}$ (2M) until pH = 11. The product was extracted

into CH_2Cl_2 (4x50mL) and dried over K_2CO_3. Filtration followed by solvent removal and drying in *vacuo* yielded a yellow oil.

Yield = 0.76g (90.1%)

^{1}H NMR (300MHz, $CDCl_3$) δ: 7.31-7.25 (m, 5H, Ar*H*), 3.76 (s, 2H, ArCH_2), 3.41-3.37 (br, 4H, CH_2NHCSNHCH_2), 2.83 (t, ^{3}J = 5Hz, 2H, ArCH$_2$NHCH_2), 1.55 (m, 2H, NHCH$_2$CH_2CH$_2$), 1.28 (m, 6H, CH_2CH_2CH_2CH$_3$), 0.86 (t, ^{3}J = 6Hz, 3H, CH_3)

ESMS m/z: 294.2 $[M + H^+]^+$

Receptor 11

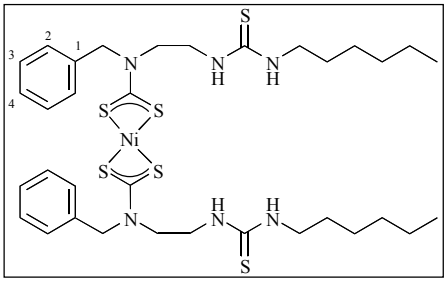

1-(2-Benzylamino-ethyl)-3-hexyl-thiourea (0.82g, 2.8mmol) was dissolved in THF:H_2O (5:1 v/v, 60mL) and KOH (0.15g, 2.8mmol) was added and stirred under $N_{2(g)}$ until dissolved. CS_2 (0.22g, 2.9mmol) was added and the solution stirred for 30 minutes. $Ni(CH_3CO_2)_2{\cdot}4H_2O$ (0.35g, 1.4mmol) was added to the yellow solution and the mixture stirred for 15 hours. H_2O (100mL) was added and the product extracted into CH_2Cl_2 (6x50mL) and dried over K_2CO_3. Filtration followed by solvent removal and recrystallisation from CH_2Cl_2/Et_2O yielded a light green powder, which was dried in *vacuo*.

Yield = 0.30g (27.2%)

^{1}H NMR (300MHz, $CDCl_3$) δ: 7.24 (m, 10H, Ar*H*), 6.04 (br, 2H, CSN*H*CH$_2$CH$_2$CH$_2$), 5.94 (br, 2H, NCH$_2$CH$_2$N*H*CS), 4.77 (s, 4H, ArCH_2), 3.72 (br, 4H, NCH$_2$CH_2NHCS), 3.67 (br, 4H, NCH_2), 3.27 (m, 4H, CSNHCH_2CH$_2$CH$_2$), 1.52 (m, 4H, NHCH$_2$CH_2CH$_2$), 1.31 (m, 12H, CH_2CH_2CH_2CH$_3$), 0.75 (s, 6H, CH_3)

^{13}C NMR (75.5MHz, DMSO-d_6) δ: 207.3 (*C*S$_2$), 183.2 (*C*S), 135.1 (Ar*C*^{1}), 129.5 (Ar*C*^{2}), 128.8 (Ar*C*^{3}), 128.7 (Ar*C*^{4}), 52.6 (*C*H$_2$), 48.2 (*C*H$_2$), 44.2 (*C*H$_2$), 42.0 (*C*H$_2$), 31.7 (*C*H$_2$), 29.3 (*C*H$_2$), 26.9 (*C*H$_2$), 22.8 (*C*H$_2$), 14.6 (*C*H$_3$)

UV/visible (MeCN:DMSO 4:1) λ/nm (ε/dm^3 mol^{-1} cm^{-1}): 326 (31.8), 390 (6.7), 428 sh (1.6)

IR (Nujol®) ν/cm^{-1}: 3332 & 3242 (NH), 1498 (CN), 982 (CS_{as}), 742 (CS(Thiocarbonyl)), 652 (CS_s)

ESMS m/z: 817.2 $[M + Na^+]^+$

Elemental Analysis %:	Calculated + 2 H_2O	C	50.1	H	6.9	N	10.3
	Experimental	C	49.8	H	6.6	N	10.4

Tetraethyleneglycolditosylate 12[3]

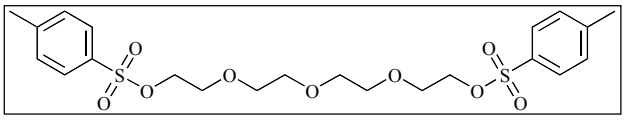

Tetraethyleneglycol (10.95g 56.0mmol) was dissolved in THF (35mL) and to this was added NaOH (14.0g, 350.0mmol) and water (35mL) and the mixture was stirred under $N_{2(g)}$. *p*-Toluenesuphonylchloride (25.0g, 131.0mmol) was dissolved in THF (35mL) and added drop wise over 30 minutes with the temperature being maintained below 5ºC. The mixture was stirred for a further 2 hours and then poured onto ice/water (100mL). The product was extracted into CH_2Cl_2 (4x50mL) and washed again with H_2O (2x100mL) followed by $NaCl_{(aq)}$ (100mL, saturated) solution and dried over $MgSO_4$. Filtration followed by solvent removal and drying in *vacuo* yielded a colourless oil.

Yield = 23.75g (72.2%)

^{1}H NMR (300MHz, $CDCl_3$) δ: 7.78 (d, ^{3}J = 8Hz, 4H, *o*-Ar*H*), 7.33 (d, ^{3}J = 8Hz, 4H, *p*-Ar*H*), 4.14 (m, 4H, SOCH_2), 3.67 (m, 4H, $SOCH_2CH_2$), 3.55 (s, 8H, OCH_2CH_2O), 2.44 (s, 6H, $ArCH_3$)

ESMS m/z: 502.5 $[M]^+$, 525.5 $[M + Na^+]^+$, 541.5 $[M + K^+]^+$

3,4-[15]Crown-5-benzaldehyde 13[4]

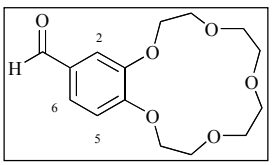

3,4-Dihydroxybezaldehyde (6.53g, 47.0mmol) and CsF (35.7g, 240.0mol) were dissolved in MeCN (300mL). Tetraethyleneglycolditosylate (23.75g, 47.0mmol) was dissolved in MeCN (500mL) and added drop wise with stirring. The mixture was stirred for 24 hours and then filtered through 0.5cm of Celite® and the solvent removed. The product was re-dissolved in $CHCl_3$ (100mL) and washed with $NaOH_{(aq)}$

(100mL, 10% w/w) and dried over $MgSO_4$. Filtration followed by solvent removal and recrystallisation from isopropyl ether yielded a cream solid, which was dried in *vacuo*.

Yield = 4.26g (30.6%)

^{1}H NMR (300MHz, $CDCl_3$) δ: 9.83 (s, 1H, *H*CO), 7.31 (d, ^{3}J = 8Hz, 1H, Ar*H*^{6}), 7.39 (s, 1H, Ar*H*^{2}), 6.94 (d, ^{3}J = 8Hz, 1H, Ar*H*^{5}), 4.21 (m, 4H, ArOC*H*$_2$), 3.93 (m, 4H, ArOCH$_2$C*H*$_2$), 3.77 (m, 8H, OC*H*$_2$C*H*$_2$OC*H*$_2$C*H*$_2$O)

ESMS m/z: 319.1 $[M + Na^+]^+$, 335.1 $[M + K^+]^+$

(3,4-[15]Crown-5)-*N*-hexyl-benzylamine 14

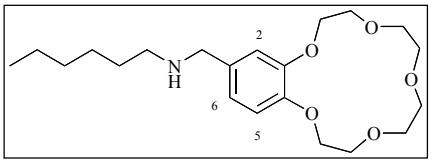

Method the same as that of **10**, except hexylamine (0.52g, 5.0mmol) and 3,4-[15]crown-5-benzaldehyde (1.00g, 5.0mmol) were used yieldeding a brown oil.

Yield = 0.52g (27.4%)

^{1}H NMR (300MHz, $CDCl_3$) δ: 6.98 (s, 1H, Ar*H*^{2}), 6.87 (s, 1H, N*H*), 6.83 (d, ^{3}J = 6Hz, 1H, Ar*H*^{6}), 6.78 (d, ^{3}J = 6Hz, 1H, Ar*H*^{5}), 4.13 (m, 4H, ArOC*H*$_2$), 3.91 (m, 4H, ArOCH$_2$C*H*$_2$), 3.75 (m, 8H, OC*H*$_2$C*H*$_2$OC*H*$_2$C*H*$_2$O), 2.61 (m, 2H, NHC*H*$_2$), 1.56 (m, 2H, NHCH$_2$C*H*$_2$), 1.28 (m, 6H, C*H*$_2$C*H*$_2$C*H*$_2$CH$_3$), 0.87 (t, ^{3}J = 7Hz, 3H, C*H*$_3$)

Receptor 15

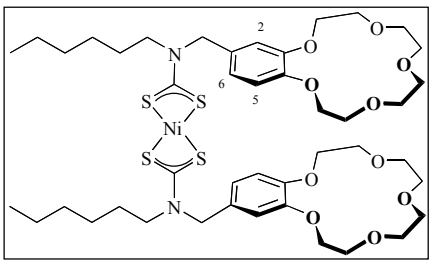

(3,4-[15]Crown-5)-*N*-hexyl-benzylamine (0.50g, 1.2mmol) was dissolved in THF:H_2O (2:1 v/v, 60mL) and TBAOH (1.0g, 3.9mmol) was added and stirred under $N_{2(g)}$ until dissolved. CS_2 (0.10g, 1.2mmol) was then added and the solution stirred for 30 minutes. $Ni(CH_3CO_2)_2{\cdot}4H_2O$ (0.16g, 0.6mmol) was added to the yellow solution and the mixture stirred for 15 hours. Filtration followed by washing with Et_2O (20mL), yielded a green powder, which was dried in *vacuo*.

Yield = 0.24g (41.2%)

^{1}H NMR (300MHz, $CDCl_3$) δ: 6.82 (br, 6H, Ar*H*), 4.70 (s, 4H, ArCH_2), 4.15 (br, 8H, ArOCH_2), 3.92 (br, 8H, $ArOCH_2CH_2$), 3.76 (br, 16H, OCH_2CH_2O), 3.42 (br, 4H, CH_2N), 1.57 (br, 4H, CH_2CH_2N), 1.24 (br, 12H, $CH_3CH_2CH_2CH_2CH_3$), 0.87 (br, 6H, CH_3)

^{13}C NMR (75.5MHz, $CDCl_3$) δ: 204.0 (CS_2), 149.7 (Ar*C*), 149.2 (Ar*C*), 127.4 (Ar*C*), 121.7 (Ar*C*), 114.8 (Ar*C*), 114.5 (Ar*C*), 71.3 (CH_2O), 70.8 (CH_2O), 69.8 (CH_2O), 69.3 (OCH_2), 51.8 ($ArCH_2N$), 48.5 (NCH_2), 31.5 (NCH_2CH_2), 26.8 ($NCH_2CH_2CH_2$), 26.5 ($NCH_2CH_2CH_2$), 22.6 ($NCH_2CH_2CH_2CH_3$), 14.2 (CH_3)

UV/visible (MeCN:DMSO 4:1) λ/nm (ε/dm^3 mol^{-1} cm^{-1}): 326 (34.8), 395 (6.0) , 424 (1.2)

IR (Nujol®) ν/cm^{-1}: 1504 (CN), 1002 (CS_{as}), 656 (CS_s)

ESMS m/z: 508.2 $[M + 2Na^+]^{2+}$, 993.4 $[M + Na^+]^+$, 1009.4 $[M + K^+]^+$

Elemental Analysis %:	Calculated	C	54.4	H	7.0	N	2.9
	Experimental	C	49.9	H	6.0	N	2.8

(3,4-[15]Crown-5)-benzylamine 16[5]

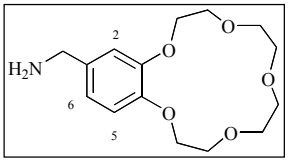

MeOH (50mL) saturated with NH_3 (see below) and Raney Ni (0.10g, excess) was placed in a stainless steel hydrogen reduction apparatus. 3,4-[15]Crown-5-benzaldehyde (1.40g, 4.7mmol) was added and heated at 50ºC with stirring. The mixture was stirred in an H_2 atmosphere (10bar) for 2 hours. Filtering through Celite® followed by solvent removal yielded a yellow oil which was dissolved in $CHCl_3$ (50mL). This was removed and the product re-dissolved and solvent removed a further three times in order to remove any residual ammonia. The product was then dissolved in $CHCl_3$ (200mL), washed with $HCl_{(aq)}$ (2x50mL, 1M), the aqueous layers collected. $NaOH_{(aq)}$ (100mL, 1M) was added, the product extracted into CH_2Cl_2 (3x75mL) and dried over $MgSO_4$. Filtration followed by solvent removal and drying in *vacuo* yielded a yellow oil.

Yield = 0.53g (38.0%).

^{1}H NMR (300MHz, $CDCl_3$) δ: 7.02 (s, 2H, N*H*$_2$), 6.87 (d, ^{3}J = 9Hz, 1H, Ar*H*^{6}), 6.80 (s, 1H, Ar*H*^{2}), 6.66 (d, ^{3}J = 9Hz, 1H, Ar*H*^{5}), 4.30 (d, ^{3}J = 5Hz, 2H, ArC*H*$_2$), 4.11 (m, 4H, ArOC*H*$_2$), 3.89 (m, 4H, ArOCH$_2$C*H*$_2$), 3.76 (m, 8H, OC*H*$_2$C*H*$_2$OC*H*$_2$C*H*$_2$O)

ESMS m/z: 320.0 $[M + Na^+]^+$

Preparation of ammonia saturated methanol: Aqueous NH_3 solution (400mL, 33%) was heated to 50ºC in a 1L flask fitted with a condenser. NH_3 vapour passed from the top of the condenser through KOH pellets, then through the MeOH (150mL) with cooling and finally through solid KOH again. This was continued until approximately 40g of NH_3 had been dissolved in the MeOH.

_N_-(3,4-[15]Crown-5-benzyl)-2-chloro-acetamide 17

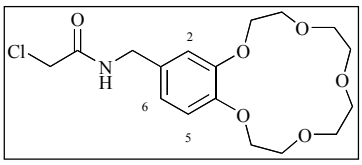

Method the same as that of **1**, except (3,4-[15]crown-5)-benzylamine (0.53g, 1.8mmol), $NaOH_{(aq)}$ (20mL, 10% w/w) and chloroacetyl chloride (0.20g, 1.8mmol) were used and stirring continued for 1 hour yielding a yellow oil.

Yield = 0.67g (quantitative)

^{1}H NMR (300MHz, $CDCl_3$) δ: 6.82 (m, 4H, CON*H,* Ar*H*^{2} & Ar*H*^{5} & Ar*H*^{6}), 4.40 (d, ^{3}J = 5Hz, 2H, ArC*H*$_2$), 4.14 (m, 4H, ArOC*H*$_2$), 4.09 (s, 2H, C*H*$_2$Cl), 3.92 (m, 4H, ArOCH$_2$C*H*$_2$), 3.75 (s, 8H, OC*H*$_2$C*H*$_2$OC*H*$_2$C*H*$_2$O)

ESMS m/z: 396.6 $[M + Na^+]^+$

_N_-(3,4-[15]Crown-5-benzyl)-2-hexylamino-acetamide 18

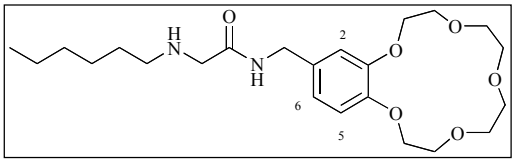

Hexylamine (10mL, excess) was heated to 40ºC and *N*-(3,4-[15]crown-5-benzyl)-2-chloro-acetamide (0.67g, 1.8mmol) dissolved in $CHCl_3$ (10mL) was added portion wise with stirring. The mixture was stirred for 12 hours. H_2O (200mL) was added and the product extracted into CH_2Cl_2 (4x50mL) and then washed again with H_2O (200mL) and

dried over K_2CO_3. Filtration followed by solvent removal and drying in *vacuo* at 40ºC yielded a yellow oil.

Yield = 0.50g (63.3%)

^{1}H NMR (300MHz, $CDCl_3$) δ: 7.55 (br, 1H, CON*H*), 6.81 (m, 3H, ArH^2 & ArH^5 & ArH^6), 4.38 (d, ^{3}J = 6Hz, 2H, ArCH_2), 4.12 (m, 6H, ArOCH_2, COCH_2), 3.90 (m, 4H, ArOCH_2CH_2), 3.76 (s, 8H, OCH_2CH_2OCH_2CH_2O) 2.58 (m, 2H, NHCH_2), 1.42 (m, 2H, NHCH_2CH_2), 1.26 (m, 12H, CH_2CH_2 CH_2CH_3), 0.87 (m, 6H, CH_3)

ESMS m/z: 461.8 $[M + Na^+]^+$, 477.8 $[M + K^+]^+$

Receptor 19

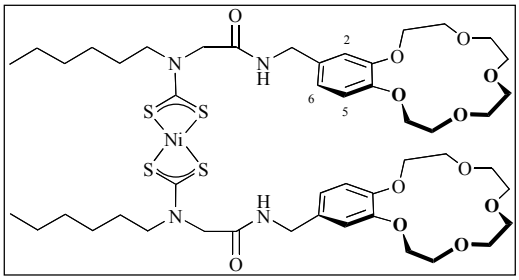

N-(3,4-[15]Crown-5-benzyl)-2-hexylamino-acetamide (0.25g, 0.6mmol) was dissolved in THF:H_2O (3:1 v/v, 60mL) and KOH (0.5g, 0.6mmol) was added and stirred under $N_{2(g)}$ until dissolved. CS_2 (0.05g, 0.6mmol) was then added and the solution stirred for 30 minutes. $Ni(CH_3CO_2)_2{\cdot}4H_2O$ (0.07g, 0.3mmol) was added to the yellow solution and the mixture stirred for 15 hours. H_2O (100mL) was added with stirring and filtration of the solid followed by washing with EtOH (5mL) and Et_2O (5mL) yielded a green powder, which was dried in *vacuo*.

Yield = 0.26g (79.8%)

^{1}H NMR (300MHz, $CDCl_3$) δ: 6.83 (m, 8H, CON*H* & ArH^2 & H^5 & H^6), 4.40 (d, ^{3}J = 4Hz, 4H, ArCH_2), 4.25 (m, 4H, COCH_2), 4.12 (m, 8H, ArOCH_2), 3.91 (m, 8H, ArOCH_2CH_2), 3.75 (s, 16H, OCH_2CH_2OCH_2CH_2O), 3.50 (m, 4H, NCH_2CH_2), 1.37 (m, 4H, NCH_2CH_2), 1.28 (m, 12H, $CH_2CH_2CH_2CH_3$), 0.88 (m, 6H, CH_3)

^{13}C NMR (75.5MHz, $CDCl_3$) δ: 207.1 (CS_2), 165.9 (*C*O), 149.2 (Ar*C*), 148.1 (Ar*C*), 132.6 (Ar*C*), 120.4 (Ar*C*), 114.4 (Ar*C*), 113.4 (Ar*C*), 70.9 & 70.5 & 69.7 & 69.3 ((OCH_2CH_2OCH_2CH_2)$_2$O), 51.7 (ArCH_2), 42.6 (NCH_2CO), ~40.0 (NCH_2CH_2), 31.5 (NCH_2CH_2), 26.8 (N$CH_2CH_2CH_2$), 26.4 (N$CH_2CH_2CH_2CH_2$), 22.6 (CH_2CH_3), 14.6 (CH_3)

UV/visible (MeCN:DMSO 4:1) λ/nm (ε/dm^3 mol^{-1} cm^{-1}): 303 (35.5), 323 (25.0) , 382 (5.2), 416 sh (1.7)

IR (Nujol®) ν/cm^{-1}: 3278 (NH), 1654 (Amide I), 1558 (Amide II), 1510 (CN), 972 (CS_{as})

ESMS m/z: 1108.6 $[M + Na^+]^+$, 1124.6 $[M + K^+]^+$

Elemental Analysis %:	Calculated + 2 H_2O	C	51.4	H	7.0	N	5.0
	Experimental	C	51.4	H	7.5	N	4.4

Receptor 20

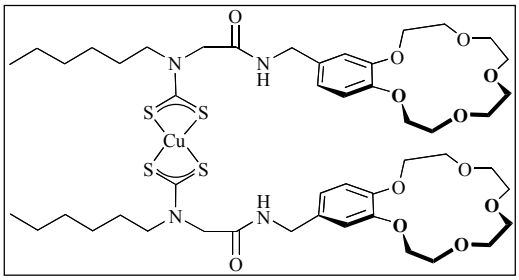

Method the same as that of **19**, except *N*-(3,4-[15]crown-5-benzyl)-2-hexylamino-acetamide (0.25g, 0.6mmol), KOH (0.5g, 0.6mmol), CS_2 (0.05g, 0.6mmol) and $Cu(CH_3CO_2)_2{\cdot}H_2O$ (0.06g, 0.3mmol) were used yieldeding a brown powder.

Yield = 0.18g (55.1%)

UV/visible (MeCN:DMSO 4:1) λ/nm (ε/dm^3 mol^{-1} cm^{-1}): 274 (40.0), 288 sh (28.8), 439 (9.9)

IR (Nujol®) ν/cm^{-1}: 3282 (NH), 1658 (Amide I), 1554 (Amide II), 1510 (CN), 982 (CS_{as}), 654(CS_s)

ESMS m/z: 1112.2 $[M + Na^+]^+$, 1128.2 $[M + K^+]^+$

Elemental Analysis %:	Calculated + 2 H_2O	C	51.2	H	7.0	N	5.0
	Experimental	C	51.0	H	7.0	N	4.4

(3-Aminomethyl-benzyl)-carbamic acid *tert*-butyl ester 21[2]

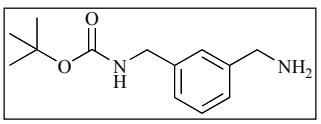

Method the same as that of **6**, except di-*tert*-butoxy carbonyl (2.45g, 11.0mmol) in 1,4-dioxane (30mL) and *m*-xylene diamine (6.12g, 45.0mmol) in 1,4-dioxane (30mL) were used and the combined organic fractions were washed with H_2O (6x50mL) yielding a yellow oil.

Yield = 1.63g (61.4%)

^{1}H NMR (300MHz, $CDCl_3$) δ: 7.35-7.13 (m, 4H, Ar*H*), 4.90 (br, 1H, CON*H*), 4.29 (d, ^{3}J = 5Hz, CH_2NHCO), 3.84 (s, 2H, CH_2NH$_2$), 1.44 (s, 9H, (CH_3)$_3$)

ESMS m/z: 164.2 $[M - OC(CH_3) + H^+]^+$

[3-(3-Hexyl-thioureidomethly)-benzyl]-carbamic acid *tert*-butyl ester 22

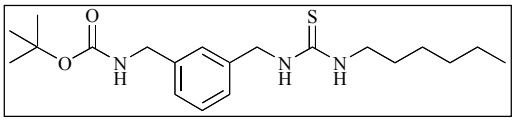

(3-Aminomethyl-benzyl)-carbamic acid *tert*-butyl ester (1.05g, 4.4mmol) was dissolved in CH_2Cl_2 (100mL) and to this was added hexyl isothiocyanate (0.67g, 4.5mmol) and the mixture was refluxed for 1 hour. H_2O (100mL) was added and the product extracted into CH_2Cl_2 (4x50mL) and dried over K_2CO_3. Filtration followed by solvent removal and drying in *vacuo* yielded a yellow crystalline solid.

Yield = 1.68g (95.0%)

^{1}H NMR (300MHz, $CDCl_3$) δ: 7.30 - 7.10 (m, 4H, Ar*H*), 6.40 (br, 1H, ArCH$_2$N*H*CS), 6.19 (br, 1H, NHCSN*H*), 5.07 (br, 1H, CON*H*), 4.64 (d, ^{3}J = 5, 2H, ArCH_2NHCS), 4.21 (d, ^{3}J = 6Hz, 2H, ArCH_2NHCO), 3.36 (br, 2H, NCH_2CH$_2$), 1.94 (m, 2H, NCH$_2$CH_2), 1.42 (s, 9H, (CH_3)$_3$), 1.26 (m, 6H, CH_2CH_2CH_2CH$_3$), 0.86 (m, 3H, CH_3)

[3-(3-Benzyl-thioureidomethyl)-benzyl]-carbamic acid *tert*-butyl ester 23

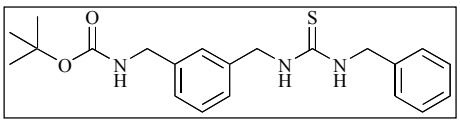

Method the same as that of **22**, except (3-aminomethyl-benzyl)-carbamic acid *tert*-butyl ester (1.05g, 4.4mmol) and benzyl isothiocyanate (0.67g, 4.5mmol) were used, which yielded a yellow crystalline solid.

Yield = 1.51g (88.0%)

^{1}H NMR (300MHz, $CDCl_3$) δ: 7.40 - 7.00 (m, 10H, Ar*H* & ArCH$_2$N*H*CO), 6.44 (br, 2H, ArCH$_2$N*H*CSN*H*), 4.55 (br, 4H, ArCH_2NHCSNHCH_2), 4.07 (d, ^{3}J = 6Hz, 2H, ArCH_2NHCO), 1.32 (s, 9H, (CH_3)$_3$)

1-(3-Aminomethyl-bezyl)-3-hexyl-thiourea 24

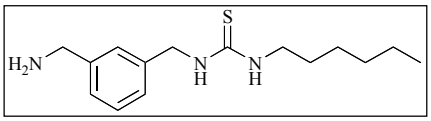

Method the same as that of **9**, except [3-(3-hexyl-thioureidomethly)-benzyl]-carbamic acid *tert*-butyl ester (1.01g, 2.6mmol) was used which yielded a pale yellow oil.

Yield = 0.84g (Quantitative)

^{1}H NMR (300MHz, $CDCl_3$) δ: 7.30 - 7.0(m, 4H, Ar*H*), 6.29 (br, 1H, $ArCH_2NHCS$), 6.03 (br, 1H, $ArCH_2NHCSNH$), 4.65 (br, 2H, $ArCH_2NHCS$), 3.82 (s, 2H, $ArCH_2NH_2$), 3.35 (br, 2H, NCH_2CH_2), 1.52 (m, 2H, NCH_2CH_2), 1.25 (m, 6H, $CH_2CH_2CH_2CH_3$), 0.86 (m, 3H, CH_3)

1-(3-Aminomethyl-benzyl)-3-benzyl-thiourea 25

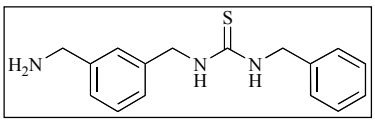

Method the same as that of **9**, except **[**3-(3-benzyl-thioureidomethly)-benzyl]-carbamic acid *tert*-butyl ester (1.01g, 2.6mmol) was used which yielded a pale yellow oil.

Yield = 0.84g (Quantitative)

^{1}H NMR (300MHz, $CDCl_3$) δ: 7.30 - 7.00 (m, 9H, Ar*H*), 6.32 (br, 2H, $NHCSNH$), 4.60 (br, 4H, $CH_2NHCSNHCH_2$), 4.17 (m, 2H, $ArCH_2NH_2$)

1-Hexyl-3-(3-hexylaminomethyl-benzyl)-thiourea 26

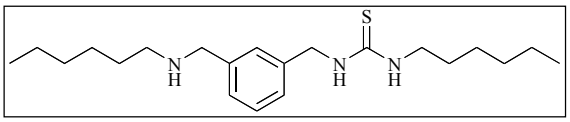

Method the same as that of **10**, except 1-(3-aminomethyl-benzyl)-3-hexyl-thiourea (1.90g, 7.0mmol) and hexanal (0.71g, 7.0mmol) were used, which yielded a colourless oil.

Yield = 2.54g (91.0%)

^{1}H NMR (300MHz, $CDCl_3$) δ: 7.40 - 7.00 (m, 4H, Ar*H*), 6.19 (br, 1H, $ArCH_2NHCS$), 5.98 (br, 1H, $NHCSNH$), 4.83 (br, 1H, $ArCH_2NH$), 4.65 (br, 2H, $ArCH_2NHCS$), 3.69 (s, 2H, $ArCH_2NH_2$), 3.35 (m, 2H, $SCNHCH_2CH_2$), 2.60 (m, 2H, $CH_2NHCH_2CH_2$), 2.03 (m, 2H, $SCNHCH_2CH_2CH_2$), 1.52 (m, 2H, NCH_2CH_2), 1.28 (m, 6H, $CH_2CH_2CH_2CH_3$), 1.25 (m, 6H, $CH_2CH_2CH_2CH_3$), 0.86 (m, 6H, CH_3)

1-Benzyl-3-(3-hexylaminomethyl-benzyl)-thiourea 27

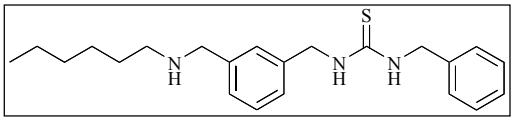

Method the same as that of **10**, except 1-(3-aminomethyl-bezyl)-3-benzyl-thiourea (1.90g, 7.0mmol) and hexanal (0.71g, 7.0mmol) were used, which yielded a colourless oil.

Yield = 2.50 (Quantitative)

^{1}H NMR (300MHz, $CDCl_3$) δ: 7.40 - 7.00 (m, 9H, Ar*H*,), 6.28 (br, 2H, $ArCH_2NHCSNH$), 4.60 (br, 4H, $CH_2NHCSNHCH_2$), 4.25 (m, 2H, $ArCH_2NHCH_2$), 2.58 (m, 2H, $NHCH_2CH_2$) 1.42 (m, 2H, $NHCH_2CH_2$), 1.25 (m, 6H, $CH_2CH_2CH_2CH_3$), 0.89 (3H, m, CH_3)

2-Chloro-*N*-[2-(2-chloro-acetylamino)-ethyl]-acetamide 33

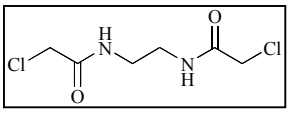

Ethylenediamine (0.60g, 10.0mmol) was dissolved in $CHCl_3$ (50mL) and to this was added $NaOH_{(aq)}$ (20mL, 40% w/w, excess). Chloroacetyl chloride (2.26g, 20.0mmol) was dissolved in $CHCl_3$ (50mL) and added drop wise to the mixture with stirring. After 15 minutes the solid was filtered off and washed with Et_2O (20mL). Drying in *vacuo* yielded a white solid.

Yield = 1.77g (83.1%)

^{1}H NMR (300MHz, DMSO-d_6) δ: 8.27 (br, 2H, N*H*), 4.02 (s, 4H, CH_2Cl), 3.15 (d, ^{3}J = 2Hz, 4H, CH_2NH)

ESMS m/z: 213.1 $[M + H^+]^+$

2-Chloro-*N*-[3-(2-chloro-acetylamino)-2,2-dimethyl-propyl]-acetamide 34

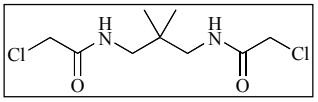

Method the same as that of **33**, except 1,3-diamino-2,2-dimethyl propane (2.04g, 20.0mmol) and chloroacetyl chloride (4.52g, 40.0mmol) were used, which yielded a white solid.

Yield = 4.24g (83.0%)

^{1}H NMR (300MHz, DMSO-d_6) δ: 7.44 (br, 2H, N*H*), 4.10 (s, 4H, CH_2Cl), 3.09 (d, ^{3}J = 7Hz, 4H, CH_2NH), 0.93 (s, 6H, CH_3)

ESMS m/z: 277.1 $[M + Na^+]^+$

2-Chloro-*N*-[2-(2-chloro-acetylamino)-phenyl]-acetamide 35

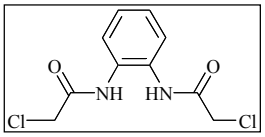

Method the same as that of **33**, except 1,2-phenyldiamine (2.16g, 20.0mmol), chloroacetyl chloride (4.52g, 40.0mmol) and KOH (2.36g, 40.0mmol) in H_2O (20mL) were used, which yielded a pink solid.

Yield = 5.12g (98.1%)

^{1}H NMR (300MHz, DMSO-d_6) δ: 8.67 (br, 2H, N*H*), 7.52 (d of d, ^{3}J = 6Hz, ^{4}J = 3Hz, 2H, Ar*H*), 7.32 (d of d, ^{3}J = 6Hz, ^{4}J = 3Hz, 2H, Ar*H*), 4.24 (s, 4H, CH_2Cl)

ESMS m/z: 283.1 $[M + Na^+]^+$

2-Chloro-*N*-[3-(2-chloro-acetylamino)-phenyl]-acetamide 36

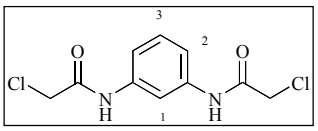

Chloroacetyl chloride (9.03g, 80.0mmol) was dissolved in $CHCl_3$ (50mL). 1,3-Phenyldiamine (1.08g, 10.0mmol) and NEt_3 (2.03g, 20.0mmol) were dissolved in $CHCl_3$ (50mL) and added drop wise to the mixture with stirring. After 15 minutes the solid was filtered off and washed with Et_2O (20mL). Drying in *vacuo* yielded a white solid.

Yield = 2.61g (99.9%)

^{1}H NMR (300MHz, DMSO-d_6) δ: 10.39 (s, 2H, N*H*), 7.92 (s, 1H, ArH^1), 7.32-7.27 (m, 3H, ArH^2 & ArH^3), 4.23 (s, 4H, CH_2Cl)

ESMS m/z: 283.0 $[M + Na^+]^+$

2-Chloro-*N*-[4-(2-chloro-acetylamino)-phenyl]-acetamide 37

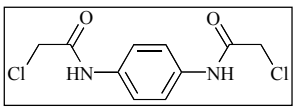

Method the same as that of **33**, except 1,4-phenyldiamine (2.16g, 20.0mmol), chloroacetyl chloride (4.52g, 40mmol) and KOH (2.36g, 40mmol) in H_2O (20mL) were used, which yielded a purple solid.

Yield = 5.00g (96.7%)

^{1}H NMR (300MHz, DMSO-d_6) δ: 10.31 (s, 2H, N*H*), 7.53 (s, 4H, Ar*H*), 4.22 (s, 4H, CH_2Cl)

ESMS m/z: 283.1 $[M + Na^+]^+$

2-Hexylamino-*N*-[2-(2-hexylamino-acetylamino)-ethyl]-acetamide 38

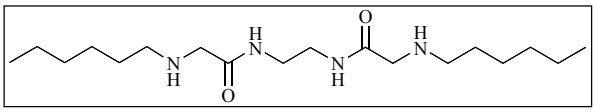

Hexylamine (10mL, excess) was heated to 40ºC and 2-chloro-*N*-[2-(2-chloro-acetylamino)-ethyl]-acetamide (1.77g, 8.3mmol) was added portion wise with stirring. The mixture was stirred for 12 hours. H_2O (200mL) was added and the product extracted into CH_2Cl_2 (4x50mL) and then washed again with H_2O (200mL) and dried over K_2CO_3. Filtration followed by solvent removal and heating at 40ºC in *vacuo* yielded a white solid.

Yield = 1.68g (59.2%)

^{1}H NMR (300MHz, $CDCl_3$) δ: 7.56 (br, 2H, CON*H*), 3.42 (t, ^{3}J = 3Hz, 4H, CONHCH_2), 3.24 (s, 4H, COCH_2), 2.57 (t, ^{3}J = 7Hz, 4H, NHCH_2CH$_2$), 1.44 (m, 4H, NHCH$_2$CH_2), 1.29 (m, 12H, CH_2CH_2CH_2CH$_3$), 0.89 (t, ^{3}J = 7Hz, 6H, CH_3)

ESMS m/z: 343.3 $[M + H^+]^+$

2-Hexylamino-*N*-[3-(2-chloro-acetylamino)-2,2-dimethyl-propyl]-acetamide 39

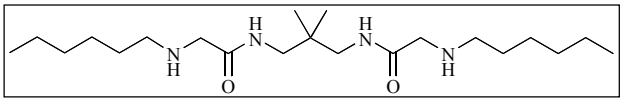

Method the same as that of **38**, except 2-chloro-*N*-[3-(2-chloro-acetylamino)-2,2-dimethyl-propyl]-acetamide (4.24g, 16.6mmol) was used which yielded a yellow oil.

Yield = 4.14g (65.0%)

^{1}H NMR (300MHz, $CDCl_3$) δ: 7.85 (t, ^{3}J = 7Hz, 2H, CON*H*), 3.28 (s, 4H, CONHCH_2), 3.03 (d, ^{3}J = 7Hz, 4H, COCH_2), 2.59 (t, ^{3}J = 8Hz, 4H, NHCH_2CH$_2$), 1.47 (m, 4H, NHCH$_2$CH_2), 1.28 (m, 12H, CH_2CH_2CH_2CH$_3$), 0.87 (t, ^{3}J = 7Hz, 6H, CH_3)

ESMS m/z: 385.5 $[M + H^+]^+$

2-Hexylamino-*N*-[2-(2-chloro-acetylamino)-phenyl]-acetamide 40

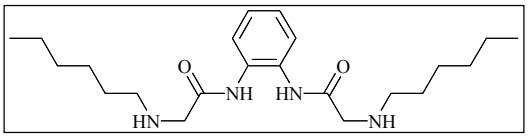

Method the same as that of **38**, except 2-chloro-*N*-[2-(2-chloro-acetylamino)-phenyl]-acetamide (4.24g, 16.6mmol) was used, which yielded a yellow oil.

Yield = 2.83g (63.0%)

^{1}H NMR (300MHz, $CDCl_3$) δ: 9.42 (t, ^{3}J = 7Hz, 2H, CON*H*), 7.60 (d of d, ^{3}J = 6Hz, ^{4}J = 4Hz, 2H, Ar*H*), 7.17 (d of d, ^{3}J = 6Hz, ^{4}J = 4Hz, 2H, Ar*H*), 3.39 (s, 4H, COCH_2), 2.64 (t, ^{3}J = 8Hz, 4H, NHCH_2CH$_2$), 1.49 (m, 4H, NHCH$_2$CH_2), 1.29 (m, 12H, CH_2CH_2CH_2CH$_3$), 0.87 (t, ^{3}J = 7Hz, 6H, CH_3)

ESMS m/z: 391.4 $[M + H^+]^+$

2-Hexylamino-*N*-[3-(2-chloro-acetylamino)-phenyl]-acetamide 41

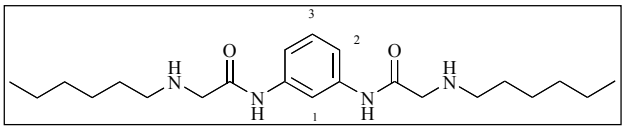

Method the same as that of **38**, except 2-chloro-*N*-[3-(2-chloro-acetylamino)-2,2-dimethyl-propyl]-acetamide (2.61g, 10.0mmol) was used which yielded a yellow oil.

Yield = 1.68g (43.0%)

^{1}H NMR (300MHz, $CDCl_3$) δ: 9.40 (s, 2H, CON*H*), 7.87 (s, 1H, ArH^1), 7.37-7.26 (m, 3H, ArH^2 & ArH^3), 3.37 (s, 4H, COCH_2), 2.66 (t, ^{3}J = 7Hz, 4H, NHCH_2CH$_2$), 1.52 (m, 4H, NHCH$_2$CH_2), 1.31 (m, 12H, CH_2CH_2CH_2CH$_3$), 0.89 (t, ^{3}J = 7Hz, 6H, CH_3)

ESMS m/z: 391.4 $[M + H^+]^+$

2-Hexylamino-*N*-[3-(2-chloro-acetylamino)-phenyl]-acetamide 42

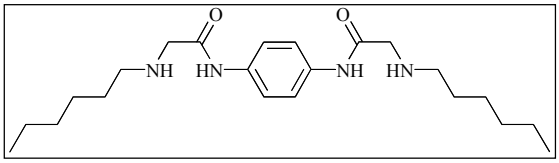

Hexylamine (10mL, excess) was added to DMF (10mL) and heated to 40ºC and 2-chloro-*N*-[4-(2-chloro-acetylamino)-2,2-dimethyl-propyl]-

acetamide (5.00g, 19.2mmol) was added portion wise with stirring. The mixture was stirred for 12 hours. H_2O (200mL) and CH_2Cl_2 (50mL) were added and the product filtered off and washed with Et_2O (20mL), yielding a white solid.

Yield = 2.85g (38.0%)

^{1}H NMR (300MHz, DMSO-d_6) δ: 10.80 (s, 2H, CON*H*), 7.56 (s, 4H, Ar*H*), 3.89 (s, 4H, COCH_2), 2.92 (t, ^{3}J = 8Hz, 4H, NHCH_2CH$_2$), 1.61 (m, 4H, NHCH$_2$CH_2), 1.25 (m, 12H, CH_2CH_2CH_2CH$_3$), 0.89 (t, ^{3}J = 7Hz, 6H, CH_3)

ESMS m/z: 391.5 $[M + H^+]^+$

Receptor 43

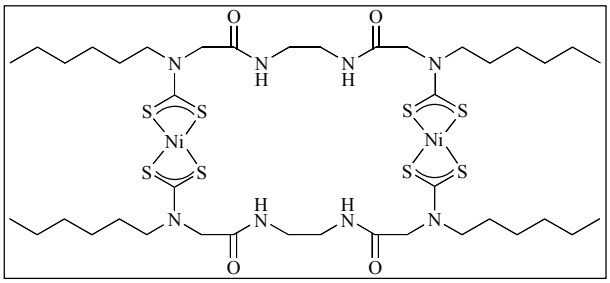

2-Hexylamino-*N*-[2-(2-hexylamino-acetylamino)-ethyl]-acetamide (0.56g, 1.6mmol) was dissolved in THF:H_2O (2:1 v/v, 30mL) and KOH (0.18g, 3.2mmol) was added and stirred under $N_{2(g)}$ until dissolved. CS_2 (0.24g, 3.2mmol) was then added and the solution stirred for 30 minutes. Ni$(CH_3CO_2)_2$·4H_2O (0.41g, 1.6mmol) was added to the yellow solution and the mixture stirred for 15 hours. H_2O (100mL) was added with stirring, filtration followed by recrystallisation from DMSO/Et_2O followed by filtering and washing with EtOH (20mL) and Et_2O (20mL) yielded a light green powder which was dried in *vacuo*.

Yield = 0.63g (71.6%)

^{1}H NMR (300MHz, DMSO-d_6) δ: 8.06 & 7.91 (br, 2x2H, CON*H*), 4.27 & 4.18 (br, 2x4H, COCH_2), 3.55 (br, 8H, CONHCH_2), 3.12 (br, 8H, NHCH_2CH$_2$), 1.61 (br, 8H, NHCH$_2$CH_2), 1.26 (m, 24H, CH_2CH_2CH_2CH$_3$), 0.85 (br, 12H, CH_3)

^{13}C NMR (75.5MHz, DMSO-d_6) δ: 207.4 (*C*S$_2$), 166.0 (*C*O), 57.5 & 57.3 (*C*H$_2$CO), 39.0 (*C*H$_2$), 31.6 (*C*H$_2$), 26.8 (*C*H$_2$), 26.5 (*C*H$_2$), 22.7 (*C*H$_2$), 14.6 (*C*H$_3$)

UV/visible (MeCN:DMSO 4:1) λ/nm (ε/dm^3 mol^{-1} cm^{-1}): 324 (16.0), 387 (2.8), 423 sh (0.8)

IR (Nujol®) ν/cm^{-1}: 3284 (NH), 1662 (Amide I), 1530 (Amide II), 1488 (CN), 962 (CS_{as}), 660 (CS_s)

ESMS m/z: 1141.4 $[M + K^+]^+$, 1101.3 $[M - H^+]^-$

Elemental Analysis %:	Calculated + H_2O	C	42.9	H	6.7	N	10.0
	Experimental	C	43.1	H	8.5	N	10.2

Receptor 44

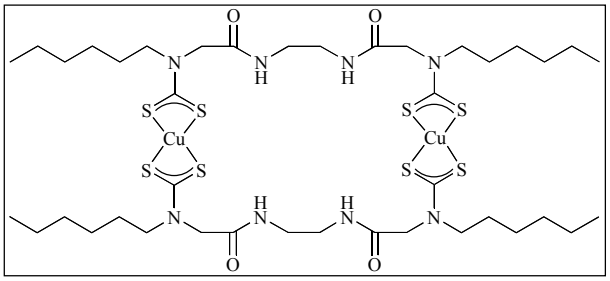

Method the same as that of **43**, except $Cu(CH_3CO_2)_2{\cdot}H_2O$ (0.32g, 1.6mmol) was used, which yielded a brown powder.

Yield = 0.45g (50.1%)

UV/visible (MeCN:DMSO 4:1) λ/nm (ε/dm^3 mol^{-1} cm^{-1}): 274 (48.3), 443 (13.7)

IR (Nujol®) ν/cm^{-1}: 3266 (NH), 1650 (Amide I), 1552 (Amide II), 1482 (CN), 956 (CS_{as}), 648 (CS_s)

ESMS m/z: 1112.4 $[M + K^+]^+$, 1111.2 $[M - H^+]^-$

Elemental Analysis %:	Calculated	C	41.8	H	6.7	N	9.8
	Experimental	C	42.3	H	5.9	N	9.6

Receptor 45

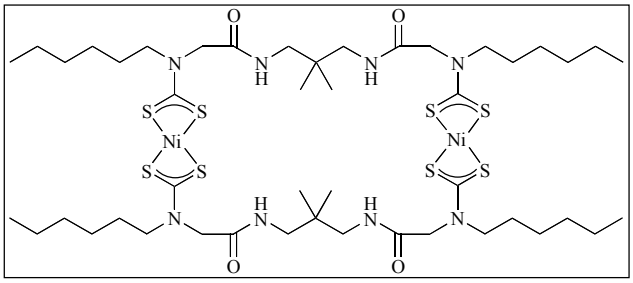

Method the same as that of **43**, except that 2-hexylamino-*N*-[3-(2-chloro-acetylamino)-2,2-dimethyl-propyl]-acetamide (1.38g, 3.6mmol), KOH (0.41g, 7.3mmol), CS_2 (0.55g, 7.3mmol) and $Ni(CH_3CO_2)_2{\cdot}4H_2O$ (0.89g, 3.6mmol) were used. H_2O (100mL) was added with stirring, filtration of the solid followed by washing with EtOH (20mL) and Et_2O (20mL) yielded a light green powder which was dried in *vacuo*.

Yield = 0.51g (23.9%)

^{1}H NMR (300MHz, DMSO-d_6) δ: 7.99 (br, 4H, CON*H*), 4.25 (br, 8H, COCH_2), 3.56 (br, 8H, CONHCH_2), 2.89 (br, 8H, NHCH_2CH$_2$), 1.56 (br, 8H, NHCH$_2$CH_2), 1.24 (m, 24H, CH_2CH_2CH_2CH$_3$), 0.84 (br, 12H, CH_3), 0.76 (br, 12H, CCH_3)

^{13}C NMR (75.5MHz, DMSO-d_6) δ: 207.3 (*C*S$_2$), 166.3 (*C*O), 51.6 (*C*H$_2$CO), 46.7 (*C*H$_2$CO), ~40 (*C*H$_2$), 37.2 (*C*(CH$_3$)$_2$), 31.6 (*C*H$_2$), 26.8 (*C*H$_2$), 26.4 (*C*H$_2$), 23.9 (C*C*H$_3$), 22.7 (*C*H$_2$), 14.6 (*C*H$_3$)

UV/visible (MeCN:DMSO 4:1) λ/nm (ε/dm^3 mol^{-1} cm^{-1}): 322 (68.7), 388 (12.6), 422 sh (4.5)

IR (Nujol®) ν/cm^{-1}: 3280 (NH), 3176 (NH), 1674 (Amide I), 1536 (Amide II), 1484 (CN), 956 (CS$_{as}$), 644 (CS$_s$)

ESMS m/z: 1204.7 [M + H_2O]$^+$

Elemental Analysis %:	Calculated	C	46.5	H	7.1	N	9.4
	Experimental	C	46.3	H	6.9	N	9.0

Receptor 46

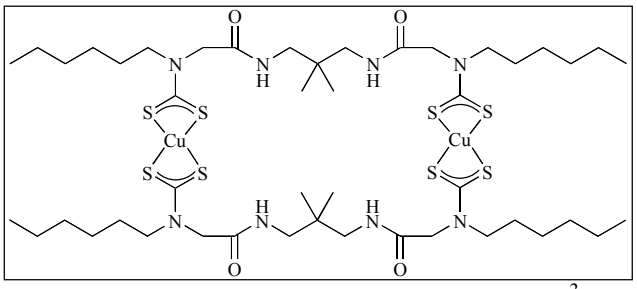

Method the same as that of **45**, except Cu(CH$_3$CO$_2$)$_2$·H$_2$O (0.72g, 3.6mmol) was used which yielded a brown powder.

Yield = 1.10g (51.3%)

UV/visible (MeCN:DMSO 4:1) λ/nm (ε/dm^3 mol^{-1} cm^{-1}): 272 (48.2), 291 sh (36.4), 439 (11.3)

IR (Nujol®) ν/cm^{-1}: 3288 (NH), 3174 (NH), 1650 (Amide I), 1534 (Amide II), 1460 (CN), 944 (CS$_{as}$), 650 (CS$_s$)

ESMS m/z: 1219.3 [M + Na$^+$]$^+$, 1235.4 [M + K$^+$]$^+$

Elemental Analysis %:	Calculated + 4 H_2O	C	43.5	H	7.3	N	8.8
	Experimental	C	43.6	H	7.1	N	8.9

Receptor 47

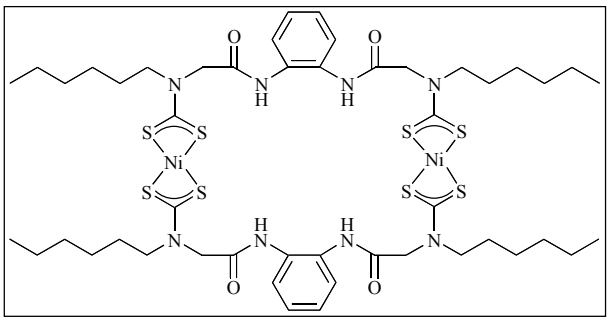

Method the same as that of **45**, except 2-hexylamino-*N*-[2-(2-chloro-acetylamino)-phenyl]-acetamide (0.94g, 2.4mmol), KOH (0.27g, 4.8mmol), CS_2 (0.37g, 4.8mmol) and $Ni(CH_3CO_2)_2{\cdot}4H_2O$ (0.59g, 2.4mmol) were used which yielded a green powder.

Yield = 0.99g (68.6%)

^{1}H NMR (300MHz, DMSO-d_6) δ: 9.40 (br, 4H, CON*H*), 7.42 (br, 4H, Ar*H*), 7.22 (br, 4H, Ar*H*), 4.70 & 4.47 (br, 2x4H, COCH_2), 3.37 (br, 8H, NHCH_2CH$_2$), 1.75 & 1.63 (br, 8H, NHCH$_2$CH_2), 1.27 (m, 24H, CH_2CH_2CH_2CH$_3$), 0.84 (br, 12H, CH_3)

^{13}C NMR (75.5MHz, DMSO-d_6) δ: 207.8 (*C*S$_2$), 165.0 (*C*O), 130.8 (Ar*C*), 126.3 (Ar*C*), 125.7 (Ar*C*), 52.2 & 51.5 (*C*H$_2$CO), ~40 (*C*H$_2$), 31.6 (*C*H$_2$), 27.0 (*C*H$_2$), 26.5 (*C*H$_2$), 22.8 (*C*H$_2$), 14.6 (*C*H$_3$)

UV/visible (MeCN:DMSO 4:1) λ/nm (ε/dm^3 mol^{-1} cm^{-1}): 323 (53.8), 383 (10.6), 425 sh (4.0)

IR (Nujol®) ν/cm^{-1}: 3252 (NH), 1678 (Amide I), 1537 (Amide II), 1500 (CN), 962 (CS$_{as}$)

ESMS m/z: 1237.6 [M + K$^+$]$^+$, 1197.2 [M - H$^+$]$^-$

Elemental Analysis %:							
	Calculated	C	48.1	H	6.1	N	9.4
	Experimental	C	48.2	H	6.1	N	9.4

Receptor 48

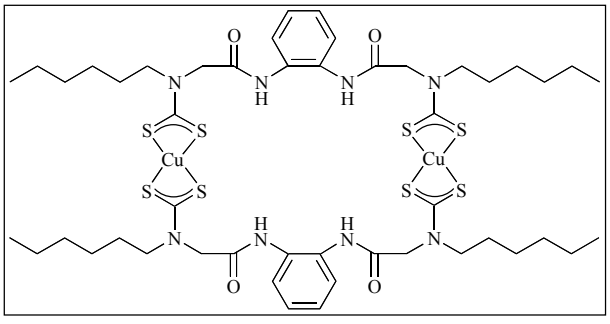

Method the same as that of **47**, except $Cu(CH_3CO_2)_2{\cdot}H_2O$ (0.48g, 2.4mmol) was used, which yielded a brown powder.

Yield = 1.18g (81.3%)

UV/visible (MeCN:DMSO 4:1) λ/nm (ε/dm^3 mol^{-1} cm^{-1}): 272 (42.0), 443 (8.8)

IR (Nujol®) ν/cm^{-1}: 3224 (NH), 1664 (Amide I), 1532 (Amide II), 1486 (CN), 960 (CS_{as}), 648 (CS_s)

ESMS m/z: 1231.3 $[M + Na^+]^+$, 1247.3$[M + K^+]^+$

Elemental Analysis %: Calculated C 48.0 H 6.0 N 9.3

Experimental C 48.0 H 6.0 N 9.4

Receptor 49

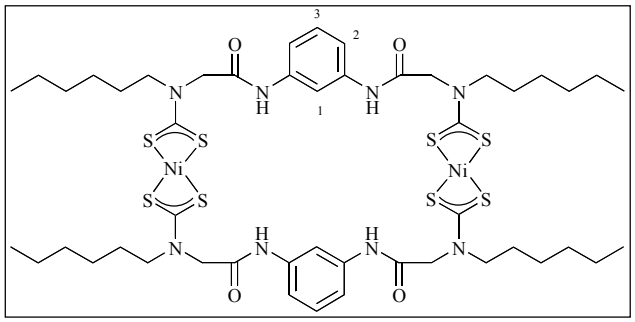

Method the same as that of **45**, except 2-hexylamino-*N*-[3-(2-chloro-acetylamino)-phenyl]-acetamide (0.56g, 1.4mmol), KOH (0.16g, 2.8mmol), CS_2 (0.22g, 2.8mmol) and $Ni(CH_3CO_2)_2{\cdot}4H_2O$ (0.36g, 1.4mmol) were used which yielded a green powder.

Yield = 0.65g (75.6%)

^{1}H NMR (300MHz, DMSO-d_6) δ: 10.2 (br, 4H, CON*H*), 7.98 & 7.86 (br, 2x1H, ArH^1), 7.23 & 7.19 (br, 2x3H, ArH^2 & ArH^3), 4.41 & 4.37 (br, 2x4H, COCH_2), 3.57 (br, 8H, NHCH_2CH$_2$), 1.59 (br, 8H, NHCH$_2$CH_2), 1.24 (m, 24H, CH_2CH_2CH_2CH$_3$), 0.84 (br, 12H, CH_3)

^{13}C NMR (75.5MHz, DMSO-d_6) δ: 207.5 (*C*S_2), 164.7 (*C*O), 139.6 (Ar*C*), 129.9 (Ar*C*), 115.0 (Ar*C*), 115.0 (Ar*C*), 52.2 & 51.7 (*C*H$_2$CO), 39.4 (*C*H$_2$), 31.5 (*C*H$_2$), 26.9 (*C*H$_2$), 26.4 (*C*H$_2$), 22.6 (*C*H$_2$), 14.6 (*C*H$_3$)

UV/visible (MeCN:DMSO 4:1) λ/nm (ε/dm^3 mol^{-1} cm^{-1}): 322 (72.7), 386 (13.6), 422 sh (5.6)

IR (Nujol®) ν/cm^{-1}: 3248 (NH), 1668 (Amide I), 1538 (Amide II), 1486 (CN), 958 (CS_{as}), 650 (CS_s)

ESMS m/z: 1237.5 $[M + K^+]^+$

Elemental Analysis %: Calculated C 48.1 H 6.1 N 9.4

Experimental C 48.2 H 6.0 N 9.0

Receptor 50

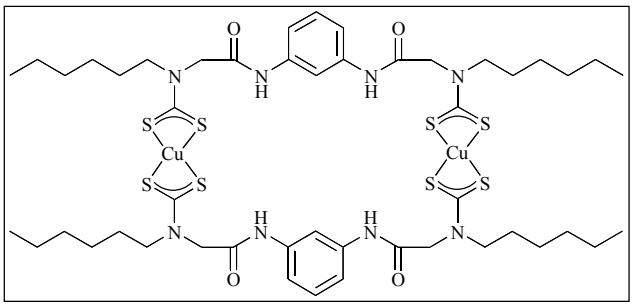

Method the same as that of **49**, except $Cu(CH_3CO_2)_2 \cdot H_2O$ (0.29g, 1.4mmol) was used which yielded a brown powder.

Yield = 0.66g (76.2%)

UV/visible (MeCN:DMSO 4:1) λ/nm (ε/dm^3 mol^{-1} cm^{-1}): 270 (64.8), 286 sh (38.8), 438 (17.8)

ESMS m/z: 1207.2 $[M + H^+]^+$

IR (Nujol®) ν/cm^{-1}: 3282 (NH), 1698 (Amide I), 1536 (Amide II), 1484 (CN), 958 (CS_{as}), 650 (CS_s)

Elemental Analysis %:							
	Calculated	C	47.7	H	6.0	N	9.3
	Experimental	C	48.3	H	5.3	N	9.0

Receptor 51

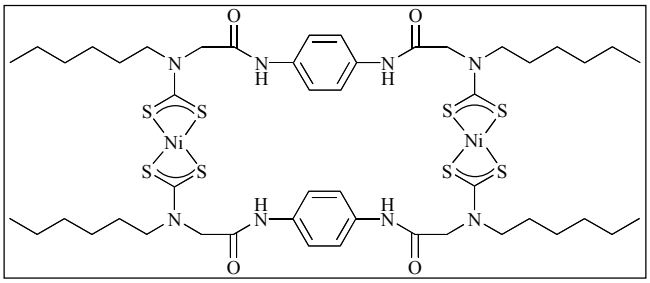

Method the same as that of **45**, except 2-hexylamino-*N*-[4-(2-chloro-acetylamino)-phenyl]-acetamide (0.95g, 2.4mmol), KOH (0.16g, 2.8mmol), CS_2 (0.22g, 2.8mmol) and $Ni(CH_3CO_2)_2 \cdot 4H_2O$ (0.61g, 2.4mmol) were used, which yielded a green powder.

Yield = 0.41g (28.1%)

^{1}H NMR (300MHz, DMSO-d_6) δ: 10.16 (br, 4H, CON*H*), 7.53 (br, 8H, Ar*H*), 4.39 (br, 8H, COCH_2), 3.66 (br, 8H, NHC$H_2$$CH_2$), 1.65 (br, 8H, NHCH$_2CH_2$), 1.31 (m, 24H, C$H_2CH_2CH_2$$CH_3$), 0.91 (br, 12H, C$H_3$)

^{13}C NMR (75.5MHz, DMSO-d_6) δ: 207.4 (*C*S_2), 164.4 (*C*O), 134.9 (Ar*C*), 120.2 (Ar*C*), 119.9 (Ar*C*), 53.2 & 52.7 & 52.5 & 52.0 (*C*H_2CO), ~40 (*C*H_2), 31.5 (*C*H_2), 26.8 (*C*H_2), 26.3 (*C*H_2), 22.6 (*C*H_2), 14.5 (*C*H_3)

UV/visible (MeCN:DMSO 4:1) λ/nm (ε/dm^3 mol^{-1} cm^{-1}): 323 (53.5), 388 (9.1), 427 sh (2.6)

IR (Nujol®) ν/cm^{-1}: 3264 (NH), 1660 (Amide I), 1554 (Amide II), 1488 (CN), 958 (CS_{as}), 649 (CS_s)

ESMS m/z: 1237.7 $[M + K^+]^+$

Elemental Analysis %:	Calculated + 4 H_2O	C	45.4	H	6.1	N	8.5
	Experimental	C	45.6	H	6.1	N	8.3

Receptor 52

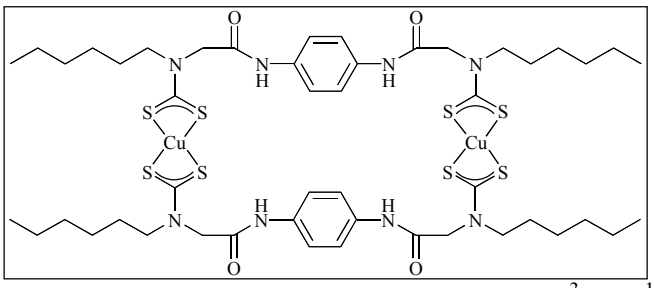

Method the same as that of **51**, except $Cu(CH_3CO_2)_2{\cdot}H_2O$ (0.48g, 2.4mmol) was used which yielded a brown powder.

Yield = 0.35g (20.7%)

UV/visible (MeCN:DMSO 4:1) λ/nm (ε/dm^3 mol^{-1} cm^{-1}): 270 (64.8), 286 sh (38.8), 438 (17.8)

IR (Nujol®) ν/cm^{-1}: 3252 (NH), 1678 (Amide I), 1558 (Amide II), 1494 (CN), 946 (CS_{as}), 646 (CS_s)

ESMS m/z: 1247.7 $[M + K^+]^+$

Receptor 53

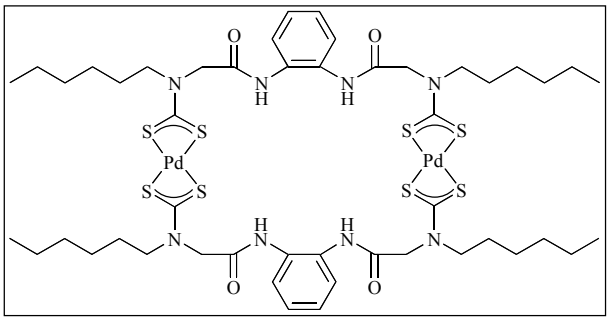

47 (0.5g, 0.4mmol) was dissolved in THF:H_2O (10:1 v/v, 110mL) and K_2PdCl_4 (0.26g, 0.8mmol) was added portion wise. The mixture was stirred for 10 minutes $N_{2(g)}$. H_2O (100mL) was added and the product extracted into CH_2Cl_2 (6x50mL) and dried over $MgSO_4$. Filtration followed by solvent removal yielded an orange solid, which was dried in *vacuo*.

Yield = 0.40g (77.0%)

^{1}H NMR (300MHz, DMSO-d_6) δ: 8.29 (s, 4H, CON*H*), 7.43 - 7.46 (m, 4H, Ar*H*), 7.25 - 7.28 (m, 4H, Ar*H*), 4.74 & 4.6 (br, 8H, COCH_2), 3.74 (br, 8H, NHCH_2CH$_2$), 1.72 (br, 8H, NHCH$_2$CH_2), 1.37 (m, 24H, CH_2CH_2CH_2CH$_3$), 0.88 (br, 12H, CH_3)

^{13}C NMR (75.5MHz, DMSO-d_6) δ: 211.1 (*C*S$_2$), 165.3 (*C*O), 139.9 (Ar*C*), 128.7 (ArC), 125.6 (Ar*C*), 52.5 & 51.8 (*C*H$_2$CO), ~40 (*C*H$_2$), 35.0 (*C*H$_2$), 31.6 (*C*H$_2$), 31.1 (*C*H$_2$), 22.6 (*C*H$_2$), 14.6 (*C*H$_3$)

UV/visible (MeCN:DMSO 4:1) λ/nm (ε/dm^3 mol^{-1} cm^{-1}): 302 (70.0), 348 sh (16.2)

IR (Nujol®) ν/cm^{-1}: 3196 (NH), 1704 (CO), 1524 (CN), 970 (CS$_{as}$), 664 (CS$_s$)

ESMS m/z: 1331.2 [M + K$^+$]$^+$

Elemental Analysis %:

Calculated	C	45.5	H	5.6	N	8.6
Experimental	C	45.3	H	6.1	N	8.0

2-Cyclohexylamino-*N*-[2-(2-cyclohexylamino-acetylamino)-ethyl]-acetamide 54

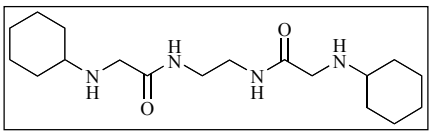

Method the same as that of **38**, except cyclohexylamine (10mL, excess) and 2-chloro-*N*-[2- (2-chloro-acetylamino)-ethyl]-acetamide (1.77g, 8.3mmol) were used which yielded a white solid.

Yield = 1.69g (60.3%)

^{1}H NMR (300MHz, $CDCl_3$) δ: 7.67 (br, 2H, CON*H*), 3.38 (t, ^{3}J = 3Hz, 4H, CONHCH_2), 3.23 (s, 4H, COCH_2), 2.32 (m, 2H, NHC*H*), 1.83-1.58 (m, 12H, C*H* (cyclohexyl) & N*H*), 1.27-0.94 (m, 12H, C*H* (cyclohexyl))

ESMS m/z: 339.3 [M]$^+$

Receptor 55

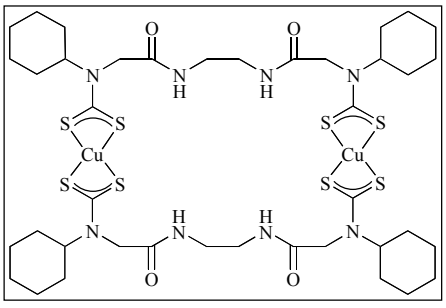

Method the same as that of **43**, except 2-cyclohexylamino-*N*-[2-(2-cyclohexylamino-acetylamino)-ethyl]-acetamide (0.56g, 1.7mmol), KOH (0.18g, 3.2mmol), CS_2 (0.19g, 3.4mmol) and Cu(CH$_3$CO$_2$)$_2$·H$_2$O (0.33g, 1.7mmol) were

used. H_2O (100mL) was added and the product extracted into CH_2Cl_2 (4x50mL) and dried over K_2CO_3. Filtration followed by solvent removal and recrystallisation from CH_2Cl_2/EtOH yielded a brown powder, which was dried in *vacuo*.

Yield = 0.50g (26.6%)

UV/visible ($CHCl_3$) λ/nm (ε/dm^3 mol^{-1} cm^{-1}): 272 (57.6), 440 (19.2)

IR (Nujol®) ν/cm^{-1}: 3292 (NH), 1660 (Amide I), 1524 (Amide II), 1488 (CN), 964 (CS_{as}), 660 (CS_s)

ESMS m/z: 552.1 $[M]^{2+}$

Elemental Analysis %:	Calculated + 2 H_2O	C	42.1	H	6.0	N	9.8
	Experimental	C	42.8	H	6.2	N	9.9

2-Chloro-*N*-[12-(2-chloro-acetylamino)-dodecyl]-acetamide 56

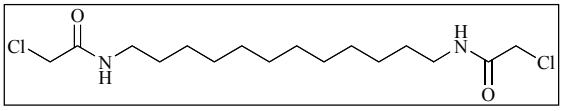

Method the same as that of **1**, except 1,12-diaminododecane (1.00g, 5.0mmol), $KOH_{(aq)}$ (10mL, 40% w/w, excess) and chloroacetyl chloride (1.13g, 10.0mmol) were used. After stirring for 15 minutes H_2O (50mL) was added and the product was extracted into $CHCl_3$ (3x50mL) and dried over K_2CO_3. Filtration followed by solvent removed and drying in *vacuo* yielded a while solid.

Yield = 1.57g (88.9%)

^{1}H NMR (300MHz, $CDCl_3$) δ: 7.26 (br, 2H, N*H*), 4.06 (s, 2H, CH_2Cl), 3.30 (q, ^{3}J = 7Hz, 4H, NHCH_2), 1.56 (m, 8H, NHCH$_2$CH_2), 1.36 (m, 16H, NHCH$_2$CH$_2$CH_2CH_2CH_2CH_2), 0.78 (t, 3H, ^{3}J = 6Hz, CH_3)

ESMS m/z: 375.2 $[M + Na^+]^+$

2-Hexylamino-*N*-[12-(2-hexylamino-acetylamino)-dodecyl]-acetamide 57

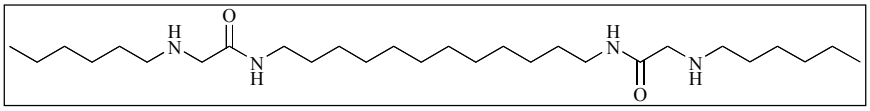

Method the same as that of **38**, except hexylamine

(15mL, excess) and 2-chloro-*N*-[12-(2-chloro-acetylamino)-dodecyl]-acetamide (1.57g, 4.5mmol) were used, which yielded a yellow oil.

Yield = 1.24g (58.0%)

^{1}H NMR (500MHz, $CDCl_3$) δ: 7.30 (br, 2H, CON*H*), 3.24 (q, ^{3}J = 6Hz, 4H, C*H*$_2$NHCO), 3.21 (s, 4H, COC*H*$_2$), 2.55 (t, ^{3}J = 7Hz, 2H, C*H*$_2$NHCH$_2$CO), 1.47 (m, 4H, CONHCH$_2$C*H*$_2$), 1.42 (m, 4H, C*H*$_2$CH$_2$NHCH$_2$CO), 1.27 (m, 20H, CH$_3$C*H*$_2$C*H*$_2$C*H*$_2$ & CONHCH$_2$CH$_2$C*H*$_2$C*H*$_2$C*H*$_2$C*H*$_2$), 0.85 (t, ^{3}J = 7Hz, 6H, C*H*$_3$)

ESMS m/z: 521.6 $[M + K^+]^+$

Receptor 58

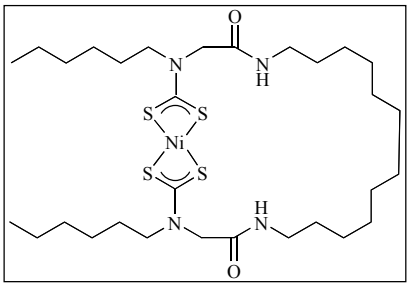

Method the same as that of **43**, except 2-hexylamino-*N*-[12-(2-hexylamino-acetylamino)-dodecyl]-acetamide (0.62g, 1.3mmol), THF:H_2O (5:1 v/v, 30mL), KOH (0.15g, 2.6mmol), CS_2 (0.20g, 2.6mmol) and $Ni(CH_3CO_2)_2{\cdot}4H_2O$ (0.32g, 1.3mmol) were used. After stirring for 15 hours the THF was removed under reduced pressure, H_2O (100mL) was added and the product extracted into $CHCl_3$ (3x50mL). Drying over K_2CO_3 and filtration of the followed by solvent removal yielded a green powder, which was dried in *vacuo*.

Yield = 0.75g (73.0%)

^{1}H NMR (300MHz, DMSO-d$_6$) δ: 8.06 (t, ^{3}J = 7Hz, 2H, CON*H*), 4.17 (s, 4H, COC*H*$_2$), 3.54 (t, ^{3}J = 6Hz, 4H, C*H*$_2$N), 3.04 (q, ^{3}J = 6Hz, 4H, CONHC*H*$_2$), 1.55 (m, 4H, CONHCH$_2$C*H*$_2$), 1.42 (m, 4H, C*H*$_2$CH$_2$N), 1.24 (m, 20H, CH$_3$C*H*$_2$C*H*$_2$C*H*$_2$ & CONHCH$_2$CH$_2$C*H*$_2$C*H*$_2$C*H*$_2$C*H*$_2$), 0.85 (t, ^{3}J = 7Hz, 6H, C*H*$_3$)

^{13}C NMR (75.5MHz, DMSO-d$_6$) δ: 205.7 (*C*S$_2$), 164.3 (*C*O), 50.7 (*C*H$_2$CO), 38.5 (*C*H$_2$), 31.0 (*C*H$_2$), 30.8 (*C*H$_2$), 30.7 (*C*H$_2$), 29.0 (*C*H$_2$), 28.9 (*C*H$_2$), 26.1 (*C*H$_2$), 26.0 (*C*H$_2$), 25.7 (*C*H$_2$), 22.1 (*C*H$_2$), 21.9 (*C*H$_2$), 13.9 (*C*H$_3$)

UV/visible (MeCN:DMSO 4:1) λ/nm (ε/dm^3 mol^{-1} cm^{-1}): 324 (35.0), 388 (6.2), 428 sh (2.0)

IR (Nujol®) ν/cm^{-1}: 3310 (NH), 1648 (Amide I), 1562 (Amide II), 1506 (CN), 970 (CS_{as}), 688 (CS_s)

ESMS m/z: 731.2 $[M + K^+]^+$

Elemental Analysis %:	Calculated + H_2O	C	50.8	H	8.2	N	7.9
	Experimental	C	51.5	H	8.2	N	7.9

Receptor 59

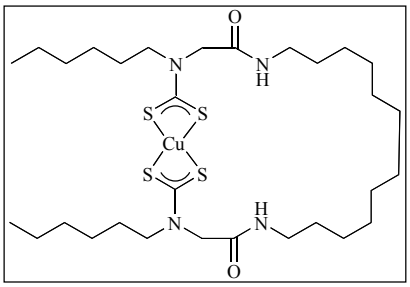

Method the same as that of **58**, except $Cu(CH_3CO_2)_2{\cdot}H_2O$ (0.26g, 1.3mmol) was used which yielded a brown powder.

Yield = 0.85g (91.4%)

UV/visible (MeCN:DMSO 4:1) λ/nm (ε/dm^3 mol^{-1} cm^{-1}): 271 (26.6), 288 sh (16.5), 435 (8.7)

IR (Nujol®) ν/cm^{-1}: 3292 (NH), 1646 (Amide I), 1560 (Amide II), 1500 (CN), 974 (CS_{as})

ESMS m/z: 736.3 $[M + K^+]^+$

Elemental Analysis %:	Calculated	C	51.7	H	8.1	N	8.0
	Experimental	C	51.1	H	8.8	N	7.8

(2-{3-[2-(3,3-Dimethyl-butyrylamino)-ethyl]-thioureido}-ethyl)-carbamic acid *tert*-butyl ester 60

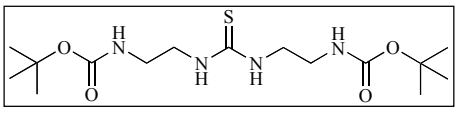

(2-Amino-ethyl)-carbamic acid *tert*-butyl ester (1.28g, 8.0mmol), triethylamine (0.81g, 4.0mmol) and CS_2 (0.30g, 4.0mmol) were dissolved in MeOH (100mL). The mixture was refluxed under $N_{2(g)}$ for 12 hours. H_2O (100mL) and $HCl_{(aq)}$ (20mL, 2M) were added and the product was extracted into CH_2Cl_2 (4x50mL) and dried over K_2CO_3. Filtration followed by solvent removal and drying in *vacuo* yielded a yellow oil.

Yield = 1.16g (80.5%)

^{1}H NMR (300MHz, $CDCl_3$) δ: 7.11 (br, 2H, N*H*CS), 5.35 (br, 2H, N*H*CO), 3.58 (m, 4H, CH_2NHCS), 3.30 (m, 4H, CH_2NHCO), 1.39 (s, 18H, (CH_3)$_3$)

3,5-Di-*tert*-butyl-benzaldehyde 61[6]

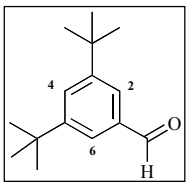

3,5-Di-*tert*-butyl toluene (25.0g, 120mmol), *N*-bromosuccinimide (32.9g, 180mmol) and 2,2'-azobis(2-methyl-propionitrile) (0.11g, 0.7mmol) were refluxed in 1,2-dichloroethane for 4 hours. The solvent was removed and hexamethylenetetramine (47.2g, 340mmol), H_2O (33mL) and EtOH (33mL) were added. The mixture was refluxed for 4 hours and cooled to room temperature. $HCl_{(aq)}$ (32%, 33mL) was added and the mixture refluxed for a further 30 minutes. The mixture was cooled to room temperature, poured into Et_2O (200mL) and washed with H_2O (2x200mL) and $NaCl_{(aq)}$ (2x200mL, saturated). The Et_2O layer was dried over K_2CO_3, filtration followed by solvent removal and drying in *vacuo* yielded a yellow solid.

Yield = 21.5g (82.1%)

^{1}H NMR (500MHz, $CDCl_3$) δ: 10.0 (s, 1H, C*H*O), 7.75 (d, ^{4}J = 1Hz, 2H, ArH^2 & ArH^6), 7.74 (t, ^{4}J = 1Hz, 1H, ArH^4), 1.35 (s, 18H, CH_3)

ESMS m/z: 203.3 $[M - CH_3^+]^+$

[2-(3,5-Di-*tert*-butyl-benzylamino)-ethyl]-carbamic acid *tert*-butyl ester 62

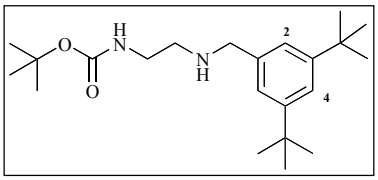

Method the same as that of **10**, except *N*-(*tert*-butoxycarbonyl)ethylene-1, 2-diamine (1.60g, 10.0mmol) and 3,5-di-*tert*-butyl-benzaldehyde (2.18g, 10.0mmol) were used, which yielded a yellow oil.

Yield = 3.12g (86.0%)

^{1}H NMR (300MHz, $CDCl_3$) δ: 7.32 (d, ^{4}J = 2Hz, 1H, ArH^4), 7.14 (d, ^{4}J = 2Hz, 2H, ArH^2), 5.04 (br, 1H, N*H*CO), 3.78 (s, 2H, ArCH_2), 3.25 (q, ^{3}J = 7Hz, 2H, CONHCH_2), 2.79 (t, ^{3}J = 6Hz, 2H, CH_2NH), 1.46 (s, 9H, (CH_3)$_3$), 1.35 (s, 18H, ArCH_3)

ESMS m/z: 363.3 $[M + H^+]^+$

N^1-(3,5-Di-*tert*-butyl-benzyl)-ethane-1,2-diamine 63

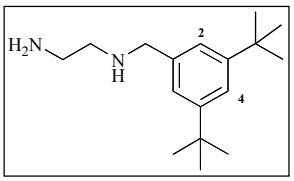

Method the same as that of **9**, except [2-(3,5-di-*tert*-butyl-benzylamino)-ethyl]-carbamic acid *tert*-butyl ester (3.12g, 8.6mmol) was used which yielded a yellow oil.

Yield = 2.26g (Quantitative)

^{1}H NMR (300MHz, $CDCl_3$) δ: 7.32 (d, ^{4}J = 2Hz, 1H, Ar*H*^{4}), 7.17 (d, ^{4}J = 2Hz, 2H, Ar*H*^{2}), 3.81 (s, 2H, ArC*H*$_2$), 2.85 (t, ^{3}J = 7Hz, 2H, C*H*$_2$), 2.76 (t, ^{3}J = 6Hz, 2H, C*H*$_2$), 1.34 (s, 18H, (C*H*$_3$)$_3$)

ESMS m/z: 263.3 $[M + H^+]^+$

1,3-Bis-[2-(3,5-di-*tert*-butyl-benzylamino)-ethyl]-thiourea 64

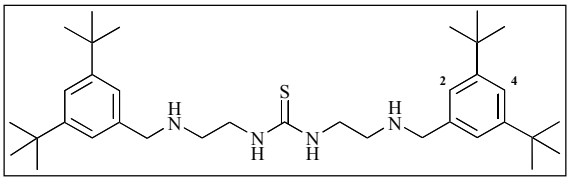

N^1-(3,5-Di-*tert*-butyl-benzyl)-ethane-1,2-diamine (2.26g, 8.6mmol) and 1,1'-thiocarbonyldi-2(1H)-pyridone (1.00g, 4.3mmol) were dissolved in CH_2Cl_2 (50mL). The mixture was refluxed under $N_{2(g)}$ for 1 hour. H_2O (100mL) was added and the product was extracted into CH_2Cl_2 (3x50mL) and dried over K_2CO_3. Filtration followed by solvent removal and recrystallisation from hot MeOH yielded a beige solid.

Yield = 0.65g (25.0%)

^{1}H NMR (300MHz, $CDCl_3$) δ: 7.35 (d, ^{4}J = 2Hz, 2H, Ar*H*^{4}), 7.16 (d, ^{4}J = 2Hz, 4H, Ar*H*^{2} & Ar*H*^{6}), 5.70 (br, 2H, CSN*H*), 4.78 (s, 4H, C*H*$_2$NHCS), 3.57 (s, 8H, C*H*$_2$), 1.33 (s, 36H, C*H*$_3$)

ESMS m/z: 575.7 $[M - C_2H_6 + K^+]^+$

N,N'-Dibenzyl-*m*-xylylenediamine 68

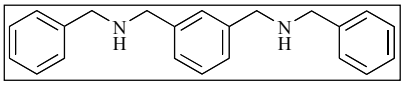

Method the same as that of **10**, except benzylamine (1.58g, 14.7mmol) and benzene-1, 3-dicarbaldehyde (0.98g, 7.3mmol) were used, which yielded a colourless oil.

Yield = 2.08g (89.4%)

^{1}H NMR (500MHz, $CDCl_3$) δ: 7.35-7.23 (m, 14H, Ar*H*), 3.82 (s, 4H, CH_2), 3.81 (s, 4H, CH_2)

ESMS m/z: 317.1 $[M + H^+]^+$

2,6-Bis-(benzylamino-methyl)-4-methyl-phenol 69

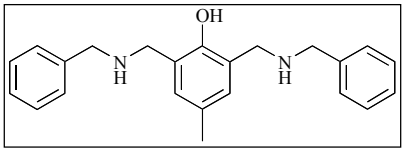

Method the same as that of **10**, except 2-hydroxy-5-methyl-benzene-1, 3-dicarbaldehyde (0.49g, 3.0mmol) and benzylamine (0.64g, 6.0mmol) were used, which yielded a yellow oil.

Yield = 0.94g (90.4%)

^{1}H NMR (300MHz, $CDCl_3$) δ: 7.35-7.26 (m, 12H, Ar*H*), 6.86 (s, 2H, N*H*), 3.90 (s, 4H, CH_2), 3.83 (s, 4H, CH_2), 2.25 (s, 3H, CH_3)

ESMS m/z: 347.2 $[M + H^+]^+$

2,6-Bis-(hexylamino-methyl)-4-methyl-phenol 70

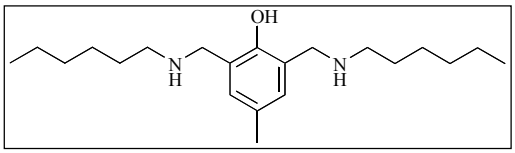

Method the same as that of **10**, except 2-hydroxy-5-methyl-benzene-1, 3-dicarbaldehyde (0.52g, 3.2mmol) and hexylamine (0.65g, 6.4mmol) were used, which yielded a yellow oil.

Yield = 0.88g (82.2%)

^{1}H NMR (300MHz, $CDCl_3$) δ: 6.78 (s, 2H, Ar*H*), 4.76 (br, 2H, N*H*), 3.81 (s, 4H, ArCH_2NH), 2.60 (t, ^{3}J = 7Hz, 4H, NHC$H_2$$CH_2$), 2.19 (s, 3H, ArC$H_3$), 1.49 (m, 4H, $NHCH_2$CH_2), 1.26 (m, 12H, CH_2CH_2C$H_2$$CH_3$), 0.85 (t, ^{3}J = 7Hz, 6H, CH_3)

ESMS m/z: 242.9 $[M - C_6H_{14}N - CH_3 + Na^+]^+$

2,6-Bis-bromomethyl-pyridine 71[7]

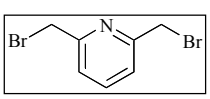

2,6-Bis-hydroxymethyl-pyridine (1.50g, 10.8mmol) was dissolved in HBr (48% in AcOH, 14mL) and refluxed under $N_{2(g)}$ for 1 hour. H_2O (50mL)

followed by $NaOH_{(aq)}$ (50mL, 2M) was added and the resulting precipitate was collected by filtration and dried in *vacuo* yielding a white powder.

Yield = 0.57g (20.0%)

^{1}H NMR (300MHz, $CDCl_3$) δ: 7.71 (t, ^{3}J = 8Hz, 1H, PyrH^4), 7.37 (d, ^{3}J = 8Hz, 2H, PyrH^3 & H^5), 4.54 (s, 4H, CH_2)

2,6-Bis-butylaminomethyl-pyridine 72

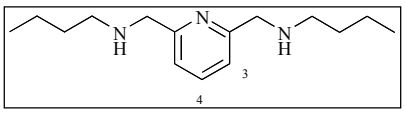

2,6-Bis-bromomethyl-pyridine (0.57g, 2.2mmol) was added portion wise to butylamine (20mL, excess) with stirring. The mixture was stirred under $N_{2(g)}$ for 30 minutes, H_2O (100mL) was added and the product extracted into CH_2Cl_2 (3x50mL) and dried over K_2CO_3. Filtration followed by solvent removal and drying in *vacuo* yielded a yellow oil.

Yield = 0.52g (96.3%)

^{1}H NMR (300MHz, $CDCl_3$) δ: 7.54 (t, ^{3}J = 8Hz, 1H, PyrH^4), 7.11 (d, ^{3}J = 8Hz, 2H, PyrH^3), 3.84 (s, 4H, PyrCH_2N), 2.61 (t, ^{3}J = 7Hz, 4H, NCH_2CH$_2$), 1.92 (br, 2H, NH), 1.46 (m, ^{3}J = 7Hz, 4H, NCH$_2$CH_2), 1.33 (m, ^{3}J = 7Hz, 4H, CH_2CH$_3$), 0.87 (t, ^{3}J = 7Hz, 6H, CH_3)

ESMS m/z: 250.2 $[M + H^+]^+$

Receptor 73

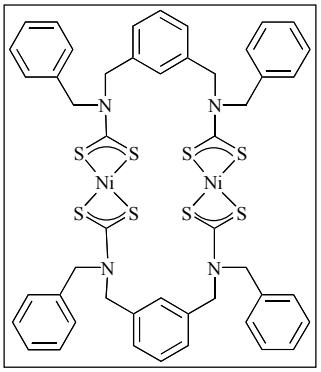

N,*N*'-Dibenzyl-*m*-xylylenediamine (1.04g, 3.3mmol) was dissolved in EtOH:H_2O (2:1 v/v, 75mL) and KOH (0.41g, 7.3mmol) was added and stirred under $N_{2(g)}$ until dissolved. CS_2 (0.55g, 7.2mmol) was then added and the solution stirred for 30 minutes. $Ni(CH_3CO_2)_2{\cdot}4H_2O$ (0.82g, 3.3mmol) was added to the yellow solution and the mixture stirred for 15 hours. The green solid was filtered off and extracted into CH_2Cl_2 (200mL). Solvent removal and recrystallisation from CH_2Cl_2/EtOH yielded a green powder, which was dried in *vacuo*.

Yield = 0.90g (51.9%)

^{1}H NMR (300MHz, $CDCl_3$) δ: 7.51-7.14 (m, 28H, Ar*H*), 4.74-4.68 (m, 16H, CH_2)

^{13}C NMR : Too insoluble to obtain a spectrum.

UV/visible (CH_2Cl_2:MeCN 7:3) λ/nm (ε/dm^3 mol^{-1} cm^{-1}): 323 (42.0), 402 (7.7), 442 sh (0.2)

IR (Nujol®) ν/cm^{-1}: 1476 (CN), 984 (CS_{as}), 660 (CS_s)

ESMS m/z: 1072.8 [M + Na$^+$]$^+$, 1089.0 [M + K$^+$]$^+$

Elemental Analysis %:	Calculated + 2 H_2O	C	53.1	H	4.5	N	5.2
	Experimental	C	52.9	H	4.2	N	5.0

Receptor 74

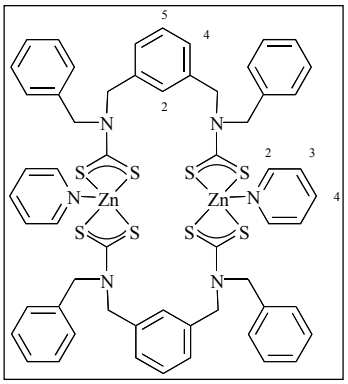

Method the same as that of **73**, except $Zn(CH_3CO_2)_2{\cdot}2H_2O$ (0.72g, 3.3mmol) was used which yielded a white power which was dissolved in pyridine (50mL) and filtered. Solvent removal yielded a brown solid that was dried in *vacuo*.

Yield = 0.51g (36.2%)

^{1}H NMR (300MHz, $CDCl_3$) δ: 8.74 (t of d, ^{3}J = 6Hz ^{4}J = 2Hz, 4H, PyrH^2), 8.14 (d of t, ^{3}J = 6Hz ^{4}J = 2Hz, 2, PyrH^4), 7.83 (s, 2H, ArH^2), 7.70 (t, ^{3}J = 6Hz, 4H, PyrH^3), 7.54 (d, ^{3}J = 8Hz, 4H, ArH^4), 7.41-7.29 (m, 20H, Ar*H*), 7.17 (t, ^{3}J = 8Hz, 2H, ArH^5), 4.23 (s, 8H, CH_2), 4.03 (s, 8H, CH_2)

^{13}C NMR (75.5MHz, $CDCl_3$) δ: 207.15 (CS_2), 149.7 (PyrC^2), 137.4 (PyrC^3) 135.9 (Ar*C*), 135.0 (Ar*C*), 129.1 (Ar*C*), 129.0 (Ar*C*), 128.4 (Ar*C*), 127.9 (Ar*C*), 126.6 (Ar*C*), 124.5 (PyrC^4), 56.7 (CH_2), 55.9 (CH_2)

UV/visible (CH_2Cl_2:MeCN 7:3) λ/nm (ε/dm^3 mol^{-1} cm^{-1}): 267 (72.6), 287 sh (38.0)

IR (Nujol®) ν/cm^{-1}: 1482 (CN), 988 (CS_{as})

ESMS m/z: 1062.8 [M - 2 Pyr + H$^+$]$^+$, 1087.0 [M - 2 Pyr + Na$^+$]$^+$, 1102.6 [M - 2 Pyr + K$^+$]$^+$

Elemental Analysis %:	Calculated	C	57.0	H	4.5	N	6.9
	Experimental	C	56.5	H	4.5	N	7.1

Receptor 75

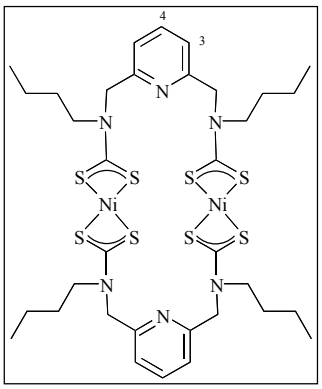

2,6-Bis-butylaminomethyl-pyridine (0.50g, 2.0mmol) was dissolved in MeCN:H_2O (5:1 v/v, 60mL) and KOH (0.22g, 4.0mmol) was added and stirred under $N_{2(g)}$ until dissolved. CS_2 (0.31g, 4.0mmol) was then added and the solution stirred for 30 minutes. $Ni(CH_3CO_2)_2{\cdot}4H_2O$ (0.50g, 2.0mmol) was added to the yellow solution and the mixture stirred for 15 hours. The green solid was filtered off and extracted into CH_2Cl_2 (200mL). Solvent removal yielded a light green powder, which was dried in *vacuo*.

Yield = 0.70g (76.4%)

^{1}H NMR (300MHz, $CDCl_3$) δ: 7.70 (t, ^{3}J = 7Hz, 2H, Pyr*H*^{4}), 7.33 (d, ^{3}J = 5Hz, 4H, Pyr*H*^{3}), 4.85 (br, 8H, PyrC*H*$_2$N), 3.65 (br, 8H, NC*H*$_2$CH$_2$), 1.62 (m, 8H, NCH$_2$C*H*$_2$), 1.36 (q, ^{3}J = 8Hz, 8H, C*H*$_2$CH$_3$), 0.93 (t, ^{3}J = 8Hz, 12H, C*H*$_3$)

^{13}C NMR (75.5MHz, $CDCl_3$) δ: 208.6 (*C*S$_2$), 154.5 (Pyr*C*^{2}), 138.2 (Pyr*C*^{4}), 121.9 (Pyr*C*^{3}), 53.6 (*C*H$_2$), 50.0 (*C*H$_2$), 29.3 (*C*H$_2$), 20.4 (*C*H$_2$), 14.2 (*C*H$_3$)

UV/visible (CH_2Cl_2:MeCN 7:3) λ/nm (ε/dm^3 mol^{-1} cm^{-1}): 321 (81.4), 396 (13.7), 434 sh (3.6)

IR (Nujol®) ν/cm^{-1}: 1498 (CN), 992 (CS_{as}), 640 (CS_s)

ESMS m/z: 915.7 $[M + H^+]^+$, 938.6 $[M + Na^+]^+$

Elemental Analysis %:

Calculated	C	44.6	H	5.5	N	9.2
Experimental	C	45.2	H	5.3	N	9.1

Receptor 76

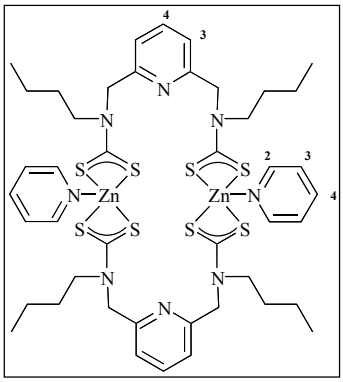

Method the same as that of **75**, except 2,6-bis-butylaminomethyl-pyridine (0.38g, 1.5mmol), KOH (0.17g, 3.0mmol), CS_2 (0.23g, 3.0mmol) and $Zn(CH_3CO_2)_2{\cdot}2H_2O$ (0.33g, 1.5mmol) were used, which yielded a white powder which was dissolved in pyridine (50mL) and filtered. Solvent removal yielded a brown solid that was dried in *vacuo*.

Yield = 0.30g (36.8%)

^{1}H NMR (300MHz, $CDCl_3$) δ: 8.66 (d, ^{3}J = 6Hz, 4H, ZnPyr*H*^{2}), 7.68 (d of t, ^{3}J = 8Hz ^{4}J = 2Hz, 4H, Pyr*H*^{2} & ZnPyr*H*^{4}), 7.31-7.20 (m, 8H, Pyr*H*^{3} & ZnPyr*H*^{3}), 5.15 (s, 8H, PyrC*H*$_2$N), 3.86 (t, ^{3}J = 6Hz, 8H, NC*H*$_2$CH$_2$), 1.69 (t, ^{3}J = 6Hz, 8H, NCH$_2$C*H*$_2$), 1.27 (q, ^{3}J = 8Hz, 8H, C*H*$_2$CH$_3$), 0.86 (t, ^{3}J = 8Hz, 12H, C*H*$_3$)

^{13}C NMR (75.5MHz, $CDCl_3$) δ: 205.5 (*C*S$_2$), 155.2 (PyrC^2), 149.0 (ZnPyrC^2), 138.4 (PyrC^4), 137.9 (ZnPyr C^4), 125.2 (PyrC^3), 121.6 (ZnPyrC^3), 55.7 (*C*H$_2$), 51.5 (*C*H$_2$), 28.4 (*C*H$_2$), 20.6 (*C*H$_2$), 14.4 (*C*H$_3$)

UV/visible (CH_2Cl_2:MeCN 7:3) λ/nm (ε/dm^3 mol^{-1} cm^{-1}): 262 (23.7)

IR (Nujol®) ν/cm^{-1}: 1480 (CN), 1002 (CS_{as})

ESMS m/z: 953.0 [M - 2 Pyr + Na$^+$]$^+$, 967.0 [M - 2 Pyr + K$^+$]$^+$

Elemental Analysis %:							
	Calculated + 2 H_2O	C	47.0	H	5.7	N	10.0
	Experimental	C	46.0	H	5.6	N	9.7

Receptor 77

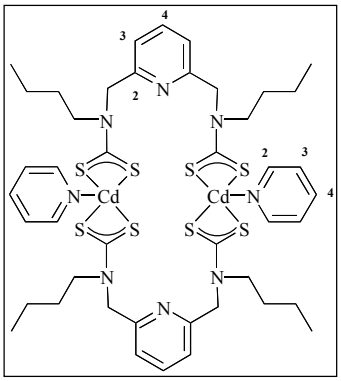

Method the same as that of **75**, except 2,6-bis-butylaminomethyl-pyridine (0.38g, 1.5mmol), KOH (0.17g, 3.0mmol), CS_2 (0.23g, 3.0mmol) and $CdCl_2 \cdot ½H_2O$ (0.34g, 1.5mmol) were used, which yielded a white powder that was dissolved in pyridine (50mL) and filtered. Solvent removal yielded a brown solid that was dried in *vacuo*.

Yield = 0.15g (16.9%)

^{1}H NMR (300MHz, $CDCl_3$) δ: 8.64 (d, ^{3}J = 8Hz, 4H, CdPyr*H*^{2}), 7.69 (d of t, ^{3}J = 8Hz ^{4}J = 2Hz, CdPyr*H*^{4}), 7.50 (t, ^{3}J = 6Hz, 2H, Pyr*H*^{4}), 7.35-7.27 (m, 4H, CdPyr*H*^{3}), 7.17 (d, ^{3}J = 8Hz, 4H, Pyr*H*^{3}), 5.20 (br, 8H, PyrC*H*$_2$N), 4.06 (br, 8H, NC*H*$_2$CH$_2$), 1.77 (t, ^{3}J = 7Hz, 8H, NCH$_2$C*H*$_2$), 1.30 (q, ^{3}J = 7Hz, 8H, C*H*$_2$CH$_3$), 0.91 (t, ^{3}J = 7Hz, 12H, C*H*$_3$)

^{13}C NMR (75.5MHz, $CDCl_3$) δ: 205.6 (*C*S_2), 154.8 (Pyr*C*^{2}), 149.9 (CdPyr*C*^{2}), 137.3 (Pyr*C*^{4}), 136.6 (CdPyr*C*^{4}), 124.1 (Pyr*C*^{3}), 120.9 (CdPyr*C*^{3}), 53.6 (*C*H_2), 50.0 (*C*H_2), 29.3 (*C*H_2), 20.4 (*C*H_2), 14.2 (*C*H_3)

UV/visible (CH_2Cl_2:MeCN 7:3) λ/nm (ε/dm^3 mol^{-1} cm^{-1}): 262 (65.7)

IR (Nujol®) ν/cm^{-1}: 1480 (CN), 964 (CS_{as})

ESMS m/z: 1024.9 [M - 2 Pyr + H$^+$]$^+$

Elemental Analysis %:	Calculated + 2 H_2O	C	43.4	H	5.3	N	9.2
	Experimental	C	42.6	H	4.8	N	9.2

Receptor 78

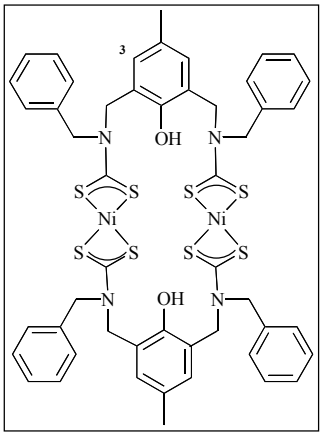

Method the same as that of **73**, except 2,6-bis-(benzylamino-methyl)-4-methyl-phenol (0.47g, 1.4mmol), KOH (0.15g, 2.7mmol), CS_2 (0.22g, 2.9mmol) and $Ni(CH_3CO_2)_2{\cdot}4H_2O$ (0.35g, 1.4mmol) were used, which yielded a light green powder.

Yield = 0.72g (95.3%)

^{1}H NMR (300MHz, $CDCl_3$) δ: 7.35-7.20 (m, 20H, Ar*H*), 6.87 (br, 4H, Ar*H*^{3}), 4.68 (br, 16H, C*H*$_2$), 2.25 (s, 6H, C*H*$_3$)

^{13}C NMR (75.5MHz, $CDCl_3$) δ: 208.2 (*C*S_2), 151.0 (Ar*C*OH), 134.0 (Ar*C*), 132.1 (Ar*C*), 130.3 (Ar*C*), 129.2 (Ar*C*), 129.1 (Ar*C*), 128.5 (Ar*C*), 120.5 (Ar*C*), 51.4 (*C*H_2), 47.1 (*C*H_2), 21.0 (Ar*C*H_3)

UV/visible (CH_2Cl_2:MeCN 7:3) λ/nm (ε/dm^3 mol^{-1} cm^{-1}): 328 (67.3), 398 (12.0), 437 sh (2.8)

IR (Nujol®) ν/cm^{-1}: 3322 (OH), 1484 (CN), 1008 (CS_{as}), 660 (CS_s)

ESMS m/z: 1132.8 [M + Na$^+$]$^+$, 1148.8 [M + K$^+$]$^+$

Elemental Analysis %:	Calculated + H_2O	C	53.2	H	4.5	N	5.0
	Experimental	C	53.2	H	4.5	N	4.8

Receptor 79

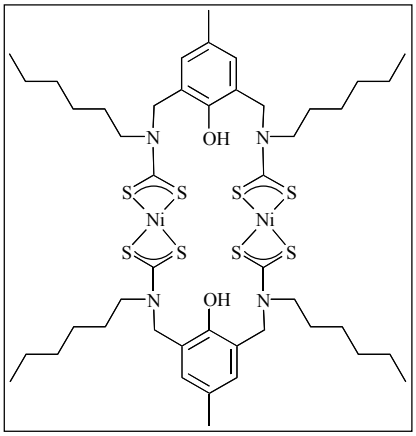

Method the same as that of **73**, except 2,6-bis-(hexylamino-methyl)-4-methyl-phenol (0.44g, 1.3mmol), KOH (0.15g, 2.7mmol), CS_2 (0.22g, 2.9mmol) and $Ni(CH_3CO_2)_2{\cdot}4H_2O$ (0.38g, 1.5mmol) were used, which yielded a light green powder.

Yield = 0.74g (71.6%)

^{1}H NMR (300MHz, $CDCl_3$) δ: 6.97 (br, 4H, Ar*H*), 4.83 (br, 8H, ArC*H*$_2$), 3.49 (br, 8H, NCH$_2$C*H*$_2$), 2.31 (br, 6H, ArC*H*$_3$), 1.28 (br, 24H, C*H*$_2$C*H*$_2$C*H*$_2$CH$_3$), 0.89 (br, 12H, C*H*$_3$)

^{13}C NMR (75.5MHz, $CDCl_3$) δ: 206.5 (*C*S$_2$), 150.9 (Ar*C*OH), 131.7 (Ar*C*), 130.3 (Ar*C*), 120.7 (Ar*C*), 48.9 (*C*H$_2$), 47.7 (*C*H$_2$), 31.6 (*C*H$_2$), 26.9 (*C*H$_2$), 26.7 (*C*H$_2$), 22.9 (*C*H$_2$), 21.0 (Ar*C*H$_3$), 14.5 (*C*H$_3$)

UV/visible (CH_2Cl_2:MeCN 7:3) λ/nm (ε/dm^3 mol^{-1} cm^{-1}): 325 (77.2), 392 (13.3), 431 sh (3.1)

IR (Nujol®) ν/cm^{-1}: 3182 (OH), 1482 (CN), 1008 (CS_{as}), 656 (CS_s)

ESMS m/z: 1086.8 $[M + H^+]^+$, 1124.8 $[M + K^+]^+$

Elemental Analysis %:	Calculated + 2 H_2O	C	49.2	H	6.8	N	5.0
	Experimental	C	47.7	H	5.4	N	4.7

Receptor 80

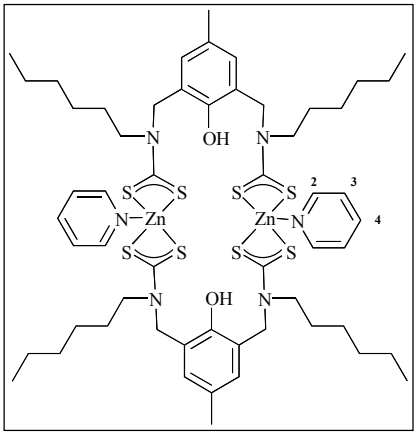

Method the same as that of **73**, except 2,6-bis-(hexylamino-methyl)-4-methyl-phenol (0.44g, 1.32mmol), KOH (0.15g, 2.7mmol), CS_2 (0.22g, 2.9mmol) and $Zn(CH_3CO_2)_2{\cdot}2H_2O$ (0.30g, 1.4mmol) were used, which yielded a white powder which was dissolved in pyridine (50mL) and filtered. Solvent removal yielded a brown solid that was dried in *vacuo*.

Yield = 0.64g (38.5%)

^{1}H NMR (300MHz, $CDCl_3$) δ: 8.77 (d, ^{3}J = 8Hz, 4H, ZnPyr*H*^{2}), 7.73 (d of t, ^{3}J = 8Hz ^{4}J = 2Hz, 2H, ZnPyr*H*^{4}), 7.37 (t, ^{3}J = 6Hz, 2H, ZnPyr*H*^{3}), 6.95 (br, 4H, Ar*H)*, 4.92 (br, 8H, ArCH_2), 3.80 (br, 8H, CH_2CH_2), 2.32 (br, 6H, ArCH_3), 1.78 (br, 8H, CH_2CH_2), 1.38 (br, 24H, CH_2CH_2CH_2CH_3), 0.83 (br, 12H, CH_3)

^{13}C NMR (75.5MHz, $CDCl_3$) δ: 204.2 (*C*S_2), 151.6 (Ar*C*OH), 149.4 (Pyr*C*^{2}), 139.7 (Pyr*C*^{4}), 131.2 (Ar*C*), 129.5 (Ar*C*), 125.5 (Pyr*C*^{3}), 121.6 (Ar*C*), 54.0 (*C*H_2), 53.7 (*C*H_2), 31.6 (*C*H_2), 26.7 (*C*H_2), 26.5 (*C*H_2), 22.8 (*C*H_2), 20.9 (Ar*C*H_3), 14.3 (*C*H_3)

UV/visible (CH_2Cl_2:MeCN 7:3) λ/nm (ε/dm^3 mol^{-1} cm^{-1}): 264 (114.8), 279 sh (81.2)

IR (Nujol®) ν/cm^{-1}: 3194 (OH), 1482 (CN), 1006 (CS_{as}), 656 (CS_s)

ESMS m/z: 1100.4 [M - 2 Pyr + H$^+$]$^+$

Elemental Analysis %:	Calculated + H_2O	C	52.7	H	6.6	N	6.6
	Experimental	C	52.7	H	6.3	N	6.5

N^1,*N*^{6}-Dihexyl-hex-2-ene-1,6-diamine 81

Method the same as that of **18**, except hexylamine (20mL, excess) and 1,4-dichloror-2-butyne (2.45g, 20mmol) were used, which yielded an orange oil.

Yield = 4.12g (81.9%)

^{1}H NMR (300MHz, $CDCl_3$) δ: 3.38 (t, ^{3}J = 5Hz, 4H, CC*H*$_2$), 2.63 (q, ^{3}J = 7Hz, NHC*H*$_2$CH$_2$), 1.40 (m, 4H, NHCH$_2$C*H*$_2$), 1.26 (m, 12H, C*H*$_2$C*H*$_2$C*H*$_2$CH$_3$), 0.84 (t, ^{3}J = 7Hz, 6H, C*H*$_3$)

ESMS m/z: 253.3 [M + H$^+$]$^+$

82

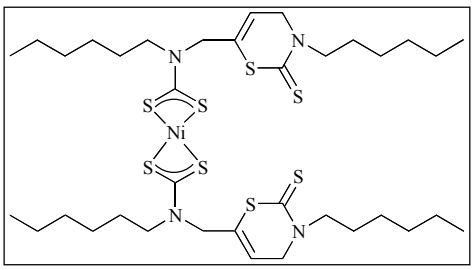

Method the same as that of **58**, except *N*^{1},*N*^{6}-dihexyl-hex-2-ene-1,6-diamine (2.06g, 8.1mmol), KOH (0.91g, 16.2mmol), CS_2 (1.23g, 16.2mmol) and $Ni(CH_3CO_2)_2{\cdot}4H_2O$ (0.77g, 8.1mmol) were used.

Recrystallisation from CH_2Cl_2/EtOH yielded a green powder, which was dried in *vacuo*.

^{1}H NMR (300MHz, $CDCl_3$) δ: 5.50 (t, ^{3}J = 7Hz, 2H, C*H*), 4.75 (s, 4H, SCC*H*$_2$), 4.09 (d, ^{3}J = 7Hz, 4H, SCNC*H2*), 3.77 (t, ^{3}J = 7Hz, 4H, NC*H*$_2$CH$_2$), 3.46 (t, ^{3}J = 7Hz, 4H, NC*H*$_2$CH$_2$), 1.56-1.68 (m, 8H, NCH$_2$C*H*$_2$), 1.28-1.32 (m, 24H, C*H*$_2$C*H*$_2$C*H*$_2$CH$_3$), 0.89 (br, 6H, C*H*$_3$)

ESMS m/z: 887.4 $[M + Na^+]^+$

N-Bis (4-carbomethoxybenzyl) amine 83[8]

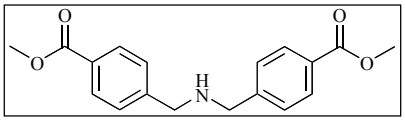

Methyl-4-amino methyl benzoate·HCl (1.40g, 6.9mmol) was dissolved in $NaOH_{(aq)}$ (50mL, 1M) and the amine was extracted into CH_2Cl_2 (4x50mL) and dried over K_2CO_3. Filtering followed by solvent removal and drying in *vacuo* yielded a yellow oil (1.09g, 6.6mmol). Method the same as that of **10**, except 4-formyl benzoate (1.08g, 6.6mmol) was used which yielded a yellow oil.

Yield = 1.65g (81.0%)

^{1}H NMR (300MHz, $CDCl_3$) δ: 7.99 (d, ^{3}J = 8Hz, 4H, Ar*H*), 7.41 (d, ^{3}J = 8Hz, 4H, Ar*H*), 3.90 (s, 6H, C*H*$_3$), 3.84 (s, 4H, C*H*$_2$), 1.68 (s, 1H, N*H*)

N-(*tert*-Butoxycarbonyl)bis (4-carbomethoxybenzyl) amine 84[8]

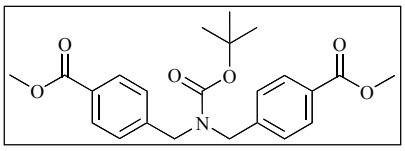

N-Bis (4-carbonylbenzyl) amine (1.65g, 5.3mmol), di-*tert*-butoxy carbonyl (1.15g, 5.3mmol) and DMAP (catalytic) were dissolved in $CHCl_3$ (100mL) and the mixture was stirred under $N_{2(g)}$ for 12 hours. $HCl_{(aq)}$ (100mL, 2M) was added and the product was extracted into CH_2Cl_2 (4x50mL) and dried over K_2CO_3. Filtration followed by solvent removal and drying in *vacuo* yielded a yellow oil.

Yield = 2.14g (97.0%)

^{1}H NMR (300MHz, $CDCl_3$) δ: 7.98 (d, ^{3}J = 8Hz, 4H, Ar*H*), 7.25 (d, ^{3}J = 8Hz, 4H, Ar*H*), 4.48 (br, 2H, C*H*$_2$), 4.38 (br, 2H, C*H*$_2$), 3.89 (s, 6H, OC*H*$_3$), 1.44 (s, 9H, (C*H*$_3$)$_3$)

Bis-(4-hydroxymethyl-benzyl)-carbamic acid *tert*-butyl ester 85[8]

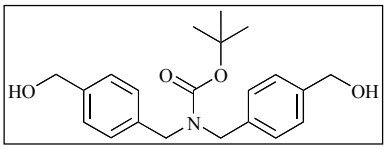

N-(*tert*-butoxycarbonyl)bis (4-carbomethoxybenzyl) amine (2.14g, 5.2mmol) was dissolved in THF (100mL). $LiAlH_4$ (0.78g, 20.1mmol) was added carefully and the mixture refluxed for 30 minutes under $N_{2(g)}$ and then $HCl_{(aq)}$ (2M) was added carefully until pH = 3. The product was extracted into CH_2Cl_2 (4x50mL) and dried over K_2CO_3. Filtration followed by solvent removal and drying in *vacuo* yielded a yellow oil.

Yield = 1.06g (57.1%)

^{1}H NMR (300MHz, $CDCl_3$) δ: 7.29 (d, ^{3}J = 8Hz, 4H, Ar*H*), 7.16 (br, 4H, Ar*H*), 4.66 (br, 4H, C*H*$_2$OH), 4.37 (br, 2H, C*H*$_2$N), 4.31 (br, 2H, C*H*$_2$N), 2.33 (br, 2H, O*H*), 1.49 (s, 9H, (C*H*$_3$)$_3$)

Bis-(4-formyl-benzyl)-carbamic acid *tert*-butyl ester 86[8]

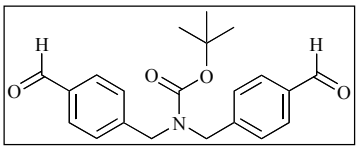

Pyridinium chlorochromate (1.44g, 6.7mmol) was dissolved in CH_2Cl_2 (25mL) and bis-(4-hydroxymethyl-benzyl)-carbamic acid *tert*-butyl ester (1.19g, 3.4mmol) was added and the mixture stirred under $N_{2(g)}$ for 2 hours. H_2O (50mL) was added and the product was extracted into CH_2Cl_2 (4x50mL) and dried over K_2CO_3. Filtration followed by solvent removal and drying in *vacuo* yielded a dark brown oil.

Yield = 0.95g (80.0%)

^{1}H NMR (300MHz, $CDCl_3$) δ: 10.02 (s, 2H, C*H*O), 7.85 (d, ^{3}J = 8Hz, 4H, Ar*H*), 7.35 (br, 4H, Ar*H*), 4.53 (br, 2H, C*H*$_2$N), 4.43 (br, 2H, C*H*$_2$N), 1.47 (s, 9H, (C*H*$_3$)$_3$)

Bis-[4-(benzylamino-methyl)-benzyl]-carbamic acid *tert*-butyl ester 87[8]

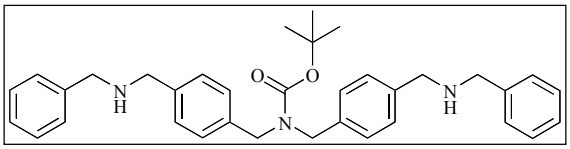

Method the same as that of **10**, except bis-(4-hydroxymethyl-benzyl)-carbamic acid *tert*-butyl ester (0.95g, 2.6mmol) and benzylamine (0.51g, 5.2mmol) were used, which yielded a dark brown oil.

Yield = 1.27g (88.2%)

^{1}H NMR (300MHz, $CDCl_3$) δ: 7.35-7.19 (m, 18H, Ar*H*), 4.42 (br, 2H, CH_2), 4.33 (br, 2H, CH_2), 3.81 (br, 8H, CH_2), 1.57 (br, 2H, N*H*), 1.47 (s, 9H, (CH_3)$_3$)

Bis-[4-(benzylamino-methyl)-benzyl]-amine 88[8]

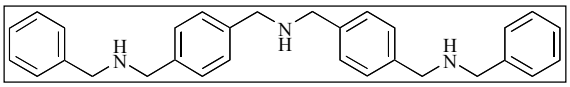

Method the same as that of **9**, except bis-[4-(benzylamino-methyl)-benzyl]-carbamic acid *tert*-butyl ester (1.27g, 2.4mmol) was used which yielded a yellow oil.

Yield = 0.80g (76.3%)

^{1}H NMR (300MHz, $CDCl_3$) δ: 7.35-7.25 (m, 18H, Ar*H*), 3.81-3.73 (m, 12H, CH_2), 1.66 (br, 3H, N*H*)

ESMS m/z: 436.2 $[M + H^+]^+$, 458.2 $[M + Na^+]^+$, 474.2 $[M + K^+]^+$

{3-[(3-{[3-(*tert*-Butoxycarbonylamino-methyl)-benzylamino]-methyl}-benzylamino)-methyl]-benzyl}-carbamic acid *tert*-butyl ester 91

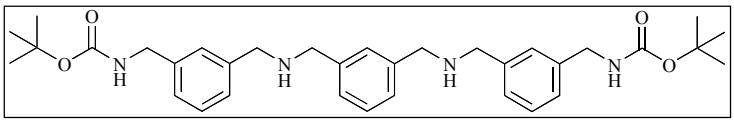

Method the same as that of **10**, except isopthalic dicarboxaldehyde (0.46g, 3.4mmol) and (3-aminomethyl-benzyl)-carbamic acid *tert*-butyl ester (1.63g, 6.9mmol) were used, which yielded a yellow oil.

Yield = 0.50g (88.2%)

^{1}H NMR (300MHz, $CDCl_3$) δ: 7.33-7.20 (m, 12H, Ar*H*), 4.98-4.92 (m, 4H, CH_2NHCO), 4.29 (d, ^{3}J = 3Hz, 4H, ArCH_2NHCO), 3.85-3.76 (m, 8H, ArCH_2NHCH_2ArCH_2NHCH_2Ar), 1.44 (s, 18H, (CH_3)$_3$)

ESMS m/z: 575.1 $[M + H^+]^+$

3-({3-[(3-Aminomethyl-benzylamino)-methyl]-benzylamino}-methyl)-benzylamine 92

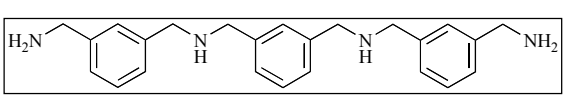

Method the same as that of **9**, except {3-[(3-{[3-

(*tert*-butoxycarbonylamino-methyl)-benzylamino]-methyl}-benzylamino)-methyl]-benzyl}-carbamic acid *tert*-butyl ester (0.74g, 1.3mmol) was used which yielded a pale yellow oil.

Yield = 0.35g (72.9%)

^{1}H NMR (300MHz, $CDCl_3$) δ: 7.32-7.18 (m, 12H, Ar*H*), 3.87-3.81 (m, 12H, CH_2), 1.66 (br, 6H, N*H*)

(3,5-Di-*tert*-butyl-benzyl)-(3-{[3-({3-[(3,5-di-*tert*-butyl-benzylamino)-methyl]-benzylamino}-methyl)-benzylamino]-methyl}-benzyl)-amine 93

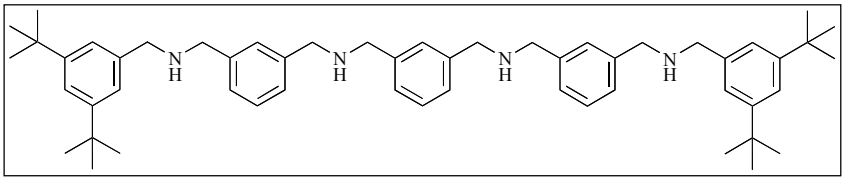

Method the same as that of **10**, except 3,5-di-*tert*-butyl-benzaldehyde (0.39g, 1.8mmol) and 3- ({3-[(3-aminomethyl-benzylamino)-methyl]-benzylamino}-methyl)-benzylamine (0.35g, 0.9mmol) were used, which yielded a yellow oil.

Yield = 1.10g (78.9%)

^{1}H NMR (300MHz, $CDCl_3$) δ: 7.33-7.18 (m, 18H, Ar*H*), 3.85-3.82 (m, 16H, CH_2), 1.34 (s, 4H, (CH_3)$_3$)

ESMS m/z: 779.9 $[M + H^+]^+$

Receptor 96

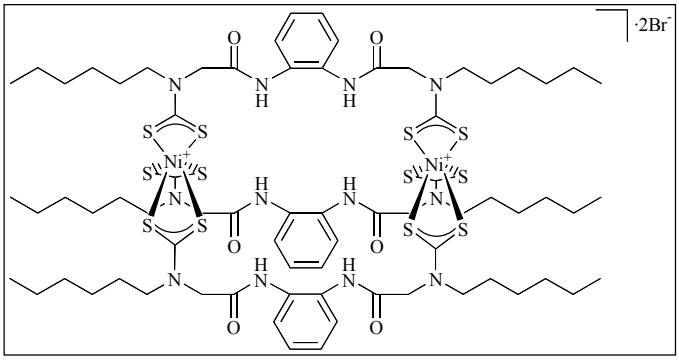

47 (0.50g, 4.2mmol) was dissolved in $CHCl_3$ (100mL) and *N*-bromosuccinimide (0.30g, 8.4mmol) was added portion wise. The mixture was stirred for 1 hour under $N_{2(g)}$. H_2O (100mL) was added and the product extracted into CH_2Cl_2 (4x50mL) and dried over $MgSO_4$. Filtration followed by solvent removal and recrystallisation from CH_2Cl_2/EtOH yielded a red/brown solid, which was dried in *vacuo*.

Yield = 0.40g (75.7%)

UV/visible ($CHCl_3$) λ/nm (ε/dm^3 mol^{-1} cm^{-1}): 265 sh (80.0), 335 (30.8), 388 (13.8), 435 (11.6), 495 sh (9.6), 556 sh (6.0)

IR (Nujol®) ν/cm^{-1}: 3186 (NH), 1660 (Amide I), 1548 (Amide II), 1518 (CN), 962 (CS_{as}), 652 (CS_s)

ESMS m/z: 869.4 $[M - 2Br^-]^{2+}$

Elemental Analysis %:							
	Calculated	C	45.5	H	5.7	N	8.9
	Experimental	C	46.2	H	5.6	N	9.1

Receptor 97

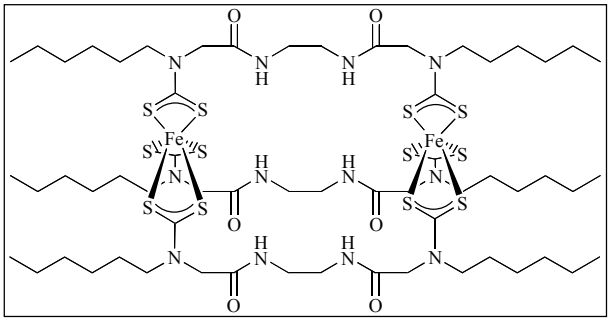

Method the same as that of **43**, except 2-hexylamino-*N*-[2-(2-hexylamino-acetylamino)-ethyl]-acetamide (0.56g, 1.6mmol), KOH (0.18g, 3.2mmol), CS_2 (0.24g, 3.2mmol) and $FeCl_3$ (0.17g, 1.0mmol) were used, which yielded a black powder, which was dried in *vacuo*.

Yield = 0.48g (55.1%)

UV/visible (DMSO) λ/nm (ε/dm^3 mol^{-1} cm^{-1}): 281 sh, 351 sh, 402, 509 sh, 597 sh (ε not determined as the receptor precipitated from solution)

IR (Nujol®) ν/cm^{-1}: 3300 (NH), 1666 (Amide I), 1556 (Amide II), 1486 (CN), 962 (CS_{as})

ESMS m/z: 1589.7 $[M + H^+]^+$, 794.4 $[M]^{2+}$

Elemental Analysis %:							
	Calculated	C	45.3	H	6.9	N	10.6
	Experimental	C	45.3	H	6.8	N	9.5

Receptor 98

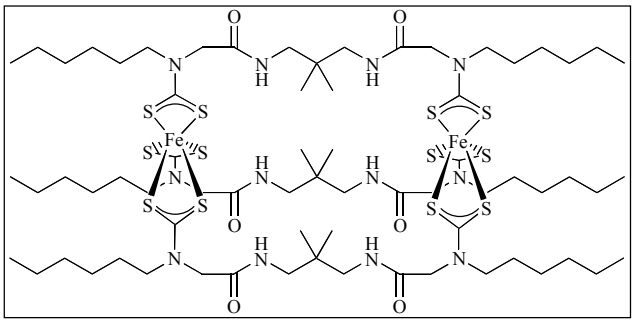

Method the same as that of **43**, except 2-hexylamino-*N*-[3-(2-chloro-acetylamino)-2,2-dimethyl-propyl]-acetamide (1.38g, 3.6mmol), KOH (0.41g, 7.3mmol), CS_2 (0.55g, 7.3mmol) and $FeCl_3$ (0.39g, 2.3mmol) were used, which yielded a black powder.

Yield = 1.10g (26.8%)

UV/visible (DMSO) λ/nm (ε/dm^3 mol^{-1} cm^{-1}): 354 sh, 402 sh, 505 sh, 592 sh (ε not determined as the receptor precipitated from solution)

IR (Nujol®) ν/cm^{-1}: 3268 (NH), 3162 (NH), 1660 (Amide I), 1530 (Amide II), 1480 (CN), 960 (CS_{as}), 648 (CS_s)

ESMS m/z: 1717.0 $[M + H^+]^+$, 1756.0 $[M + K^+]^+$, 590.4 $[M]^{2+}$

Elemental Analysis %:	Calculated + 4 H_2O	C	46.3	H	7.6	N	9.4
	Experimental	C	45.1	H	7.2	N	8.9

Receptor 99

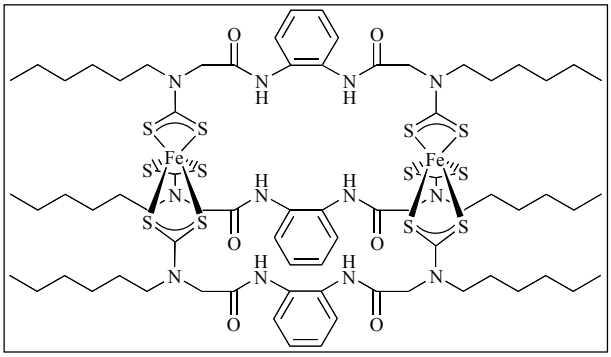

Method the same as that of **43**, except 2-hexylamino-*N*-[2-(2-chloro-acetylamino)-phenyl]-acetamide (0.94g, 2.4mmol), KOH (0.27g, 4.8mmol), CS_2 (0.37g, 4.8mmol) and $FeCl_3$ (0.29g, 1.6mmol) were used, which yielded a black powder.

Yield = 0.91g (65.6%)

UV/visible (DMSO) λ/nm (ε/dm^3 mol^{-1} cm^{-1}): 354 sh (10.4), 389 sh (15.0), 503 sh (4.3), 602 sh (2.3)

IR (Nujol®) ν/cm^{-1}: 3214 (NH), 1676 (Amide I), 1518 (Amide II), 1482 (CN), 960 (CS_{as}), 644 (CS_s)

ESMS m/z: 1733.7 $[M + H^+]^+$, 866.7 $[M]^{2+}$

Elemental Analysis %:	Calculate	C	49.9	H	6.3	N	9.7
	Experimental	C	49.9	H	6.0	N	9.8

Receptor 100

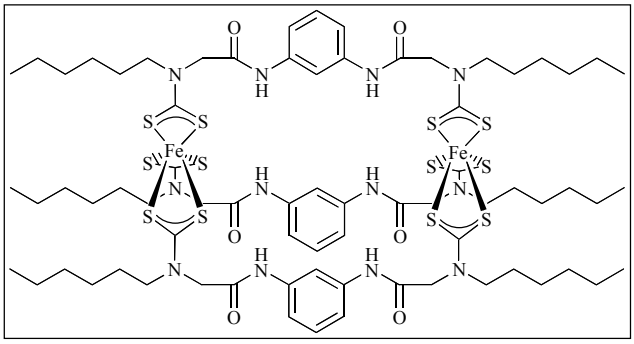

Method the same as that of **43**, except 2-hexylamino-*N*-[3-(2-chloro-acetylamino)-phenyl]-acetamide (0.94g, 2.4mmol), KOH (0.27g, 4.8mmol), CS_2 (0.37g, 4.8mmol) and $FeCl_3$ (0.16g, 0.9mmol) were used, which yielded a black powder.

Yield = 0.91g (65.6%)

UV/visible (DMSO) λ/nm (ε/dm^3 mol^{-1} cm^{-1}): 345 (20.4), 394 sh (15.6), 512 sh (4.9), 586 sh (3.7)

IR (Nujol®) ν/cm^{-1}: 3284 (NH), 1686 (Amide I), 1532 (Amide II), 1484 (CN), 964 (CS_{as})

ESMS m/z: 866.7 $[M]^{2+}$

Elemental Analysis %:	Calculated	C	49.9	H	6.3	N	9.7
	Experimental	C	49.7	H	5.7	N	9.4

Receptor 101

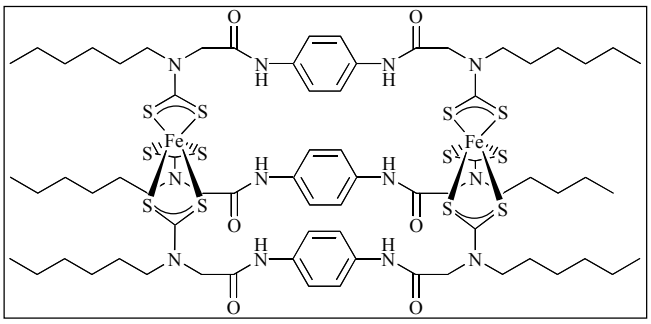

Method the same as that of **43**, except 2-hexylamino-*N*-[4-(2-chloro-acetylamino)-phenyl]-acetamide (0.95g, 2.4mmol), KOH (0.27g, 4.8mmol), CS_2 (0.37g, 4.9mmol) and $FeCl_3$ (0.26g, 1.6mmol) were used, which

yielded a black powder.

Yield = 0.52g (37.0%)

UV/visible : Too insoluble to obtain a spectrum.

IR (Nujol®) ν/cm^{-1}: 3292 (NH), 1674 (Amide I), 1550 (Amide II), 1484 (CN), 966 (CS_{as}), 646 (CS_s)

ESMS m/z: 866.6 $[M]^{2+}$

Elemental Analysis %:	Calculated + 4 H_2O	C	47.9	H	6.5	N	9.0
	Experimental	C	47.6	H	6.7	N	9.3

***N*-(2-{Bis-[2-(2-chloro-acetylamino)-ethyl]-amino}-ethyl)-2-chloro-acetamide 102**

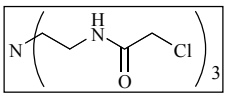

Method the same as that of **1**, except tris-(2-aminoethyl) amine (1.48g, 10.1mmol), $NaOH_{(aq)}$ (20mL, 40% w/w, excess) and chloroacetyl chloride (3.43g, 30.4mmol) was used. After 15 minutes stirring the solid was filtered off and washed with EtOH (20mL) and Et_2O (20mL). Drying in *vacuo* yielded a white solid.

Yield = 3.10g (82.7%)

^{1}H NMR (300MHz, $CDCl_3$) δ: 7.14 (br, 3H, N*H*), 4.23 (s, 6H, CH_2Cl), 3.41 (q, ^{3}J = 6Hz, 6H, CH_2NH), 2.71 (t, ^{3}J = 6Hz, 6H, NCH_2)

ESMS m/z: 375.0 $[M + H^+]^+$

***N*-(2-{Bis-[2-(2-hexylamino-acetylamino)-ethyl]-amino}-ethyl)-2-hexylamino-acetamide 103**

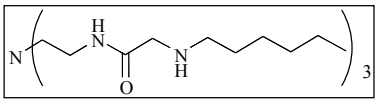

Method the same as that of **38**, except hexylamine (15mL, excess), H_2O (10mL) and *N*-(2-{bis-[2-(2-chloro-acetylamino)-ethyl]-amino}-ethyl)-2-chloro-acetamide (3.10g, 8.3mmol) were used, which yielded a yellow oil.

Yield = 4.08g (86.6%)

^{1}H NMR (300MHz, $CDCl_3$) δ: 7.51 (t, ^{3}J = 5Hz, 3H, CON*H*), 3.28 (q, ^{3}J = 6Hz, 6H, C*H*$_2$NHCO), 3.24 (s, 6H, C*H*$_2$CO), 2.60 (m, 12H, NHC*H*$_2$CH$_2$ & NC*H*$_2$CH$_2$), 1.46 (m, 6H, NHCH$_2$C*H*$_2$), 1.28 (m, 12H, C*H*$_2$C*H*$_2$C*H*$_2$CH$_3$), 0.85 (t, ^{3}J = 7Hz, 9H, C*H*$_3$)

ESMS m/z: 570.5 $[M + H^+]^+$

Receptor 104

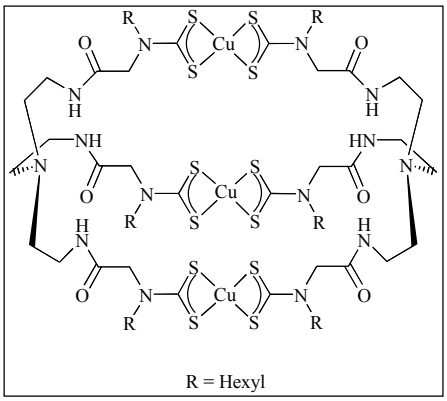

Method the same as that of **58**, except *N*-(2-{bis-[2-(2-hexylamino-acetylamino)-ethyl]-amino}-ethyl)-2-hexylamino-acetamide (1.36g, 2.4mmol), THF:H_2O (5:1 v/v, 60mL), KOH (0.40g, 7.1mmol), CS_2 (0.55g, 7.2mmol) and $Cu(CH_3CO_2)_2{\cdot}H_2O$ (0.72g, 3.6mmol) were used, which yielded a brown powder.

Yield = 0.75g (35.1%)

UV/visible ($CHCl_3$) λ/nm (ε/dm^3 mol^{-1} cm^{-1}): 275 (55.6), 439 (16.8)

IR (Nujol®) ν/cm^{-1}: 3266 (NH), 1662 (Amide I), 1538 (Amide II), 1486 (CN), 956 (CS_{as}), 650 (CS_s)

ESMS m/z: 1820.8 $[M + K^+]^+$

Elemental Analysis %:

Calculated	C	44.5	H	6.8	N	11.0
Experimental	C	46.1	H	7.1	N	10.2

Receptor 105

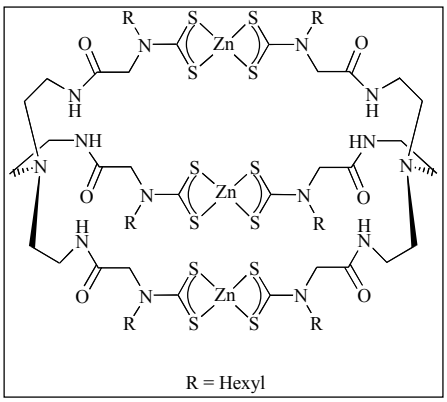

Method the same as that of **76**, except *N*-(2-{bis-[2-(2-hexylamino-acetylamino)-ethyl]-amino}-ethyl)-2-hexylamino-acetamide (0.59g, 1.0mmol), KOH (0.17g, 3.0mmol), CS_2 (0.23g, 3.0mmol) and $Zn(CH_3CO_2)_2{\cdot}2H_2O$ (0.34g, 1.5mmol) were used. H_2O (100mL) was added with stirring, filtration of the solid followed by washing with

EtOH (20mL) and Et_2O (20mL) yielded a cream powder, which was dried in *vacuo*.

Yield = 0.17g (21.2%)

^{1}H NMR (300MHz, DMSO) δ: 7.44 (br, 6H, CON*H*), 4.47 (br, 12H, CH_2CO), 3.86 (t, ^{3}J = 7Hz, 12H, NCS$_2$CH_2CH$_2$), 3.20 (q, ^{3}J = 7Hz, 12H, NCH$_2$CH_2), 2.62 (t, ^{3}J = 7Hz, 12H, NCH_2CH$_2$), 1.71 (m, 12H, NCS2CH$_2$CH_2), 1.30 (m, 12H, CH_2CH_2CH_2CH$_3$), 0.88 (t, ^{3}J = 7Hz, 9H, CH_3)

^{13}C NMR : Too insoluble to obtain a spectrum.

UV/visible : Too insoluble to obtain a spectrum.

IR (Nujol®) ν/cm^{-1}: 3286 (NH), 1662 (Amide I), 1540 (Amide II), 1486 (CN), 962 (CS$_{as}$)

ESMS m/z: 1825.8 [M + K$^+$]$^+$

Elemental Analysis %:	Calculated + 6 H_2O	C	41.8	H	7.0	N	10.4
	Experimental	C	41.9	H	6.3	N	10.4

***N*-(2-{Bis-[2-(4-chloro-butyrylamino)-ethyl]-amino}-ethyl)-4-chloro-butyramide 106**

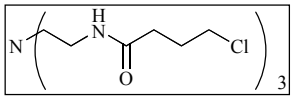

Method the same as that of **1**, except tris-(2-amino ethyl) amine (1.48g, 10mmol), KOH (1.77g, 30mmol), H_2O (10mL) and chlorobutyryl chloride (3.43g, 30mmol) was used. After stirring for 15 minutes H_2O (100mL) was added and the product extracted into $CHCl_3$ (3x50mL). Drying over K_2CO_3 and filtration followed by solvent removal yielded a white solid which was dried in *vacuo*.

Yield = 3.44g (75.0%)

^{1}H NMR (300MHz, $CDCl_3$) δ: 7.26 (t, ^{3}J = 7Hz, 3H, N*H*), 3.62 (t, ^{3}J = 6Hz, 6H, CH_2Cl), 3.29 (q, ^{3}J = 5Hz, 6H CH_2NH), 2.56 (t, ^{3}J = 5Hz, 6H, NCH_2), 2.43 (t, ^{3}J = 8Hz, 6H, COCH_2), 2.13 (m, 6H, CH$_2$CH_2CH$_2$)

ESMS m/z: 459.2 [M + H$^+$]$^+$

Nickel(II) bis(*N*,*N*-diethyl dithiocarbamate)

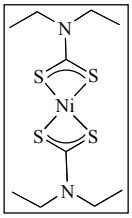

Diethylamine (0.88g, 12.0mmol) was dissolved in THF:H_2O (5:1 v/v, 60mL) and KOH (0.67g, 12.0mmol) was added and stirred under $N_{2(g)}$ until dissolved. CS_2 (0.92g, 12.0mmol) was then added and the solution stirred for 30 minutes. $Ni(CH_3CO_2)_2{\cdot}4H_2O$ (1.49g, 6.0mmol) was added to the yellow solution and the mixture stirred for 15 hours. The THF was removed under reduced pressure, H_2O (100mL) was added with stirring and the product was extracted into $CHCl_3$ (4x50mL) and dried over K_2CO_3. Filtration followed by solvent removal and drying in *vacuo* then recrystallisation from $CHCl_3$/EtOH yielded a green crystalline solid.

Yield = 1.25g (58.4%)

^{1}H NMR (300MHz, $CDCl_3$) δ: 3.58 (q, ^{3}J = 7Hz, 8H, NCH_2), 1.22 (t, ^{3}J = 7Hz, 12H, CH_3)

UV/visible (CH_2Cl_2:MeCN 7:3) λ/nm (ε/dm^3 mol^{-1} cm^{-1}): 327 (36.9), 399 (5.8), 427 sh (1.6)

IR (Nujol®) ν/cm^{-1}: 1516 (CN), 992 (CS_{as}), 636 (CS_s)

ESMS m/z: 355.3 $[M]^+$

Elemental Analysis %:	Calculated	C	33.8	H	5.7	N	7.9
	Experimental	C	33.9	H	5.7	N	8.0

Copper(II) bis(*N*,*N*-diethyl dithiocarbamate)

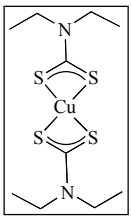

Method the same as that of nickel(II) bis(diethyl) dithiocarbamate, except $Cu(CH_3CO_2)_2{\cdot}H_2O$ (1.20g, 6.0mmol) was used which yielded a brown crystalline solid.

Yield = 1.30g (60.2%)

UV/visible (MeCN:DMSO 4:1) λ/nm (ε/dm^3 mol^{-1} cm^{-1}): 269 (32.9), 287 sh (18.0), 433 (11.8)

IR (Nujol®) ν/cm^{-1}: 1508 (CN), 996 (CS_{as})

ESMS m/z: 360.1 $[M]^+$

Elemental Analysis %:	Calculated	C	33.4	H	5.6	N	7.8
	Experimental	C	33.4	H	5.8	N	7.9

Zinc(II) bis(*N*,*N*-diethyl dithiocarbamate)

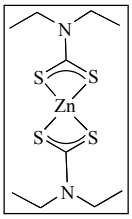

Method the same as that of nickel(II) bis(diethyl) dithiocarbamate, except $Zn(CH_3CO_2)_2{\cdot}2H_2O$ (1.32g, 6.0mmol) was used which yielded a pale yellow crystalline solid.

Yield = 1.45g (66.6%)

^{1}H NMR (300MHz, $CDCl_3$) δ: 3.96 (q, ^{3}J = 7Hz, 8H, NCH_2), 1.35 (t, ^{3}J = 7Hz, 12H, CH_3)

UV/visible (CH_2Cl_2:MeCN 7:3) λ/nm (ε/dm^3 mol^{-1} cm^{-1}): 264 (31.6), 287 sh (22.2)

IR (Nujol®) ν/cm^{-1}: 1504 (CN), 994 (CS_{as}), 666 (CS_s)

ESMS m/z: 747.4 $[2M + Na^+]^+$

Elemental Analysis %:	Calculated	C	33.2	H	5.6	N	7.7
	Experimental	C	33.4	H	5.6	N	7.7

Cadmium(II) bis(*N*,*N*-diethyl dithiocarbamate)

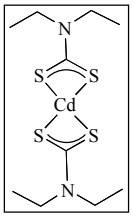

Method the same as that of nickel(II) bis(diethyl) dithiocarbamate, except $CdCl_2.½H_2O$ (1.16g, 5mmol) was used which yielded a pale yellow crystalline solid.

Yield = 1.49g (60.5%)

^{1}H NMR (300MHz, $CDCl_3$) δ: 3.58 (q, ^{3}J = 7Hz, 8H, NCH_2), 1.22 (t, ^{3}J = 7Hz, 12H, CH_3)

UV/visible (CH_2Cl_2:MeCN 7:3) λ/nm (ε/dm^3 mol^{-1} cm^{-1}): 264 (35.4), 282 sh (15.3)

IR (Nujol®) ν/cm^{-1}: 1494 (CN), 982 (CS_{as})

ESMS m/z: 747.4 $[2M + Na^+]^+$

Elemental Analysis %:	Calculated	C	29.4	H	4.9	N	6.9
	Experimental	C	29.7	H	5.4	N	6.8

Iron(II) tris(*N*,*N*-diethyl dithiocarbamate)

Method the same as that of nickel(II) bis(diethyl) dithiocarbamate, except $FeCl_3$ (0.65g, 4.0mmol) was used which yielded a black crystalline solid.

Yield = 1.26g (62.8%)

^{1}H NMR (300MHz, $CDCl_3$) δ: 39.83 (br, 8H, NC*H*$_2$), 1.53 (br, 12H, C*H*$_3$)

UV/visible (MeCN:DMSO 4:1) λ/nm (ε/dm^3 mol^{-1} cm^{-1}): 343 (6.8), 384 sh (4.4), 506 (1.8), 593 (1.4)

IR (Nujol®) ν/cm^{-1}: 1504 (CN), 992 (CS_{as})

ESMS m/z: 500.2 $[M]^+$

Elemental Analysis %:							
	Calculated	C	35.9	H	6.0	N	8.4
	Experimental	C	36.0	H	6.0	N	8.5

Nickel(IV) tris(*N*,*N*-diethyl dithiocarbamate) bromide

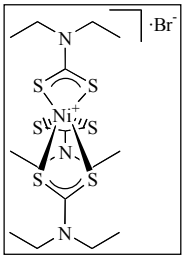

Nickel(II) bis(*N*,*N*-diethyl dithiocarbamate) (1.00g, 2.8mmol) was dissolved in $CHCl_3$ (50mL) and *N*-bromosuccinimide (0.50g, 2.8mmol) was added and the mixture stirred under $N_{2(g)}$ for 1 hour. H_2O (100mL) was added with stirring and the product was extracted into $CHCl_3$ (3x50mL) and dried over K_2CO_3. Filtration followed by solvent removal and drying in *vacuo* followed by recrystallisation from $CHCl_3/Et_2O$ yielded a purple powder.

Yield = 0.80g (66.5%)

^{1}H NMR (300MHz, $CDCl_3$) δ: 3.22 (q, ^{3}J = 7Hz, 12H, NC*H*$_2$), 1.36 (t, ^{3}J = 7Hz, 18H, C*H*$_3$)

UV/visible ($CHCl_3$) λ/nm (ε/dm^3 mol^{-1} cm^{-1}): 267 sh (30.4), 331 (27.3), 425 (6.9), 484 sh (5.0), 560 sh (3.0)

IR (Nujol®) ν/cm^{-1}: 1538 (CN), 970 (CS_{as}), 654 (CS_s)

ESMS m/z: 502.0 $[M - Br^-]^+$

Elemental Analysis %:							
	Calculated	C	30.9	H	5.2	N	7.3
	Experimental	C	31.3	H	5.3	N	7.3

Tetrabutylammonium tetrafluoroboride

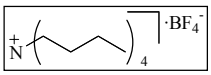

Tetrabutylammonium hydroxide (75mL, 40%, 116.0mmol) was dissolved in H_2O (150mL). Tetrafluoroboric acid (25mL, 48%, 137.0mmol) was added drop wise with stirring and the white precipitate was filtered and washed with H_2O (2x25mL). The solid was dissolved in the minimum amount of CH_2Cl_2, the organic layer separated and added to Et_2O (200mL) drop wise with stirring. Filtration and washing with Et_2O (2x25mL) yielded a white solid that was dried in *vacuo*.

4 References

[1] L. M. Harwood, C. J. Moody, *Experimental Organic Chemistry Principles and Practice*, Blackwell Scientific Publishers, 1989, 294.
[2] A. P. Krapcho, C. S. Kuell, *Synth. Comm.*, 1990, **20**, 2559.
[3] M. Ouchi, Y. Inone, Y. Liu, S. Nagamune, S. Nakamura, K.Wada, T. Hakushi, *Bull. Chem. Soc. Jpn.*, 1990, **63**, 1260
[4] F. Camps, J. Coll, S. Ricart, *J. Heterocycl. Chem.*, 1983, **20**, 249.
[5] J. Cookson, *Part II Thesis*, Oxford University, 2000, 21.
[6] M. S. Newman, L. F. Lee, *J. Org. Chem.*, 1972, **26**, 4460.
[7] M. A. Reppy, M. E. Cooper, J. L. Smithers, L. G. Douglas, *J. Org. Chem.*, 1999, **64**, 4191.
[8] P. R. Ashton, M. P. T Glink, S. Menzer, J. F. Stoddart, P. A. Tasker, A. J. P. White, D. J. Williams, *Chem. Eur. J.*, 1996, **2**, 729.

Appendices

Appendix 1	**^{1}H NMR Titrations**
Appendix 2	**UV/visible**
Appendix 3	**Cyclic and Square Wave Voltammetry**
Appendix 4	**Electrospray Mass Spectrometry**
Appendix 5	**Crystallographic Data of receptor 47**
Appendix 6	**Thin Layer Coulometry**
Appendix 7	**Rotating Disk Voltammetry**
Appendix 8	**SQUID**
Appendix 9	**U-Tube Transport**
Appendix 10	**Summary of Receptors for Chapter 2**
Appendix 11	**Summary of Receptors for Chapter 3**
Appendix 12	**Summary of Receptors for Chapter 4**
Appendix 13	**Summary of Receptors for Chapter 5**

Appendix One

^{1}H NMR Titrations

Tetrabutyl ammonium (TBA) salts of benzoate, dihydrogen phosphate and chloride were stored in a desiccator under vacuum containing self-indicating silica. TBA acetate was stored in a desiccator under vacuum that contained phosphorous pentoxide and self-indicating silica.

NMR Spectra were recorded on a Varian Mercury 300 machine. In a typical experiment, aliquots of the guest (2.5×10^{-4} mol in 0.5mL of deuterated solvent) were added to a solution of the host (5×10^{-6} in 0.5mL of deuterated solvent) at 298K. The chemical shift of a specific proton on the host was monitored for fourteen titration points (10x2μL, 1x10μL, 1x20μL and 1x50μL), corresponding to 0, 0.2, 0.4, 0.6, 0.8, 1, 1.2, 1.4, 1.6, 1.8, 2, 3, 5 and 10 equivalents of guest. The resulting data was analysed by the computer program EQNMR.[1]

The values of the observed chemical shift and the host and guest concentrations were entered into the program for every titration point. Estimates for each binding constant, the limiting chemical shifts and the complex stoichiometry were also added to the input file. The various parameters were refined by non-linear least-squares analysis to achieve the best fit between observed chemical shifts and calculated chemical shifts. The program plots the observed and calculated chemical shifts versus guest concentration, which reveals the accuracy of the experimental data and the suitability of the model. It also gives the best-fit values of the stability constants together with their errors. The parameters were varied until the values for the stability constants converged.

[1] M. J. Hynes, *J. Chem. Soc. Dalton Trans.*, 1993, 311.

Appendix Two

UV/visible Titrations

Tetrabutyl ammonium (TBA) salts of benzoate, dihydrogen phosphate, chloride and perrhenate were stored in a desiccator under vacuum containing self-indicating silica. TBA acetate was stored in a desiccator under vacuum that contained phosphorous pentoxide and self-indicating silica.

UV/visible absorption spectra were acquired on a Perkin Elmer Lambda 6 Spectrometer using Perkin Elmer Computerised Spectroscopy Software. The spectra were recorded ~293K at one minute intervals with the following parameters: Ordinate Mode A, Slit 4, Speed 960. Background correction was made with neat solvent (3mL) in the reference cell and an empty sample cell.

In a typical experiment, aliquots of guest (6.25×10^{-5}mol in 25mL) were added to a 3mL solution of the host (2.5×10^{-5}M) at 293K. Twenty eight aliquots were added (13x2µL, 1x4µL, 6x5µL, 4x15µL, 4x60µL), corresponding to 0, 0.06, 0.13, 0.20, 0.26, 0.33, 0.40, 0.46, 0.53, 0.60, 0.66, 0.73, 0.80, 0.86, 1.00, 1.10, 1.30, 1.45, 1.60, 1.75, 1.90, 2.35, 2.80, 3.25, 3.70, 5.50, 7.30, 9.10, 10.90 equivalents of guest. Spectra were recorded and the data was analysed by the computer program Specfit™.[1] The spectra together with the host and guest concentrations were read into the program for every titration point and the complex stoichiometry and whether the components species were coloured was entered. The parameters were refined by global analysis that uses singular value decomposition and non-linear modelling by the Levenberg-Marquardt method. Using the calculated stability constants, the program plots the predicted spectra of the component species together with the observed and calculated absorption versus guest concentration at a given wavelength, both of which reveal the accuracy of the experimental data and the suitability of the model. The program also gives the best-fit values of the stability

constants together with their errors. The parameters were varied until the values for the stability constants converged.

UV/visible Job Plots

It was possible to obtain Job plots form the data from the UV/visible titrations. This was done by taking the absorption data at a wavelength where the largest changes were observed at 1, 0.9, 0.8, 0.7, 0.6, 0.5, 0.4, 0.3, 0.2 and 0.1 mole fraction of host, and multiplying the absorption by the mole fraction giving Abs(HG_1), Abs($HG_{0.9}$)... This value was multiplied by (volume of solution/3mL) to give the corrected values Abs(HG_{1corr}), Abs($HG_{0.9corr}$)... The absorption of the host at these mole fractions was given by multiplying the absorption of at Abs(HG_{1corr}) by the mole fraction giving Abs(H_1), Abs($H_{0.9}$)... These two values were subtracted, Abs(HG_{1corr}) - Abs(H_1), Abs($HG_{0.9corr}$) - Abs($H_{0.9}$)... to give the difference in absorption at each value of mole fraction due to the guest binding. This value is proportional to the concentration of the host:guest complex and the Job plot was given by plotting these differences against the mole fraction of host. This way of obtaining binding stoichiometries has been verified experimentally.

[1] R. A. Binstead, A. D. Zuberbuhler, B. Jung, *Specfit 3.0.30*, Spectrum Software Associates, 2002.

Appendix Three

Cyclic and Square Wave Voltammetry

Cyclic and square wave voltammetry were performed on a EG & G Princeton Applied Research Potentiostat/Galvanostat model 273 linked to a computer using a National Instruments GPIB-PCII/IIA interface and controlled by EG & G Princeton Applied Research Model 270/250 Research Electrochemistry Software. Typical settings for all electrochemical techniques were as follows: Purge Time pass, Condition Time pass, Condition Potential pass, Deposition Potential pass, Equilibration time pass, Acquisition Mode 4/4, Rise Time high stability, Working Electrode solid, IR Mode none, Uncompensated Resistance 0Ω, Filter 5.3Hz, Auxiliary no.

The electrochemical set-up is shown below in **Figure 1** and measurements recorded at 293K. The solutions were degassed with argon before use and the whole set-up was maintained under argon at all times. The working electrode had a surface area of 0.3cm^2 and was cleaned between scans using Kemet Diamond Polish Sprays 6, 1 and ¼ micron particle size.

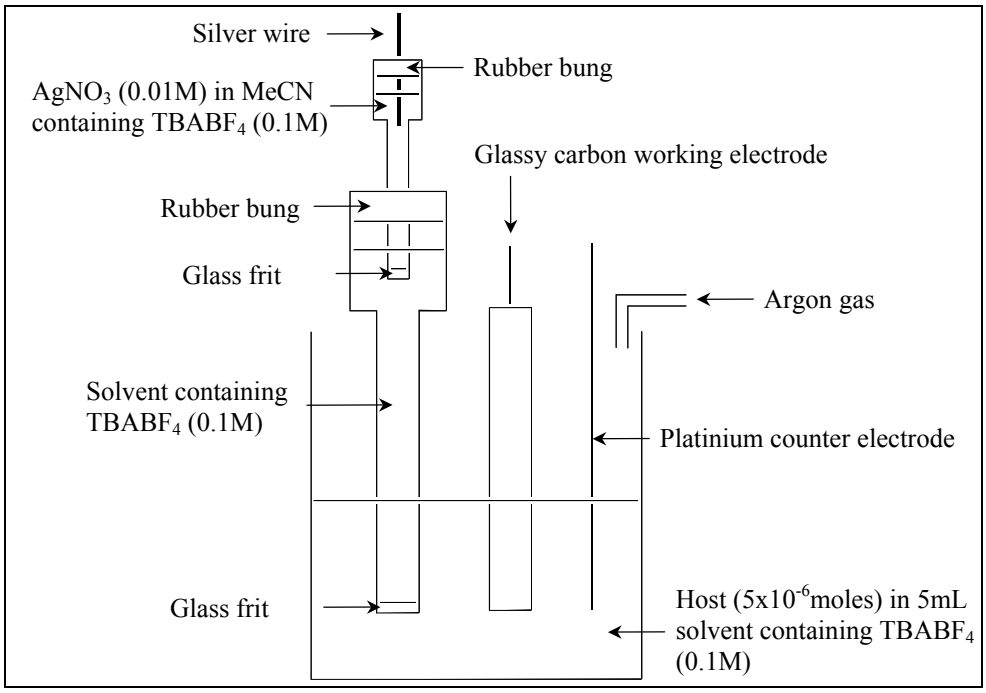

Figure 1 *Electrochemical apparatus set-up*

Using this apparatus ferrocene showed quasi-reversible behaviour in both $CHCl_3$:MeCN (4:1) and DMF solutions and **Table 1** shows the electrochemical data.

Ferrocene	**$CHCl_3$:MeCN (4:1)**	**DMF**
E_{pa} (V)	0.215	0.125
E_{pc} (V)	0.09	0.020
ΔE_p (V)	0.125	0.100
I_{pa}/I_{pc}	1.0	1.1
E_p (V)	0.155	0.070

Table 1 *Electrochemical data of ferrocene in $CHCl_3$:MeCN (4:1) and DMF containing 0.1M $TBABF_4$, potentials given with reference to Ag/Ag^+ at 293K, scan rate = 100mVs^{-1}, E_p - peak potential in square wave voltammogram*

In a typical experiment, the host ($5x10^{-6}$moles) was dissolved in 5ml of a solution containing $TBABF_4$[1] (0.1M) and the cyclic[2] and square wave[3] voltammogram were recorded. For the cyclic voltammetry scan rates of 20, 40 60, 80, 100 mV/s were used to test for reversibility.

Typical settings for cyclic voltammetry were: Scan Rate 100mV/s, Scan Increment 2mV, Strep Time 0.020s, Vertex 2 Delay pass, Vertex 2 Potential pass, Number of Cycles 2, Store Cycle 2. Typical settings for Square wave voltammetry were: Pulse Height, 0.025V, Frequency 60Hz, Scan Increment 2mV.

Tetrabutyl ammonium (TBA) salts of benzoate, dihydrogen phosphate, chloride and perrhenate were stored in a dessicator under vacuum containing self-indicating silica. TBA acetate was stored in a dessicator under vacuum that contained phosphorous pentoxide and self-indicating silica.

Titrations were performed by addition of an aliquot (20μL, 5 equivalents) of the guest solution ($5x10^{-4}$moles in 2mL) to the host solution, stirred and the cyclic and square wave voltammograms recorded. The data was smoothed using a cubic Savitsky-Golay method.[4]

[1] See Experimental chapter for synthesis.

[2] a) Southampton Electrochemical Group, *Instrumental Methods in Electrochemistry*, Ellis-Horwood, 1985, 178; b) A. J. Bard, L. R. Faulkner, *Electrochemical Methods Fundamentals and Applications*, J. Wiley & Sons, 21; c) T. E. Edmonds, *Chemical Sensors*, Blackie, 1988, 193.
[3] a) Southampton Electrochemical Group, *Instrumental Methods in Electrochemistry*, Ellis-Horwood, 1985, 72; b) T. E. Edmonds, *Chemical Sensors*, Blackie, 1988, 203.
[4] A. Savitsky, M. J. E. Golay, *Anal. Chem.*, **36**, 1627.

Appendix Four

Electrospray Mass Spectrometry

Electrospray mass spectrometry (ESMS)[1] was performed on a Micromass LCT controlled by Masslynx LCTOF v.3.4 software. Typical settings were as follows: Capillary 3200V, Sample Cone 50V, Extraction Cone 10V, RFLens 200, Desolvation Temperature 80°C, Source Temperature 60°C, RF DC Offset 1 3, RF DC Offset 2 3, Aperture 3, Acceleration 200, Focus 0, Steering 0, MCP Detector 2700, Manual Pusher 100, Ion Energy 40, Tube Lens 20, Grid 2 50, TOF Flight Tube 4678, Reflection 1790.

In a typical experiment $2x10^{-6}$moles of the compound was dissolved in 0.5mL. 50µL of this solution was taken and 0.5mL of either MeCN or MeOH was added. A 50µL portion of this more dilute solution was injected into the spectrometer with the carrier solvent (MeCN of MeOH) running at 50µL per minute.

The conditions for obtaining the best spectrum varied dependent upon the individual compound being studied. The main parameters that affected the spectrum were capillary voltage, sample cone voltage, desolvation temperature and source temperature. Capillary voltage varied 3000V - 4000V, sample cone voltage 5V - 200V, desolvation temperature 60°C - 140°C, source temperature 40°C - 120°C. The choice of carrier solvent also sometimes affected the final spectrum. When operated in positive mode, the addition of 50µL of a MeCN KPF_6 solution to the sample enhanced the intensity of the peak corresponding to molecular ion:potassium adduct. The negative mode parameters are given in the section below concerning the anion competition studies. When nitrosonium tetrafluoroborate[2] was used to perform dithiocarbamate oxidation reactions, it was either added in excess to the sample before injection or was injected into the spectrometer in MeOH or MeCN and after allowing the machine to run for one minute, the sample was injected.

The data in the highest intensity region of ion counts was summed and background ion counts were subtracted from this. The software automatically calibrated the data set. Smoothing and performing a background correction obtained the final spectrum.

Cation competition studies were carried out using hexafluorophosphate (PF_6) or perchlorate (ClO_4) salts of Na, K, Rb and Cs. $CsPF_6$ and $RbPF_6$ were synthesised using the method reported by Lange.[3] In a typical experiment $2x10^{-6}$moles of the receptor was dissolved in 0.5mL of solvent. A 50μL potion of this solution was taken and 0.5mL of MeOH was added. 50μL of each of the cation metal salt solutions ($2x10^{-4}$moles in 5mL of MeOH) was added and 50μL of the resulting solution was injected into the spectrometer with the MeOH as the carrier solvent running at 50μL per minute. The parameters used were as described above with the exception of: Capillary 3200V, Sample Cone 100V, Extraction Cone 10V, Desolvation Temperature 80°C, Source Temperature 60°C.

The attempted anion competition studies were carried out using tetrabutyl ammonium (TBA) salts of acetate, benzoate, dihydrogen phosphate and chloride. TBA acetate was stored in a dessicator, under vacuum, that contained phosphorous pentoxide and self-indicating silica whereas the other salts were stored in a dessicator, under vacuum, containing self-indicating silica. In a typical experiment a $2x10^{-6}$moles of the receptor was dissolved in 0.5mL of a solvent the compound was soluble in. 50μL of this solution was taken and 0.5mL of CH_2Cl_2 was added. 50μL of each of the TBA anion salts solutions ($2x10^{-4}$moles in 5mL of CH_2Cl_2) was added and 50μL of the resulting solution was injected into the spectrometer with the CH_2Cl_2 as the carrier solvent running at 50μL per minute. The parameters used were as described above with the exception of: Capillary 4000V, Sample Cone 100V, Extraction Cone 10V, Desolvation Temperature 140°C, Source Temperature 120°C.

[1] N. B. Cech, C. G. Enke, *Mass Spectrom. Rev.*, 2001, **20**, 362.
[2] A. M. Bond, R. Colton, A. D'Agostino, J. Harvey, J. J. Traeger, *Inorg. Chem.*, 1993, **32**, 3952.
[3] W. Lange, E. Muller, *Ber. Der Deutsch Chem. Ges. Zu Berlin,* 1930, **63**, 1064.

Appendix Five

Crystallographic Data of Receptor 47

Crystals of receptor **47** were grown from 100mL of a $2.5x10^{-6}$M MeCN:$CHCl_3$ (99:1) solution over three weeks at ~293K. A single crystal having dimensions approximately 0.04 x 0.12 x 0.24 mm was mounted on a glass fibre using perfluoropolyether oil and cooled rapidly to 150K in a stream of cold N_2 using an Oxford Cryosystems CRYOSTREAM unit. Diffraction data were measured using an Enraf-Nonius KappaCCD diffractometer (graphite-monochromated MoK_α radiation, λ = 0.71073Å). Intensity data were processed using the DENZO-SMN package.[1]

Examination of the systematic absences of the intensity data showed the space group to be either *C c* or *C* 2/*c*. The structure was solved in the space group *C* 2/*c* using the direct-methods program SIR92,[2] which located all non-hydrogen atoms of the macrocycle. The non-hydrogen atoms of the alkyl side chains and disordered solvent were located in difference Fourier maps. Subsequent full-matrix least-squares refinement was carried out using the CRYSTALS program suite.[3] Coordinates and anisotropic thermal parameters of all ordered non-hydrogen atoms were refined. Geometric restraints were applied to the solvent (C-C 1.47(1) Å, C-N 1.13(1) Å, C-C-N 180(1)°) and the coordinates and isotropic thermal parameters of its non-hydrogen atoms refined. Hydrogen atoms were positioned geometrically after each cycle of refinement. A 3-term Chebychev polynomial weighting scheme was applied. Refinement converged satisfactorily to give R = 0.0457, wR = 0.0524.

An attempt was also made to solve and refine the structure in the space group *C c*. This did not resolve the disorder and the structure could not be refined satisfactorily.

The complex is situated on a crystallographic centre of inversion. One of the alkyl side chains exhibits large anisotropic thermal parameters, suggesting it may be disordered, however,

it was not possible to resolve this disorder. The solvent is also disordered and Fourier maps show a continuous zigzag band of electron density rather than discrete molecules. This has been satisfactorily modelled as being due to overlapping acetonitrile molecules, but the presence of other species cannot be excluded. **Figure 1** shows the crystal structure together with atom labels.

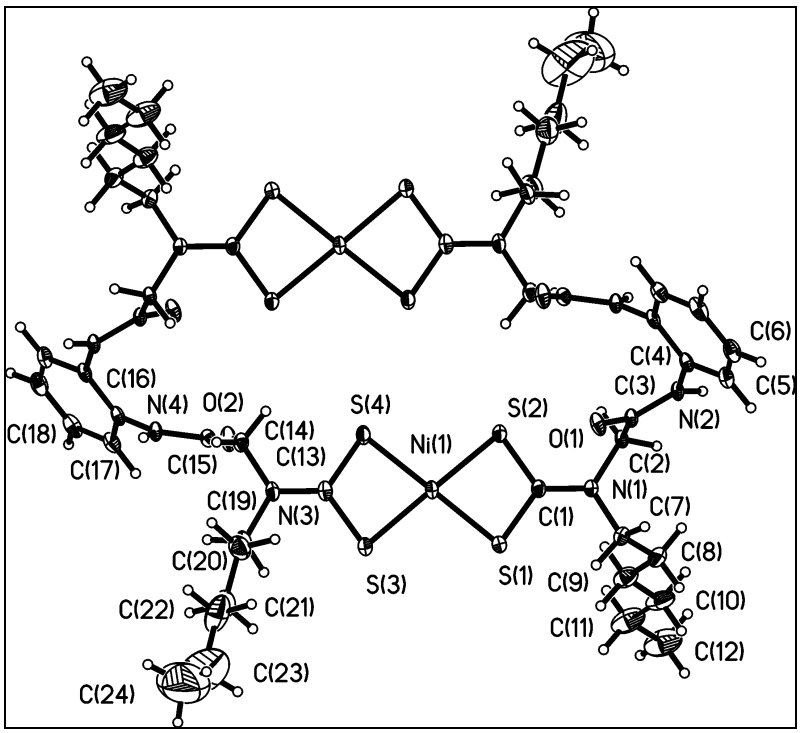

Figure 1 *Crystal structure of **47** together with atom labels (Thermal ellipsoids shown at 30% probability)*

[1] Z. Otwinowski, W. Minor, *Processing of X-ray Diffraction Data Collected in Oscillation Mode, Methods Enzymol.*, 1997, **276**, Eds. C. W. Carter and R. M. Sweet, Academic Press.
[2] A. Altomare, G. Cascarano, G. Giacovazzo, A. Guagliardi, M. C. Burla, G. Polidori, M. Camalli, *J. Appl. Cryst*. 1994, **27**, 435.
[3] D. J. Watkin, C. K. Prout, J. R. Carruthers, P. W. Betteridge, R. I. Cooper, *CRYSTALS issue 11*, Chemical Crystallography Laboratory, Oxford, UK, 2001.

Crystal identification	ARC139
Chemical formula	$C_{50}H_{71}N_9Ni_2O_4S_8$
Formula weight	1236.08
Temperature (K)	150
Wavelength (Å)	0.71073
Crystal system	Monoclinic
Space group	*C* 2/*c*
a (Å)	34.0525(6)
b (Å)	19.3859(4)
c (Å)	9.4251(2)
α (°)	90
β (°)	102.058(3)
γ (°)	90
Cell volume (Å^3)	6084.6
Z	4
Calculated density (Mg/m^3)	1.349
Absorption coefficient (mm^{-1})	0.942
F_{000}	2606.022
Crystal size (mm)	0.04 x 0.12 x 0.24
Description of crystal	Green plate
Absorption correction	Semi-empirical from equivalent reflections
Transmission coefficients (min,max)	0.89, 0.96
θ range for data collection (°)	$5.0 \leq \theta \leq 27.5$
Index ranges	$-44 \leq h \leq 43$, $0 \leq k \leq 25$, $0 \leq l \leq 12$
Reflections measured	45757
Unique reflections	7118
R_{int}	0.057
Observed reflections ($I > 3\sigma(I)$)	4758
Refinement method	Full-matrix least-squares on *F*
Parameters refined	328
Weighting scheme	Chebychev 3-term polynomial
Goodness of fit	1.0330
R	0.0457
wR	0.0524
Residual electron density (min,max) (eÅ^{-3})	-0.41, 1.01

Table 1 *Crystal data and refinement details*

Atom	x	y	z	U_{equiv}	Occupancy
Ni(1)	0.157204(12)	0.27965(2)	0.30734(4)	0.0275	
S(1)	0.10289(2)	0.22749(4)	0.18641(9)	0.0369	
S(2)	0.18442(2)	0.19876(4)	0.19421(8)	0.0324	
S(3)	0.12914(2)	0.35926(4)	0.41968(9)	0.0346	
S(4)	0.21103(2)	0.32858(4)	0.44061(8)	0.0321	
O(1)	0.15809(8)	0.01852(11)	0.2168(2)	0.0345	
O(2)	0.24540(8)	0.52038(12)	0.5358(2)	0.0399	
N(1)	0.12494(7)	0.12256(12)	0.0324(2)	0.0249	
N(2)	0.16947(8)	-0.04542(12)	0.0277(2)	0.0248	
N(3)	0.18689(8)	0.42249(13)	0.6164(3)	0.0302	
N(4)	0.25844(8)	0.54129(12)	0.7779(2)	0.0254	
C(1)	0.13566(9)	0.17447(15)	0.1225(3)	0.0269	
C(2)	0.15444(9)	0.07674(14)	-0.0095(3)	0.0239	
C(3)	0.16035(9)	0.01384(14)	0.0892(3)	0.0243	
C(4)	0.18199(9)	-0.10470(15)	0.1158(3)	0.0260	
C(5)	0.15868(11)	-0.16373(16)	0.1025(3)	0.0347	
C(6)	0.17056(12)	-0.21869(16)	0.1953(4)	0.0397	
C(7)	0.0827(1)	0.10044(17)	-0.0143(4)	0.0353	
C(8)	0.06619(11)	0.1121(2)	-0.1748(4)	0.0497	
C(9)	0.06420(12)	0.1880(3)	-0.2163(4)	0.0539	
C(10)	0.04652(13)	0.2014(3)	-0.3758(5)	0.0677	
C(11)	0.04454(16)	0.2779(4)	-0.4153(6)	0.0828	
C(12)	0.0275(2)	0.2899(5)	-0.5740(7)	0.1060	
C(13)	0.1775(1)	0.37805(15)	0.5077(3)	0.0283	
C(14)	0.2283(1)	0.43298(15)	0.6934(3)	0.0302	
C(15)	0.24434(9)	0.50282(15)	0.6602(3)	0.0271	
C(16)	0.28208(9)	0.60122(14)	0.7800(3)	0.0265	
C(17)	0.27036(11)	0.65674(16)	0.6873(3)	0.0327	
C(18)	0.29460(12)	0.71523(16)	0.6994(4)	0.0399	
C(19)	0.15555(12)	0.45813(19)	0.6743(4)	0.0433	
C(20)	0.14347(15)	0.4134(3)	0.8019(5)	0.0599	
C(21)	0.10451(17)	0.4387(3)	0.8343(6)	0.0702	
C(22)	0.0916(2)	0.4014(4)	0.9558(6)	0.0964	
C(23)	0.0514(4)	0.4256(12)	0.9863(15)	0.2312	
C(24)	0.0422(8)	0.417(2)	1.094(3)	0.4155	
C(25)	0.0082(6)	0.1015(7)	0.2582(19)	0.117(5)*	0.5
C(26)	0.0075(4)	0.0534(6)	0.3772(11)	0.078(3)*	0.5
N(5)	0.0061(3)	0.0188(5)	0.471(1)	0.083(3)*	0.5

Table 2 *Atomic coordinates, equivalent isotropic thermal parameters ($Å^2$) and site occupancies (where not unity) of non-hydrogen atoms *refined value of U_{iso} (N(5), C(25) and C(26) are due to MeCN in the structure)*

Atom	x	y	z	U_{iso}	Occupancy
H(21)	0.1806	0.1017	-0.0003	0.0291	
H(22)	0.1447	0.0617	-0.1123	0.0291	
H(51)	0.1334	-0.1667	0.0263	0.0428	
H(61)	0.1537	-0.2614	0.1861	0.0499	
H(71)	0.0659	0.1271	0.0420	0.0417	
H(72)	0.0809	0.0501	0.0070	0.0417	
H(81)	0.0839	0.0878	-0.2309	0.0578	
H(82)	0.0385	0.0923	-0.2007	0.0578	
H(91)	0.0921	0.2072	-0.1932	0.0641	
H(92)	0.0473	0.2124	-0.1573	0.0641	
H(101)	0.0635	0.1773	-0.4351	0.0801	
H(102)	0.0187	0.1821	-0.3994	0.0801	
H(111)	0.0723	0.2976	-0.3906	0.0976	
H(112)	0.0272	0.3020	-0.3575	0.0976	
H(121)	0.0268	0.3406	-0.5946	0.1259	
H(122)	0.0448	0.2664	-0.6330	0.1259	
H(123)	-0.0003	0.2708	-0.5998	0.1259	
H(141)	0.2294	0.4298	0.8001	0.0349	
H(142)	0.2455	0.3961	0.6639	0.0349	
H(171)	0.2448	0.6547	0.6126	0.0402	
H(181)	0.2867	0.7549	0.6316	0.0503	
H(191)	0.1658	0.5041	0.7134	0.0512	
H(192)	0.1313	0.4647	0.5948	0.0512	
H(201)	0.1651	0.4175	0.8913	0.0724	
H(202)	0.1404	0.3639	0.7713	0.0724	
H(211)	0.1076	0.4887	0.8604	0.0855	
H(212)	0.0830	0.4332	0.7448	0.0855	
H(221)	0.1127	0.4082	1.0459	0.1181	
H(222)	0.0893	0.3513	0.9310	0.1181	
H(231)	0.0505	0.4766	0.9703	0.2889	
H(232)	0.0302	0.4029	0.9114	0.2889	
H(241)	0.0149	0.4369	1.0900	0.4752	
H(242)	0.0620	0.4400	1.1735	0.4752	
H(243)	0.0417	0.3663	1.1145	0.4752	
H(251)	0.0221	0.0795	0.1864	0.1408	0.5
H(252)	0.0228	0.1444	0.2974	0.1408	0.5
H(253)	-0.0200	0.1134	0.2095	0.1408	0.5

Table 3 *Atomic coordinates, isotropic thermal parameters ($Å^2$) and site occupancies (where not unity) of hydrogen atoms (H(251), H(252) and H(253) are due to MeCN in the structure)*

Atom	U_{11}	U_{22}	U_{33}	U_{23}	U_{13}	U_{12}
Ni(1)	0.0341(2)	0.02417(19)	0.02423(18)	-0.00774(14)	0.00611(14)	-0.00309(15)
S(1)	0.0306(4)	0.0376(4)	0.0406(4)	-0.0173(3)	0.0034(3)	0.0027(3)
S(2)	0.0308(4)	0.0343(4)	0.0320(4)	-0.0131(3)	0.0062(3)	-0.0030(3)
S(3)	0.0361(4)	0.0303(4)	0.0354(4)	-0.0115(3)	0.0025(3)	0.0016(3)
S(4)	0.0345(4)	0.0317(4)	0.0322(4)	-0.0124(3)	0.0115(3)	-0.0082(3)
O(1)	0.0618(15)	0.0286(11)	0.0156(9)	-0.0010(8)	0.0139(9)	0.005(1)
O(2)	0.0692(17)	0.0349(12)	0.0155(9)	-0.0020(8)	0.009(1)	-0.0018(11)
N(1)	0.0297(13)	0.0237(12)	0.0213(11)	-0.0024(9)	0.0054(9)	-0.002(1)
N(2)	0.0379(14)	0.0226(11)	0.014(1)	-0.0032(8)	0.0062(9)	-0.002(1)
N(3)	0.0406(15)	0.0256(12)	0.0237(12)	-0.0069(9)	0.005(1)	0.0003(11)
N(4)	0.0386(14)	0.0238(12)	0.014(1)	-0.0028(8)	0.0068(9)	-0.004(1)
C(1)	0.0330(15)	0.0274(14)	0.0194(12)	-0.0028(11)	0.0036(11)	-0.0000(12)
C(2)	0.0338(15)	0.0227(13)	0.0162(12)	-0.002(1)	0.0077(11)	-0.0008(11)
C(3)	0.0347(15)	0.0225(13)	0.0160(11)	-0.002(1)	0.0061(11)	-0.0031(11)
C(4)	0.0408(16)	0.0224(13)	0.0179(12)	-0.002(1)	0.0132(11)	0.0007(12)
C(5)	0.0466(19)	0.0248(15)	0.0356(16)	-0.0075(12)	0.0147(14)	-0.0049(13)
C(6)	0.057(2)	0.0236(15)	0.0443(18)	-0.0033(13)	0.0234(16)	-0.0064(15)
C(7)	0.0320(16)	0.0331(16)	0.0393(17)	-0.0080(13)	0.0041(13)	-0.0064(13)
C(8)	0.038(2)	0.067(3)	0.0391(19)	-0.0165(18)	-0.0025(15)	-0.0005(18)
C(9)	0.040(2)	0.083(3)	0.0373(19)	0.0043(19)	0.0047(15)	-0.003(2)
C(10)	0.036(2)	0.121(4)	0.043(2)	0.008(2)	0.0017(16)	0.009(2)
C(11)	0.057(3)	0.129(5)	0.058(3)	0.034(3)	0.002(2)	-0.007(3)
C(12)	0.074(4)	0.177(8)	0.064(3)	0.035(4)	0.007(3)	0.008(4)
C(13)	0.0413(17)	0.0220(13)	0.0221(13)	-0.001(1)	0.0080(12)	-0.0043(12)
C(14)	0.0399(17)	0.0277(15)	0.0198(13)	-0.0007(11)	-0.0010(12)	0.0024(13)
C(15)	0.0356(16)	0.0300(14)	0.0154(12)	-0.000(1)	0.0049(11)	0.0034(12)
C(16)	0.0423(17)	0.0217(13)	0.0188(12)	-0.003(1)	0.0137(12)	0.0018(12)
C(17)	0.0506(19)	0.0281(15)	0.0218(13)	0.0031(11)	0.0130(13)	0.0084(14)
C(18)	0.068(2)	0.0244(15)	0.0332(16)	0.0054(13)	0.0250(16)	0.0076(15)
C(19)	0.050(2)	0.0394(19)	0.0382(18)	-0.0167(15)	0.0046(15)	0.0086(16)
C(20)	0.069(3)	0.066(3)	0.046(2)	-0.009(2)	0.015(2)	0.012(2)
C(21)	0.077(3)	0.074(3)	0.063(3)	-0.016(2)	0.021(2)	-0.013(3)
C(22)	0.111(5)	0.119(5)	0.065(3)	-0.016(3)	0.032(3)	-0.070(4)
C(23)	0.15(1)	0.42(3)	0.152(11)	0.015(13)	0.098(9)	-0.096(13)
C(24)	0.27(3)	0.62(5)	0.30(3)	-0.18(3)	-0.07(2)	0.22(3)

Table 4 *Anisotropic thermal parameters ($Å^2$)*

Ni(1) - S(1)	2.2048(9)
Ni(1) - S(2)	2.2062(8)
Ni(1) - S(3)	2.1998(9)
Ni(1) - S(4)	2.2080(8)
S(1) - C(1)	1.716(3)
S(2) - C(1)	1.722(3)
S(3) - C(13)	1.720(3)
S(4) - C(13)	1.711(3)
O(1) - C(3)	1.224(3)
O(2) - C(15)	1.229(3)
N(1) - C(1)	1.318(4)
N(1) - C(2)	1.456(4)
N(1) - C(7)	1.478(4)
N(2) - C(3)	1.352(4)
N(2) - C(4)	1.430(4)
N(3) - C(13)	1.325(4)
N(3) - C(14)	1.458(4)
N(3) - C(19)	1.469(4)
N(4) - C(15)	1.339(4)
N(4) - C(16)	1.411(4)
C(2) - C(3)	1.521(4)
C(4) - C(5)	1.383(4)
C(4) - C(16)	1.401(4)
C(5) - C(6)	1.385(5)
C(6) - C(18)	1.380(6)
C(7) - C(8)	1.517(5)
C(8) - C(9)	1.522(7)
C(9) - C(10)	1.520(6)
C(10) - C(11)	1.528(9)
C(11) - C(12)	1.505(7)
C(14) - C(15)	1.517(4)
C(16) - C(17)	1.391(4)
C(17) - C(18)	1.393(5)
C(19) - C(20)	1.605(6)
C(20) - C(21)	1.505(7)
C(21) - C(22)	1.496(7)
C(22) - C(23)	1.530(17)
C(23) - C(24)	1.14(3)
C(25) - C(26)	1.462(9)
C(26) - N(5)	1.122(8)

Table 5 *Bond lengths (Å) H atoms have been excluded (N(5), C(25) and C(26) are due to MeCN in the structure)*

S(1) - Ni(1) - S(2)	79.39(3)	N(1) - C(7) - C(8)	112.8(3)
S(1) - Ni(1) - S(3)	99.71(3)	C(7) - C(8) - C(9)	112.8(3)
S(2) - Ni(1) - S(3)	179.03(4)	C(8) - C(9) - C(10)	114.0(4)
S(1) - Ni(1) - S(4)	176.47(4)	C(9) - C(10) - C(11)	113.2(5)
S(2) - Ni(1) - S(4)	101.41(3)	C(10) - C(11) - C(12)	112.4(6)
S(3) - Ni(1) - S(4)	79.47(3)	S(3) - C(13) - S(4)	110.40(16)
Ni(1) - S(1) - C(1)	85.4(1)	S(3) - C(13) - N(3)	124.3(2)
Ni(1) - S(2) - C(1)	85.2(1)	S(4) - C(13) - N(3)	125.2(2)
Ni(1) - S(3) - C(13)	85.0(1)	N(3) - C(14) - C(15)	112.0(2)
Ni(1) - S(4) - C(13)	84.94(11)	O(2) - C(15) - N(4)	124.0(3)
C(1) - N(1) - C(2)	121.8(2)	O(2) - C(15) - C(14)	121.9(3)
C(1) - N(1) - C(7)	122.3(3)	N(4) - C(15) - C(14)	114.1(2)
C(2) - N(1) - C(7)	115.3(2)	N(4) - C(16) - C(4)	117.5(2)
C(3) - N(2) - C(4)	120.1(2)	N(4) - C(16) - C(17)	122.7(3)
C(13) - N(3) - C(14)	121.9(3)	C(4) - C(16) - C(17)	119.8(3)
C(13) - N(3) - C(19)	121.0(3)	C(16) - C(17) - C(18)	119.4(3)
C(14) - N(3) - C(19)	116.8(2)	C(6) - C(18) - C(17)	120.3(3)
C(15) - N(4) - C(16)	125.1(2)	N(3) - C(19) - C(20)	110.1(3)
S(1) - C(1) - S(2)	110.03(16)	C(19) - C(20) - C(21)	110.5(4)
S(1) - C(1) - N(1)	124.8(2)	C(20) - C(21) - C(22)	114.2(5)
S(2) - C(1) - N(1)	125.2(2)	C(21) - C(22) - C(23)	114.5(9)
N(1) - C(2) - C(3)	109.5(2)	C(22) - C(23) - C(24)	123.2(21)
O(1) - C(3) - N(2)	123.5(3)	C(25) - C(25) - C(26)	92.3(30)
O(1) - C(3) - C(2)	120.9(2)	C(25) - C(25) - C(26)	67.6(26)
N(2) - C(3) - C(2)	115.6(2)	C(26) - C(25) - C(26)	100.8(12)
N(2) - C(4) - C(5)	121.1(3)	C(25) - C(26) - C(25)	20.1(16)
N(2) - C(4) - C(16)	118.6(3)	C(25) - C(26) - N(5)	176.7(14)
C(5) - C(4) - C(16)	120.3(3)	C(25) - C(26) - N(5)	158.2(15)
C(4) - C(5) - C(6)	119.5(3)	C(26) - N(5) - N(5)	156.2(18)
C(5) - C(6) - C(18)	120.7(3)		

Table 6 *Bond angles (°) H atoms have been excluded*

Appendix Six

Thin Layer Coulometry

Thin layer coulometry was performed on a EG & G Princeton Applied Research Potentiostat/Galvanostat model 273 linked to a computer using a National Instruments GPIB-PCII/IIA interface and controlled by EG & G Princeton Applied Research Model 270/250 Research Electrochemistry Software.

The same electrochemical set-up was used as described in **Appendix 3** except that the working electrode was of a thin layer design (**Figure 1**).

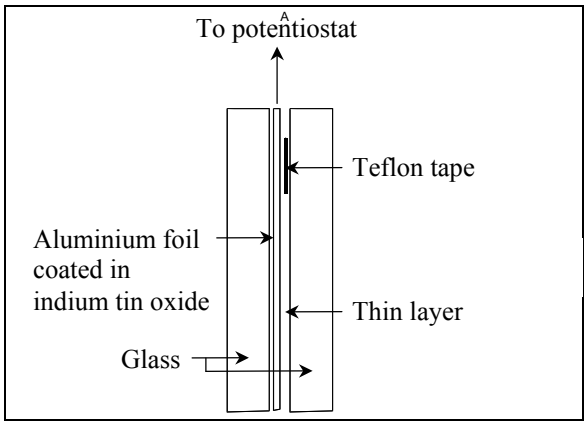

Figure 1 *Design of thin layer working electrode*

In a typical experiment, the compound to be studied ($5x10^{-6}$ moles) was dissolved in 5ml of a solution containing $TBABF_4$ (0.1M). A linear sweep voltammogram was recorded and the potential of the maximum was noted (E_{max}). Typical settings were as described in **Appendix 3** with the following additional parameters: Scan Rate 100mV/s, Scan Increment 2mV, Step Time 0.020s. A chronoamperometry experiment was run at the potential of the electrochemical process and the current recorded as a function of time. Typical settings were as described in **Appendix 3** with the following additional parameters: Time Per Point 0.060s, Number of Points 2000, Sop On pass, Initial Potential 0, Potential Step 1 E_{max}, Time Step 1 120s, Potential Step 2 pass, Time

Step 2 pass. The data was smoothed using a cubic Savitsky-Golay method.[1] The charge was calculated (Q = i x time) and plotted against time.

An example of receptor **47** and ferrocene is shown below in **Figure 2** together with the associated calculations.

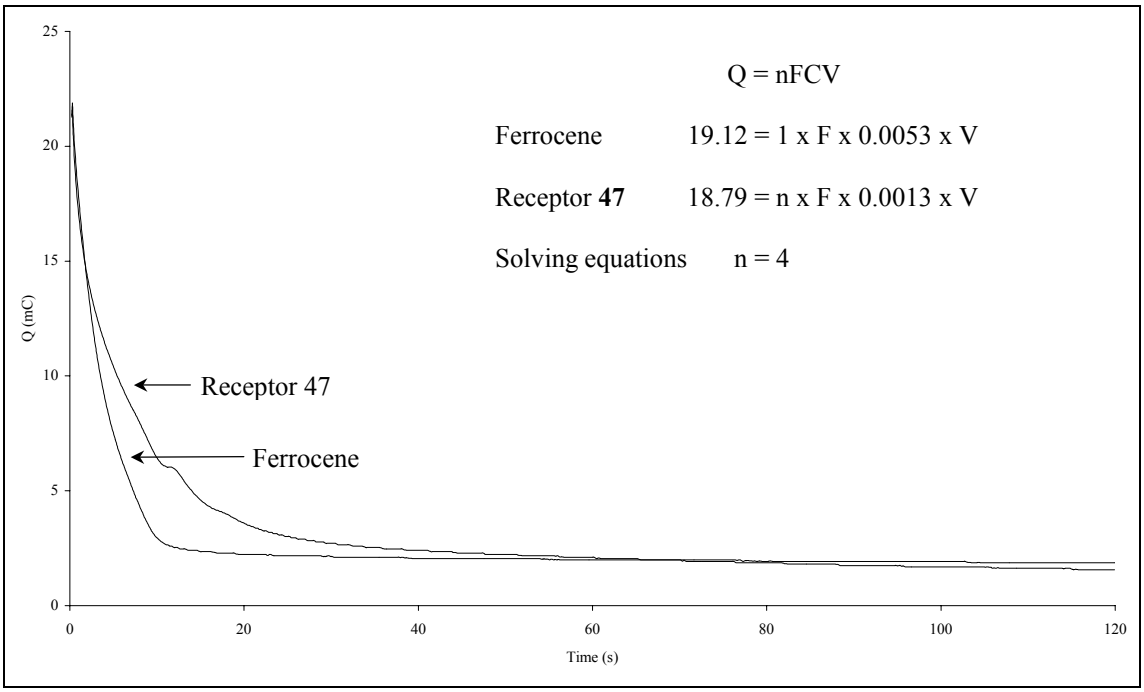

Figure 2 *Charge against time plot for receptor **47** and ferrocene in a thin layer electrode*

The process being observed was a two electron oxidation of two nickel(II) dithiocarbamate groups, i.e. four electrons should be needed.

[1] A. Savitsky, M. J. E. Golay, *Anal. Chem.*, **36**, 1627.

Appendix Seven

Rotating Disk Voltammetry

Rotating disk electrochemistry were performed on a EG & G Princeton Applied Research Potentiostat/Galvanostat model 273 and a Electrode Rotator model 636 linked to a computer using a National Instruments GPIB-PCII/IIA interface and controlled by EG & G Princeton Applied Research Model 270/250 Research Electrochemistry Software.

The same electrochemical set-up was used as described in **Appendix 3** except that the working electrode was a EG & G Princeton Applied Research Model 636 Electrode Rotator.

In a typical experiment, the molecule ($5x10^{-6}$moles) was dissolved in 5ml of a solution containing $TBABF_4$ (0.1M). The linear sweep voltammogram was recorded between potentials that contained the electrochemical process of interest and the data was smoothed using a cubic Savitsky-Golay method.[1] Typical settings used were as described in **Appendix 3** with the following additional parameters: Scan Rate 100mV/s, Scan Increment 2mV, Step Time 0.020s, Acquisition Mode 4/4.

[1] A. Savitsky, M. J. E. Golay, *Anal. Chem.*, **36**, 1627.

Appendix Eight

SQUID

Variable temperature magnetic data was collected on a Quantum Design MPMS-5 super conducting quantum interference device (SQUID) controlled by MPMS v.2.21 software.

In a typical experiment, 50mg – 100mg of finely ground compound was placed into an agar capsule. This was placed in a plastic straw as shown below in **Figure 1**. Small holes were made in the straw along its whole length to allow air to escape.

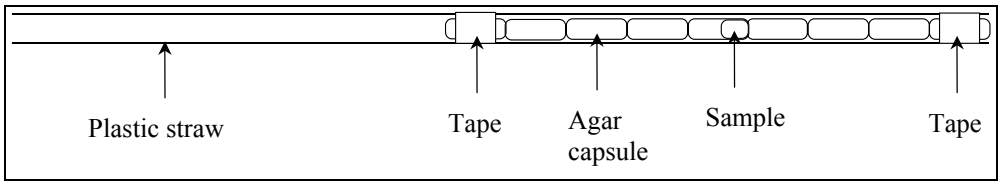

Figure 1 *Sample mounting for variable temperature magnetic studies*

The straw was inserted into the machine and the sample centred automatically using the software. Two different experiments were used, zero-field cooled and field cooled. The value at each temperature was divided by the number of moles in the sample and this value was divided by the applied field. Contributions due to diamagnetism were then subtracted, to give the molar magnetic susceptibility, χ_m.

Calculation of the best fit parameters for variable temperature magnetic measurements were carried out using the Solver function in Microsoft Excel 2000.

Appendix Nine

U-Tube Transport

U-tube transport studies were performed at 293K using a cell design as shown below in **Figure 1**. Caesium picrate was kindly synthesised by Dr. P. Hopkins.

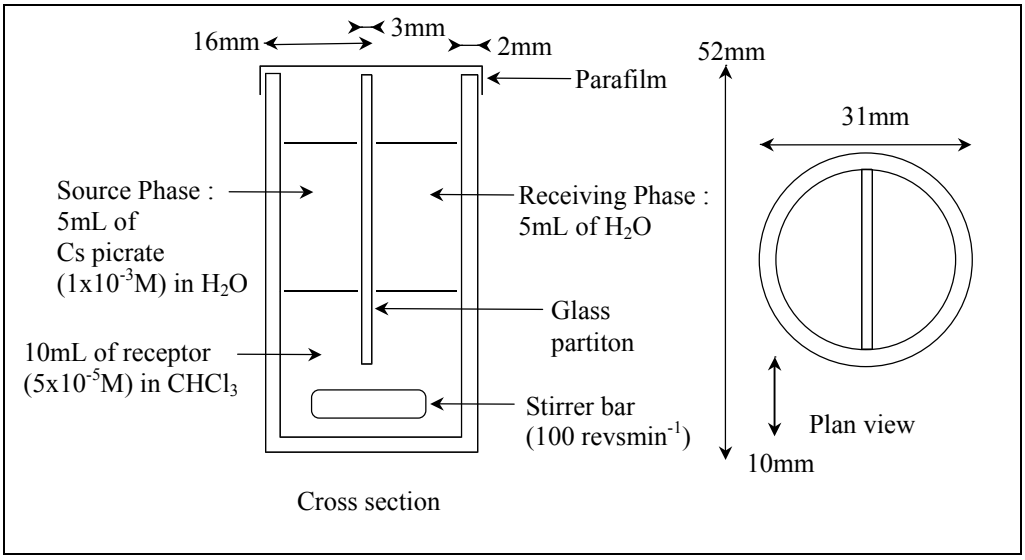

Figure 1 *U-tube design for transport studies*

At one-day intervals, for five days, a 0.25mL aliquot of the receiving phase was withdrawn and made up to 3mL with H_2O. The UV/visible spectrum of the sample was recorded on a Perkin Elmer Lambda 6 Spectrometer using Perkin Elmer Computerised Spectroscopy Software. The spectra were recorded with the following parameters: Ordinate Mode A, Slit 4, Speed 960. Background correction was made with 3mL of H_2O in the reference cell and an empty sample cell. At the same time, 0.25mL of the source phase was also removed and disposed of. The amount of caesium picrate in the receiving phase was calculated by monitoring the maximum in the spectrum at 356nm.

Appendix Ten

Summary of Receptors for Chapter 2

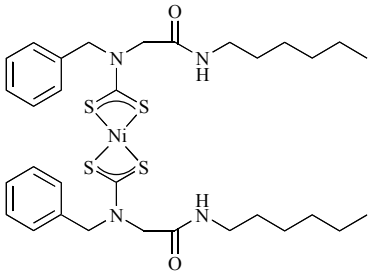

4

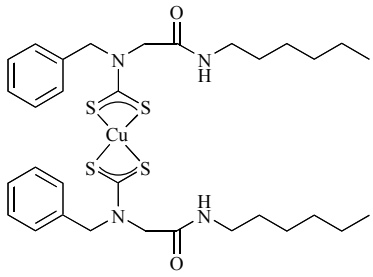

5

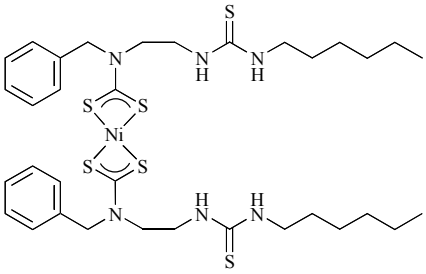

11

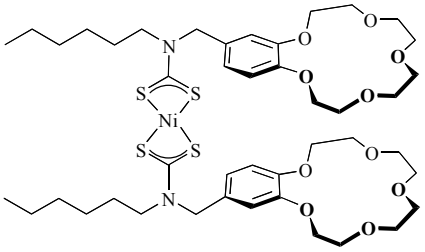

15

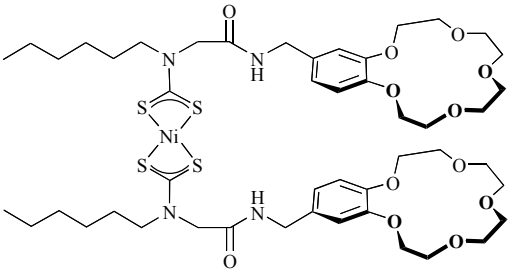

19

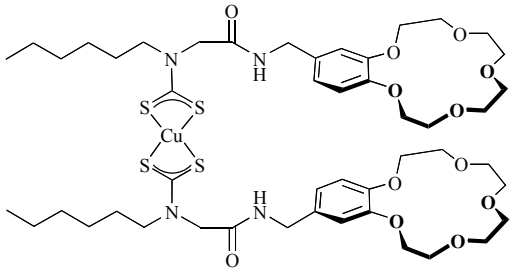

20

Appendix Eleven

Summary of Receptors for Chapter 3

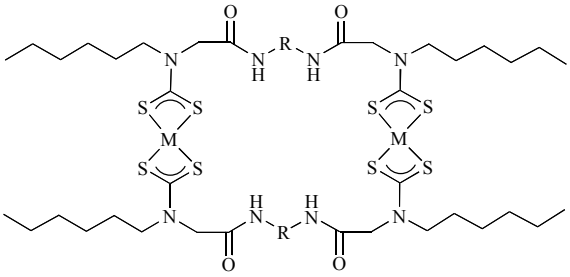

R=				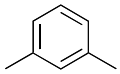	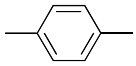
M = Ni(II)	**43**	**45**	**47**	**49**	**51**
M = Cu(II)	**44**	**46**	**48**	**50**	**52**

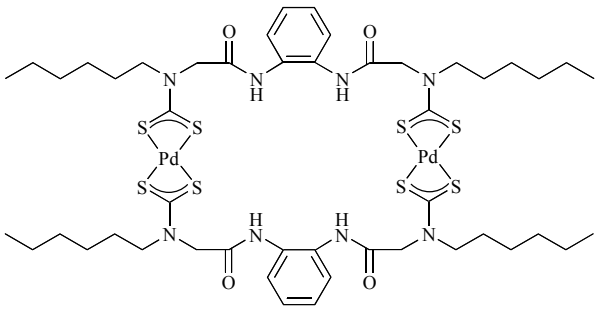

53

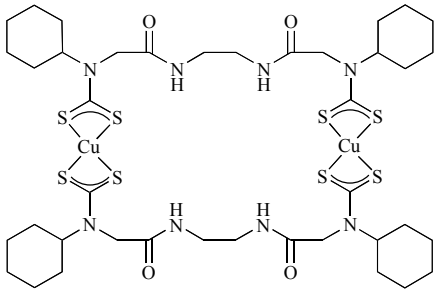

55

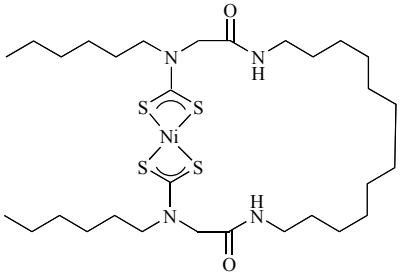

58

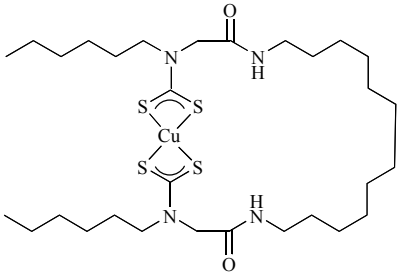

59

Appendix Twelve

Summary of Receptors for Chapter 4

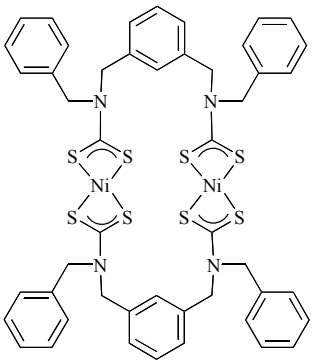

73

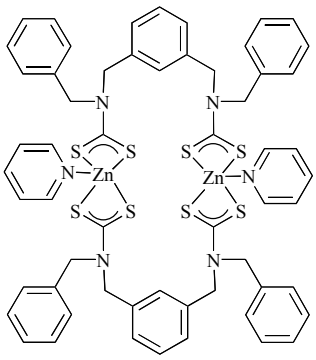

74

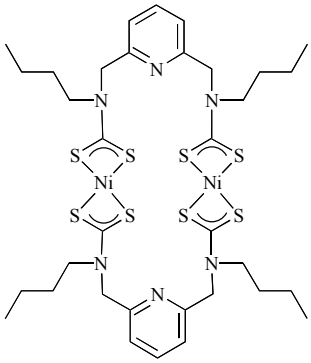

75

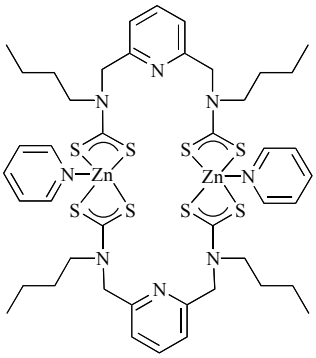

76

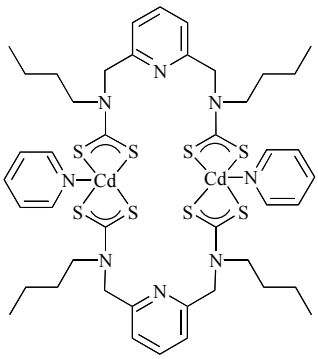

77

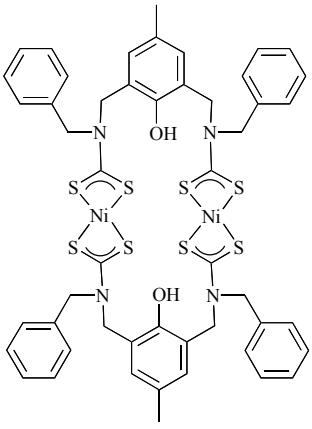

78

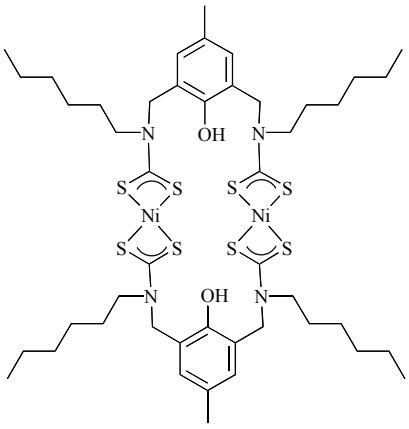

79

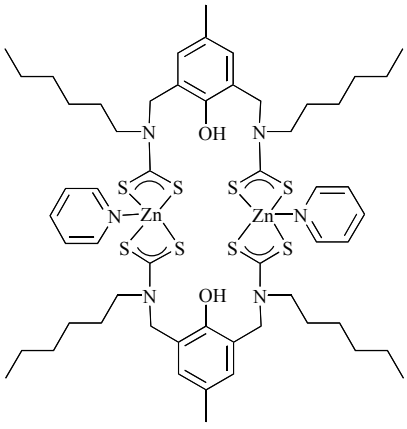

80

Appendix Thirteen

Summary of Receptors for Chapter 5

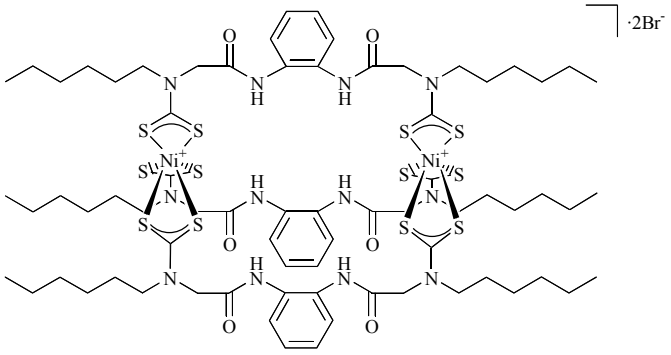

96

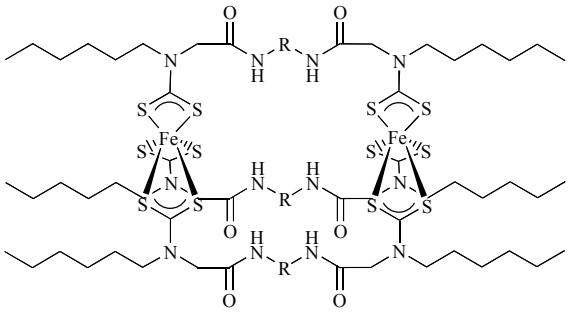

R=

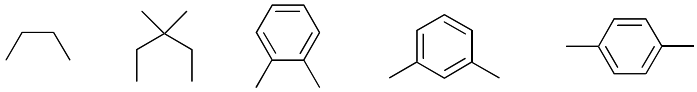

97 **98** **99** **100** **101**

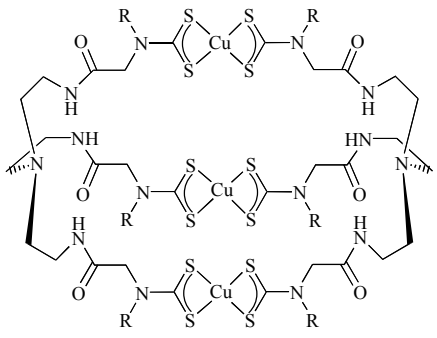

104

R = Hexyl

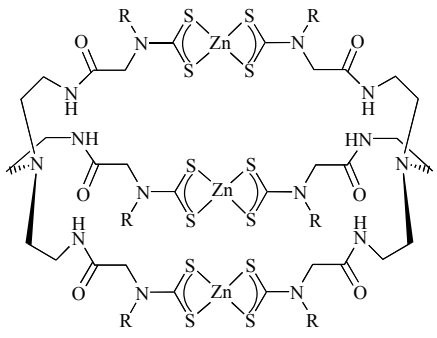

105

R = Hexyl